People's Democratic Republic of Algeria

Ministry of Higher Education and Scientific Research

Amar Telidji University - Laghouat

Faculty of Sciences

PhD Thesis in Sciences

Specialty: Chemistry

Presented and defended publicly

October 09th, 2021

By

Ahmed ABDELMOUIZ

THEME

Proposal of an optimal process for the removal of carbon dioxide and hydrogen sulfide contained in natural gas (IN SALAH)

Supervisory and Examining Committee :

Mr	Abdelaziz GHERIB	Chair of Defense	Pr	UAT Laghouat
Mr	Mokhtar FODILI	External examiner	Pr	UZA Djelfa
Mr	Ali BOUCENNA	External examiner	Pr	UMB Boumerdes
Mr	Med Ben Abdellah TAOUTI	Examiner	Pr	UAT Laghouat
Mr	Ahmed HAMDI	Examiner	MCA	UAT Laghouat
Mr	Abdenacer GUIBADJ	Supervisor	Pr	UAT Laghouat
Mr	Ahmed HADJADJ	Co-supervisor	Pr	UMB Boumerdes
Mr	Amr HENNI	Co-Supervisor abroad	Pr	Uregina(Canada)

2020/2021

Abstract

The primary focus of this research is on developing comprehensive reaction rate/kinetics models that take into account the coupling between the chemical equilibrium and chemical kinetics of all possible chemical reactions for the absorption of CO_2 into aqueous solutions of MDEA,PZ, blended (MDEA –PZ),blended (PZ –Sulfolane) , and blended (MDEA –Sulfolane) in order to explore the potential of these solvents for capturing CO_2 in terms of reaction kinetics.

The reaction kinetics of carbon dioxide in the aqueous mixed solvent solutions of (PZ+ Sulfolane) , and (MDEA+ Sulfolane) were studied for the first time using the stopped-flow technique. The absorption rates of carbon dioxide in the aqueous mixed solvent solutions of (PZ+ Sulfolane), and (MDEA+ Sulfolane) were higher than those of standalone PZ and MDEA at the same concentrations at all temperatures from (298.15 to 313.15) K.

The study confirms the advantage of the commercially available Sulfinol technologies over standalone amine-based processes.

The solubility results over a wide range of temperature are useful for studying the solution properties in the chemical, biochemical, environmental protection, and energy industries.

The solubility of CO_2 in aqueous solutions of blended (MDEA-Sulfolane), and (MDEA-PZ) decreases as temperature increases because the solubility of CO_2 declines with increasing temperature; thus, the system tends toward CO_2 desorption rather than CO_2 absorption. For the effect of CO_2 partial pressure, the equilibrium solubility of CO_2 increases as CO_2 partial pressure increases due to the higher driving force for CO_2 absorption at higher CO_2 partial pressure.

The physical Solubility in the mixed aqueous solvent of (MDEA-Sulfolane) is higher than that of aqueous mixed (MDEA-PZ), as if there was a kind of “enhancement” in the solubility when MDEA was used with Sulfolane.

It is predicted that replacement of Sulfinol-M solvent has better performance and suitable economics compared to present solvent and other amine solvents, reduce energy consumption and reduce investment costs.

Based on the results obtained from this research in terms of reaction kinetics and absorption capacity, it can be concluded that the aqueous solution of blended (MDEA-Sulfolane) have good potential to be used as the alternative solvents for capturing acid gas.

Key words: Kinetics, Piperazine, Zwitterion, Stopped flow, Sulfolane, Mixed solvents

---

ملخص

ينصب التركيز الأساسي لهذا البحث على تطوير نماذج معدل التفاعل/ الحركية الشامل, التي تأخذ بعين الإعتبار التوازن الكيميائي والحركية الكيميائية لجميع التفاعلات الكيميائية الممكنة لإمتصاص ثاني أكسيد الكربون في المحاليل المائية التالية: البيبرازين ، مثيل ديإيثانول أمين، مزيج (المثيل ديإيثانول أمين - البيبرازين)، مزيج (المثيل ديإيثانول أمين - السيلفولان), ومزيج (البيبرزين - السيلفولان) من أجل استكشاف إمكانات هذه المذيبات لإمتصاص ثاني أكسيد الكربون من حيث حركية التفاعل.

تمت دراسة حركية التفاعل لثاني أكسيد الكربون في المحاليل المائية المذيبة المختلطة (المثيل ديإيثانول أمين - السيلفولان), و (البيبرزين - السيلفولان) ولأول مرة باستخدام تقنية التدفق المتوقف. كانت معدلات إمتصاص ثاني أكسيد الكربون في محاليل المذيبات المختلطة المائية ل (البيبرزين - السيلفولان) , و(المثيل ديإيثانول أمين - السيلفولان) أعلى من تلك الموجودة في البيبرازين ،و المثيل ديإيثانول أمين عند نفس التراكيز في جميع درجات الحرارة. تؤكد الدراسة ميزة تقنيات السيلفينول المتاحة تجاريًا على التقنيات القائمة على الأمين المستقلة.

دراسة نتائج الذوبانية على مجال واسع من درجات الحرارة مفيدة لدراسة خصائص المحاليل في الصناعات الكيميائية ،الكيمياء الحيوية ،حماية البيئة وصناعات الطاقة.

تنخفض قابلية ذوبان ثاني أكسيد الكربون في المحاليل المائية الختلطة : (المثيل ديإيثانول أمين - البيبرازين)، و(المثيل ديإيثانول أمين - السيلفولان) مع زيادة درجة الحرارة لأن قابلية ذوبان ثاني أكسيد الكربون تتناقص مع زيادة درجة الحرارة ؛ وبالتالي ، يميل النظام نحو إدمصاص ثاني أكسيد الكربون بدلاً من إمتصاصه. إرتفاع الضغط الجزئي لثاني أكسيد الكربون يسبب إرتفاع القوة الدافعة للإمتصاص مما يؤدي إلى إرتفاع قابلية ذوبان هذا المركب. الذوبانية الفيزيائية في المذيب المائي المختلط ل (المثيل ديإيثانول أمين - السيلفولان), أعلى من المذيب المائي المختلط ل (المثيل ديإيثانول أمين - البيبرازين)، مما يؤكد وجود نوع من "التعزيز" في الذوبانية عند استخدام المثيل ديإيثانول أمين مع السيلفولان . من المتوقع أن يكون لمذيب (السلفينول- م) أداء إقتصادي أفضل ومناسب مقارنة بالمذيب الحالي والمذيبات الأمينية الأخرى ، وهذا كونه يقليل من استهلاك الطاقة و من تكاليف الاستثمار.

استنادًا إلى النتائج المتحصل عليها من هذا البحث من حيث حركيات التفاعل وقدرة الامتصاص ، يمكن استنتاج أن المحلول المائي المختلط (المثيل ديإيثانول أمين – السيلفولان) لديه إمكانية جيدة لاستخدامه كمذيبات بديلة لإمتصاص الغاز الحمضي.

الكلمات المفتاحية : الحركية ، زويتيرين ، بيبرازين ، سيلفولان ، ، مذيبات مختلطة.

Résumé

L'objectif principal de cette recherche est de développer des modèles complets de la cinétique de réaction qui prennent en compte le couplage entre l'équilibre chimique et la cinétique chimique de toutes les réactions chimiques possibles pour l'absorption du CO_2 dans des solutions aqueuses de MDEA, PZ, mélange (MDEA - PZ), mélange (PZ –Sulfolane) , et le mélange (MDEA – Sulfolane) afin d'explorer le potentiel de ces solvants pour absorber le CO_2 en termes de cinétique de réaction. La cinétique de réaction du dioxyde de carbone dans les solutions aqueuses de solvants mixtes de (PZ + Sulfolane) et (MDEA + Sulfolane) a été étudiée pour la première fois en utilisant la technique à flux arreté. Les taux d'absorption du dioxyde de carbone dans les solutions aqueuses de solvants mixtes de (PZ+Sulfolane) et (MDEA+Sulfolane) étaient plus élevés que ceux du PZ et du MDEA aux mêmes concentrations à toutes températures de (298,15 à 313,15) K. L'étude confirme l'avantage des technologies Sulfinol disponibles dans le commerce par rapport aux procédés autonomes à base d'amine. Les résultats de solubilité sur une large plage de températures sont utiles pour étudier les propriétés de la solution dans les industries chimiques, biochimiques, de protection de l'environnement et énergétiques. La solubilité du CO_2 dans les solutions aqueuses de mélange (MDEA-Sulfolane) et (MDEA-PZ) diminue à mesure que la température augmente car la solubilité du CO_2 diminue avec l'augmentation de la température ; ainsi, le système tend vers la désorption du CO_2 plutôt que l'absorption. Pour l'effet de la pression partielle de CO_2, la solubilité à l'équilibre du CO_2 augmente à mesure que sa pression partielle augmente en raison de la force motrice plus élevée pour l'absorption de CO2 à une pression partielle plus élevée.

La solubilité physique dans le solvant aqueux mixte du (MDEA-Sulfolane) est supérieure à celle du mélange aqueux (MDEA-PZ), comme s'il y avait une sorte d'« amélioration » de la solubilité lorsque le MDEA était utilisé avec le Sulfolane. Il est prévu que le remplacement du solvant Sulfinol-M a de meilleures performances et une économie appropriée par rapport au solvant

actuel et à d'autres solvants aminés, réduit la consommation d'énergie et réduit les coûts d'investissement. Sur la base des résultats obtenus à partir de cette recherche en termes de cinétique de réaction et de capacité d'absorption, on peut conclure que la solution aqueuse de mélange (MDEA-Sulfolane) a un bon potentiel pour être utilisée comme solvants alternatifs pour capturer les gaz acides.

Mots clés : Cinétique, Pipérazine, Zwitterion, flux arrêté, Sulfolane, Solvants mixtes

Acknowledgements

Foremost, I would like to express my appreciation and acknowledgement to the Ministry of Higher Education and Scientific Research of Algeria for the financial support to conduct this interesting research. I am very grateful to them for the funding they have provided that has aided me greatly in the completion of this work.

I have been fortune enough to have been given the opportunity to travel to Canada to continue my research work in the international Test Centre for CO_2 Capture (ITC), and Research innovation center (RIC) (Faculty of Engineering and Applied Science, University of Regina, Canada), under the supervision of prof Amr Henni. He gave me the freedom to define my thesis statement and always acted as a very helpful sounding board for my ideas. Whenever I was bereft of ideas, my discussions with him and his insights always helped me get back on the right track. His trustworthy advice and support throughout all phases of the research was most welcome and appreciated. I am really thankful to him for his kind supervision during the achievement of this work. It was always inspiring to work with him. I would like to thank him and the staff of the University of Regina for their kindness, encouragement and hospitality.

My acknowledgement also extends to my supervisors, Pr. Abdenacer Guibadj and, Pr. Ahmed Hadjadj, for their invaluable guidance, support, and encouragement throughout my study. I appreciate all their contributions of time and their passion, which exceptionally inspire and enrich my growth as a researcher. Special thanks and acknowledge to them for their personal guidance, constant support, and mentorship over the course of this thesis.

My gratitude to my late parents is beyond measure – all through my life, they have always sacrificed to ensure that I had the best opportunities possible and they have constantly believed in me and encouraged me to dream big and to pursue those dreams. I cannot put into words what their support has meant to me over the years and I dedicate this thesis to them.

I would also like to thank my thesis committee members, Pr: Abdelaziz. Gherib, Pr.Mokhtar. Fodili , Pr .Ali. Boucenna, Pr : Mohammed Benabdallah. Taouti , and Dr: Ahmed. Hamdi, ,for their valuable suggestions and advices.

My deepest thanks from all my heart to all the staff of the University of Amar Telidji, Laghouat, especially those of process engineering department.

Finally, I would like to express my sincere appreciation to everyone who made this work possible, both directly and indirectly through their assistance and support.

Finally, I would like to express my sincere appreciation to everyone who made this work possible, both directly and indirectly through their assistance and support.

Dedication

This work is dedicated to

My late parents: Aboubaker and Messaouda. They have been the best models. Their constant prayers and encouragements made all these hard years enjoyable. (No words can explain how much I am thankful to them).

My wife (Fatiha), and kids(Aboubaker, Saber, Mouataz, Razane, and Firas), for their patience, love, and their continual support of my work. Their love made my daily pilgrimage to the laboratory in very cold temperatures, and for long nights a bearable task.

My brothers, sisters, and aunts.

Table of Contents

List of Tables

List of Figures

Nomenclature

A	Arrhenius constant
A_i	Temperature dependence coefficient
B	Base (amine, water or hydroxyl ion)
C_p^{ig}	Ideal gas heat capacity
E_{act}	Activation energy
f	*Fugacity*
$G_m^{*,E}$	Molar excess Gibbs free energy
H_i	Henry's constant for component i
H_m^*	Molar enthalpy
$H_m^{*,E}$	Molar excess enthalpy (* refers to the asymmetrical reference state)
I_x	Ionic strength
K_0	Observed pseudo-first-order reaction rate constant
K_{-1}	Backward first-order reaction rate constant
K_2	Forward second-order reaction rate constant
Ka	Equal to $K_2 K_{amine} / K_{-1}$
K_{base}	Rate constant for the deprotonation of the Zwitterion by a base (amine, water, or hydroxyl ion).
K_B	Equal to $K_2 K_{base} / K_{-1}$
K_w	Equal to $K_2 K_{water} / K_{-1}$
N_A	Avogadro number
n_{CO2}^g	Moles of CO_2 in gas phase at equilibrium
n_i	Number of moles of component i
P	Pressure
P_{CO2}	Equilibrium partial pressure of CO_2

r_{CO2}	Rate of reaction with respect to CO_2
R	Universal gas constant (0.008315 kJ /mol. K).
S	Entropy
t	Time (second)
T	Temperature
T_r	Reduced temperature
T_{Ci}	Critical temperature
T^{ref}	Reference temperature (298.15 k)
V_m	Molar volume
$V_i^{\infty,aq}$	Brelvi -O'Connell partial molar volume for component i.
x_i	Molar fraction of component i
Z_i	Compressibility factor
[ ]	Concentration (mol/ m^3)

Greek symbols

A_{ϕ}	Debije-Hückel parameter
α	CO_2 loading (mol of CO_2 per mol of amine)
α_i	Activity of component i
γ_i	Activity coefficient of component i
C	Equilibrium concentration of gas at interface (mol/L)
$\Delta_f H_w^{*,ig}$	Standard enthalpy of formation for ideal gas (kJ/mol)
ω_i	Acentric factor
ϕ_i^v	Vapor fugacity coefficient
ϕ_i^0	Liquid pure component fugacity coefficient of component i
Q_e	Electron charge
ε_w	Dielectric constant of water
ρ	Density (g/Cm^3)
τ	Binary Interaction Parameter in NRTL Equation

Abbreviations

AAD	Absolute average deviation
AMP	2-amino-2-methyl-1-propanol
CO_2	Carbon dioxide
COS	Carbonyl sulfide
CS_2	Carbon disulfide
DEA	Diethanolamine
DEAB	4-(diethylamine)-2-butanol
DGA	Diglycolamine
DIPA	Diisopropanolamine
DIPPR	Design Institute for Physical properties
DMMEA	Di-methyl-monoethanolamine
EOS	Equation of state
E-NRTL	Electrolyte non-random two-liquid
H_2S	Hydrogen sulfide
HCl	Hydrochloric acid
MEA	Monethanolamine
MDEA	Methyldiethanolamine
MRD	Mean relative deviation
N_2	Nitrogen
NRTL	Non-random two-liquid
PDH	Pitzer-Debye- Hückel

PZ	Piperazine
TEA	Triethanolamine
TMS	Tetramethylene sulfone(Sulfolane)
VLE	Vapour-liquid equilibrium
UNIQUAC	Universal quasi Chemical

General Introduction

General Introduction

Rapid economic growth has contributed to today's ever increasing demand for energy. An obvious consequence of this is an increase in the use of fuels, particularly conventional fossil fuels (i.e. coal, oil and natural gas) that have become key energy sources since the industrial revolution. According to the report of International Energy Agency (IEA, 2014), fossil fuels still account for over 80% of the world energy supply. Natural gas has been a popular energy source for many decades, and its demand as a fuel is continuously increasing worldwide.

There is a prediction of considerable growth in the natural gas sector over the next two decades; natural gas is also occasionally predicted to even overtake other conventional fossil fuels (e.g., oil) as the main fuel between 2020 and 2030 (Bp, 2013; Economides and wood, 2009**)** At the end of 2013, the known worldwide natural gas reserves were reported to be approximately 185.7 trillion cubic meters, a volume that is estimated to be sufficient for 55.1 years of global demand (Bp, 2014). Natural gas is therefore expected to have a significant impact on the industrial, transport, power, residential and commercial sectors (Correljé, 2013; liss, 2012).

Natural gas is mostly considered to be a "clean" fuel with respect to the emission of pollutants from its combustion. Methane is the cleanest hydrocarbon fuel source. It releases approximately 30% less carbon dioxide than oil and 43% less carbon dioxide than coal (Langston, 2010).

It's composed of methane with a variety of other components, including higher hydrocarbons, water, carbon dioxide, hydrogen sulfide, and other impurities such as mercaptans (R-SH), helium, and nitrogen. H_2S, CO_2 and SO_2 are termed as acid gases since they dissociate to form weak acidic solution when they come into contact with water or an aqueous medium. These amines are known as weak organic bases. After its treatment by the usual separation process for the removal of liquefiable hydrocarbons, normally contains considerable moisture and a substantial amount of undesirable compounds, principally hydrogen sulphide and carbon dioxide. These compounds are collectively known as "Acid gases" and they are very undesirable, as they cause corrosion and present major safety risks. Because of the highly toxicity of H_2S and the lack of heating value of CO_2 ,natural gas should be cleaned from acid gases to meet the pipe-line quality standard specifications as a consumer fuel, enhance the calorific value of the natural gas, avoid pipelines and equipment corrosion and further overcome related process bottle necks.

According to the Standard American Society for Testing and Materials (ASTM) test method for the analysis of hydrogen sulfide in gaseous fuels (lead acetate reaction rate method), which is ASTM D4084-07 (2012), This method is used in the industry to determine the concentration of hydrogen sulfide and to verify compliance with operational and environmental needs. The sales gas criteria as per the US pipeline specifications are as follows: **(1)** minimum gross calorific value of 950 BTU/SCF, **(2)** maximum water content of 7.0 lbs/ MMcf, **(3)** maximum H_2S content of 4 ppm vol, **(4)** maximum total inert gases content of 4% (maximum CO_2 content of 2%), and **(5)** maximum hydrocarbon dew point of (-10 °C) at operating pressure maximum. The calorific value is the main parameter to represent the sales gas because it quantifies the energy that can be obtained from the gas as a fuel. Additionally, it determines the price of the produced gas in the market. To maintain the calorific value higher than the limit, inert gases such as nitrogen and carbon dioxide must be removed to a maximum of 04 mol%, of which only a maximum of 02 mol% carbon dioxide is allowed. The removal of acid gases (CO_2, H_2S and other sulfur components) from natural gas is often referred to as gas sweetening process. The removal of acid gases, including CO_2 and H_2S, is challenging, and the existence of these gases in the natural gas increases the risk associated with the gas plant and requires the usage of special materials that can withstand the corrosive environment. A variety of acid gas purification technologies are used depending upon operability , flexibility and economics such as :

• Absorption Processes (Chemical and Physical absorption)

• Adsorption Process (Solid Surface)

• Physical Separation (Membrane, Cryogenic Separation)

• Hybrid Solution (Mixed Physical and Chemical Solvents)

A recent study by (Li et al., 2013) found that more than 1000 patents have been published on CO_2 capture by solvents, sorbents and membranes, and about 38% of these patents are on solvent technology.

The selecting of the acid gas removal process can be simplified by gas composition and operating conditions. High CO_2 partial pressure in the feed gas enhances the possibilities of employing physical solvent, while the presence of significant amount of heavy hydrocarbon

discourages the use of physical solvent. Low CO_2 partial pressures and low outlet pressure of the product stream may favour application of chemical solvents (Tennyson et al., 1977).

The most conventional method of acid gas sweetening that has applied in industry is the chemical absorption through aqueous alkanol-amine solutions, because of its acid gas removal capacity to low levels at low pressures. Moreover , The loss of these aqueous solutions is not substantial the solubility of hydrocarbons in it is very low (Shirazizadeh, 2019) Some examples of industrial importance are the primary amines mono-ethanolamine (MEA) and di-glycol-amine (DGA), the secondary amines di-ethanolamine (DEA) and diisopropanolamine (DIPA), the tertiary amines methyldiethanolamine (MDEA) and triethanolamine (TEA), and the amine blend comprising MDEA and piperazine (PZ)) (Kohl and Riesenfeld, 1997). In chemical solvents, N-methyldiethanolamine (MDEA) is a tertiary alkanolamine that its aqueous solutions are widely used in the gas treatment units. In spite of its low reaction rate with CO_2, the aqueous MDEA solution seems to be an effective solvent for CO_2 removal from gas streams due to its high solution concentration, high CO_2 loading, slow degradation rate, low corrosiveness, low regeneration heat of reaction, and low evaporation loss (Huang et al., 2011). The choice of a certain amine (single or blended amine) is mainly based on the absorption capacity, reaction kinetics and regenerative potential and facility. Piperazine (PZ) is a cyclic, diamine that has previously been studied as a promoter for amine systems such as MDEA/PZ or MEA/PZ blends to improve CO_2 mass transfer rates.

Combining the absorption characteristics of each amine, blended amines have been suggested for the absorption of acid gases (Chakravarty, et al 1985).

Blended amine solvents, which consist of a mixture of primary or secondary amine with a sterically hindered or tertiary amine, combine the higher CO_2 reaction rates of the primary or secondary amine with the higher CO_2 loading capacity of the sterically hindered or tertiary amine (Chakravarty et al., 1985).

Blending MDEA and PZ (both chemical solvents) has the potential to combine the high CO_2 capacity of MDEA and the favorable kinetics of PZ to improve the absorption of carbon dioxide, while decreasing energy during regeneration and reaching the usual specifications of In-Salah gaseous region (Krechba field) . A chemical absorption process of Activated

Methyldiethanolamine (a-MDEA) is used for the treatment of the export gas of Krechba gaseous field to meet the product gas specifications and which must be less than or equal to 0.3 mol% CO_2 and 2.0 mg / cm^3 in H_2S. The high energy requirements for the regeneration of the absorbent appear as the main disadvantage, therefore the development of solvents capable of processing larger quantities of acid gases with lower energy demands is a challenge for the capture technology**.** The use of these processes for world-wide CO_2 capture is inhibited by high energy and plant expenditures.

The possibility of employing alkanolamines in hybrid solvents (chemical and physical solvents) in order to remove acid gases has attracted great interest, and several research groups have studied the use of aqueous and non-aqueous solutions of alkanolamines in the separation of acid gases. In physical solvents, the absorption is not restricted by the stoichiometry, and the regeneration of the solvent could be done by reduction of the pressure. In addition, the sulphur compounds such as COS and thiols could be removed by this method (Mirzaei et al., 2015). In fact, using a mixed-solvent allows one to take the advantages of both types of physical and chemical solvents. The previous studies showed that the CO_2 absorption capacity of a physical solvent is lower than a chemical solvent at low pressures, but it can be enhanced to higher gas loadings at high partial pressures due to lack of stoichiometry limits(Wang et al.,2010).Therefore desired solvent characteristics are as following :

1) High capacity and low enthalpy of absorption: This characteristic is most important as it directly relates to the energy expended (KJ/mol of CO_2 captured), but the laws of thermodynamics connect the absorption capacity and enthalpy of solution (Mathias, and O'Connell, 2012), and thus independent variation may be restricted.

2) High mass transfer and chemical kinetics: This characteristic desirable because it reduces equipment sizes, and for the same equipment and flow higher mass transfer and chemical kinetics will decrease capacity because the system will operate closer to the equilibrium limit.

3) Cost and availability: A multiple-use chemical is usually preferred because it costs less and is widely available.

4) Low viscosity: Lower solvent viscosity usually leads to faster mass transfer and higher heat-transfer rates (Mangers and Ponter, 1980), which reduces pumping costs.

5) Low degradation tendency: Lower degradation tendency reduces the need for solvent replacement or reclaiming, and allows the regenerator to operate at higher pressure (i.e., higher temperature), which increases thermal efficiency.

6) Low volatility: Lower solvent volatility decreases solvent slip in the absorber bed, and hence reduces the capacity required for the wash system.

7) Toxicity/environmental: Of particular concern here is the formation of toxic by-products like nitrosamines, or environmental impacts from volatility losses.

8) Low fouling tendency: This characteristic is closely related to the solvent melting point and indicates whether it may precipitate as a solid. Solvent degradation may also cause fouling and increase solvent corrosivity.

In amine-based acid gas capture, acid gas reacts with an aqueous amine solution, forming different electrolyte species. In electrolyte solutions a larger variety of interactions and phenomena exist than in non-electrolyte solutions. Besides physical and chemical molecule-molecule interactions, ionic reactions and interactions occur (molecule-ion and ion-ion).

Modeling electrolyte systems is challenging and requires models which can cope with the strong non-idealities of the liquid, caused by the presence of cationic and anionic species. The absorption kinetics represents one of the important key parameters required for simulating , and optimizing a process for acid gas capture from natural gas streams because it provides us with how fast acid gas reacts with amines.

The knowledge of the phase behaviour and equilibrium solubility of acid gases in solvents is of fundamental importance, the thermophysical properties of solvents are necessary for solvent selection and subsequent process simulation and design of acid gas treatment equipment.

Rigorous and accurate representation of the thermodynamic properties of these electrolyte systems is essential for successful modeling and simulation of such chemical products and processes (Chen and Mathias, 2002). The accuracy of any simulation model depends on the accuracy of thermodynamic model used and the completeness of property data, including

those of reactions that occur in the process. Accurate modeling of thermodynamic properties requires availability of reliable experimental data.

The solubility of gases in liquids is a fundamental property for the design of gas absorption and stripping columns and gas-liquid and gas-liquid-solid reactors in the chemical industry.

Sulfolane is a physical solvent which is used in the processing of gases. It is a polar organic compound which has a strong affinity for the acid gases (H_2S and CO_2) which are present in many natural and refinery gas streams. Unlike other physical solvents such as methanol, sulfolane is rarely used alone but rather in admixture with a chemical solvent such as an alkanolamine solution. The use of mixed solvents is an attractive alternative to either chemical or physical solvents alone. In some respects the process is similar to a chemical process, but the presence of the physical solvent enhances the capacity of the solution for acid gases, especially when the gas stream to be treated is at elevated pressure and the acid gases are present in high concentrations (Jou et al., 1990). Sulfolane which's known as tetramethylene sulfone (TMS) has high physical absorption capacity for acid gases, hence used in physical and hybrid solvent processes.(Angaji et al., 2013). The aqueous mixture of (MDEA + TMS) is used in the Shell Sulfinol process since its gas loading capacity is high for the simultaneous absorption of acid gases.(Xu et al., 1993).

In this study Sulfolane has been chosen as one of the solvents of the hybrid solvent system. The mixing of the chemical solvent MDEA and the physical solvent Sulfolane is expected to increase the Kinetic reaction rate, the acid gas loading capacity, and selectivity than the pure solvent. The main objectives of this research can be summarized as follows:

1- To obtain new experimental kinetics data for CO_2 absorption into aqueous solutions of aqueous PZ, aqueous MDEA, aqueous blended(MDEA-PZ),aqueous blended (PZ-Sulfolane), and blended(MEA-Sulfolane).

2- To develop comprehensive reaction rate/kinetics models for CO_2 absorption into aqueous solutions of blended (MDEA+PZ), blended (PZ+ Sulfolane), and blended (MDEA-Sulfolane) that take into account the coupling between the chemical equilibrium, and chemical kinetics of all possible chemical reactions**.**

3- To establish the predictive correlation for calculating the reaction order constant that governs the (CO_2-MDEA-PZ), (CO_2-PZ-Sulfolane) , and (CO_2-MDEA-Sulfolane) reactions.

4- To determine a consistent thermodynamic model which can describe the acid gas-alkanolamine mixtures over extensive pressure, temperature and amine concentration range.

5- To experimentally investigate the effect of temperature and pressure on the solubility of CO_2, and the effect of increasing sulfolane, and amine concentrations as a physical and chemical solvent, respectively, on the solubility of CO_2 in the mixed solvents.

This study is divided into five chapters.

After a general introduction about the acid gas removal processes, the thesis is organized as follows:

Chapter one summarizes the most common technologies used in natural acid gas removal processes. Reaction kinetics of acid gas absorption into reactive amine solutions, kinetic apparatuses and procedures that have been used are presented in Chapter two. Chapter Three provides a general literature review of the thermodynamic published models, and our case appropriate model.

All the experimental apparatuses procedures that have been used throughout this research, and the results and discussions, are presented in Chapter four, and five.

Finally, the thesis includes overall conclusions and recommendations for future research.

Chapter I

Comprehensive Review Of Different Processes Available and Suitable for Removal of Acid Gas From Natural Gas

Chapter I: Comprehensive Review of Different Processes Available and Suitable for Removal of Acid Gas from Natural Gas

Introduction:

Like other non-renewable fossil fuels, natural gas is essentially formed from the decomposition of living matters such as plants, animals and micro-organisms that lived over millions of years ago and became an inanimate mixture of gases. Although there are various theories about the origin of fossil fuels, the most widely accepted theory states that fossil fuels are usually formed when organic matters are decayed and compressed under the earth's crust at high pressure and for a very long time. This kind of formation is technically referred to as thermogenic methane. This type of natural gas is formed by the decomposition process of the piled and compressed organic matters that are covered in mud, sediment and debris at high temperature beneath the crust of the earth. In another way, natural gas can also be formed by the action of tiny methane-producing microorganisms and it is technically termed as biogenic methane. In this case, methane formation usually takes place close to the earth's surface and the methane produced is usually dissipated into the atmosphere. However, in some cases, this methane can be trapped underground and recovered as natural gas. As a third theory, natural gas is formed by abiogenic processes where this process takes place at extremely underneath the earth's crust, where hydrogen-rich gases and carbon molecules are dominant. These gases may interact with minerals found in the underground in the absence of oxygen by the time the gases gradually rise towards the surface of the earth. In such processes reaction will take place and forms gaseous compounds such as nitrogen, carbon dioxide, oxygen, water and inert gases like argon. Hence, the condition will form methane deposits at very high pressure, similar to that of the thermogenic methane (NaturalGas.org, 2010). The natural gas processed at the wells will have different range of composition depending on type, depth, and location of the underground reservoirs of porous sedimentary deposit and the geology of the area. Most often, oil and natural gas are found together in a reservoir. When the natural gas is produced from oil wells, it is categorized as associated with (dissolved in) crude oil or non-associated.

Natural gas consists primarily of methane as the prevailing element but it also contains considerable amounts of light and heavier hydrocarbons as well as contaminating compounds of CO_2, Hg, He, H_2S and etc. Thus, the impurities must be removed to meet the pipe-line quality

standard specifications as a consumer fuel, enhance the calorific value of the natural gas, avoid pipelines and equipment corrosion and further overcome related process bottle necks.

I-1) Natural gas consumption statistics:

In consideration of the state of the art green technology requirements in promoting low-and zero-emission through the wise use of natural resources for the available reserves, natural gas becomes one of the most attractive, fastest and the premium growing fuel of world primary energy consumption (Economides and Wood, 2009). According to the technical report that was released on June 2011 by the International Energy Outlook 2010, the global utilization of natural gas raises to 44% from the reference year 2007 (108 trillion cubic feet) to the predicted year of 2035 (156 trillion cubic feet). In 2008, the need for natural gas was lowered due to the global economic recession that affects the global fuel markets, and in the following year, the worldwide natural gas utilization was reduced approximately by 1.1% (Energy Information and Administration, 2011). Nevertheless, the worldwide need for natural gas has revived as the global economies starts to make progress from the economic recession. Accordingly, the spending of natural gas rise on average by 1.8 percent per annum as of the year 2007 to the predicted year of 2020. However, far from the predicted year 2020 to 2035, the increase in natural gas utilization of natural gas is estimated to slow down to 0.9 percent per annum on average, due to the high prices on the natural gas product and its resources that will be introduced to the worldwide sell. Natural gas, also called “the prince of hydrocarbons” as it has many applications. The proportion of the natural gas consumed for energy production in major fields including industrial, commercial, residential, transportation and in generating electricity for the year 2009 is shown on Figure I.1.

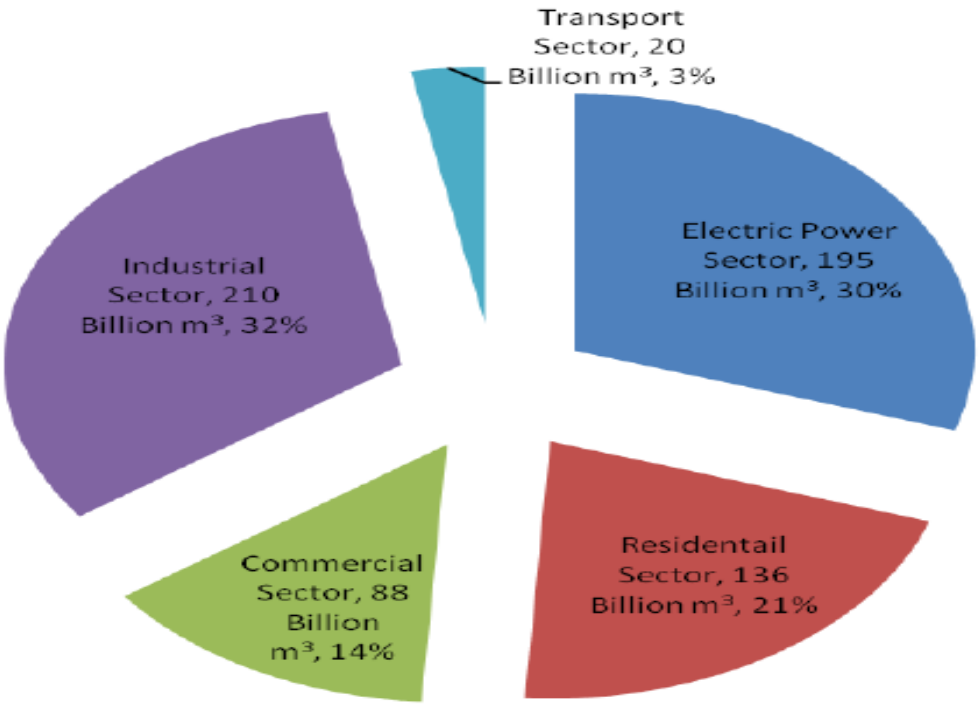

FigureI.1. Natural gas consumption statistics by different sectors (Energy Information and Administration 2011)

Again, according to the International Energy Outlook 2010 on its June 2011 release, natural gas was reported to be one of the main energy sources for industrial and electrical power generation applications. From the total worldwide natural gas consumption statistics for the year 2007, the industrial field shared almost 40 percent and it is predicted to maintain that share through 2035. In applications for electric power field, natural gas is usually preferred for new power plants. Moreover, when combusting natural gas, it usually emits less CO_2 than does other fuels such as petroleum or coal so it is expected that the use of natural gas will be encouraged by government decision and policy makers to at least reduce the impact of GHG (Energy Information and Administration 2011).

I.2) Acid gas removal technologies for natural gas purification:

As one of the major contaminates in natural gas feeds, carbon dioxide must optimally be removed as it reduces the energy content of the gas and affect the selling price of the natural gas. Moreover, it becomes acidic and corrosive in the presence of water that has a potential to damage the pipeline and the equipment system. The removal of CO2from the natural gas through

the purification processes is vital for an improvement in the quality of the product (Dortmundt and Doshi, 1999). The processes that are used to remove acid gas are broad and the existing technologies are many that effective selection of process becomes a critical concern. This is because each of the processes has their own advantages and limitations relatives to others. Although common decisions in selecting an acid gas removal process can generally be simplified, factors such as nature and amount of contaminants in the feed gas, the amount of every contaminants present in feed gas and the targeted removal capacity, amount of hydrocarbon in the gas, pipeline specification, capital and operating cost, amount of gas to be processed, desired selectivity, and conditions at which the feed gas is available for processing are the major factors that should also be considered (Dortmundt and Doshi,1999).

I.3) Absorption process:

Absorption process is one of the most important unit operations in natural gas purification process where a component of a gaseous phase is contacted with a liquid in which it is preferentially soluble. Absorption is usually carried out in a countercurrent tower (column), through which liquid descends and gas ascends. As per the needed surface area for gas-liquid contact, the absorption tower may be fitted with required trays, filled with packing, or fitted with sprays or other internals. As overall selection criteria, the characteristics of a good solvent for absorption process fulfils the following main features: high gas solubility, high solvent selectivity, high volatility, low effects on product and environment, high chemical stability, low cost and more availability, non-corrosive, low viscosity, non-flammable and low freezing point. At equilibrium conditions, solubility of gases is referred as the quantity of gas dissolved in a given quantity of solvent. Further at equilibrium, the partial pressure (fugacity) of a component in the gas is equal to the fugacity of the same component in the liquid. This defines the equilibrium thermodynamic criterion for the relation of the concentration of a component in the gas and its corresponding concentration in the liquid (Meyers, 2001).

The important fundamental principles for physical absorption are solubility and mass transfer; the principles of reaction equilibria and reaction kinetics are for chemical absorption. When the gas (as a solute) is absorbed into a solution containing a reagent that reacts chemically with it,

the amount of absorption (concentration profile) becomes dependent on the reaction kinetics and the concentration of the reacting reagent in the liquid (Meyers, 2001).

The reverse process (which is also termed as stripping process, desorption, or regeneration), is employed when it is needed to remove the absorbed gases from the solvent for the purpose of recovery of the gas or the solvent or both. In the process of absorption, the selective solvent (absorbent) in a plate of packed column is contracted counter-currently with the gas to be processed (absorbate). As applied to gas purification process and based on the nature of interaction of absorbent and absorbate, absorption process is generally divided into physical and chemical absorption. In physical absorption, the desired gas component being absorbed (absorbate) is more soluble in the liquid solvent (absorbent) than other components in the gas phase but does not react chemically with the absorbent. Whereas in chemical absorption, the absorbate react chemically with the absorbent or a component within the absorbent. When the absorbent reaches its equilibrium level, regeneration step will take place by reducing the partial pressure in the gas phase and by thermal or chemical gradient for the case of physical and chemical absorption respectively (Kohl and Nielsen, 1997; Scott, 1998).

I.4) Physical absorption:

I.4.1) Basic separation principles for physical absorption process:

Physical absorption processes are the type of absorption processes where the solvent interacts only physically with the dissolved gas. In this process, the solvent is used as an absorbent with thermodynamic properties such that the relative absorption of acid gas is more favored over the other components of the gas mixture. Mostly, physical solvent systems are used when the feed gas is characterized by high CO_2 partial pressure and low temperatures. Although heavy hydrocarbon restricts the wide use of physical solvent, its absorption capacity can be higher than chemical solvents. In addition, low CO_2 partial pressures as well as low outlet pressure of the product stream may also discourage the application of physical solvents (Ebenezer and Gudmunsson, 2005).

Removal of acid gas from the feed gas by physical solvent absorption is based on the solubility of acid gas within the solvents. The partial pressure and the temperature of the feed gas are the

two major factors that determine the solubility of the acid gas. In physical absorption, the interaction between CO_2 and the absorbent is weak relative to chemical solvents, decreasing the energy requirement for regeneration. Regeneration of solvents is assisted by either heating, pressure reduction or a combination of both. Mostly, physical solvent scrubbing of CO_2 is well established. Selexol, a liquid glycol-based solvent, has been used for decades to process natural gas, both for bulk CO_2 removal and H_2S removal (Davison, Freund et al., 2001). Glycol is effective for capturing both CO_2 and H_2S at higher concentration. However, the CO_2 is released at near atmospheric pressure, requiring recompression for transportation and geologic storage. The Rectisol process, based on low temperature methanol, is another physical solvent process that has been used for removing CO_2. Glycerol carbonate is interesting because of its high selectivity for CO_2, but it has a relatively low capacity (Kovvali and Sirkar, 2002).

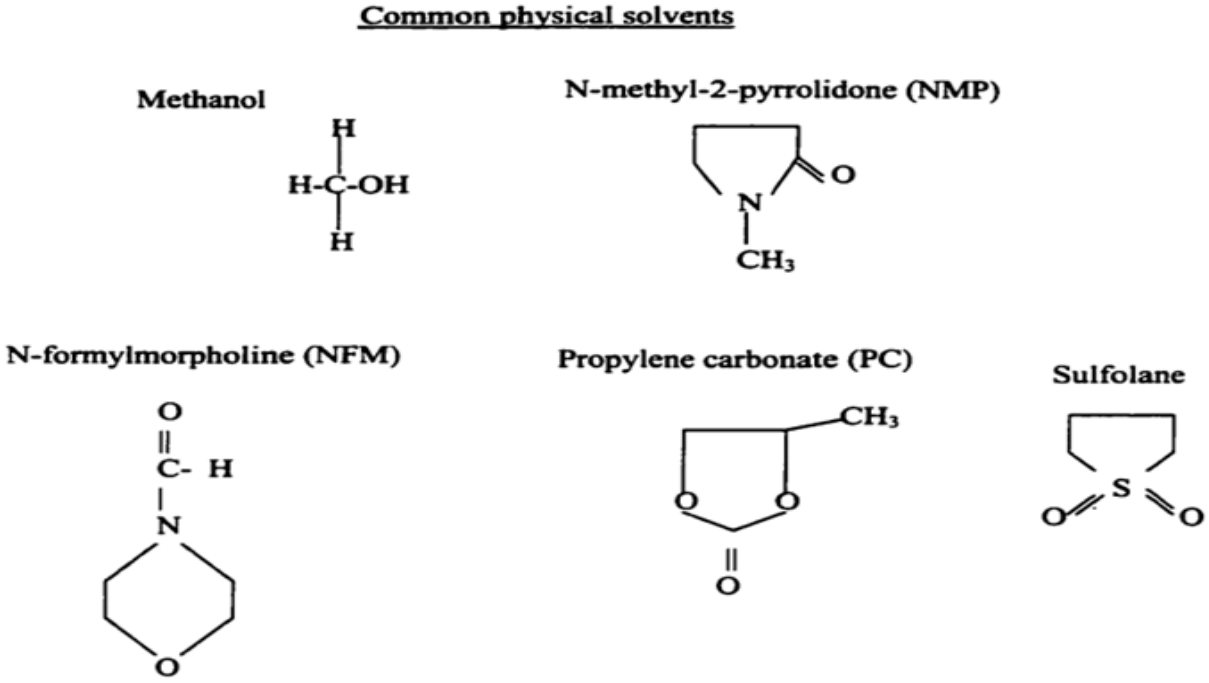

Figure I.2. Common physical solvents (Henni, 2002)

I.5) Chemical absorption:

I.5.1) Basic separation principles for chemical absorption process:

In natural gas purification plant, chemical absorption processes are used to remove acid gases such as CO_2 in the gas stream by the action of exothermic reaction of the solvent with the gases.

Many alkanolamines are most widely used as the chemical solvent gas treating process for acid gas removal in the natural gas and petroleum processing industries. These processes use a solvent, either an alkanolamine or an alkali-salt (hot potassium carbonate processes) in an aqueous solution.

The common amine based solvents used for the absorption process are mono-ethanolamine (MEA), di-ethanolamine (DEA) and methyldiethanolamine (MDEA) that reacts with the acid gas to form a complex or bond. H_2S, CO_2 and SO_2 are termed as acid gases since they dissociate to form weak acidic solution when they come into contact with water or an aqueous medium. These amines are known as weak organic bases. The basicity is provided by the amine function, and it provides reactivity to remove the acid gases. The hydroxyl groups serve to increase the solubility of amine in water. This effect reduces the vapor pressure of the amines so that less is lost out the top of the absorber or stripper (Glasscock, 1990).

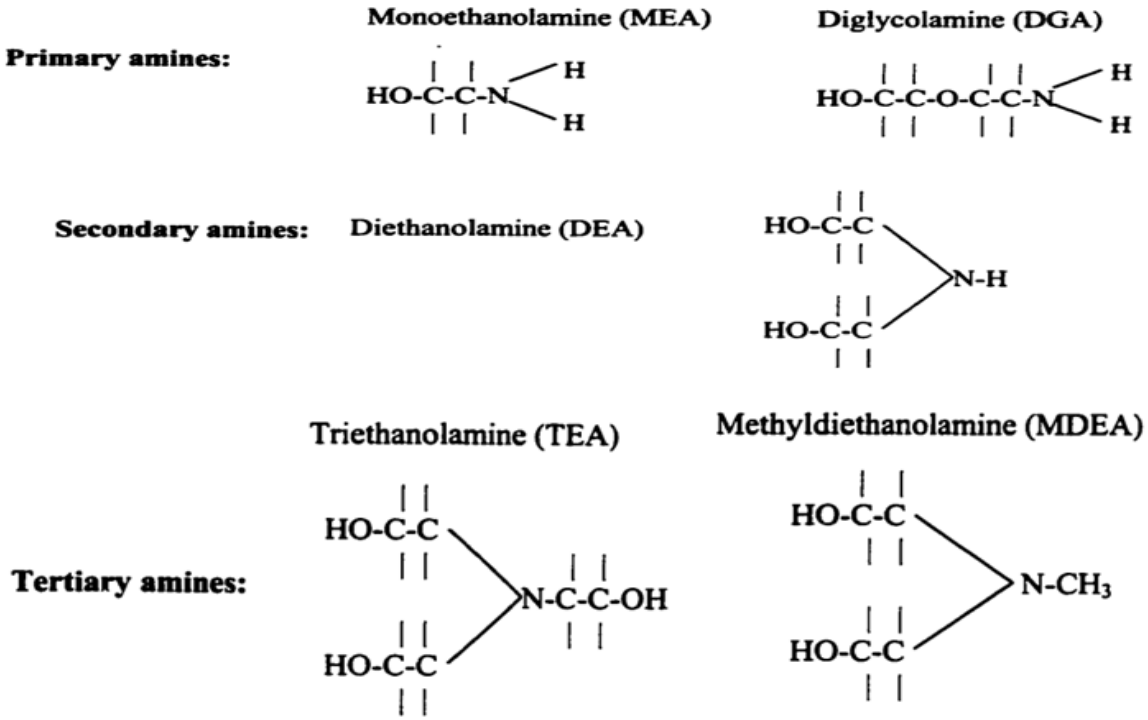

Figure I-3. Common Chemical solvents (Alkanolamines), (Henni, 2002)

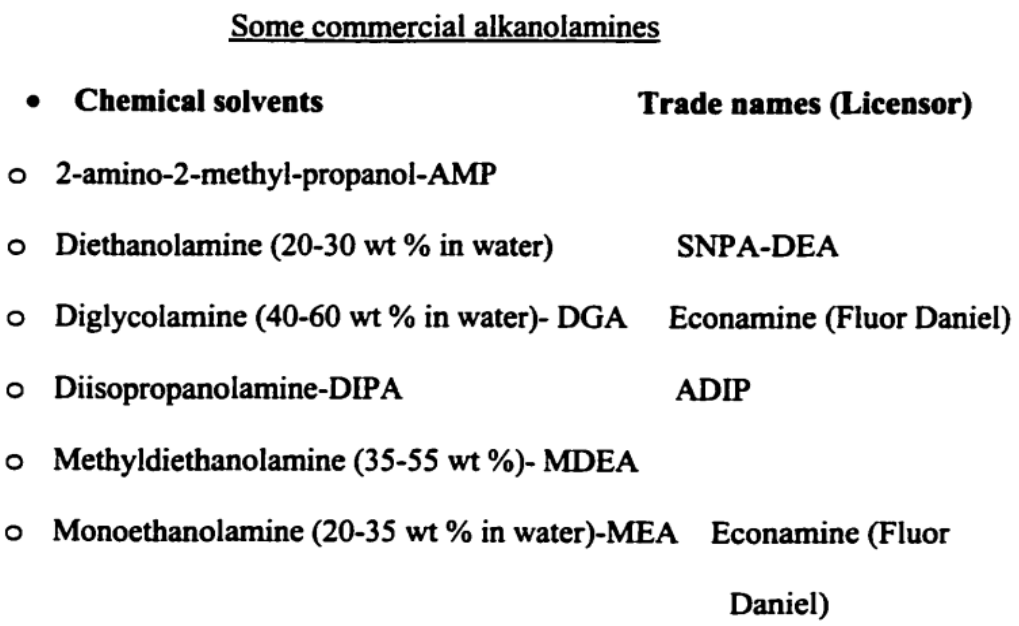

Figure I.4. Commercial Alkanolamines (Henni, 2002).

A simplified schematic representation for the flow of a typical gas treating operation using amine solvents are shown in Figure I.5.

In the typical process, a sour gas is introduced to absorber from its bottom at high-pressure and goes to rise up and counter currently contacts an aqueous alkanolamine solution that is routed to the top of the absorber. The resulting amine solution that contains high CO_2 is then transported to the heat exchangers to raise its temperature. Then, it is directed to the top of a regenerator (stripper) to counter-currently contact steam at high temperature and low pressure. Afterwards, the steam strips the CO_2 and H_2S from solution and the lean alkanolamine solution is routed through the heat exchanger, where it is cooled, and reintroduced at the top of absorber.

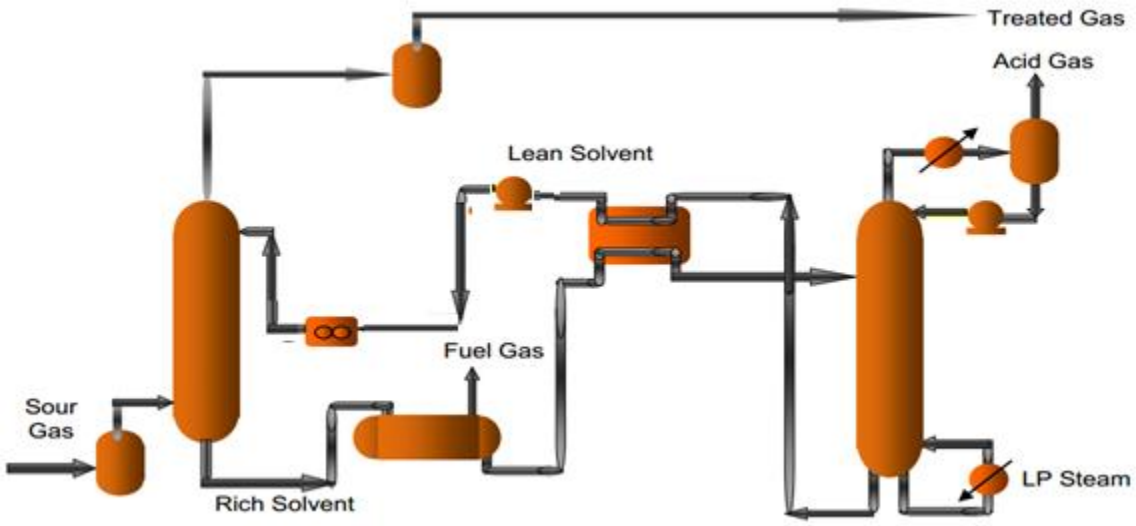

Figure I.5. Simplified schematic representation for the flow of a typical gas treating operation using amine solvents.

As the process proceeds, the complex or bond is subsequently reversed in the regenerator at elevated temperatures and reduced acid gas partial pressures releasing the acid gas and regenerating the solvent for reuse. These are well suited for low pressure applications where the acid gas partial pressures are low and low levels of acid gas are desired in the residue gas since their acid gas removal capacity is relatively high and insensitive to acid gas partial pressures as compared to physical solvents (Kohl and Nielsen, 1997).

In most oil refineries sector, since stripped gas is mostly H2S, much of which often comes from hydro-desulfurization (sulfur-removing process). The clause process is then used to convert the H_2S-rich stripped gas to elemental sulfur. In some plants, it is common to share a common regenerator unit for more than one amine absorber unit (Kohl and Nielsen, 1997).

Recently, 2-amino-2-methyl-1-propanol (AMP) as another group of alkanolamines which called sterically hindered amines (SHAs), has received great deal of focus as it needs less energy for their regeneration. A hindered amine was originally defined by (Sartori and Savage, 1983) as an amine belonging to one of the following categories: **(1)** a primary amine in which the amino group is attached to a tertiary carbon; **(2)** a secondary amine in which the amino group is attached to at least one secondary or tertiary carbon.

It offers absorption capacity, absorption rate, selectivity, and degradation resistance advantages over conventional amines for CO_2 removal from gases (Sartori and Savage, 1983; Say et al, 1984; Goldstein et al., 1984).

Moreover, blending of alkanolamines has also been researched as to obtain their potential synergy than the individual favorable features, e.g. high absorption capability coupled with thermal energy demand for regeneration (Rodriguez, Mello et al., 2011). Generally, the chemical solvent processes are characterized by a relatively high heat of acid gas absorption and require a substantial amount of heat for regeneration. Combining the absorption characteristics of each amine, blended amines have been suggested for the absorption of acid gases.(Chakravarty et al., 1985) .

Blended amine solvents, which consist of a mixture of primary or secondary amine with a sterically hindered or tertiary amine, combine the higher CO_2 reaction rates of the primary or secondary amine with the higher CO_2 loading capacity of the sterically hindered or tertiary amine.(Chakravarty et al.,1985). The concept of using amine mixtures is based on utilizing and combining the advantages of the amines in the mixture, or of customizing the amine solution to a particular use. Aqueous blends of primary or secondary amines with tertiary amines are very attractive for bulk CO_2 removal, as these blends combine the higher reaction rates between CO_2 and primary or secondary amines with the easier regeneration and higher absorption capacities of tertiary amines.

Table I.1. Comparison of the major acid gas absorption processes (Ritter and Ebner, 2007)

	Chemical absorption		**Physical Solvent Absorption**
	Alkanol amine	**Inorganic Carbonate**	
Type of absorbents	MEA,DEA,DGA,MDEA, DIPA	K_2CO_3, (K_2CO_3-MEA), (K_2CO_3-DEA)	Selexol, Rectisol, Purisol
CO_2 absorption mechanism	Chemical reaction CO_2: $2RNH_2+CO_2+H_2O\leftrightarrow(RNH_3)_2CO_3$ $(RNH_3)_2CO_3+CO_2+H_2O\leftrightarrow2RNH_3+HCO_3$	Chemical reaction CO_2: $Na_2CO_3+CO_2+H_2O\leftrightarrow2NaHCO_3$	Physical dissolution
Operating gauge pressure, mmHg	Insensitive to pressure	> 10,337.76	12,922.2-51,688
Operating Temp, ^oC	37.78-204.44	93.33-121.11	Ambient temperature
Absorbent Recovery	Reboiled stripper	Stripper	Flash, reboiler, or steam stripper
Swing variables (Temp. or Pressure)	Temperature principally	Both, but pressure principally	Pressure principally
Selectivity CO_2 vs. H_2S	Only MDEA selective for H_2S	May be selective for H2S	Some selectivity for H_2S
Meets ppmv CO_2	Yes	Yes	Yes
Utility Cost	High	Medium	Low to medium

I.5.2) Limitation and challenges: The solvent used in absorption process such as amines and Benfield solution causes corrosion of the units (Polasek and Bullin, 1984). When the solvent react with some corrosion inhibitors, it will cause erosion of the unit, high tendency for foaming and solid suspension thus reduce CO_2 solvent loading and require injection of antifoaming agents to reduce the surface tension of the solvent and to ensure better contact between the solvent and the CO_2, the regenerated solution leaving the stripper is at its saturated temperature and partially vaporize in the pump suction, resulting in vibration and excessive wear of the pump impellers. Moreover, since all of the solvents cannot be recycled back to the absorber column, the disposal

of the solvents causes environmental hazards and thus showed the common disadvantages of using the absorption process (Bord, Cretier et al. 2004; Ebenezer and Gudmunsson, 2006).

I.6) Adsorption process:

I.6.1) Basic separation principles for adsorption process :

In gas separation application, the process of adsorption is described as the adhesion or retention of selective components of feed gas stream brought into contact to the surface of certain solid adsorbent as the result of the force of field at the surface. As the surface of an adsorbing material may exhibit different affinities for the various components of a fluid, it offers a straightforward means of purification (removal of undesirable components from a fluid mixture) as well as a potentially useful method of bulk separation (separation of a mixture into two or more streams of enhanced value). Although adsorption process is rarely applied for bulk separation of CO_2 from CH_4, there are kinetics-based adsorption processes that have been implemented in USA for the recovery of methane from landfill gas. These gases mainly comprises of methane (50-65%), carbon dioxide (35-50%), a trace amount of nitrogen and sulfur compounds. In this process, carbon molecular sieve is used as the adsorbent. In use of this process, it can be possible to recover more than 90% methane with 87-89% purity (Yang, 1997). One of the successful applications for bulk separation of CO_2 from CH4 is performed by using Engelhard molecular gate, a commercial brand name adsorbent developed by Engelhard Corporation. The first application of molecular gate CO_2 removal system is at the Tidelands Oil Production Company operated facility in Long Beach, California. The feed source for this unit is hydrocarbon rich associated gas from enhanced oil recovery section. The feed more typically operates at 30- 40% of CO_2 and the adsorbent able to reduce CO_2 level less than 2% (Ritter and Ebner, 2007).

Depending on the nature and strength of the surface forces, adsorptive gas separation process can be divided into two types: physical adsorption and chemisorption.

Chemisorption can be considered as the formation of a chemical bond between the sorbate and the solid surface (covalent interaction of CO_2 and the surface of the adsorbent) that gives scope for much larger increases in adsorption capacity. Such interactions are strong, highly specific, and often not easily reversible. Chemisorption systems are sometimes used for removing trace

concentrations of contaminants, but the difficulty of regeneration makes such systems unsuitable for most process applications (Meyers, 2001).

In most operations, adsorption processes depend on physical adsorption. The forces of physical adsorption are weaker (a combination of Van der Waals forces and electrostatic forces) than the forces of chemisorption so the heats of physical adsorption are lower and the adsorbent is more easily regenerated as no covalent bonds are formed and heat is released upon adsorption. During capture, the chemical potential of the adsorbed CO_2 is lower than the chemical potential of CO_2 in the gas mixture. Several different types of force are involved. For nonpolar systems the major contribution is generally from dispersion repulsion (van der Waals) forces, which are a fundamental property of all matter. When the surface is polar, depending on the nature of the sorbate molecule, there may also be important contributions from polarization, dipole, and quadrupole interactions. Selective adsorption of a polar species such as water or a quadrupolar species such as CO_2 from a mixture with other nonpolar species can therefore be accomplished by using a polar adsorbent. Indeed, adjustment of surface polarity is one of the main ways of tailoring adsorbent selectivity (Meyers, 2001).

Physical adsorption at a surface is so fast, and the kinetics of physical adsorption are usually controlled by mass or heat transfer rather than by the intrinsic rate of the surface process (Meyers, 2001). Most of the separation processes is based upon equilibrium mechanism and the separation is accomplished by the adsorption equilibrium capacity difference of the adsorbent among the adsorbate.

The main advantage of physical adsorption methods is its low energy requirement for the regeneration of the sorbent material with short period of time associated with the change in pressure. The widely used adsorption processes includes the metal oxide (metal organic frame works), molecular sieves (zeolites, activated carbon) and promoted hydrotalcites based processes. Zeolite systems can produce nearly pure streams of CO_2, but have high energy expenses due to vacuum pumps and dehumidification equipment. As most effective adsorbent, the use of hydrotalcites at high temperatures (177-327°C) is widely for adsorption of CO_2 in or near combustion or gasification chambers. However, more study is still required to decrease the

pressure difference requirement and enhance the capacity of current adsorbents (Hermann, Bosshar et al., 2005).

Commercial adsorbents that show ultra-porosity have been used for the selective separation of gases, and included activated carbons, charcoal, activated clays, silica gel, activated alumina, and crystalline aluminosilicate zeolites.

The major advantages of using adsorption processes are simplicity of operation, the relative capability of the molecular sieve beds to withstand mechanical degradation and the possibility of simultaneous dehydration of gases and acid removal. Once saturation of the adsorbent is reached, regeneration is carried out by either applying heat or by lowering pressure (concentration).Based on regeneration methods, adsorption process is most commonly divided into temperature swing adsorption (TSA), pressure swing adsorption (PSA) and displacement desorption.

TableI.2. Typical loading capacities of some commercial adsorbents towards acid gases with their corresponding regeneration methods

Adsorbent	Adsorbate	T (^oC)	P (mmHg)	Loading (mol/kg)	Regeneration Method
Activated Carbon	CO_2	25-300	500	1.5-2.0 at 25^oC 0.1-0.2 at 300^oC	PSA
5A zeolite	CO_2	25-250	500	~ 3.0 at 25^oC 0.2 at 250^oC	PSA
Titanosilicates	CO_2	25-200	760 - 6x10^5	-	PSA
HTlc (K-promoted)	CO_2	300-400	200-700	0.4-0.7	PSA
Solid amine (supported PEI)	CO_2	75	760	1.5 - 3.0	PSA
Double-layer hydroxides	CO_2	375	230	1.5	PSA
Alumina (un-doped)	CO_2	400	500	0.06	PSA
Alumina (doped w/Li2O)	CO_2	400	500	0.52	PSA
alumina(basic)	CO_2	300	500	0.3	PSA
Li zirconate	CO_2	500	760	3.4-4.5	TSA
CaO	CO_2	500	150	4-8 at 500^oC 7 at 500^oC	TSA

I.6.2) Thermal swing adsorption:

The use of cyclic thermal swing processes (TSA) is widely applicable for the purification operations such as removal of $CO_2$from natural gas or drying. In TSA, desorption is achieved by increasing the temperature of the adsorption bed by applying heat to the bed or more commonly by purging with a hot purge gas. At higher temperatures the adsorption equilibrium constant is reduced so that even quite strongly adsorbed species can be removed with a comparatively small purge gas volume. TSA is generally used for purification of the process such as drying or removal of CO2 from natural gas (Meyers, 2001). Thermal swing adsorption is very reliable to remove minor component. The limitation in thermal swing adsorption process is the adsorption cycle time that is required to cool down the bed. Other obstacles are the high energy requirements and large heat loss (Mersmann, Kind et al., 2011).

I.6.3) Pressure swing adsorption:

Pressure swing adsorption (PSA) is one of the most known industrial processes for gas separation. PSA is well known a technology for the removal of CO_2 from gaseous streams containing methane In such process, the removal of CO_2 from natural gas streams by adsorption processes are based on materials with selective adsorption to CO_2 by different equilibrium capacities or by differences in uptake rates (Cavenati, Carlos et al., 2006). In PSA, regeneration is carried out by lowering the operating partial pressure to desorb the adsorbate (Kerry, 2007). This can be obtained either by depressurization or by evacuation or by both. PSA is more suitable for bulk separation. Moreover, PSA is also used for drying of air and industrial gases. Air pre-purification (purification of air prior to cryogenic distillation by removal of CO_2, water, and hydrocarbons) is also at developing stage for PSA (Yang and Wiley, 2003). As the most important decision in any adsorption-based technology is the adsorbent selection, zeolites as microporous materials that adsorb CO_2 strongly, are mostly used in PSA processes. Zeolites have good records for separation of CO_2 than activated carbons in the PSA (Cavenati, Carlos et al., 2006)**.** The major advantages of PSA system are low capital and maintenance costs, high purity product, rapid shutdown and start-up characteristics, lack of corrosions problems, absence of heat requirement and pipe insulation and comparative straight forward operation.

I.6.4) Displacement desorption:

Displacement desorption, is similar to purge gas stripping as the temperature and pressure are maintained constant, but instead of an inert purge, an adsorbable species is used to displace the adsorbed component from the bed similar to displacement chromatography. Displacement desorption is usually used when desorption by pressure swing or thermal swing fails to be practical. Steam stripping process can be considered as a combination of thermal swing and displacement desorption as it is mostly used in the regeneration of solvent recovery system using an activated carbon adsorbent. In a typical displacement desorption, the displacing component should be adsorbed somewhat less strongly than the preferentially adsorbed species so that the adsorption desorption equilibrium can be shifted by varying the concentration of the desorbent. Such processes run more or less isothermally and offer a useful alternative to thermal swing processes for strongly adsorbed species when thermal swing would require temperatures high enough to cause cracking, coking, or rapid aging of the adsorbent (Meyers, 2001).

I.6.4) Limitation and challenges:

As compared to other methods, for adsorption to be economical, ideal adsorbents should have high transfer rates, high regenerability and high capacity that allow for thermal swing adsorption (TSA) or low pressure swing adsorption (PSA). At the adsorption equilibria, the loading usually decreases with increasing temperature for a given partial pressure or concentration of the adsorptive in the fluid. In an isothermal system, the loading decreases with decreasing partial pressure or concentration. A further regeneration process is based on the replacement of the adsorbate by another adsorptive with a greater affinity to the adsorbent (Mersmann, Kind et al.,

2011).

Table I.3. Advantages and limitations of the regeneration method (Meyers, 2001)

Adsorbent	Adsorbate	T (^oC)	P (mmHg)	Loading (mol/kg)	Regeneration Method
Activated Carbon	CO_2	25-300	500	1.5-2.0 at 25^oC 0.1-0.2 at 300^oC	PSA
5A zeolite	CO_2	25-250	500	~ 3.0 at 25^oC 0.2 at 250^oC	PSA
Titanosilicates	CO_2	25-200	760 - $6x10^5$	-	PSA
HTlc (K-promoted)	CO_2	300-400	200-700	0.4-0.7	PSA
Solid amine (supported PEI)	CO_2	75	760	1.5 - 3.0	PSA
Double-layer hydroxides	CO_2	375	230	1.5	PSA
Alumina (un-doped)	CO_2	400	500	0.06	PSA
Alumina (doped w/Li2O)	CO_2	400	500	0.52	PSA
alumina(basic)	CO_2	300	500	0.3	PSA
Li zirconate	CO_2	500	760	3.4-4.5	TSA
CaO	CO_2	500	150	4-8 at 500^oC 7 at 500^oC	TSA

I.7) Cryogenic process:

I.7.1) Basic separation principle for cryogenic process:

Cryogenic separation (also known as low temperature distillation) uses a very low temperature (-73.30 ^oC) for purifying gas mixtures in the separation process (Ebenezer and Gudmunsson, 2005).

The major industrial application of low-temperature processes involves the separation and purification of gases. Much of the commercial oxygen and nitrogen, and all the neon, argon, krypton, and xenon, are obtained by the distillation of liquid air (Meyers, 2001). Commercial helium is separated from helium-bearing natural gas by a well-established low temperature process. Cryogenics has also been used commercially to separate hydrogen from various sources of impure hydrogen (Meyers, 2001).

The cryogenic method is better at extraction of the lighter liquids, such as ethane, than is the alternative absorption method. Essentially, cryogenic processing consists of lowering the temperature of the gas stream to around (-84.44 ^{o}C). While there are several ways to perform this function the turbo expander process is most effective, using external refrigerants to chill the gas stream. The quick drop in temperature that the expander is capable of producing condenses the hydrocarbons in the gas stream, but maintains methane in its gaseous form (Tobin J., Shambaugh P. et al., 2006). While cryogenic separation is used commercially to liquefy and purify CO_2 from streams that have high CO_2 concentrations (typically greater than (50-70 percent), it has not been applied to large scale CO_2capture from flue gas due to the low concentration of CO_2 that makes the application of this technique not economical. Cryogenic separation can separate CO_2 from other gases using pressure and temperature control resulting in solid or liquid CO_2 particulate matter and other contaminants are also removed in the process. Cryogenics use condensation of gases as the main principle. When CO_2 is cooled below its boiling point, it begins to condense and separate and turns into a liquid state. Differences in boiling points cause the gases to separate because each gas will turn to a liquid at a different point, but separation into pure components can also be influenced by the composition of the gas being cooled (Tobin , Shambaugh et al., 2006). The advantages of this process are the suitability to liquefy and purify the feed gas with high concentration of CO_2 and for producing a liquid CO_2 ready for transportation by pipeline and does not require compression since there is no additional chemicals used.

I.7.2) Limitation and challenges :

The main disadvantage of cryogenic separation is that the process is highly energy intensive for regeneration and can significantly decrease the overall plant efficiency when applied to streams with low CO_2 concentration. Moreover, tendency for blockage of process equipment is high and some cryogenic fluids are flammable and toxic such as (acetylene, ethane) (Ebenezer and Gudmunsson, 2005).

I.8) Membrane process :

I.8.1) Basic principle of membrane process:

In essence, gas separation membranes are thin films that selectively transport gases through the membrane based on differences in permeabilities of the species flowing through the membrane. The permeability of gases in a membrane is related as a function of membrane properties (physical and chemical structure), the nature of the permeant species (size, shape, and polarity), and the interaction between membrane and permeant species (Stern 1994; Burggraaf 1996; Shekhawat, Luebke et al., 2003). The membrane properties and the nature of the permeant species determine the diffusional characteristics of a penetrant gas through a given membrane. The interaction between membrane and permeant, refers to the sorptivity or solubility of the gas in the membrane. The permeability coefficient (or permeability) of a penetrant is the product of the solubility coefficient or the sorptivity (thermodynamic parameter) and the diffusion coefficient (kinetic parameter). The permeability coefficient denotes the rate at which a penetrant crosses a membrane. The solubility (sorptivity coefficient) is a measurement of the amount of gas sorbed by the membrane when equilibrated with a given pressure of gas at a given temperature. The diffusion coefficient indicates how fast a penetrant is transported through the membrane in the absence of obstructive sorption. The selectivity of the membrane to specific gas or liquid molecules is subject to the ability of the molecules to diffuse through the membrane. The permselectivity or ideal separation factor is simply the ratio of the pure gas permeability of the gases being separated. Membranes utilized in separations need to possess both high selectivity and high permeation. The higher the permeability, the less membrane area is required for a given separation and therefore the lower the membrane cost. The higher the selectivity is the lower the losses of methane and therefore the higher the volume of the product that can be recovered (Porter 1990; Shekhawat, Luebke et al., 2003). Gas transport through porous membranes takes place through a number of mechanisms, such as molecular sieving, Knudsen diffusion, surface diffusion, capillary condensation and micropore diffusion. Brief descriptions of these mechanisms are provided as follows.

Molecular diffusion: In molecular diffusion, the mean free path of the gas molecules is smaller than the pore size and diffusion occurs primarily through molecule-molecule collisions. Here, the

driving force is the composition gradient. If a pressure gradient is applied in such pore regimes bulk (laminar) flow occurs, the transport is described by Poiseuille flow or viscous flow (De Lange, Keizeret al., 1995; Javaid, 2005).

Knudsen diffusion: This mode of transport is significant when the mean free path of the gas molecules is greater than the pore size. In such situations, the collisions of the molecules with the pore wall are more frequent than the collisions among molecules. Separation selectivities with this mechanism are proportional to the ratio of the inverse square root of the molecular weights (De Lange, Keizer et al., 1995; Javaid, 2005).

Surface diffusion: It takes place when the permeating species exhibit a strong affinity for the membrane surface and adsorb along the pore walls. In this mechanism, separation occurs due to the differences in the amount of adsorption of the permeating species. Surface diffusion often occurs in parallel with other transport mechanisms such as Knudsen diffusion (De Lange, Keizer et al., 1995; Javaid, 2005).

The activation energy for the diffusion is strongly correlated with the heat of adsorption. Since it is assumed that diffusion takes place by molecules which jump from one site to another, the activation energy is a fraction of heat adsorption (Gilliland, Baddour et al, 1974). This implies that: **a)** strongly adsorbed molecules**,** and **b)** the total flux will decrease as the temperature is increased since the increased diffusivity is overruled by the decrease in surface concentration (De Lange, Keizer et al., 1995).

Capillary condensation: It is one form of surface flow where one of the gases is a condensable gas. Typically in mesopores and small macropores, at certain critical relative pressures as determined by the Kelvin equation, the pore gets completely filled by the condensed gas. Due to the formation of menisci at both ends of the pore, transport can take place through hydrodynamic flow generated by capillary pressure difference between the two ends. This mechanism of gas transport can be considered as the limiting case adsorption process when the pressure is increased. Theoretically capillary condensation can be used to achieve very high selectivities, as the formation of the liquid layer of the condensable gas will block and prevent the flow of the non-condensable gas (Javaid, 2005).

Configurational or micropore diffusion: This type of diffusion may be considered as the limiting value of surface diffusion where the pore size becomes comparable to the molecular size. In this mechanism, diffusion is perceived as an "activated" process and separation is a strong function of molecular shape, molecular size, pore size, and the interactions between the pore wall and gas molecules. This type of mechanism is dominant in microporous inorganic membranes such as zeolite and carbon molecular sieves membranes (Javaid, 2005).

In another dimension, membranes can be coupled with a solvent to capture desired gases such as CO_2 and the process is known as membrane gas absorption. In such process, the CO_2 diffuses between the pores in the membrane and is then absorbed by the solvent. The membrane maintains the surface area between gas and liquid phases. This type of membrane is used when the CO_2 has a low partial pressure, such as in flue gases, because the driving force for gas separation is small. Although a range of configurations exists either simply as gas separation devices or incorporating liquid absorption stages, the process has not yet been applied on a large scale and there are challenges related to the composition and temperature of the feed gases

Currently, most researches are focussed on developing effective solvents and optimising the reaction time. The general advantages of the membranes process and mainly for the removal of CO_2 from natural gas includes: enhanced weight and space efficiency which make it more applicable for off shore environment, high adaptability to variation of CO_2 content in the feed gas and separation at low pressure and temperature, easy to combine with other separation process and use of other chemicals is not required, periodic removal and handling of spent solvent or adsorbent making the system more environmental friendly, relatively no moving parts make the process more flexible to operate, control and also easy to scale-up, low maintenance requirement, reduced energy consumption unless compression used, and low capital costs. However, it has some limitations as the separated CO_2 is at low pressure, it needs additional energy for compression of the feed gas to and meet pipeline pressure standard. Hence, economics remains a challenge while working towards pipeline specifications (Ebenezer and Gudmunsson, 2005).

I.8.2) Membrane selection for natural gas separation:

For more than two decades membranes have been known to constitute a mature technology that has been applied in natural gas processing. Currently membranes are used for CO_2 removal from natural gas at processing rates from million standard cubic feet per day (MMSCFD) to 250 MMSCFD. New units are also in design or construction stage to handle volumes up to 500 MMSCFD (Sridhar, Smitha et al., 2007). The important criteria for selecting membrane materials for gas separation are based on the following key factors **(a)** intrinsic membrane permselectivity **(b)** ability of the membrane material to resist swelling induced plasticization (chemical resistance, which is quite rare but mostly fulfilled by inorganic membranes) and **(c)** ability to process the membrane material into a useful asymmetric morphology with good mechanical strength under adverse thermal and feed mixture conditions. The polymer membrane material should have good interaction and sorption capacity preferably with one of the components of the mixture for an effective separation. Molecular structure, specific nature and arrangement of chemical groups attached to the main chain are also some of the important factors, which affect the membrane properties and hence, their performance. Molecular weight distribution and membrane polarity are other parameters of interest for the development of novel membranes in natural gas separation. In the field of removal of acid gases from natural gas, a feed stream constituting CH_4, CO_2 and H_2S must be dealt with an integration of three relevant areas such as material selection, membrane synthesis and system configuration. A clear choice of membrane materials not only render high permeability ratios, but also yield good permeabilities. The specific membrane chemistry is also equally important which depends upon the type of separation to be achieved. Therefore, membrane material selection is an area of high significance.

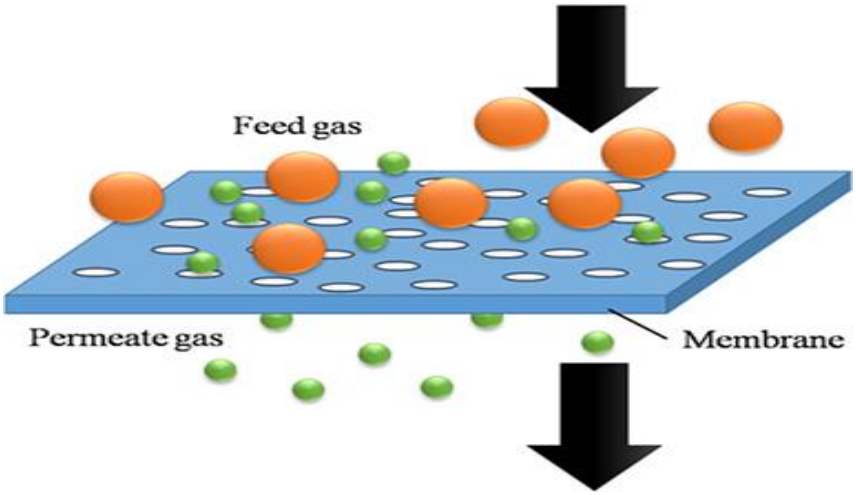

Figure I.6 . Membrane separation technology in CO_2 Capture

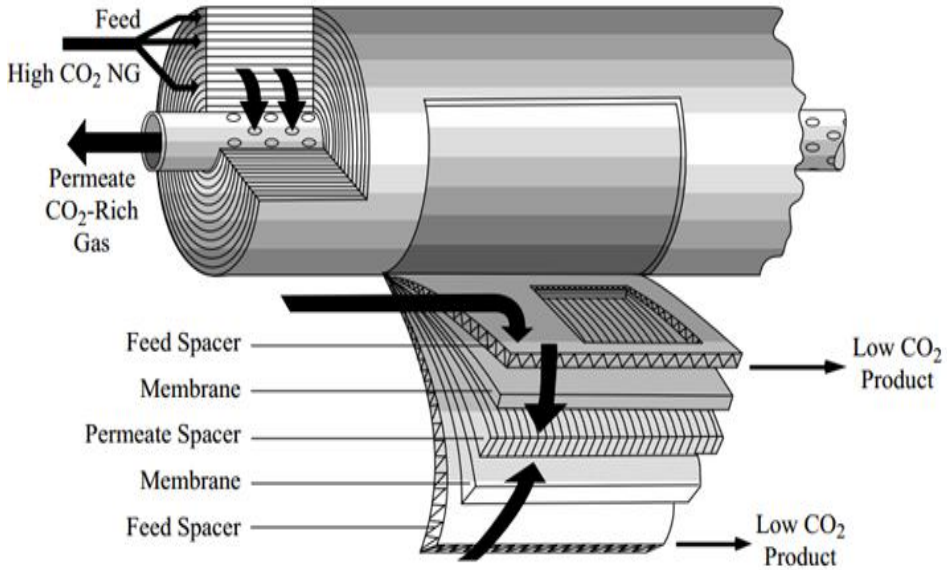

Figure I.7 . Acid gas removal using membrane

I.8.3) Polymeric membranes:

Polymeric membranes are most commercially used for the bulk separation of gases in many processes such as recovery of nitrogen from air, separation of oxygen-nitrogen mixture and hydrocarbons in petrochemical industries and also purification of natural gas. With regards to the separation of CO_2 from gas streams, primarily for natural gas sweetening; these membranes

selectively transmit CO_2 versus CH_4. The driving force for the separation is pressure gradient across the membrane. As such, compression is required for the feed gas in order to provide the driving force for permeation, and the separated CO_2 is at low pressure and it requires additional compression to meet pipeline pressure requirements (Pandey and Chauhan, 2001; Sridhar, Smitha et al., 2007; Bernardo, Drioli et al., 2009). The two types of polymeric membranes that are commercially available for gas separations are glassy and rubbery membranes. Glassy membranes are rigid and glass-like, and operate below their glass transition temperatures. On the other hand, rubbery membranes are flexible, soft and operate above their glass transition temperatures. Mostly, rubbery polymers show a high permeability, but a low selectivity, whereas glassy polymers exhibit a low permeability but a high selectivity. Glassy polymeric membranes dominate industrial membrane separations because of their high gas selectivities, along with good mechanical properties. Generally, polymeric membranes have been known for their excellent intrinsic transport properties, high processability and their low cost.

I.8.4) Inorganic membranes:

Inorganic membranes (also known as ceramic membranes) are used for gas separation due to their superior thermal, mechanical and chemical stability, good erosion resistance, insensitivity to bacterial action and a long operational life (Caro, Noack et al., 2000). Microporous and dense membranes are the two types of inorganic membranes that are suitable for high-temperature gas separation applications. Dense, nonporous inorganic membranes are made of polycrystalline ceramic material, in particular made of perovskites, palladium and its alloys, silver, nickel and stabilized solid electrolytes (zirconia). Mostly, they have been used or evaluated for separating gaseous components in laboratory work to characterize membrane properties. They are prepared as unsupported ones as well as thin films on porous supports. Application of dense membranes is primarily for highly selective separation of hydrogen (i.e.H_2 through Pd) and oxygen (i.e.O_2 through perovskites); transport occurs via charged particles. Dense membranes are impermeable to all gases except for a very limited number of gases that can permeate the material or can be incorporated into the structure of the membrane and transported through the material However, their applications are rarely been used in membrane separation processes because of their low permeability as they have relatively thick membranes which limited their application for

practical separation processes as compared to porous inorganic membranes (Ismail and David, 2001; Baker, 2004).

Microporous inorganic membranes made of glass, metal, alumina, zirconia, zeolite and carbon membranes are commercially used as porous inorganic membranes. Other inorganic materials, such as cordierite, silicon carbide, silicon nitride, Titania, mullite, tin oxide and mica also have been used to produce porous inorganic membranes. These membranes vary greatly in pore size, support material and configuration. A microporous ceramic membrane system generally consists of a microporous ceramic support, some ceramic intermediate layers, and eventually a highly selective top layer. The support provides mechanical strength to the system. The intermediate layers bridge the gap between the large pores of the support and the small pores of the top layer. The top layer has separating capacities (Baker, 2004). Although inorganic membranes are more expensive than polymeric membranes, they possess advantages of temperature and wear resistance, well-defined stable pore structure, chemically inertness, and better selectivity than the polymeric membranes. However, due to the lack of technology to form continuous and defect-free membranes, high cost of production and handling issues e.g., brittleness, the commercial applications of inorganic membranes are still limited. For example, according to (Vu, 2001; Baker, 2004), a zeolite membrane module would cost around US$ 3000/m^2 of active membrane area compared to US$ 20/m^2 for existing gas separation polymeric hollow-fiber membrane modules (Vu, 2001; Baker, 2004).

Table I.4. Advantages and limitations of inorganic membranes over polymeric membranes (Caro, Noack et al, 2000)

Advantages for inorganic membranes	Limitation for inorganic membranes
High stability at high temperatures	High capital costs
High resistance to harsh environments	Brittleness (membrane cracking) due to extremely high sensitivity of membranes to temperature gradient
High resistance to high pressure drops	Low membrane surface per module volume
High resistance to microbiological degradation	Challenging in achieving high selectivities in large scale microporous membranes
Ease of cleanability after fouling	Generally low permeability of the highly selective (dense) membranes at medium temperatures
Ease of catalytic activation	Challenging for proper sealing of membrane to module at high temperatures

I.8.5) Mixed matrix membranes:

The molecular-sieve type fillers used in mixed matrix membranes (MMMs) such as zeolite and carbon molecular sieve (CMS) are capable to discriminate between different molecules present in the feed mixture, usually on the basis of size and shape of molecules (Pal, 2007; Shimekit, Mukhtar et al., 2009). Gas transport through a mixed matrix membrane is considered as complex phenomena. Due to its heterogeneity, a number of theoretical permeation models have been used to predict the permeation properties of mixed matrix (heterogeneous) membranes as a function of the permeabilities of the continuous and dispersed phases (Hashemifard, Ismail et al., 2010)

Generally, permeation in MMMs occurs by a combination of diffusion through the polymer phase and diffusion through the permeable zeolite particles. The relative permeation rates through the two phases are determined by their intrinsic permeabilities (Baker, 2004). The available models used in the prediction of the permeability of gases in mixed matrix membrane can be referred from (Shimekit, Mukhtar et al., 2011).

The market for the separation of acid gases by membranes can be divided as follows:

(1) Very small systems (less than 5 MMSCFD): At such flow rate, membrane units are very attractive and usually, the permeate gas is used or flared as fuel. Moreover, the system is a simple bank of membrane modules.

(2) Small systems (5-40 MMSCFD): Two-stage membrane systems are used to reduce methane loss. In this gas flow range, amine and membrane systems compete and the choice depends on site specific factors.

(3) Medium to large systems (more than 40 MMSCFD): In this range, membrane systems are too expensive to compete with amine plants. However, a number of large membrane systems have been installed on offshore platforms, at carbon dioxide oilfield flood operations, or where site-specific factors particularly favor membranes (Baker, 2004).

I.8.6) Limitation and challenges :

The application of membranes today for CO_2 separation in natural gas processing is mainly used for moderate-volume gas streams. For large-volume gas streams, membrane separation today cannot yet compete with the standard amine absorption as the flux and selectivity of the membranes are too low for processing large gas volumes.

Membranes are used in situations where the produced gas contains high levels of CO_2. However, a key sensitivity with these current membranes is that they must be protected from the heavier C_5^+ hydrocarbons present in wet natural gas streams. Exposure to these compounds immediately degrades performance and can cause irreversible damage to the membranes. Thus, in order to fully exploit the use of membranes in natural gas purification, development of more selective, higher-flux and cost effective new membranes are still critical concerns. And hence, the outcome will make membrane processes much more competitive with other technologies such as amine absorption for large scale systems (Baker, 2004).

Although the choice of acid gas removal technology depends on the needs of the gas processor, the current market trend showed that membranes have also proven their usefulness to compete with absorption (amines) technology. Nevertheless, the absorption technology based on amine treatment is still an efficient method although the amine units are large and heavy. Table 9 compares amines and membranes for CO_2 removal systems (Baker, 2004).

Table I.5. Comparison of Amines and Membranes for CO_2 Removal Systems (Baker, 2004)

Operating Issues	Amines	Membranes
User Comfort Level	Very familiar	Still considered new technology
Hydrocarbon Losses	Very low	Losses depend upon conditions
Meets Low CO_2 Spec.	Yes (ppm levels)	No (<2% economics are challenging)
Meets Low H_2S Spec.	Yes (<4 ppm)	Sometimes
Energy Consumption	Moderate to high	Low, unless compression used
Operating Cost	Moderate	Low to moderate
Maintenance Cost	Low to moderate	Low, unless compression used
Ease of Operation	Relatively complex	Relatively simple
Environmental Impact	Moderate	Low
Dehydration	Product gas saturated	Product gas dehydrated

Table I.6. Overall comparisons of natural gas purification technologies

Process	Advantages	Disadvantages
Absorption	-Widely used technology for efficient (50-100) % removal of acid gases (CO_2 and H_2S)	-Not economical as high partial pressure is needed while using physical solvents absorption -Long-time requirement for purifying acid gas as low partial pressure is needed while using chemical solvents.
Adsorption	-High purity of products can be achieved. -Ease of adsorbent relocation to remote fields when equipment size becomes a concern.	-Recovery of products is lower - Relatively single pure product
Membrane	-Simplicity, versatility, low capital investment and operation. – Stability at high pressure - High recovery of products - Good weight and space efficiency - Less environmental impact	- Recompression of permeate - Moderate purity
Cryogenic	-Relatively higher recovery compared to other process -Relatively high purity products	-Highly energy intensive for regeneration -Not economical to scale down to very small size. -Unease of operation under different feed stream as it consists of highly integrated, enclosed system.

I.9) Hybrid separation processes:

In hybrid separation processes, an integration of one process is used with other separation process or processes in which the basic functioning of one process is joined with another physical or chemical process in a single unit operation (Bernardo, Drioli et al., 2009).

The hybrid separation processes combines the properties of physical and chemical solvent for effective and selective removal of acid gas from natural gas. One of the well acclaimed

successful hybrid separation process uses in the oil and gas industry is Sulfinol process licensed by shell E&P (energy and petrochemical companies). Sulfinol is a mixture of sulfolane (tetrahydrothiophene1-1 dioxide a physical solvent), water and either di-isopropanol-amine (DIPA) or Methyl-di-ethanol-amine (MDEA) (both chemical solvent). The dual functionality and capacity of physical and chemical solvents mixture of sulfinol make the solvent more efficient. The physical solvent for instance provides the system for bulk removal of acid gas and also allows much greater solution loading of acid gas than most pure base solvents.

Some researchers (Bhide, Voskericyan et al., 1998) also report that a membrane-amine hybrid system would be economical in comparison to an amine system alone or a membrane system alone for various conditions, such as low CO_2 compositions, and a recent study confirms the economic feasibility of another membrane-amine system design (Falk-Pedersen and Dannstrom, 1997). A study with a membrane-cryogenic distillation hybrid system also shows favourable economics as well (Vu, 2001). The membrane system offered a 30% reduction in operating cost when compared with a methyl diethanolamine (MDEA) system and significantly reduced the size of the subsequent operations (Blizzard, Parro et al., 2005; Bernardo, Drioli et al., 2009). The combination of membrane processes with another process (most commonly with amine units) for bulk removal of CO_2offers an economical advantage over amine technologies. However, this process has also the limitation of being complex as it is a combination of two processes (Baker, 2004).

A properly designed hybrid process will balance the drawbacks of the specific process and favourably combine their advantages. It is anticipated that the result will be a better separation, contributing to a sustainable process improvement by allowing the reduction of investment and operational costs (Bernardo, Drioli et al., 2009).

I.10) Ionic liquids:

The use of ionic liquids (ILs) for CO_2 capture and the removal of acid gases from natural gas and other industrial processes has been one of the foremost research applications for this unique class of non-volatile solvents. ILs have a negligible vapor pressure, and an adjustable physicochemical character. ILs can dissolve CO_2 and H_2S and are stable at temperatures up to several hundred degrees centigrade, which make them suitable candidates for CO_2 capture/gas sweetening studies

(Kumelan et al., 2006, Kim et al, 2007). Because most of the ILs interact with CO_2 because of its quadruple moment and dispersion forces (in the case of physio-sorption), with the interaction being developed between CO_2 and IL anion through a weak Lewis acid-base interaction, the regeneration process could be achieved with little heat (Figueroa et al., 2008). It could be argued that that low energy requirements for regeneration (usually performed through stripping) is a property not only for ILs but also for the absorption in any physical solvent with high boiling point in comparison to chemical absorbents. Nevertheless, recent studies reported by (Wappel et al., 2010). IL performance could be improved through the suitable selection of anion/cation combinations that would lead to better absorption ability. ILs offer promising advantages in natural gas sweetening and flue gas CO_2 absorption processes because of their unique characteristics. Their negligible vapor pressure is one of the main factors that make this class of materials superior to the conventional organic solvents. Chemical modification of ILs may produce promising results, attracting more research groups to this field. ILs have received much attention to replace volatile organic solvents. Even though the toxicity of the ILs is still in debate because of their incomplete toxicological data and low Solubility of CO_2/H_2S in common ILs. The selection of ILs consisting of cation and anion groups with appropriate functional groups could improve the interactions of ILs with CO_2/H_2S, making them as effective as the alkanolamine molecules. Their high thermal stability is also very beneficial, considering that high-pressure conditions are required while the natural gas is purified (Karadas et al., 2010).

I.11) Amine Process:

In the gas processing industry absorption with chemical solvents has been used commercially for the removal of acid gas impurities from natural gas. The currently preferred chemical solvent technology for acid gas removal is chemical absorption of acid gases by amine-based absorbents. Alkanolamines are the most commonly used category of amine chemical solvents used for acid Gas removal. Chemical absorption of CO_2 with alkanolamines as solvent has been used in a large variety of industries over years. It is notable that MDEA is advantageous over other amines due to selective removal of H_2S from its mixture with CO_2. The selectivity of absorption is due to the higher rate of the reaction of MDEA with H2S than the reaction of MDEA with CO_2 (Anufrikov et al., 2007). H_2S has H^+ that can give directly to MDEA; the proton transfer reaction is always fast and spontaneous. Moreover, comparing to other amines, MDEA is more stable, less volatile

and less corrosive, it has lower heat of reaction and higher absorption capacity (Anufrikov et al., 2007).

I.12) Process overview of In salah gas (Krechba AGRU):

The dehydrated gas from the Teg and Reg facilities combines by mixing with the dehydrated and conditioned gas from the Krechba field's own processing facilities. The resulting gas mixture is then directed to separation cyclones to ensure ultimate settling before passing through the acid gas removal unit (AGRU) where CO_2 is removed from the export gas. It is then conveyed to the export gas dehydration unit. The gas thus processed and in accordance with the specifications of the standardized marketing standards is sent to the export pipeline.

I.13) Acid gas removal unit (AGRU):

I.13.1) Design basis: A single phase absorption process of Activated Methyldiethanolamine (a-MDEA) (activated by the piperazine) is used for the treatment of the export gas to meet the product gas specifications and which must be less than or equal to 0.3 mol% CO_2 and 2.0 mg / cm^3 in H_2S. The table below summarizes the design case defining the operating conditions of the AGRU.

The AGRU acid gas removal unit is designed for an overall feed gas flow rate of 1,338,416 (Cm^3 / h) and theoretical dry gas concentrations for CO_2 and H_2S of 6.6 mole% and 15 ppmv, respectively. The CO_2 concentration of 6.6 mole% (dry basis) including the design margin of approximately 0.1 mole% is the maximum threshold expected in the gas at a design flow rate.

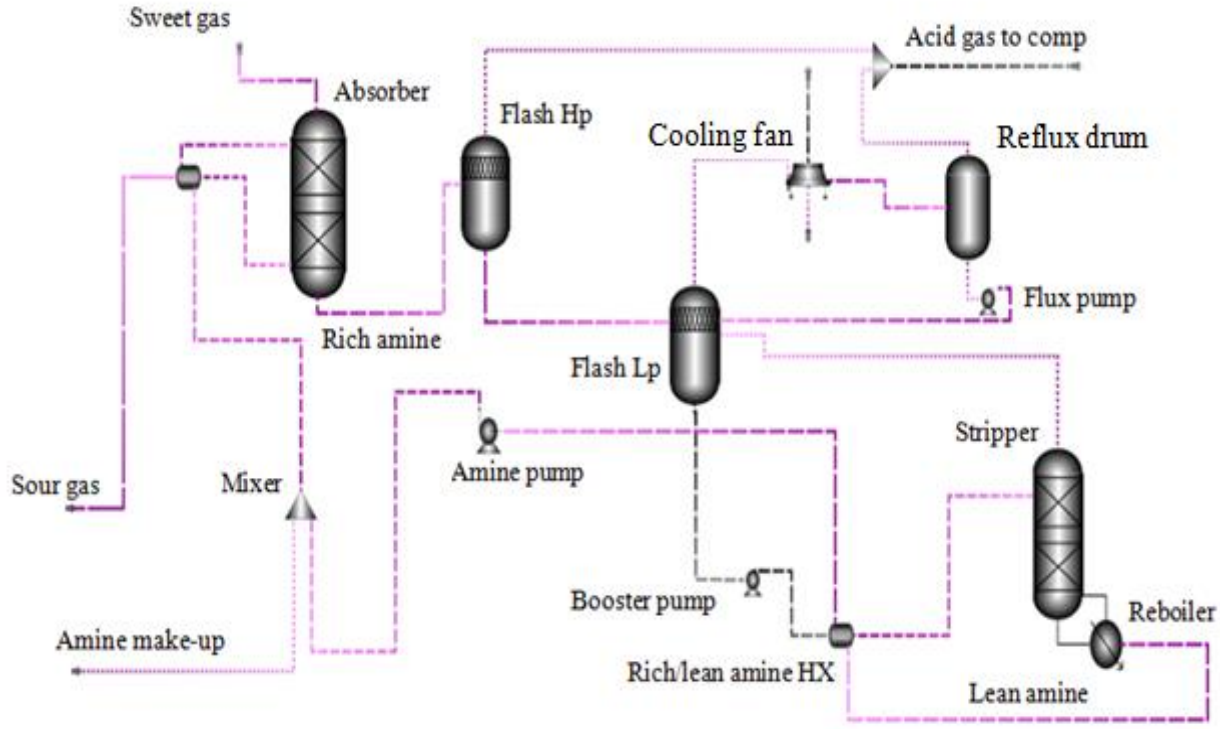

Figure I.8. Simplified process diagram (AGRU) (Krechba, In Salah, Algeria)

I.13.2) Krechba AGRU description:

The feed gas arrives at the two CO_2 extraction trains from the inlet manifold of the Krechba common treatment plants and separation cyclones at a pressure of about 72.3 bar and a variable temperature of 25ºC to 35ºC. The gas pre-heater is provided to increase and maintain the temperature of the feed gas at about 55 ° C by heat exchange with the lean amine solution previously cooled by an air cooling system. Increasing the exit temperature of the pre-heater gas to the recommended value of 55ºC generally favors a marked improvement in the kinetic response and a reduction in contact time in the absorber which optimizes the required height of the bed packing. The preheated feed gas is fed to the bottom of the vertical absorption column where it is contacted with a countercurrent flow of a poor a-MDEA solution, which enters the top of the column at about 55 ° C. via a distributor (diffuser) of liquids. The poor a-MDEA solution absorbs CO_2 and H_2S in the gas so that the gas thus treated meets the required specifications. The treated gas leaves the top of the absorption column at a pressure of 71.4 bar_a and at a temperature of about 55 °C and eventually passes to the export gas dehydration unit. In

order to reduce the entrainment of the lean amine solution from the absorber, a demister is therefore installed at the top of the column. The rich a-MDEA solution from the bottom of the absorption column at a nearby temperature of 83ºC and a required pressure of 6 bar in the HP flash drum. As the amine solution is flashed from high pressure to medium pressure in the HP flash drum, the instantaneous separation of CO_2 from the solution will result and bi-phasic flow as well. A flash gas rich in CO_2 (about 50 mol %) from the HP flash drum is conveyed under pressure control either to the reflux drum stripper to join the reinjection system or possibly to the acid gas torch. The pressure of the resulting rich amine solution is further lowered and the bi-phase mixture is then conveyed to the flash drum BP, which operates at a pressure of 1.7 bar_a, where it comes into countercurrent contact with the CO_2 head from the stripper. Since the pressure of the flash drum BP is low, the CO_2 is released from the solution and a bi-phase flow results.CO_2 distillate coming from the stripper, with a temperature of 103 ºC and a pressure of 1.8 bar_a, will feed from bottom (below the packing bed) the flash drum BP where it plays the role of exhaustion agent and improves the CO_2 separation efficiency. The acidic gas stream leaving the flash ball BP at a temperature of around 78ºC, goes to the condenser flash, where it is cooled to a temperature of 55ºC, using cooling fans. The stream of cooled acid gas then passes to the reflux drum, where the condensed water is collected and then pumped back to the flash drum BP by the reflux pumps under level control. The wet acid gas stream at a pressure of 1.5 bar_a and a temperature of 55ºC will then pass to the CO_2 compression installation for reinjection. In case of unavailability of the reinjection system, the gas is vented via the acid gas torch. The solution of rich a-MDEA coming from the flash drum BP is conveyed to the rich amine pumps increasing its discharge pressure at 5 bars, and which is then preheated to 115 ° C by heat exchange with the a-MDEA poor solution in the (poor / rich) exchanger. The bi-phasic solution of rich pre-heated a-MDEA then feeds the top of the CO_2 stripper in which the CO_2 is released from the solution. The stripper operates at a pressure of 1.8 bar_a at the top of the column and a heat transfer due to the heat exchange provided by 3 of the stripper reboilers in service. The latter use circulating hot water as a source of heat to meet heating needs. A solution of hot regenerated a-MDEA, having a temperature of 121ºC, leaves the bottom of the stripper and is cooled to 89 °C by heat transfer exchange due to the rich solution of a-MDEA in the poor / rich exchanger. The regenerated amine solution is cooled then increased in pressure to about 5 bars, by poor amine booster pumps. The cooled lean amine solution is then increased in pressure by the circulating pumps to

about 75 bar_g and then further cooled to 55 ° C against feed gas in the feed preheater and then sent to CO_2 absorber.

Conclusion:

The removal of acid gases from the natural gas has been an important unit operation for many decades. Traditionally, the motivation for this removal has been of technical and/or economical character. It has been given special emphasis aimed at increasing the heating value of natural gas, reducing pipe lines and equipment corrosion during transportation, storage and distribution and meeting environmental requirements.

The last two decades or so increased attention has been drawn to CO_2 as a greenhouse gas. Since the main source of anthropogenic CO_2 in the atmosphere is the combustion of fossil fuels, it is generally accepted that action should be taken to decrease the accumulation of CO_2 in the atmosphere. The most common technology for removing acid gases from both low and high pressure gas streams is absorption by alkanolamines. It is a mature technology in natural gas purification. The use of these processes for world-wide CO_2 capture is inhibited by high energy and plant expenditures. In order to deal with this, a better understanding of the fundamentals of these processes is necessary.

Many separation techniques, such as membrane, physical adsorption, and cryogenics, can be used to capture CO_2 from process gases. However, The currently preferred technology for acid gas removal is chemical absorption of acid gases by amine-based absorbents. It has been used commercially to capture the gas because absorption is highly effective at various CO_2 concentrations, and is relatively inexpensive.

Chapter II

General Literature Review of Reaction Kinetics Of Acid Gas Absorption Into Reactive Amine Solutions

Chapter II: General Literature Review of Reaction Kinetics of Acid Gas Absorption into Reactive Amine Solutions

Introduction:

Reaction kinetics is one of the most important parameters for the amine-based acid gas capture process because it indicates how fast acid gas reacts with amine, and it is one of the key parameters required for simulating and designing the absorption column (Kohl and Riesenfeld, 1997). The widely used processes for the removal of acid gas from natural gas and industrial gas streams are the regenerative absorption of acid gas into aqueous solutions of alkanolamines. Primary and secondary alkanolamines react rapidly with CO_2 to form carbamates. However, the heat of absorption associated with the carbamate formation is high, which results in high solvent regeneration costs. Further, the CO_2 loading capacity of such alkanolamines is limited to 0.5 mol of CO_2 per mol of amine. Tertiary alkanolamines possess no hydrogen atom attached to the nitrogen atom, as in the case of primary and secondary alkanolamines. Thus, the carbamation reaction cannot take place, resulting in a low reactivity with respect to CO_2. Instead, tertiary amines facilitate the CO_2 hydrolysis reaction forming bicarbonates. The reaction heat released in bicarbonate formation is lower than that of carbamate formation, thus reducing solvent regeneration costs. Moreover, tertiary amines have a high CO_2 loading capacity of 1 mol of CO_2 per mol of amine. The CO_2 absorption rates of tertiary amines can be enhanced by the addition of small amounts of primary or secondary amines (Chakravarty, 1985). In addition, other absorption activators such as piperazine (PZ) can also be used (Appl et al., 1982).

In order to obtain reaction kinetics data, CO_2 absorption experiments need to be performed using laboratory scale gas–liquid contactors such as stirred cell reactor, wetted wall column, laminar jet absorber, wetted sphere absorber, string of disc contactor or stopped-flow apparatus.

II.1) Stirred cell reactor:

In the stirred cell reactor (figure II. 1A), the gas and liquid phases are stirred separately using separated adjustable impellers. The gas–liquid interface needs to be smooth, and a consistent interface is achieved by controlling the agitation speed from impellers. A pressure transducer is located in the gas-phase side for measuring the total pressure in the reactor. In addition, temperature sensors are located in both the gas and liquid sides of the reactor, and baffles are

installed in the liquid side in order to avoid formation of vortices. The gas absorption rate is determined by measuring the change in total pressure in the reactor (Astarita et al., 1983; Pani et al., 1997). The advantage of the stirred cell reactor is that only gas-phase measurement is required. However, its disadvantage is the difficulty of maintaining the smooth and consistent gas–liquid interface.

II.2) Wetted wall column:

The wetted wall column diagram is presented in Figure II.1B. The liquid is continuously pumped to the bottom of the wetted wall column then overflows from the interior of the tube and forms a thin liquid film over the outer surface of the tube. This thin liquid film contacts the inlet gas counter currently. The gas absorption rate can be calculated from the gas-phase material balance by measuring the concentration and volumetric flow rate of inlet gas and outlet gas (Saha et al. ,1995; Ko and Li,2000). The disadvantages of this equipment are the possibility of creating ripples in the liquid film and inactive film at the bottom of the column (Astarita et al., 1983).

II.3) Laminar jet absorber:

In this technique, the liquid is degassed by spraying it into a vacuum and then the degassed liquid is passed through the temperature-controlled water jacket, in order to reach the desired temperature. The degassed liquid is then passed through the jet nozzle in order to continuously generate a smooth-surfaced, rod-like jet in the absorption chamber. The soap-film meter is used to measure the rate of gas absorption. A 2D microscope is used to measure jet height (h_j) and jet diameter (d_j). Finally, the discharged liquid is collected, and liquid flow rate (L) is measured (Rinker et al., 1996; Aboudheir et al., 2003)**.** The laminar jet absorber is shown in Figure II.1C. The advantage of the laminar jet absorber is that the gas–liquid interface can be measured directly from the microscope. Furthermore, this technique is suitable for very reactive liquid solvents due to the short contact time in the laminar jet absorber. However, the disadvantages of this technique are the possibility of creating turbulent liquid surface, a reduction in the liquid jet caused by gravity, and stagnant surface and ripples at the bottom of liquid jet created by the liquid jet receiver. These behaviors can be avoided by good design of the liquid jet nozzle and liquid jet receiver (Astarita et al., 1983; Aboudheir et al., 2004). Another limitation of the

laminar jet absorber is that the jet length cannot be varied over a wide range, thereby restricting the range of gas–liquid interfacial area.

II.4) Wetted sphere absorber:

The wetted sphere absorber (Figure II.1D) is similar to the laminar jet absorber. This technique introduces liquid solvent into the absorption chamber by overflowing the sphere instead of generating a liquid jet as in the laminar jet absorber (Seo and Hong, 2000). The absorption surface area can be calculated from the surface of the sphere. In addition, the operating procedure for the wetted sphere absorber is the same as the laminar jet absorber. The advantage of this technique is that the laminar liquid surface over the sphere can be generated and controlled easier than that of laminar jet absorber, since the liquid is flown over the sphere. However, the disadvantages of this equipment are that the absorption surface area cannot be varied, and the possibility of creating ripples in the liquid film and inactive film at the bottom of the sphere (Astarita et al., 1983).

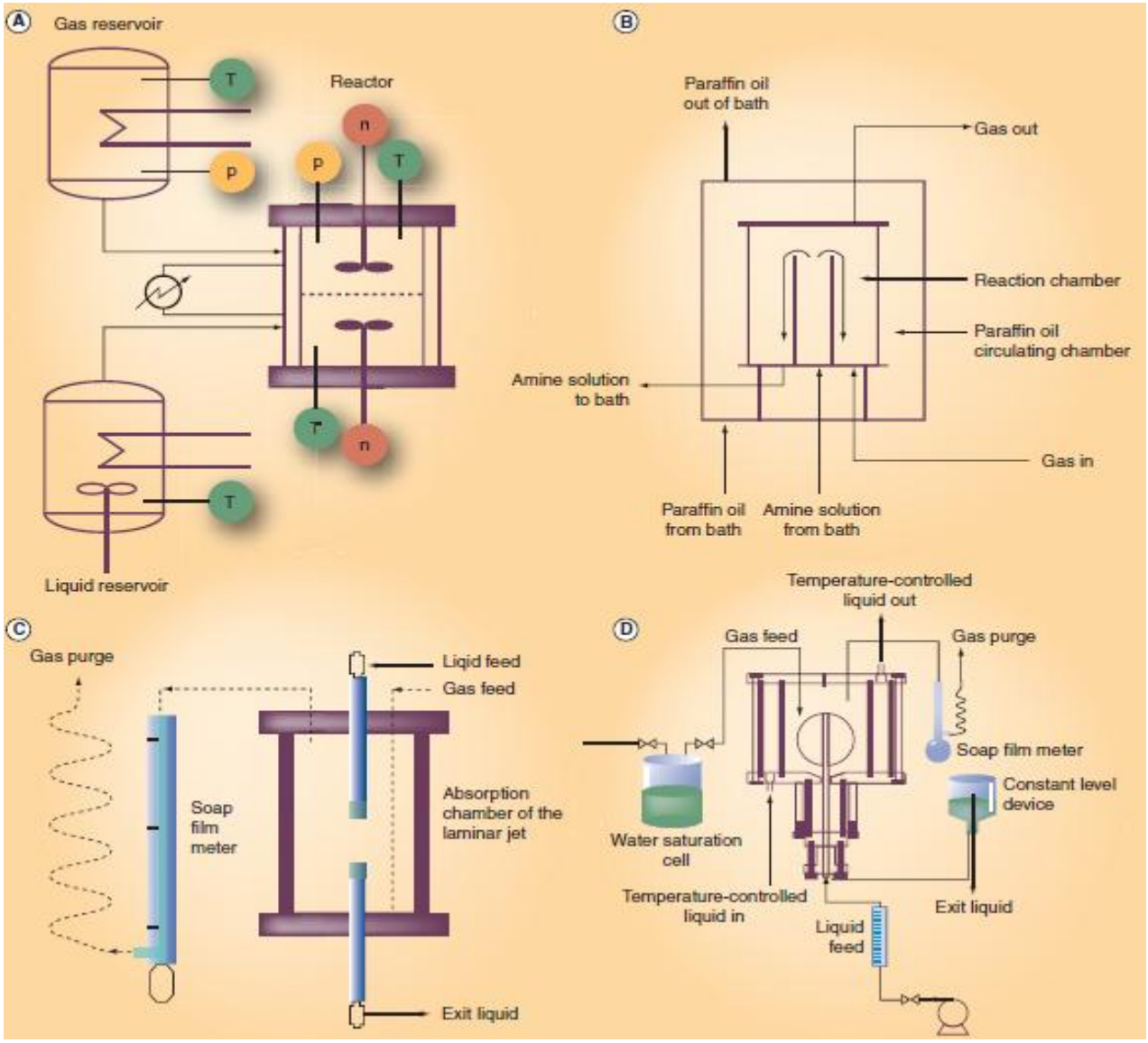

Figure II.1. Experimental equipment for measuring the CO_2 absorption rate. (A) Stirred cell reactor; (B) wetted wall column; (C) laminar jet absorber; and (D) wetted sphere absorber.
n: Molar hold-up (kmol); p: partial pressure (kPa); T: Temperature (K).

II.5) String of disc contactor:

A number of circular discs are held together by a vertical wire in the absorption column. The reactive liquid flows downward from the top of the contactor. CO_2 is introduced counter-currently from the bottom of the contactor. The active surface area can be calculated based on the diameter and number of the discs. In addition, the absorption surface area of this contactor can be varied by introducing or removing the disc elements in the column. A disadvantage of this contactor is that absorption rate at specific concentrations of liquids and/or gas cannot be achieved. This is because the concentration of CO_2 and the composition of reactive liquid are changed accordingly along the height of the string column (Danckwerts, 1979; Vaidya and Kenig, 2007). Therefore, the overall absorption rate, which can be calculated by the difference of mass flux at inlet and outlet of the column, is applied (Ma'mun, 2007).

II.6) Stopped-flow apparatus:

The stopped-flow technique is a homogeneous direct method for measuring the gas absorption into liquid solvent. Saturated gas and liquid solutions are mixed in the stopped-flow apparatus as presented in (Figure II.2). The conductivity cell monitors ion formation as a function of time, since the ion formation initiates a voltage change. Thereafter, the microcomputer automatically generates the observed pseudo first-order constant based on the output voltage values (Li et al., 2007).However, the disadvantage of this technique is that a conductivity measurement can only be done at low amine concentration. Lastly, for novel solvents screening, the stopped-flow apparatus is suggested. This is because a very small quantity of solvent is required and the experimental procedure is simple (Vaidya and Kenig, 2007; Li et al., 2007)

The stopped flow technique is the most widely used of rapid mixing techniques for CO_2-amine studies which is the subject of our kinetic study. In comparison with mass-transfer techniques, stopped-flow technique enables to determine kinetic constant usually ranged between about 0.01 and 1000 s^{-1}. Kinetic measurements with stopped-flow technique are free from gas-liquid mass transfer limitations. Signal can be directly related to the intrinsic reaction in the liquid phase which makes the method very reproducible.

Figure II.2. Experimental equipment for measuring the CO_2 absorption rate: stopped-flow apparatus.

II.7) Reaction mechanisms:

Alkanolamines are the most popular absorbents used to remove acid gas from process gas streams. Primary and secondary alkanolamines react rapidly with CO_2 to form carbamates. However, Tertiary alkanolamines possess no hydrogen atom attached to the nitrogen atom, as in the case of primary and secondary alkanolamines. Thus, the carbamation reaction cannot take place, resulting in a low reactivity with respect to CO_2. Instead, tertiary amines facilitate the CO_2 hydrolysis reaction forming bicarbonates. The reaction of CO2 with primary, secondary and sterically hindered amines is usually described by the zwitterion mechanism, whereas the reaction with tertiary amines is described by the base-catalyzed hydration of CO_2.

II.7.1) Zwitterion Mechanism:

The zwitterion mechanism was originally proposed by Caplaw (Caplaw,1968) and later reintroduced by Danckwerts (Danckwerts,1979) as a two-step reaction between CO_2 and primary or secondary amine (denoted as R_1R_2NH) through formation of a zwitterion

intermediate($R_1R_2NH^+COO^-$),and then a deprotonation of zwitterion intermediate by a base (denoted as B) to carbamate

$$CO_2 + R_1R_2NH \overset{K_2^z, K_{-1}^z}{\longleftrightarrow} R_1R_2NH^+COO^- \quad \text{(II.1)}$$

$$R_1R_2NH^+COO^- + B \overset{K_b, K_{-b}}{\longleftrightarrow} AMCOO^- + B\,H^+ \quad \text{(II.2)}$$

Where, K_2^z, K_{-1}^Z are the second-order forward rate constant and first-order reverse rate constant for Equation 1, respectively, And a superscript Z represents the zwitterion mechanism. In Equation II.2, base (B) can be R_1R_2NH, OH^- or H_2O (Blauwhoff et al, 1983): By applying the pseudo-steady state approximation for the concentration of $R_1R_2NCOO^-$, the rate of CO_2 absorption based on the zwitterion mechanism can be derived as (Blauwhoff et al, 1983):

$$r_{CO2} = \frac{K_2^z[CO_2][R_1R_2NH]}{1+\frac{K_{-1}^z}{\sum_b[B]}} = \frac{K_2^z[CO_2][R_1R_2NH]}{1+\frac{K_{-1}^z}{K_{R_1R_1NH}[R_1R_2NH]+K_{OH^-}[OH^-]+K_{H_2O}[H_2O]}} \quad \text{(II.3)}$$

In this case if $\frac{K_{-1}^z}{\sum_b[B]}$ <<1, the equation (II.3) can be simplified to be the second-order rate reaction as (Blauwhoff et al, 1983):

$$r_{CO2} = K_2^z[CO_2][R_1R_2NH] \quad \text{(II.4)}$$

If $\frac{K_{-1}^z}{\sum_b[B]}$ >>1, the equation (II.3) can be simplified to be the second-order rate reaction as (Blauwhoff et al, 1983):

$$r_{CO2} = \frac{\sum_b[B]}{K_{-1}^z} K_2^z[CO_2][R_1R_2NH] \quad \text{(II.5)}$$

Versteeg and van Swaaij, 1988), and (Laddha and Danckwerts, 1981) suggested that OH^- and H_2O are the minor contributors to a deprotonation of zwitterion (Equation II.2) due to a low concentration of OH^- and a low basicity of H_2O, compared with R_1R_2NH. Therefore, Equation (II.5) can be simplified as:

$$r_{CO2} = \frac{K_{R_1R_1NH}K_2^z}{K_{-1}^z}[CO2][R_1R_2NH]^2 \quad \text{(II.6)}$$

If R_1R_2NH is the main contribution of Equation (II.2), as suggested by Versteeg and van Swaaij (Versteeg and van Swaaij, 1988) and Laddha and Danckwerts (Laddha and Danckwerts, 1981) ,the overall reaction between CO2 and primary or secondary amine can be represented as:

$$CO_2 + R_1R_2NH \leftrightarrow R_1R_2NCOO + R_1R_2NH_2^+ \qquad \text{(II.7)}$$

Thus, it is implied from Equation (II.4) that the theoretical equilibrium loading capacity of primary and secondary amine is limited to 0.5 mol CO_2 per mol of amine . However, this statement is only applicable if the carbamate species is quite stable (e.g., carbamate species from MEA and DEA) (Saha et al, 1995)

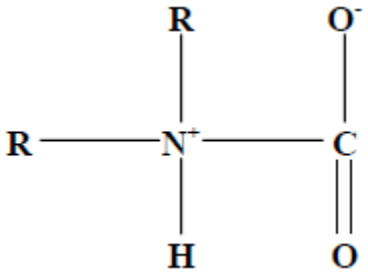

Figure II.3: Zwitterion structure

II.7.2) Termolecular mechanism:

The termolecular mechanism was originally proposed by Crooks and Donnellan, (1989) and states that the reaction is a single step where the initial product is not a zwitterion, but a loosely bound encounter complex with a mechanism of the type as shown in Figure II.4. Most of these complexes are intermediates, which break up to give reagent molecules, again, while a few react with a second molecule of either R_1R_2NH, OH-, or H_2O to give ionic products. Bond formation and charge separation occur only in the second step (Aboudheir et al., 2003 ; Da Silva and Svendsen, 2004 ; Crooks and Donnellan, 1989).

The reaction-rate expression according to the termolecular mechanism can be written as:

$$r_{CO2} = (K_{\mathrm{R_1R_1NH}}[R_1R_2NH] + K_{OH^-}[OH^-] + K_{\mathrm{H_2}O}[H_2\mathrm{O}])[CO_2][R_1R_2NH] \qquad \text{(II.8)}$$

If R_1R_2NH is assumed to be the main contributor in the termolecular mechanism, the rate expression can then be reduced (superscript T denotes termolecular mechanism):

$$r_{CO2} = K^{T}_{R_1R_1NH}[CO_2][R_1R_2NH]^2 \quad \text{(II.9)}$$

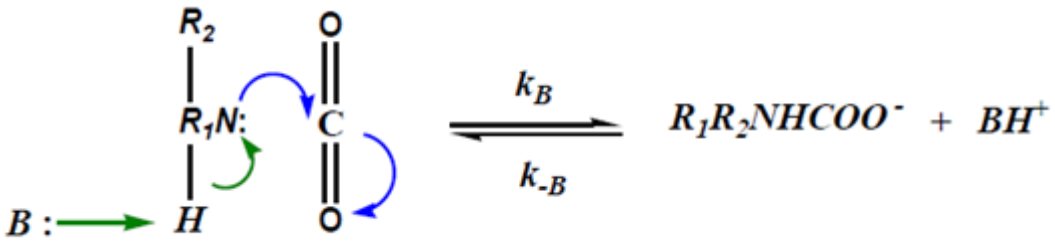

Figure II.4: Schematic drawing of single-step termolecular reaction mechanism (Crooks and Donnellan, 1989)

II.7.3) Base-catalyzed hydration mechanism:

The base-catalyzed hydration of the CO_2 mechanism by tertiary amine (denoted as R_3N) was originally proposed by Donaldson and Nguyen (1980). They proposed that the tertiary amine does not react directly with CO_2 but acts as a base that catalyzes the hydration of CO_2, as presented in Equation (II.11).

$$R_3N + CO_2 + H_2O \overset{K_{R3N}}{\longleftrightarrow} R_3NH^+ + HCO_3^- \quad \text{(II.11)}$$

The rate expression for the base-catalyzed hydration mechanism for tertiary amine can be written as (Caplaw, 1968):

$$r_{CO2} = K_{R_3N}[CO_2][R_3N] \quad \text{(II.12)}$$

In the case of the base-catalyzed hydration mechanism, the rate of CO_2 absorption is a second-order reaction rate. (K_2: m^3/ kmol.s), because K_2 directly represents the reaction kinetics (speed of the reaction) and is required for process simulation and design of the absorption column (Kohl, 1997; Danckwert, 1979, Astarita et al., 1983, Aboudheir et al., 2003).

After measuring the CO_2 absorption rate using the experimental gas–liquid contactor (e.g., stirred cell reactor, wetted wall column, laminar jet absorber, wetted sphere absorber, string of disc contactor or stopped-flow apparatus), the interpretation of the experimental kinetics data is

required for determining the second-order reaction rate constant. For the CO_2 absorption into amine solutions, several approaches have been applied, including graphical methods, simplified models based on reaction mechanism and a numerically solved comprehensive model.

II.8) Graphical method:

The graphical method was used during the 1980s until the mid-1990s for determining the order of reaction, and the reaction rate constant of MEA, DEA, TEA and AMP (Saha et al.,1995; Blauwhoff et al.,1983; Versteeg and van Swaaij,1988; Donaldson and Nguyen,1980; Alvarez et al.,1980).Assuming that the reaction between CO_2 and amine is an m^{th} order reaction with respect to concentration of dissolved CO_2 at the interface and an n^{th} order reaction with respect to amine concentration, the reaction rate expression for a single amine system can be written as (Saha et al.,1995):

$$r_{CO2} = K_{\text{mn}}\, {C^*_{CO_2}}^{m} {C^*_{Am}}^{n} \qquad \text{(II.13)}$$

Where, $K_{\text{mn}}$is the reaction rate constant (m^3/kmol.s) and $C^*_{CO_2}$ is the molar concentration of CO_2at the interface (kmol/m^3), which can be calculated by the Henry's law relationship, as presented in Equation II.14; C^*_{Am} is the molar concentration of amine (kmol/m^3) and He is Henry's law constant (kPa m^3/kmol):

$$C^*_{CO_2} = \frac{P_{CO2}}{He} \qquad \text{(II.14)}$$

II.9) Simplified model based on reaction mechanism:

In this approach, the reaction rate/kinetics data obtained from the gas–liquid contactor are interpreted based on the proposed mechanism between CO_2 and amine (i.e., zwitterion, termolecular and base-catalyzed hydration mechanisms). In addition, the single and blended amines solutions are also treated differently. First, the overall rate of CO_2 absorption (r_{ov}) is defined as (Ramachandran et al, 2006)**:**

$$r_{ov} = K_{\text{ov}}[CO_2] \qquad \text{(II.15)}$$

(K_{ov}) can be calculated via the experimental measurement of CO_2 absorption rate.

1) Primary & secondary amines:

For the primary and secondary amines (e.g., MEA and DEA), the overall reaction rate for CO_2 absorption based on the zwitterion mechanism can be written as (Blauwhoff et al,1983; Versteeg and van Swaaij,1988):

$$r_{CO2} = \quad K_{\mathrm{ov}}[CO_2] \quad = \frac{K_2^z[CO_2][R_1R_2NH]}{1+\frac{K_{-1}^z}{K_{\mathrm{R_1R_1NH}}[R_1R_2NH]+K_{OH^-}[OH^-]+K_{\mathrm{H_2O}}[H_2\mathrm{O}]}} + K_{OH^-}^{*}[OH^-][CO_2] \quad \text{(II.16)}$$

The apparent rate constant (k_{app}) is defined as (Blauwhoff et al, 1983; Versteeg and van Swaaij, 1988):

$$K_{\mathrm{app}} = K_{\mathrm{ov}} - K_{OH^-}^{*}[OH^-] \quad \text{(II.17)}$$

Therefore, k_{app} for aqueous primary or secondary amine solution can be written as (Blauwhoff et al., 1983; Versteeg and van Swaaij, 1988):

$$K_{\mathrm{app}} = \frac{K_{2,\mathrm{R_1R_1NH}}^z[CO_2][R_1R_2NH]}{1+\frac{K_{-1}^z}{K_{\mathrm{R_1R_1NH}}[R_1R_2NH]+K_{OH^-}[OH^-]+K_{\mathrm{H_2O}}[H_2\mathrm{O}]}} \quad \text{(II.18)}$$

Where, $K_{2,\mathrm{R_1R_1NH}}^z$ is a second-order reaction rate constant of primary or secondary amine based on the zwitterion mechanism for reaction (1).$K_{\mathrm{R_1R_1NH}}$, $K_{OH^-}$and $K_{\mathrm{H_2O}}$ are reaction-rate constants for deprotonation of the zwitterion intermediate (reaction 2) byR_1R_2NH, OH^- and H_2O, respectively.

The concentration of OH^- can be estimated using a relation proposed by Astarita et al (Astarita et al., 1983), as :

$$[OH^-] = \frac{K_w}{K_a}\left(\frac{1-\alpha}{\alpha}\right) \quad for\ \alpha \geqslant 10^{-3} = \sqrt{\frac{K_w}{K_a}[Amine]} \quad for\ \alpha \geqslant 10^{-3} \quad \text{(II.19)}$$

Where K_w is equilibrium dissociation constant of water (K_w= $[H^+][OH^-]$), K_a, is equilibrium deprotonation constant of amine:

$$K_a = \frac{[R_1R_2NH][H^+]}{[R_1R_2NH_2^+]} \quad \text{(II.20)}$$

And α is CO_2 loading (mol CO_2 /mol amine). In addition, OH^- can also be estimated with the vapor–liquid equilibrium model (Aboudheir et al, 2003; Ramachandran et al, 2006). The experimental values of k_{app} at specific temperatures are now correlated with the zwitterion mechanism of Equation (II.18) in order to obtain individual rate constants of $K^z_{2,\mathrm{R_1R_1NH}}$, $K_{OH^-}$and $K_{\mathrm{H_2}O}$.

In the case of the termolecular mechanism, the k_{app} for aqueous primary or secondary amine solution can be written as (Aboudheir et al., 2003):

$$K_{app} = K^T_{\mathrm{R_1R_1NH}}[R_1R_2NH] + K_{OH^-}[OH^-] + K_{\mathrm{H_2}O}[H_2\mathrm{O}])[R_1R_2NH] \qquad \text{(II.21)}$$

The experimental values of k_{app} at a specific temperature are then correlated with the termolecular mechanism of Equation (II.21) in order to obtain individual rate constants of $K^T_{\mathrm{R_1R_1NH}}$, K_{OH^-}, and $K_{\mathrm{H_2}O}$

2) Tertiary amine:

Tertiary amine (e.g., TEA and MDEA) does not react with CO_2 directly, but it acts as a base that catalyzes the hydration of CO_2 (base-catalyzed hydration mechanism). The apparent rate constant for tertiary amine based on the base-catalyzed hydration mechanism can be expressed as (Yu et al., 1985):

$$K_{app} = K_{\mathrm{R3N}}[R_3N] \qquad \text{(II.22)}$$

3) Primary sterically hindered amine:

One of the best-known hindered amines is AMP, which is the hindered amine of MEA. The reaction kinetics of AMP has been studied widely. Chakraborty et al., were among the first to study the reaction mechanism and kinetics of CO_2 absorption in AMP solution (Chakraborty et al., 1985). By using ^{13}C NMR, they observed that no carbamate peak can be detected. Therefore, they suggested the hydration of CO_2 as shown in equation II.23, as an alternative mechanism instead of carbamate formation (denoted $R'R''NH$ as AMP):

$$R'R''NH + CO_2 + H_2\mathrm{O} \;\leftrightarrow\; R'R''NH_2^+ + HCO_3^- \qquad \text{(II.23)}$$

In addition, Yi and Shen assumed that carbamate species cannot be formed in the case of AMP (Yih and Shen, 1988). Therefore, they suggested an alternative mechanism as shown in

$$R'R''NCOO^-H^+ + H_2O \leftrightarrow R'R''NH_2^+ + HCO_3^- \quad \text{(II.24)}$$

However, these mechanisms do not represent the fast absorption rate of AMP very well. Later, Alper (1990), and Bosch et al., (1990), successfully applied the zwitterion mechanism to AMP. Since an unstable carbamate species is formed in the case of AMP, the unstable carbamate is then hydrolyzed to form bicarbonate, as shown in Equation (II.25):

$$R'R''NCOO^- + H_2O \leftrightarrow R'R''NH + HCO_3^- \quad \text{(II.25)}$$

In addition, Alper (1990) and Bosch et al. ,(1990)., also found that the reaction order with respect to CO_2 concentration and AMP concentration is 1 (the overall reaction order is 2).

Based on the zwitterion mechanism, k_{app} can be written as (Bosch et al., 1990):

$$K_{\text{app}} = \frac{K^Z_{2,\text{AMP}}[CO_2][AMP]}{1+\frac{K^Z_{-1}}{K_{\text{AMP}}[R_1R_2NH]+K_{OH^-}[OH^-]+K_{\text{H}_2O}[H_2O]}} \quad \text{(II.26)}$$

4) Solvents containing polyamines:

PZ (which is a secondary cyclical amine with two secondary amine groups) has been studied the most due to its high reactivity and absorption capacity (Dang and Rochelle, 2003). Since PZ is a secondary amine, the zwitterion mechanism has been generally applied. In addition, PZ has two nitrogen atoms, and carbamate species can be formed from both of them. The reactions between CO_2 and PZ can be written as:

$$PZ + CO_2 \overset{K_b}{\leftrightarrow} PZH^+COO^- \quad \text{(II.27)}$$

$$PZH^+COO^- + B \overset{K_{2,PZ}}{\longleftrightarrow} \text{PZ}COO^- + BH^+ \quad \text{(II.28)}$$

By applying a pseudo-steady state approximation for the zwitterion, the rate expression of PZ is found to be the same as that of primary and secondary amines

$$r_{CO2} = \frac{K^{z}_{2,PZ}[CO_2][PZ]}{1+\frac{K^{z}_{-1}}{\sum_b[B]}} \quad \text{(II.29)}$$

It has been reported by several researchers that: $\frac{K^{z}_{-1}}{\sum_b[B]}$ <<1, in the case of PZ (Bishnoi and Rochelle, 2003; Ko and Li, 2000, Derks et al., 2006). This is because of the high basic strength of PZ (pKa value of PZ is 9.731).

5) Blended amine system:

Chakravarty et al. first suggested a mixing of primary or secondary amines with tertiary amines to take advantage of each amine's high-performing components (Chakravarty, 1985). This means the disadvantages of one amine are compensated for by another amine. The benefits of blended amine systems have been proven widely in the literature (e.g., MEA–MDEA, MEA–AMP, MEA–PZ, MDEA–PZ and AMP–PZ) (Edali et al., 2010; Ko and Li, 2000; Ramachandran, 2006; Caplaw, 1968; Xiao et al., 2000; Bruder et al., 2011). The simplified kinetics model for the blended amine applies the same procedure as that for single amine. The overall rate expression for the blended amine takes into accounts all of the individual amines.

II.10) Numerically solved comprehensive model:

One of the very first numerically solved comprehensive reaction rate/kinetics models, which takes into account the coupling between chemical equilibrium, mass-transfer and chemical kinetics of all possible chemical reactions, was developed by Hagewiesche et al. (Hagewiesche et al., 1995).They measured the rate of CO_2 absorption into an aqueous solution of unloaded, blended MEA–DEAB(DEAB: diethylamine-butanol) over a concentration range of 1.5 wt% MEA + 28.5 wt% MDEA to 4.5 wt% MEA + 25.5 wt% MDEA. The developed model is governed by a system of partial differential nonlinear algebraic equations based on the mass transport equation (Astarita et al., 1983). The method of lines was used to transform the partial differential equations into ordinary differential equations (ODEs); they were then solved using the code DDASSL in FORTRAN. Their developed reaction rate/kinetics model is capable of predicting the CO_2 absorption rate, the enhancement factor, and the rate coefficient of reaction between CO_2 and MEA. However, the experiment was performed with unloaded solution and at only 313 K.

Conclusion:

Reaction kinetics is one of the most important parameters for the amine-based acid gas capture process because it indicates how fast acid gas reacts with amine, and it is one of the key parameters required for simulating and designing the absorption column. In order to obtain reaction kinetics data, CO_2 absorption experiments need to be performed using laboratory scale gas–liquid contactors such as stirred cell reactor, wetted wall column, laminar jet absorber, wetted sphere absorber, string of disc contactor or stopped-flow apparatus. The stopped flow technique is the most widely used of rapid mixing techniques for CO_2-amine studies which is the subject of our kinetic study. Kinetic measurements with stopped-flow technique are free from gas-liquid mass transfer limitations. Signal can be directly related to the intrinsic reaction in the liquid phase which makes the method very reproducible. For the CO_2 absorption into our amine solutions, simplified model based on reaction mechanism approach has been applied, in which the reaction rate/kinetics data obtained from the gas–liquid contactor are interpreted based on the proposed mechanism between CO_2 and amine (i.e., zwitterion, and base-catalyzed hydration mechanisms).

Chapter III

Thermodynamics Modeling Structure

Chapter III: Thermodynamics Modeling Structure

Introduction:

The most common technology for removing acid gases from both low and high pressure gas streams is absorption by alkanolamines. The use of these processes for world-wide CO_2 capture is inhibited by high energy and plant expenditures. In order to deal with this, a better understanding of the fundamentals of these processes is necessary. Thermodynamics has important role in the design of acid gas treating plants. Thermodynamic modeling of the behavior of these systems includes consideration of both phase and chemical equilibria. Thermodynamics quantifies the driving force for mass transfer, equilibrium compositions and thus outlet concentrations. A consistent thermodynamic model also quantifies amine volatility and thermal properties of the system.

III.1) Literature review of published models:

Acid gas removal from natural gas is typically performed by physical and chemical absorption into aqueous alkanolamine solutions. A good thermodynamic description of the chemical systems used is crucial in the modelling, optimization and design of CO_2 absorption facilities. The thermodynamics represent the boundaries within which a CO_2 absorption facility can be operated. A rigorous thermodynamic model should give good predictions of the vapour liquid equilibria, the solution speciation and the heat evolved when CO_2 is absorbed.

The process industry is concerned with the modeling and simulation of wide varieties of chemical products and processes that involve electrolyte systems in aqueous or mixed solvent solutions. Example electrolyte systems include water–organics–salt mixtures, water–strong acid (such as nitric acid) mixtures, aqueous organic amines for gas treating, brines with organic additives, and extraction or crystallization of organic salts, to name a few of the foremost systems.

In amine-based acid gas capture, acid gas reacts with an aqueous amine solution, forming different electrolyte species, which means that the amine molecules ionize when they are dissolved in water. In electrolyte solutions a larger variety of interactions and phenomena exist than in non-electrolyte solutions. Besides physical and chemical molecule-molecule interactions, ionic reactions and interactions occur (molecule-ion and ion-ion).

Due to the complexity of electrolyte thermodynamics and solution chemistry, there remains a major industrial need to develop and compile public databanks of model parameters and solution chemistries for electrolyte systems of industrial significance. This effort requires skilled thermodynamicists to take measurements, compile and screen experimental data, and determine and validate model parameters.

Rigorous thermodynamic modeling requires comprehensive treatment of chemical equilibrium of the aqueous electrolyte solution chemistry, phase equilibrium of volatile non-dissociated weak electrolytes and other molecular species, and computation of activity coefficients of various ionic and molecular species in the aqueous phase. Edwards and Prausnitz used a simplified version of the emerging Pitzer model for the activity coefficient. Following Edwards et al**.** Chen et al**.,** 1979, extended the Pitzer activity coefficient model for modeling sour water stripping systems. Extension was made to the Pitzer model for computing activity coefficient of molecular solutes. The key advantage of the Pitzer model over other electrolyte activity coefficient models such as the Bromley model is its ability to represent the solution non-ideality at relatively high concentrations (up to 6 molal). It turns out that there are major issues with the use of the Pitzer model in process simulators. The Pitzer model requires both binary and ternary parameters for two-body and three body ion–ion interactions. For example, the Pitzer model would require hundreds of binary ion–ion interaction parameters and thousands of ternary ion–ion–ion interaction parameters for an aqueous solution with 10 ionic species. The issue with the Pitzer model is the empirical nature of its polynomial expressions and its highly non-ideal temperature dependencies associated with the binary and ternary interaction parameters. Another issue with the Pitzer model is that its formulation is based on the concentration scale of molality. While such a formulation allows accurate treatment of many aqueous electrolyte systems up to 6 molal, the molality-scale formulation breaks down completely and the model extrapolation goes wild as electrolyte concentration increases toward unity mole fraction and the molality approaches infinity. In practice, the Pitzer model and other similar molality-scale models can only be used for dilute aqueous electrolyte systems. This challenge called for the development of new activity coefficient models for aqueous electrolyte systems. The models would require no ternary parameters, be formulated in the concentration scale of mole fractions, represent a higher level of molecular insights, and preferably be compatible with existing well-established activity coefficient models. Compatibility with existing models would allow re-use and even expanded

use of intellectual knowledge and expertise in the industry. We set out to develop a molecular thermodynamic model for electrolyte solutions with the recognition that the liquid lattice structure of electrolyte solutions, while lacking long-range order like that of ionic crystals, must be strongly influenced by the same physical interactions extant in ionic crystals.

Two unique characteristics of the liquid lattice structure and the physical interactions were identified:

(1) like-ion repulsion, that is, around a central ion, there can only be ions of opposite charge at the immediate neighborhood of the central ion and

(2) Local electro-neutrality, that is, electro-neutrality of the solution must be maintained not only at the bulk solution level but also at the local lattice level.

After much research, we chose to develop an electrolyte model based on the semi-empirical local composition concept of non-random two-liquid (NRTL) model proposed by Prausnitz and coworkers for highly non-ideal mixtures of small molecules (Renon, and Prausnitz, 1968) The key reasons are

(1) The NRTL model is designed to account for the local physical interactions between nearest neighboring species, a key modeling consideration for electrolyte solutions,

(2) The NRTL model is algebraically simple to formulate, even when we take into account the additional physical characteristics of electrolyte solutions, i.e., like-ion repulsion and local electro-neutrality, and

(3) The NRTL model has already gained wide acceptance in the industry. The Wilson model (Wilson, 1964) was not considered because the model would not represent liquid–liquid equilibrium.

UNIQUAC (Abrams, J.M. Prausnitz, 1975) was also dropped due to its relative complexity in model formulations and because we were focusing on systems of small ionic species for which the UNIQUAC combinatorial term is of no relevance. Around 1980, Pitzer presented a reformulated electrolyte model based on the mole fraction (Pitzer, 1980). The model includes a long-range ion–ion interaction term for the Debye–Huckel limiting law and a short-range

interaction term based on the Margules equation. We presented the electrolyte NRTL model (e-NRTL) that combines the mole fraction version of the Pitzer–Debye–Huckel equation for the long-range ion–ion interaction term and the NRTL local composition equation reformulated for electrolytes (Chen et al., 1982). The resulting e-NRTL model proves to be a simple and practical molecular thermodynamic model for correlating and extrapolating thermodynamic properties of electrolyte solutions. The model reduces to the original NRTL model for nonelectrolytes. It requires only binary parameters and offers reasonable extrapolation to high concentrations as the model covers all electrolyte concentrations from infinite dilution to ionic liquids or fused salts. While electrolyte solutions follow the Debye-Huckel limiting law at low concentrations and the NRTL local composition model presents a simple perturbation on top of the Debye-Huckel limiting law, the NRTL term actually takes over as the dominant term with increasing electrolyte concentrations. Over the years, the like-ion repulsion concept has been well accepted and adopted by many researchers in their work. However, the local electroneutrality concept has been challenged and considered as a convenient way designed to "minimize" the number of model parameters. In reality, the local electro-neutrality concept and the like-ion repulsion concept together represent the molecular insights we try to capture in the model. The local electro-neutrality concept suggests that the short-range ion–solvent interaction is closely coupled with the long-range ion–ion interaction. In other words, the ion–solvent interaction of a specific ion is subject to the identity and characteristics (size, shape, polarity, charge number, etc.) of its counter-ion. These molecular insights are central to the e-NRTL model and its success. Continuing progress with the e-NRTL model over the past several decades has enabled rigorous modeling of industrial chemical processes not only with emission treatments such as sour water stripping, flue gas desulfurization, acid gas removal (Austgen et al., 1989,1991) **,** etc., but also with all types of industrial chemicals such as caustic soda (Chen et al., 1988), soda ash(sodium carbonate) (Lorant, and Davoine, 1991), phosphoric acid (Messnaoui and Bounahmidi, 2005), hydrochloric acid(Chen, L.B. Evans, 1986)**,** hydroiodic acid (Mathias et al., 2001), nitric acid (Muraoka, 2005)**,** sulfuric acid(Chen, S.M. Goldfarb, 1988), solution mining(Pinsky, G. Gruber, 1994), alumina(Khoze, P.M. Mathias, 2004), hydro-metallurgical processes(Pilate, 1988), zwitterions such as amino acids (Chen et al , 1989, Hessen et al., 2010, Zhang and Chen 2011) and antibiotics(Zhu et al., 1990), organic electrolytes (Chen et al., 2001), mixed solvent electrolytes(Mock, 1986, Chen and Song, 2004), nuclear waste treatment (Gorensek et al., 2003),

ionic liquids (Belveze et al. ,2004), etc. Not much of this progress has been published in the open literature, despite worldwide use of the model in process simulators.

The e-NRTL model has served as a comprehensive molecular thermodynamic model for virtually all types of electrolyte systems encountered in industry today.

The use of the electrolyte NRTL model covers wide varieties of aqueous and mixed-solvent electrolyte systems over the entire concentration range from pure solvents to saturated solutions or fused salts. For the rational gas treating processes the knowledge of VLE of the acid gas over alkanolamine solution is required besides the knowledge of mass transfer and kinetics. Excess Gibbs energy-based activity coefficient models provide a practical and rigorous thermodynamic framework to model thermodynamic properties of aqueous electrolyte systems, including aqueous alkanolamine systems for CO_2 capture (Chen, 2006; Zhang and Chen,2011). With the use of the electrolyte NRTL model for the liquid-phase activity coefficients, the equation of state (EOS) is used for its ability to model vapor-phase fugacity coefficients.

The excess Gibbs energy models provide rigorous thermodynamic frameworks for computing various electrolyte thermodynamic properties, including mean ionic activity coefficients, osmotic coefficients, and solute and solvent fugacities, for example. The rigorous and accurate computation of electrolyte thermodynamic properties forms a sound foundation for phase equilibrium calculations (that is, vapor–liquid equilibrium, liquid–liquid equilibrium, and salt solubilities), modeling and simulation for chemical processes involving electrolytes.

III-2) Electrolyte NRTL Model:

The e-NRTL model introduced by (Chen, 1986) is suitable for amine based processes due to its ability to handle electrolyte systems. However, this model requires that a large number of parameters are fitted against experimental data, usually partial and total pressures. It is suitable for modeling CO_2 capture/acid gas removal process, since it's able to correct the non-ideal behavior of aqueous multi-component electrolyte systems.

Thermodynamic modeling of these multi-component systems is very challenging. The reactions taking place in the solution give rise to a number of new ions and molecules. To properly

simulate and design the CO_2 absorption/stripping processes with the aqueous alkanolamine solutions, it is essential to understand the process fundamentals. Knowledge of vapor–liquid equilibrium is the basis for the simulation and design of acid gas absorption/stripping processes (Austgen et al., 1989). In addition, mass transfer rate-based simulation models require knowledge on liquid phase speciation resulting from aqueous phase reactions.

Scalable simulation, design, and optimization of the CO_2 capture processes start with modeling of the thermodynamic properties, specifically vapor-liquid equilibrium (VLE) and chemical reaction equilibrium, as well as calorimetric properties. Accurate modeling of thermodynamic properties requires availability of reliable experimental data.

In electrolyte solutions a larger variety of interactions and phenomena exist than in non - electrolyte solutions. Besides physical and chemical molecule-molecule interactions, ionic reactions and interactions occur (molecule-ion and ion-ion). For the thermodynamic modeling of this kind of systems the electrolyte non-random two-liquid model (e-NRTL) is applied (Aspen plus Technology, 2016).

Table III.1 summarizes the models and equations used for the calculation of the physical properties in the liquid and vapor phase and shows the interaction dependencies among the models

Table III.1: Applied thermodynamic models and equations within the e-NRTL model.

Thermodynamic Property	Models / equations
Liquid Phase	
Enthalpy	Electrolyte NRTL enthalpy model Required sub-models: - General pure component ideal gas heat capacity - General pure component heat of vaporization -Electrolyte NRTL activity coefficient model - Aqueous Infinite Dilution Heat Capacity
Gibbs energy	Electrolyte NRTL Gibbs free energy model Required sub-models: - General pure component ideal gas heat capacity - Electrolyte NRTL activity coefficient model -Aqueous Infinite Dilution Heat Capacity
Entropy	Relation between Gibbs free energy, Enthalpy and Entropy - Electrolyte NRTL enthalpy model - Electrolyte NRTL Gibbs free energy model
Density	Clarke aqueous electrolyte volume Required sub-model: - Rackett equation
Activity coefficients	Electrolyte NRTL activity coefficient model
Fugacity	Brelvi-O'connell model Electrolyte activity coefficient model Extended Antoine Henry's law Rackett equation Soave-Redlich-Kwong
Vapor phase	
Enthalpy, Gibbs energy, Entropy	Soave-Redlich-Kwong General pure component ideal gas heat capacity correlation
Fugacity coefficient Density	Soave-Redlich-Kwong

III.3) Liquid phase:

The following section summarizes the models used for the thermodynamic description of the liquid phase physical properties which are constantly used in the Aspen plus Technology, 2016.

III.3.1) Electrolyte NRTL enthalpy model:

The equation for the electrolyte NRTL enthalpy model is:

$$H_m^* = x_w H_w^* + \sum_s x_s H_s^{*,l} + \sum_k x_k H_k^{\infty} + H_m^{*,E} \quad \text{(III.1)}$$

The molar enthalpy H_m^* and the molar excess enthalpy $H_m^{*,E}$ are defined with the asymmetrical reference state: the pure solvent water and infinite dilution of molecular solutes and ions. (* refers to the asymmetrical reference state). x_w, x_s, x_k , are the mole fraction of water (w), non-water solvent (s) and ion or molecular solute (k),

H_w^* : is the liquid enthalpy for water,

$$H_w^* = \Delta_f H_w^{*,ig} + \int_{298.25}^{T} C_p^{ig}\, dT \quad \text{(III.2)}$$

Where**:** $\Delta_f H_w^{*,ig}$ is the Standard enthalpy of formation for ideal gas at T^{ref} (25 °C, 298.15 k), C_p^{ig} is the ideal gas heat capacity.

$H_s^{*,l}$: is the liquid enthalpy for non-water solvents

$$H_s^{*,l} = H_s^{*,ig} - \Delta H_{s,vap} \quad \text{(III.3)}$$

Where: $H_s^{*,ig}$ (J/kmol) is the ideal gas enthalpy of non-water solvents, and , $\Delta H_{s,vap}$: is the enthalpy of vaporization of non-water solvents.

H_k^{∞}: is the aqueous infinite dilution enthalpy

$$H_k^{\infty} = \Delta_f H_k^{\infty,aq} + \int_{298.25}^{T} C_p^{\infty,aq}\, dT \quad \text{(III.4)}$$

Where, $\Delta_f H_k^{\infty,aq}$ is the aqueous phase heat of formation at infinite dilution and 25 °C for ionic species and molecular solutes, and, $C_p^{\infty,aq}$ is the aqueous infinite dilution heat capacity.

C_p^{ig} is obtained from the ideal gas heat capacity model , $\Delta H_{s,vap}$: from the heat of vaporization model, $C_p^{\infty,aq}$: (J/kmol K) from the aqueous infinite dilution heat capacity model, and $H_m^{*,E}$: is calculated based on the electrolyte NRTL activity coefficient model .

Parameter requirements for the electrolyte NRTL enthalpy model are : $\Delta_f H_w^{*,ig}$(J/kmol) , $\Delta_f H_k^{\infty,aq}$ (J/kmol) .

III.3.2) Electrolyte NRTL Gibbs free energy model:

$$G_m^* = x_w \mu_w^* + \sum_s x_s \mu_s^{*,l} + \sum_k x_k \mu_k^{\infty} + RT \sum_j x_j \, ln x_j + G_m^{*,E} \quad \text{(III.5)}$$

Where: x_w, x_s, x_k are the mole fraction of water (w), non-water solvent (s) and ion or molecular solute (k), μ_w^* is the molar Gibbs free energy of pure water (thermodynamic potential), $\mu_s^{*,l}$ is the Gibbs free energy of a non-water solvent, μ_k^{∞} is the aqueous infinite dilution thermodynamic potential, $RT \sum_j x_j \, ln x_j$: is the ideal mixing term, where j refers to any component, R is the ideal gas constant, T is the temperature, and, $G_m^{*,E}$is the molar excess Gibbs free energy. The molar excess Gibbs free energy $G_m^{*,E}$ (J/kmol): is calculated based on the electrolyte NRTL activity coefficient model with the following equation:

$$G_m^{*,E} = RT \sum_i x_i \, ln \gamma_i \quad \text{(III.6)}$$

The thermodynamic potential μ_k^{∞} is calculated based on the infinite dilution aqueous phase heat capacity polynomial as followed:

$$\mu_k^{\infty} = H_k^{\infty} - TS_k^{\infty} + RT ln\left(\frac{1000}{M_w}\right) \quad \text{(III.7)}$$

$$H_k^{\infty} = \Delta_f H_k^{\infty,aq} + \int_{298.25}^{T} C_{p,k}^{\infty,aq} \, dT \quad \text{(III.8)}$$

$$S_k^{\infty} = \frac{\Delta_f H_k^{\infty,aq} - \Delta_f G_k^{\infty,aq}}{298.15} + \int_{298.25}^{T} \frac{C_{p,k}^{\infty,aq}}{T} dT \quad \text{(III.9)}$$

Where: M_w: is the molecular mass of water, $\Delta_f H_k^{\infty,aq}$ (J/kmol) is the infinite dilution aqueous phase enthalpy of formation for component k, $C_{p,k}^{\infty,aq}$ is the aqueous infinite dilution heat capacity for component k, S_k^{∞} is the mole entropy, and, $\Delta_f G_k^{\infty,aq}$ is the infinite dilution aqueous phase standard Gibbs free energy for component k. $C_{p,k}^{\infty,aq}$ is obtained from the aqueous infinite

dilution enthalpy model, and $\Delta_f H_k^{\infty,aq}$ from the input requirements of the electrolyte NRTL enthalpy model.

Parameter requirements for the electrolyte NRTL Gibbs free energy model are: $\Delta_f G_w$ (J/kmol), , $\Delta_f G_k^{\infty,aq}$ (J/kmol) ,

III.3.3) Electrolyte NRTL Activity Coefficient Model:

The electrolyte NRTL model consists of three contributions. The first contribution is the long-range contribution represented by the Pitzer-Debye-Hückel expression, which accounts for the contribution due to the electrostatic forces among all ions. The second contribution is an ion-reference-state-transfer contribution represented by the born expression. In the electrolyte NRTL model, the reference state for ionic species is always infinitely dilute state in water even when there are mixed solvents. The Born expression accounts for the change of the Gibbs energy associated with moving ionic species from a mixed solvent infinitely dilute state to an aqueous infinitely dilute state. The Born expression drops out if water is the sole solvent in the electrolyte system. The third contribution is a short-range contribution represented by the local composition electrolyte NRTL expression, which accounts for the contribution due to short-range interaction forces among all species. The electrolyte NRTL expression was developed based on the NRTL local composition concept, the like ion repulsion assumption, and the local electro-neutrality assumption. The like-ion repulsion assumption stipulates that in the first coordination shell of a cation (anion) the local composition of all other cations (anions) is zero. The local electro-neutrality assumption imposes a condition that in the first coordination shell of a molecular species the composition of cations and anion is such that the local electric charge is zero.

The NRTL expression for the local interactions, the Pitzer-Debije-Hückel expression, and the born equation are added to give equation 1 for the excess Gibbs energy. The Pitzer-Debye-Hückel expression for excess Gibbs energy, normalized to a mole fraction of unity for the solvent and zero mole fractions for ions, is given as follows:

$$\frac{G_m^{*E}}{RT} = \frac{G_m^{*E,PDH}}{RT} + \frac{G_m^{*E,Born}}{RT} + \frac{G_m^{*E,lc}}{RT} \qquad \text{(III.10)}$$

Where, "*" denotes the unsymmetric convention

PDH is the Pitzer-Debye- Hückel contribution for long range ion-ion interactions, Born is the Born Correction for change in mixed solvent reference state, and lc: is the local contribution for short range interactions.The term $G_m^{*E,PDH}$ and $G_m^{*E,Born}$ represents the long range forces contribution with reference state of the ions at infinite dilution in water.

The activity coefficient for any species i, ionic or molecular, solute or solvent, is derived from the partial derivative of the excess Gibbs energy with respect to the mole number of species i

$$ln\gamma_i = \frac{1}{RT}\left[\frac{\partial(n_i G^{*E}}{\partial n_i}\right]_{T,P,n_j\neq i} \quad \text{(III.11)}$$

i , j= molecule, cation ,anion

Where γ_i is the activity coefficient of species i in solution,n_i is the number of moles of i, and G_m^{*E} is the excess Gibbs free energy of the system, defined as

$$G_m^E = G_m - G_m^{id} \quad \text{(III.12)}$$

Where G_m is the Gibbs energy of electrolyte systems and G_m^{id} is the Gibbs energy of an ideal solution at the same conditions of temperature, pressure, and composition

This leads to: $$\mathrm{Ln}\gamma_i^* = \mathrm{Ln}\gamma_i^{*PDH} + \mathrm{Ln}\gamma_i^{*Born} + \mathrm{Ln}\gamma_i^{*lc} \quad \text{(III.13)}$$

III.3.4) Long-range interaction contribution:

The Pitzer-Debije-Hückel formula, normalized to mole fractions of unity for solvent and zero for electrolytes, is used to represent the long-range interaction contribution (Pitzer and Simonson, 1986).

$$\frac{G_m^{*E,PDH}}{RT} = -(\sum_k x_k)\left(\frac{1000}{M_s}\right)^{0.5}\left(\frac{4A_\phi I_x}{\rho}\right)\ln(1+\rho I_x^{0.5}) \quad \text{(III.14)}$$

x_k : Mole fraction of component k, M_s : Molecular weight of the solvent , A_ϕ : Debije-Hückel parameter, ρ: is the "Closest approach" parameter.

$$\mathrm{A_\phi} = \frac{1}{3}\left(\frac{2\pi \mathrm{N_A\, d}}{1000}\right)^{0.5}\left(\frac{\mathrm{Q_e^2}}{\varepsilon_w\, \mathrm{kT}}\right)^{1.5} \quad \text{(III.15)}$$

N_A : Avogadro's number, d: Density of solvent, Q_e : Electron charge, ε_w : Dielectric constant of water, T : Temperature, k : Boltzmann constant

I_x : Ionic strength (mole fraction scale): $I_x = \sum_i x_i Z_i^2$ (III.16)

x_i: Mole fraction of component i, Z_i = Charge number of ion i,

III.3.5) Born term correction to activity coefficient:

If the infinite-dilution aqueous solution is chosen as the reference state, we need to correct the change of the reference state from the mixed-solvent composition to aqueous solution for the Debye–Huckel term. The Born term (Rashin and Honig, 1985; Robinson and Stokes, 1970) is used for this purpose

$$\frac{G_m^{*E,Born}}{RT} = \frac{Q_e^2}{2kT}\left(\frac{1}{\varepsilon_s} - \frac{1}{\varepsilon_w}\right)\frac{\sum_i x_i Z_i^2}{r_i}10^{-2} \quad \text{(III.17)}$$

Where ε_s: is the dielectric constant of the solvent, and r_i : Born radius ,

The expression for the activity coefficient can be derived from (7):

$$Ln\gamma_i^{*Born} = \frac{Q_e^2}{2kT}\left(\frac{1}{\varepsilon_s} - \frac{1}{\varepsilon_w}\right)\frac{Z_i^2}{r_i}10^{-2} \qquad i: c, a \quad \text{(III.18)}$$

The dielectric constant specifies a component's ability to stabilize an ionic solution. As the dielectric constant increases, the tendency for ions to form and remain as ionic species also increases (Hilliard, 2008). The temperature dependent correlation for the dielectric constants is described with the following equation:

$$\varepsilon_i = A_i + B_i\left(\frac{1}{T} - \frac{1}{C_i}\right) \quad \text{(III.19)}$$

Where,

A_i, B_i, C_i , are coefficients, which describe the temperature dependency of the dielectric constant for a solvent i, T: temperature K

III.3.6) NRTL term for local interaction contribution:

The local contribution term accounts for the local interactions that exist at the immediate neighborhood of any species. The model assumes that there are three types of local composition

interactions. The first type consists of a central molecular species with other molecular species, cationic species, and anionic species in the immediate neighbor-hood. Here, local electro-neutrality is maintained. The other two

types are based on the like-ion repulsion assumption and have either cationic or anionic species as the central species. They also have an immediate neighborhood consisting of molecular species and oppositely charged ionic species. Accordingly, the excess Gibbs energy from local interactions for an electrolyte system can be written as follows:

$$\frac{G_m^{*E,lc}}{RT} = \sum_m x_m \frac{\sum_j x_j G_{jm}\tau_{jm}}{\sum_K x_k G_{km}} + \sum_c x_c \sum_{a'} \left(\frac{x_{a'}}{\sum_{a''} x_{a''}}\right) \frac{\sum_j x_j G_{jc,a'c}\tau_{jc,a'c}}{\sum_k x_k G_{kc,a'c}} + \cdots$$

$$\ldots + \sum_a x_a \sum_{c'} \left(\frac{x_{c'}}{\sum_{c''} x_{c''}}\right) \frac{\sum_j x_j G_{ja,c'a}\tau_{ja,c'a}}{\sum_k x_k G_{ka,c'a}} \qquad \text{(III.20)}$$

Where: j and k can be any species, and Subscripts m, c, and a, represent molecules, cations, and anions, respectively.

The short range molecular forces need to be included to account for hydrogen bonds and local interactions of molecules with molecules, molecules with ion pairs, and ion pairs with ion pairs. These interactions are described by the non-random two liquids (NRTL) theory developed by (Renon and Prausnitz, 1968).

The like-ion repulsion assumption states that the local compositions of cations around cations and anions around anions are zero. The local electro-neutrality assumption states that the local charge is always zero. The NRTL term in the excess Gibbs free energy expression is a strong function of interaction parameters, defined in equation

$$\tau_{ij,ki} = \frac{g_{ij} - g_{ki}}{RT} \qquad \text{(III.21)}$$

g_{ij}, g_{ki} are the energies of interaction of species i with species j and k respectively.

Equation (10) is the basis for the non-random distribution of species j and k around species i. The local mole fractions of j and k around i, x_{ij} and $x\,ki_{ki}$, are calculated according to equations (11) and (12), where x_j=($x_j C_j$), C_j is the charge Z for ions and unity for molecules, x_j is the total mole fraction of j in solution, and $\alpha_{ji,ki}$ is a parameter called non-randomness factor. α is a symmetric parameter: $\alpha_{ji} = \alpha_{ij}$.

$$\frac{x_{ji}}{x_{ki}} = \left(\frac{x_i}{x_k}\right) G_{ji,kj} \qquad \text{(III.22)}$$

$$G_{ji,kj} = e^{(-\alpha_{ji,kj}\tau_{ji,ki})} \quad \text{(III.23)}$$

The local composition around a species i, that can be a molecule, an anion or a cation, is determined by the relative energies of interaction of every species with species i. The τ values are impossible to measure and they have to be obtained by numerical regression. The electrolyte NRTL parameter consists of both the non-randomness factor, α , and energy parameters, τ.

A) The activity coefficient equation for molecular components is given by:

$$ln\gamma_m^{lc} = \frac{\sum_j x_j G_{jm}\tau_{jm}}{\sum_k x_k G_{km}} + \sum_{m'} \frac{x_{m'} G_{mm'}}{\sum_k x_k G_{km'}} \left(\tau_{mm'} - \frac{\sum_k x_k G_{km'}\tau_{km'}}{\sum_k x_k G_{km'}}\right) + \sum_c \sum_{a'} \frac{x_a}{\sum_{a''} x_{a''}} \frac{x_c G_{mc,a'c}}{\sum_k x_k G_{kc,a'c}} \left(\tau_{mc,a'c} - \frac{\sum_k x_k G_{kc,a'c}\tau_{kc,a'c}}{\sum_k x_k G_{kc,a'c}}\right) + \sum_a \sum_{c'} \frac{x_{c'}}{\sum_{c''} x_{c''}} \frac{x_a G_{ma,c'a}}{\sum_k x_k G_{ka,c'a}} \left(\tau_{mc,c'a} - \frac{\sum_k x_k G_{ka,c'a}\tau_{ka,c'a}}{\sum_k x_k G_{ka,c'a}}\right) \quad \text{(III.24)}$$

B)The activity coefficient equation for cations is given by:

$$\frac{1}{Z_c} ln\gamma_c^{lc} = \sum_{a'} \left(\frac{x_{a'}}{\sum_{a''} x_{a''}}\right) \frac{\sum_k x_k G_{kc,a'c}\tau_{kc,a'c}}{\sum_k x_k G_{kc,a'c}} + \sum_{m'} \frac{x_m G_{cm}}{\sum_k x_k G_{km}} \left(\tau_{cm} - \frac{\sum_k x_k G_{km}\tau_{km}}{\sum_k x_k G_{km}}\right) + \sum_a \sum_{c'} \left(\frac{x_{c'}}{\sum_{c''} x_{c''}}\right) \frac{x_a G_{ca,c'a}}{\sum_{kc} x_k G_{ka,c'a}} \left(\tau_{ca,c'a} - \frac{\sum_k x_k G_{ka,c'a}\tau_{ka,c'a}}{\sum_k x_k G_{ka,c'a}}\right) \quad \text{(III.25)}$$

C)The activity coefficient equation for anions is given by:

$$\frac{1}{Z_a} ln\gamma_a^{lc} = \sum_{c'} \left(\frac{x_{c'}}{\sum_{c''} x_{c''}}\right) \frac{\sum_k x_k G_{ka,c'a}}{\sum_k x_k G_{ka,c'a}} + \sum_m \frac{x_m G_{am}}{\sum_k x_k G_{km}} \left(\tau_{am} - \frac{\sum_k x_k G_{km}\tau_{km}}{\sum_k x_k G_{km}}\right) + \sum_c \sum_{a'} \left(\frac{x_{a'}}{\sum_{a''} x_{a''}}\right) \frac{x_c G_{ac,a'c}}{\sum_{kc} x_k G_{kc,a'c}} \left(\tau_{ac,a'c} - \frac{\sum_k x_k G_{kc,a'c}\tau_{kc,a'c}}{\sum_k x_k G_{kc,a'c}}\right) \quad \text{(III.26)}$$

D) Binary parameters:

$G_{jm} = Exp(-\alpha_{jm}\tau_{jm})$, $G_{jc,ac} = Exp(-\alpha_{jc,ac}\tau_{jc,ac})$, $G_{ja,ca} = Exp(-\alpha_{ja,ca}\tau_{ja,ca})$

$$G_{cm} = \frac{\sum_a x_a G_{ca,m}}{\sum_{a'} x_{a'}} \qquad G_{am} = \frac{\sum_c x_c G_{ca,m}}{\sum_{c'} x_{c'}}$$

$$\alpha_{mc} = \alpha_{cm} = \frac{\sum_a x_a \alpha_{ca,m}}{\sum_{a'} x_{a'}} \qquad \alpha_{ma} = \alpha_{am} = \frac{\sum_c x_c \alpha_{ca,m}}{\sum_{c'} x_{c'}}$$

$$\tau_{mc,ac} = \tau_{cm} - \tau_{ca,m} + \tau_{mc,a} \qquad \tau_{ma,ca} = \tau_{am} - \tau_{ca,m} + \tau_{mc,a}$$

The adjustable model parameters are the symmetric non-random factor parameters, α, and the asymmetric binary interaction energy parameters, τ. These parameters exist for molecule-molecule pairs ($\alpha_{mm'} = \alpha_{m'm}$, $while\ \tau_{mm'} \neq \tau_{m'm}$), molecule-electrolyte pairs ($\alpha_{m,ca} = \alpha_{ca,m}$, $while\ \tau_{m,ca} \neq \tau_{ca,m}$), and electrolyte-electrolyte pairs ($\alpha_{ca,ca'} = \alpha_{ca',ca}$, $and\ \alpha_{c'a,ca} = \alpha_{ca,c'a} while\ \tau_{ca,ca'} \neq \tau_{ca',ca}, and\ \tau_{c'a,ca} \neq \tau_{ca,c'a}$).

$$\tau_{m,ca} = C_{m,ca} + \frac{D_{m,ca}}{T} + E_{m,ca}\left[\frac{T^{ref} - T}{T} + \ln\left(\frac{T}{T^{ref}}\right)\right]$$

$$\tau_{ca,m} = C_{ca,m} + \frac{D_{ca,m}}{T} + E_{ca,m}\left[\frac{T^{ref} - T}{T} + \ln\left(\frac{T}{T^{ref}}\right)\right]$$

$$\tau_{ca,c'a} = C_{ca,c'a} + \frac{D_{ca,c'a}}{T} + E_{ca,c'a}\left[\frac{T^{ref} - T}{T} + \ln\left(\frac{T}{T^{ref}}\right)\right]$$

$$\tau_{c'a,ca} = C_{c'a,ca} + \frac{D_{c'a,ca}}{T} + E_{c'a,ca}\left[\frac{T^{ref} - T}{T} + \ln\left(\frac{T}{T^{ref}}\right)\right]$$

$$\tau_{ca,ca'} = C_{ca,ca'} + \frac{D_{ca,ca'}}{T} + E_{ca,ca'}\left[\frac{T^{ref} - T}{T} + \ln\left(\frac{T}{T^{ref}}\right)\right]$$

$$\tau_{ca',ca} = C_{ca',ca} + \frac{D_{ca',ca}}{T} + E_{ca',ca}\left[\frac{T^{ref} - T}{T} + \ln\left(\frac{T}{T^{ref}}\right)\right]$$

Where: $T^{ref} = 298$ K, and, C, D, E are the coefficients, which describe the temperature dependency of the energy parameters.

The temperature dependency of the NRTL parameters used for molecule-molecule parameters is given by:

$$\tau_{i,j} = A_{ij} + \frac{B_{ij}}{T} + FlnT + G_{ij}T$$

$$\alpha_{ij} = C_{ij} + D_{ij}(T - T^{ref})$$

III.3.7) Pure component ideal gas heat capacity:

Depending on the given properties, the ideal gas heat capacity for pure component is calculated with different equations (Aspen plus, 2016). The ideal gas heat capacity polynomial used with aqueous, solid etc. is:

$$C_{p,i}^{*,ig} = C_{1i} + C_{2i}T + C_{3i}T^2 + C_{4i}T^3 + C_{5i}T^4 + C_{6i}T^5 \quad \text{(III.27)}$$

For pure components, H_2O, CO_2 and other components, the DIPPR (DIPPR: Design Institute for Physical Properties) equation by (Aly and Lee 1981) is used:

$$C_{p,i}^{*,ig} = C_{1i} + C_{2i}\left(\frac{C_{i3}/T}{sinh(C_{i3}/T)}\right)^2 + C_{4i}\left(\frac{C_{i5}/T}{sinh(C_{i5}/T)}\right)^2 \quad \text{(III.28)}$$

The coefficients used to describe the temperature dependency of the ideal gas heat capacity for amines, H_2O and acid gas are summarized in Table below

III.3.8) Pure component enthalpy of vaporization:

Depending on the given properties, the heat of vaporization for pure components is calculated with different equations. For H_2O, acid gas and amine, the Watson heat of vaporization equation is used (Aspen plus Technologies, 2016**)**. It estimates the heat of vaporization of a pure liquid component at any temperature from the known value at a single temperature $\Delta H_i(T_1)$.

$$\Delta_{vap} H_i^*(\mathrm{T}) = \Delta_{vap} H_i^*(T_1)\left(\frac{1-T/T_{ci}}{1-T_1/T_{ci}}\right)^{a_i + b_i(1-T/T_{ci})} \quad \text{(III.29)}$$

Where, T_{ci}: is the critical temperature, T: is the temperature in K.

DIPPR heat of vaporization equation is:

$$\Delta_{vap} H_i^* = C_{1i}(1 - T_{ri})^{C_{2i} + C_{3i}T_{ri} + C_{4i}T_{ri}^2 + C_{5i}T_{ri}^3} \quad \text{for } T_{6i} \le T \le T_{7i} \quad \text{(III.30)}$$

Where, T_{ri} is the reduced temperature T/T_{ci} , T_{ci} is the critical temperature of component i, T is the temperature in K.

III.3.9) Aqueous infinite dilution heat capacity model:

The aqueous phase infinite dilution enthalpies, entropies, and Gibbs energies of aqueous and mixed solvent properties are calculated from the heat capacity polynomial.

$$C_{p,i}^{\infty,aq} = C_{1i}+C_{2i}T + C_{3i}T^2 + C_{4i}/T \quad \text{(III.31)}$$

$C_{1i}, C_{2i}, C_{3i}, C_{4i}$: Coefficients for all ionic species

III.4) Henry's constants:

The Henry's constants are an important part for the vapor liquid equilibrium of dissolved gases. Henry's law is used to predict the solubility of a gases, such as CO_2, in the solvent and is applied to molecular solutes in enthalpy and aqueous chemistry algorithms. There are two activity coefficient basis for Henry components, mixed solvent and aqueous. Thus the reference state for the activity coefficient of molecular solutes can be chosen between infinite dilution in a mixed solvent or infinite dilution in an aqueous solvent. The Henry's constant in the mixed solvent can be calculated from those of the pure solvents (Van Ness, and Abbott ,1979)

$$\ln\left(\frac{H_i}{\gamma_i^{\infty}}\right) = \sum_A x_A \ln\left(\frac{H_{iA}}{\gamma_{iA}^{\infty}}\right) \quad \text{(III.32)}$$

Where: H_{iA} The Henry's constant of supercritical component i in pure solvent A, the infinite dilution activity coefficient of supercritical component i in the mixed solvent, γ_{iA}^{∞} : the infinite dilution activity coefficient of supercritical component i in pure solvent A, and x_A the mole fraction of solvent A, and H_i is the Henry's constant of supercritical component in the mixed solvent. W_A: is used instead of x_A in Equation (3) to weigh the contributions from different solvent (Aspen plus, 2010). The parameter W_A is calculated using Equation 4:

$$w_A = \left(\frac{x_A (V_i^{\infty})^{\frac{2}{3}}}{\sum_B x_B (V_i^{\infty})^{\frac{2}{3}}}\right) \quad \text{(III.33)}$$

$\boldsymbol{V_i^{\infty}}$: represents the partial molar volume of supercritical component i at infinite dilution in pure solvent A, calculated from the Brelvi-O'connell model (Brelvi and O'Connell , 1972) with the characteristic volume for the solute ($\boldsymbol{V_{CO2}^{BO}}$) and solvent ($\boldsymbol{V_{CO2}^{BO}}$).

The correlation for Henry's constant is given as follows:

$$\ln\left(\frac{H_i}{\gamma_i^{\infty}}\right) = a_{ij} + b_{ij}\, lnT + C_{ij} lnT + d_{ij} lnT \qquad \text{(III.34)}$$

Where, $(a_{ij}, b_{ij}, c_{ij}, d_{ij})$ are the coefficients, which describe the temperature dependency of the Henry's constant, T: temperature (K).

The Henry's constant of the acid gas component i in solvent A is further corrected with the Poynting term for pressure:

$$\boldsymbol{H_{iA}(T,P) = H_{iA}\left(T, P_A^{*,l}\right) exp\,(\frac{1}{RT}\int_{P_A^{*,l}}^{P} V_i^{BO} dp} \qquad \text{(III.35)}$$

Where $\boldsymbol{H_{iA}(T,P)}$the Henry is's constant of the acid gas in solvent A at system temperature T and system pressure P. $\boldsymbol{H_{iA}\left(T, P_A^{*,l}\right)}$ is the Henry's constant of the acid gas in solvent A at system temperature and the solvent vapor pressure. The parameter $\boldsymbol{V_i^{BO}}$ (m^3/mol) is the partial molar volume of a supercritical component i at infinite dilution in solvent A. It is obtained from Brelvi-O'Connell model, $\boldsymbol{P_A^{*,l}}$, from the Antoine model, **exp** $(\frac{1}{RT}\int_{P_A^{*,l}}^{P} V_i^{BO} dp$: is the Henry´s constant pressure correction term, and $\boldsymbol{\gamma_i^{\infty}}$ is obtained from the appropriate activity coefficient model.

III.4.1) Brelvi-O'Connell-model:

The Brelvi-O'Connell model calculates the partial molar volume of a supercritical component i at infinite dilution in pure solvent A. Partial molar volume at infinite dilution is required to compute the effect of pressure on Henry's constant (see Henry's constant). The general form of the Brelvi-O'Connell model is:

$$\boldsymbol{V_i^{\infty} = f(V_i^{BO}, V_A^{BO}, V_A^{*l})} \qquad \text{(III.36)}$$

Where: $\boldsymbol{V_i^{BO} = v_{i,1} + v_{2,i} T}$, is the Brelvi-O'Connell parameter, V_A^{*l}: is the liquid molar volume of solvent A.

The above correlation applies to both solute and solvent. The liquid molar volume of solvent is obtained from the Rackett model

III.4.2) Clarke Aqueous Electrolyte Volume:

The Clarke model calculates the liquid molar volume for electrolyte solutions.

$$V_m^l = \sum_i x_i V_i^{*,l} + \sum_j x_j k_{ij} \left(V_i^{*,l} V_j^{*,l}\right) \quad \text{(III.37)}$$

Where,
x_i : is the molar fraction of component i,

$V_i^{*,l}$: is the liquid molar volume of component i, and k_{ij} : is a binary interaction parameter.

III.4.3) Rackett equation:

The Rackett equation is used to predict the density of a pure liquid dependent on temperature based on its critical properties. One density value is required to calculate the Rackett constant in the equation. Then the critical properties T_C, V_C and P_C are used to estimate new density values as the temperature changes.

$$V_i^{*,l} = \frac{RT_{CA} Z_A^{RA\left[1+(1-T_{CA})^{2/7}\right]}}{P_{CA}} \quad \text{(III.38)}$$

III.4.4) Extended Antoine equation:

$$lnP_A^{*,l} = C_{1i} + \frac{C_{2i}}{T+C_{3i}} + C_{4i} T + C_{5i} lnT + C_{6i} T^{C_{7i}} \quad \text{(III.39)}$$

III.5) Aqueous phase chemistry:

Each chemical equilibrium in the liquid phase is characterized by a chemical equilibrium constant.

The processes discussed involve both chemical equilibria and multi-component phase equilibria. The liquid phase comprises both molecular species and ionic species, which makes the modelling nontrivial. The solution chemistry involves the different chemical reactions which occur in the liquid phase.

These chemical reactions occur rapidly in solution, so chemical equilibrium conditions are assumed. Solution chemistry affects electrolyte process simulation by influencing physical properties, phase equilibrium, and other fundamental characteristics of electrolyte systems.

The equilibrium constants of the chemical reactions can be expressed as follows $(\gamma_i x_i)^{\vartheta i}$

$$K_j = \prod_i (\gamma_i x_i)^{\vartheta i} = \prod_i \alpha_i^{\vartheta i} \quad \text{(III.40)}$$

Where K_j : is the chemical equilibrium constant, α_i : is the activity, ϑi : is the reaction stoichiometric coefficient of component i, x_i : is the mole fraction of component i, and, γ_i : is the activity coefficient of component i

There are two options how to define the chemical equilibrium constants. One option is to describe the equilibrium constants by its temperature dependent function. The temperature dependency of the equilibrium constants defined in mole-fraction scale is expressed by Equation (8)

$$lnK = a + \frac{b}{T} + c\ lnT + dT \quad \text{(III.41)}$$

Or another form of the equilibrium constant, K_j, of reaction j, can take place using the reference-state Gibbs free energies, G_j^0 , of the participating components

$$-RTlnK_j = \Delta G_j^0 \quad \text{(III.42)}$$

ΔG_j^0 : is the reference state Gibbs free energy , R : is the ideas gas constant

III.6) Vapor phase:

The vapor phase is represented by Soave's modification of the Redlich-Kwong equation. This equation-of-state can be used for hydrocarbon systems that include the common light gases, such as H_2S, CO_2 and N_2. The Soave-Redlich-Kwong equation is given by the following expression:

$$P = \frac{RT}{V_m - b} - \frac{a}{V_m(V_m + b)} \quad \text{(III.43)}$$

Where: V_m: is the molar Volume, a: is the energy parameter, and, b: the size parameter.

$$a = a_0 + a_1$$

a_0: is the standard mixing quadratic term:

$$a_0 = \sum_i \sum_j x_i x_j \left(a_i a_j\right)^{0.5} (1 - k_{ij}) \quad \text{(III.44)}$$

a_1 : is an additional, asymmetric (polar) term

$$a_1 = \sum_{i=l}^{n} \left(\sum_{j=l}^{z} x_j \left(\left(a_i a_j\right)^{0.5} l_{i,j}\right)^{\frac{1}{3}}\right)^3 \quad \text{(III.45)}$$

$$b = \sum_i x_i b_i \quad \text{(III.46)}$$

$$k_{ij} = k_{ji}$$

$$a_i = \alpha_i \, 0.42478 \frac{R^2 T_{Ci}^2}{P_{Ci}} \quad \text{(III.47)}$$

$$\alpha_i = \left[1 + m_i(1 - T_{ri}^{0.5})\right]^2 \quad \text{(III.48)}$$

$$m_i = 0.48 + 1.57\omega_i - 0.176\omega_i^2 \quad \text{(III.49)}$$

$$b_i = 0.08664 \frac{RT_{Ci}}{P_{Ci}} \qquad T_r = \frac{T_{Ci}}{T}$$

Where,

x: is the molar fraction, $k_{ij}, l_{i,j}$ are binary interaction parameters, T_{Ci} is the critical temperature,

P_{Ci} is the critical pressure, T_r is the reduced temperature, and ω_i : is the acentric factor

With this model the physical properties such as enthalpy, Gibbs free energy, Entropy, density and vapor fugacity coefficient are calculated based on fundamental thermodynamic relations . (Poling, et al., 2001)

III.7) Vapor-liquid equilibrium calculations:

When the physical properties are calculated the equilibrium between the vapor and liquid phase can be calculated. At equilibrium condition the fugacity of each component in liquid and vapor phase must be equal: $f^v = f^l$

The vapor-liquid equilibrium for non-Henry component species (aspen plus Technology, 2016).

$$y_i \phi_i^v P = x_i \gamma_i \phi_i^0 P_i^0 exp\left[\frac{V_i^l (P - P_i^0)}{RT}\right] \quad \text{(III.50)}$$

Where, y_i and x_i are the molar fractions in vapor and liquid phase respectively, P and T are the system pressure and temperature, R is the ideal gas constant, ϕ_i^v the vapor fugacity coefficient of component i in the mixture, γ_i is the activity coefficient of component i in the mixture, ϕ_i^0 liquid pure component fugacity coefficient of component i, P_i^0 pure component saturation pressure for component i, $exp\left[\frac{V_i^l (P - P_i^0)}{RT}\right]$ is the Poynting correction term, and V_i^l is the partial liquid molar volume of component i.

The vapor-liquid equilibrium for Henry components can be described with the equation (aspen plus ™, 2014):

$$y_i \phi_i^v P = x_i \gamma_i \left(\frac{H_i}{\gamma_i^{\infty,aq}}\right) exp\left[\frac{V_i^{\infty,aq} (P - P_i^0)}{RT}\right] \quad \text{(III.51)}$$

Where, H_i is the Henry's constant for component i, $\gamma_i^{\infty,aq}$ is the infinite dilution activity coefficient for component, $V_i^{\infty,aq}$ is the Brevi-O'Connell partial molar volume for component i.

Conclusion:

In amine-based acid gas capture, acid gas reacts with an aqueous amine solution, forming different electrolyte species, which means that the amine molecules ionize when they are dissolved in water. In electrolyte solutions a larger variety of interactions and phenomena exist than in non-electrolyte solutions. Besides physical and chemical molecule-molecule interactions, ionic reactions and interactions occur (molecule-ion and ion-ion). A rigorous thermodynamic model should give good predictions of the vapour liquid equilibria, the solution speciation and the heat evolved when acid gas is absorbed. Due to the complexity of electrolyte thermodynamics and solution chemistry, there remains a major industrial need to develop and compile public databanks of model parameters and solution chemistries for electrolyte systems of industrial significance.

The e-NRTL model proves to be a simple and practical molecular thermodynamic model for correlating and extrapolating thermodynamic properties of electrolyte solutions which is suitable for our amine based process due to its ability to handle our electrolyte systems.

Chapter IV

Kinetics of Absorption of Carbon Dioxide in Aqueous PZ,MDEA, Blended(MDEA-PZ),(PZ-Sulfolane), and (MDEA-Sulfolane)

Chapter IV: Kinetics of Absorption of Carbon Dioxide in Aqueous MDEA, PZ, Blended (MDEA-PZ), (PZ-Sulfolane), and (MDEA-Sulfolane)

Introduction

The presence of carbon dioxide within the natural gas causes an increase in gas volume, reduces its heat value and may enhance corrosion within pipelines and processing plants. The reaction kinetics data are one of the most important parameters when selecting a chemical solvent for CO_2 absorption. When the reaction kinetics of promising solvents are measured, they provide the needed information for designing and simulation of the absorption/ regeneration columns.

The most conventional method of acid gas sweetening that has been widely used in industry is chemical absorption through aqueous alkanolamines solutions. This technology allows for acid gas removal to low levels even at low acid gas pressures. Moreover, the loss of these aqueous solutions is not substantial and solubility of hydrocarbons is very low **(**Shirazizadeh, 2019**).** Some examples of industrial importance for primary amines are Monethanolamine (MEA) and Diglycolamine (DGA), and for secondary amines Diethanolamine (DEA) and Diisopropanolamine (DIPA), and finally for tertiary amines methyldiethanolamine (MDEA) and Triethanolamine (TEA). Mixed amines are also used such as amine blends of MDEA and Piperazine (PZ).(Kohl and Riesenfeld, 1997). In an amine molecule, the basicity is provided by the amino site while the presence of the O-H group results in an increased solubility in water (Barvek and Alper, 1999).

The choice of a certain amine (single or blended amine) is mainly based on the absorption capacity, reaction kinetics and regenerative potential, corrosion, degradation, cost and the composition of the sweet gas. A complete understanding of the reaction mechanism is necessary to select amines suitable for the selective removal of acid gases (Versteeg and Van swaaij, 1988a). Combining the absorption characteristics of each amine such as in amine blends have been suggested for the absorption of acid gases**.** Chakravarty et al*.,* (1985)**.** The suitability of an alkanolamine for a certain process is among other determined by the characteristics of its kinetics with CO_2. Since the reaction of all alkanolamines with H_2S only involves a proton transfer, its rate can be considered as instantaneous with respect to mass transfer, and thus detailed knowledge of the reaction kinetics of H_2S are of no importance. The reason for the use

of such a blend is related to the relatively high rate of reaction of CO_2 with the activator combined with the advantages of tertiary amine concerning regeneration and stoichiometric loading capacity, which leads to higher rates of absorption in the absorber column while maintaining a low heat of regeneration in the stripper section. Blended amine mixture, which have mainly consisted of a mixture of primary or secondary amine with a sterically hindered or tertiary amine, combine the higher CO_2 reaction rates of the primary or secondary amine with the higher CO_2 loading capacity of the sterically hindered or tertiary amine Chakravarty et al.,(1985).

The mixtures were found to be very attractive for bulk CO_2 removal, as these blends combine the higher reaction rates between CO_2 and primary or secondary amines with the easier regeneration and higher absorption capacities of tertiary amines.

The use of piperazine (PZ) activated aqueous MDEA solutions were patented by BASF (BASF: is a German chemical group and the largest chemistry group in the world. Frederic Engelhorn founded the BASF whose abbreviation originally meant (Badische Anilin- & Soda-Fabrik.) as it proved to be successful when applied in the bulk removal of CO_2 in ammonia plants **(**Appl et al., 1982).

Zhang et al., (2001) studied the absorption of CO_2 into a mixed aqueous solution of MDEA and PZ using laboratory disk column and concluded that the reaction of PZ with CO_2 could be regarded as a rapid pseudo-first-order reaction in parallel with that of MDEA with CO_2. Bishnoi and Rochelle (2002) present data and a model of CO_2 solubility and Piperazine speciation for MDEA and PZ blends. Xu et al., (1992) studied the absorption of CO_2 from gas at ambient pressures into aqueous blends of PZ and MDEA. Sodiq et al. (2014) studied the effect of adding PZ accelerator to a sterically-hindered (AMP) and tertiary (MDEA) amines.
The main disadvantages of using aqueous alkanolamines are their limited loading, a high energy requirement and the issues of degradation and corrosion. In addition, sulfur components such as mercaptans could not be absorbed easily in alkanolamines solutions .Yeh et al., (2001).

However, a number of studies proposed the use of mixed solvents composed of a chemical solvent and a non-aqueous physical solvent to take advantage of the benefits of physical and chemical absorptions. Sulfolane was reported as a good physical solvent for carbonyl sulfide,

mercaptans, and acid gases (H_2S, CO_2). Its capacity for acid gases is almost eight times that of water at all partial pressures .Xu et al., (1991). Sulfolane is a physical solvent which is used in the processing of gases. It is a polar organic compound which has a strong affinity for the acid gases (H_2S and CO_2) which are present in many natural and refinery gas streams. Unlike other physical solvents such as methanol, sulfolane is rarely used alone but rather in admixture with a chemical solvent such as an alkanolamine solution. This mixed solvent is the basis of the industrially important Sulfinol process, the solvent in which consists of diisopropanolamine (DIPA: chemical component), sulfolane (physical component) and water Dunn et al., (1964). The use of mixed solvents is an attractive alternative to either chemical or physical solvents alone. In some respects the process is similar to a chemical process, but the presence of the physical solvent enhances the capacity of the solution for acid gases, especially when the gas stream to be treated is at elevated pressure and the acid gases are present in high concentrations.

One of the advantages of the aqueous Sulfolane–amine process for acid gas removal is the ability to simultaneously remove mercaptans and carbonyl sulphides such as COS, which are not removed by pure chemical solvents .Klinkenbijl et al., (1999). In 1964, Dunn et al. described an important industrial mixed solvent, Sulfinol, which is composed of Diisopropanolamine (DIPA), Sulfolane (TMS), and water. Roberts and Mather (1988) published equilibrium data for CO_2 and H_2S in AMP-TMS-H_2O system at (40 and 100) °C at partial pressures of the acid gases up to 6000 KPa. Xu et al., (1991) studied the kinetics of absorption of CO_2 in a mixed solvent consisting of Sulfolane, AMP, and water using a stirred-cell absorber. Macgregor and Mather (1991) reported the solubility of H_2S, CO_2, and their mixtures at (40 and 100) ^oC in a mixed-solvent consisting of MDEA (20.9 wt.%) and Sulfolane (30.5 wt.%). Henni (2002) studied the absorption of CO_2 in mixed solvent consisting of MDEA and Sulfolane using a stirred reactor. However, there has been few works reporting on the kinetic data for mixed solvents, especially the aqueous system of (MDEA+Sulfolane), widely used in natural gas sweetening plants. The main aim of this current investigation is to present the kinetic properties for the absorption of CO_2 in aqueous solutions of PZ, MDEA, MDEA mixed with PZ, PZ mixed with Sulfolane and MDEA mixed with sulfolane using the classical stopped flow technique.

IV.1) Experimental Section:

IV.1.1) Chemicals:

Reagent grade PZ with a mass purity of 99%, MDEA (99%) and Sulfolane (99%) were obtained from Sigma-Aldrich Co., Canada. All the chemicals were utilized in the supplied state without further purification. Deionized water at the laboratory was used in the appropriate amount to achieve the desired concentration of samples where needed. The purity level of the Carbon dioxide (CO_2) gas purchased from Praxair is 99.99 vol. %. For each run, an aqueous solution of carbon dioxide (CO_2) was prepared by bubbling research grade CO_2 for up to two hours into water. The solution was further diluted with water to ensure an amine concentration much in excess of that of CO_2, at least 10 times lower than amines concentration in order to achieve a pseudo first-order reaction condition. The purity level of the Carbon dioxide (CO_2) gas purchased from Praxair Inc, Canada is 99.99 vol. %.

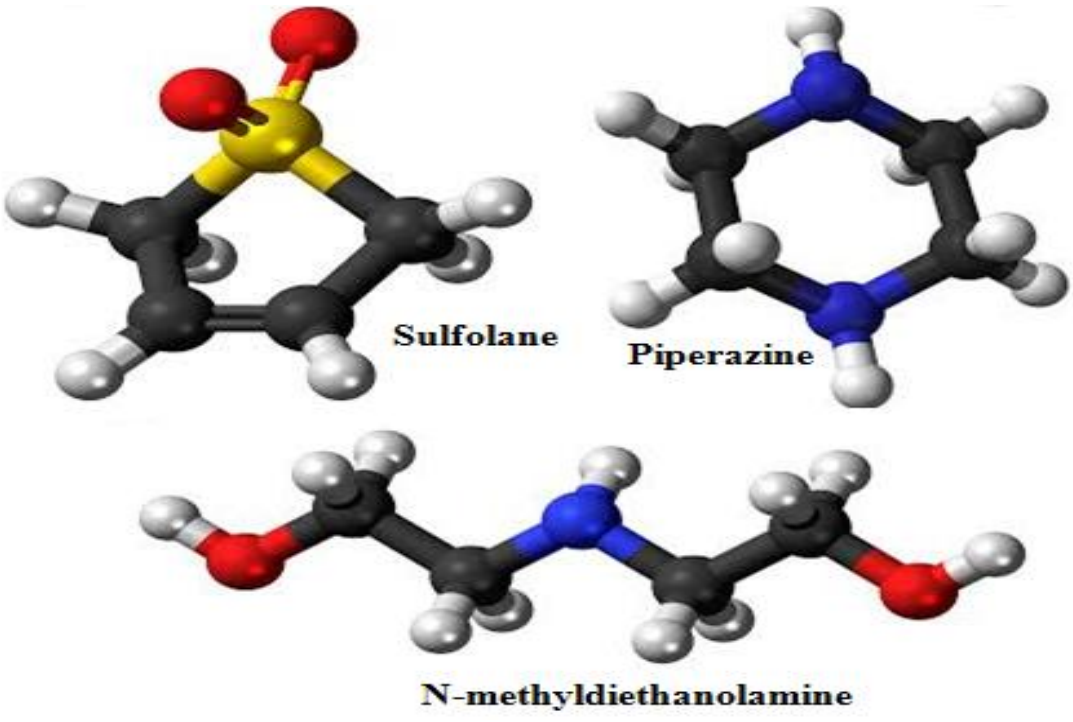

Figure IV.1. Chemical structure of the selected amines in this study

IV.1.2) Experimental Setup:

This research work involves the use of the Stopped flow technique to directly measure the pseudo first-order reaction kinetics, K_0, for aqueous solutions of different alkanolamines at various concentrations over a range of temperatures.

The equipment configuration for the stopped-flow technique consists of a standard SF-51 stopped flow unit from Hi-Tech Scientific Ltd., UK. The setup is an assembly of four equipment components; a sample-handling unit, a conductivity-detection cell, an A/D converter and a microprocessor. The external case of the sample-handling unit is made up of stainless steel which provides rigidity and support for the sample flow circuit as well as an enclosure for all the internal components. A schematic drawing of the experimental stopped-flow equipment for the sample handling unit is presented in Figure IV.2.

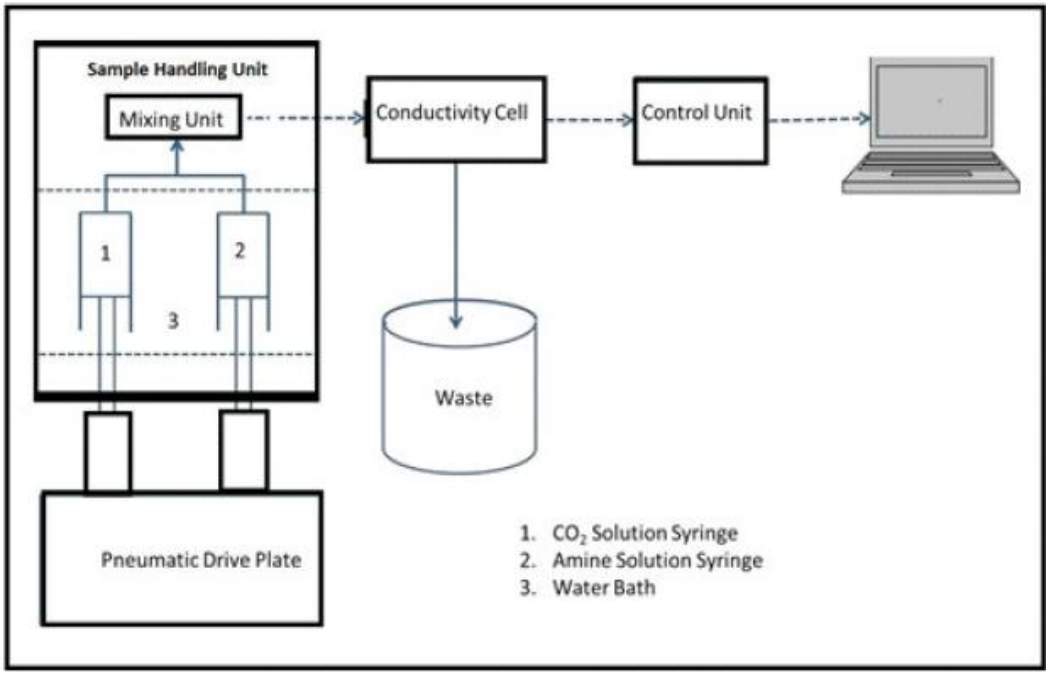

Figure IV.2. Schematic diagram of stopped-flow equipment showing the major units

The complete flow circuit, except the stop/waste syringe, is sealed off securely in a thermostat and the temperature at which the reaction takes place is kept steady by an external water bath. The temperature of the water bath can be set to desired value within ± 0.1 K. The digital display on the front panel of the sample handling unit shows the temperature at which the reaction is

taking place. The temperature on the digital display can be changed by adjusting the temperature reading on the control module for the HAAKE DC 30 attached to the water bath which can provide temperature increments of $0.1^{o}C$. The control valves on the sample handling unit are driven by compressed air supplied by an air cylinder located in the laboratory. The front panel of the unit has an air pressure indicator which shows the current air pressure is provided to drive the valves and mechanism. Other areas powered by the pneumatic air supply are the movement of the drive plate located at the bottom of the internal syringes that contain the CO_2 solution and amine solution. For each experimental procedure, a fresh solution of CO_2 was prepared and loaded into a 5ml plastic syringe along with a new solution of alkanolamines of known concentration, loaded into a second plastic syringe. An aqueous solution of CO_2 can be prepared by bubbling the gas through double-distilled water. The fresh CO_2 solution used during the experiment was prepared by bubbling research grade CO_2 for at least 02 hours through the double-distilled water until the water was completely saturated with CO_2. The bubbling procedure took place by allowing CO_2 gas supplied in a gas cylinder, to travel through a gas line completely immersed in the measured amount of water. A plastic film was used to cover the conical flask during the bubbling procedure to keep the pressure of the system constant. This saturation point was verified by measuring the pH of the solution during the bubbling process and waiting for the pH value to remain constant when the saturation point was reached. A small amount of double-distilled water was used to dilute the prepared CO_2 solution to achieve a solution whose concentration is at least ten times lower than the amine solution to fulfill pseudo first-order reaction conditions.

To run an experiment, the solvent samples were loaded into the Sample Handle Unit using plastic syringes before turning on the equipment. The valve on the air cylinder is open to allow compressed air to flow to power the pneumatic valves. By clicking the "Single shot" button within the KinetAsyst software for an experimental run, the plates drive the Stop/Waste valve based on program instructions from the software, supporting the stop syringe and allowing the valve to automatically advance to the waste position as it empties the stop syringe. After this time, the valve would proceed back to the drive position, and the pneumatic drive plate forces the fresh solution to move down the observation cell, replacing the old solution used during the previous run. The stopped-flow conductivity detection system is designed to measure the intrinsic rate of rapid homogeneous reaction directly. The sample flow circuits are fully equipped

with a temperature probe inside the observation cell to measure the temperature of the system so that the temperature of the reaction remains constant until it reaches the desired set-point. The range for the temperature control is around -0.1 K, (Yan *et al.*, 2000). It is of vital importance to state that the amine and the CO_2 solutions are drawn into sealed drive syringes, and an equal amount of the solution is injected into the observation cell of the apparatus. The rate of formation of ions is monitored closely in relation to time by the conductivity cell. The computer connected to the stopped-flow equipment automatically indicates the observed pseudo first-order constant based on the output voltage values. All other sections of the equipment coordinate the operation of the stepper motor, powering on/off all internal components and the sample handling unit, as well as driving the feature that automatically empties all waste fluid during the Drive/Waste/Flush cycle in addition to the air drive control circuitry. "KinetAsyst" software is a program that runs on the computer connected to the stopped-flow equipment via a data cable and is used to operate the pneumatically controlled drive plate which pushes the precise amount of prepared solution into the conductivity detection cell through a mixing loop. The change in conductivity is measured about time by a circuit as described by Knipe *et al.,* (1974), which produces an output voltage relative to the solution conductivity. The observed experimental data of each experimental run for the amine/CO_2 reaction was generated based on the output conductivity values. For all amine concentrations, every experiment run in the same temperature was repeated at least 10 times to ensure accurate results. The conductivity change of each experimental run with respect to time is fitted based on the relation G(t) , Knipe *et al.,* (1974) which was shown as

$$G(t) = -A\,exp(-K_0 t) + C \qquad \text{(IV.1)}$$

Where K_0 is the pseudo-first-order reaction rate constant, G(t) is the value of conductivity obtained from the conductivity meter, A is the amplitude of the signal, C is the constant conductance value at the end of observed reaction and t is the time (s). This method was deemed to not involve a gas-phase absorption, so the experiment results were able to be directly correlated with reaction rate of an intrinsic homogeneous reaction between amine and CO_2 in liquid phase.

A significant advantage to using the stopped-flow technique is that each experimental run only requires a small amount of reactants (approximately 0.1 ml each) and the equipment is easy to operate.

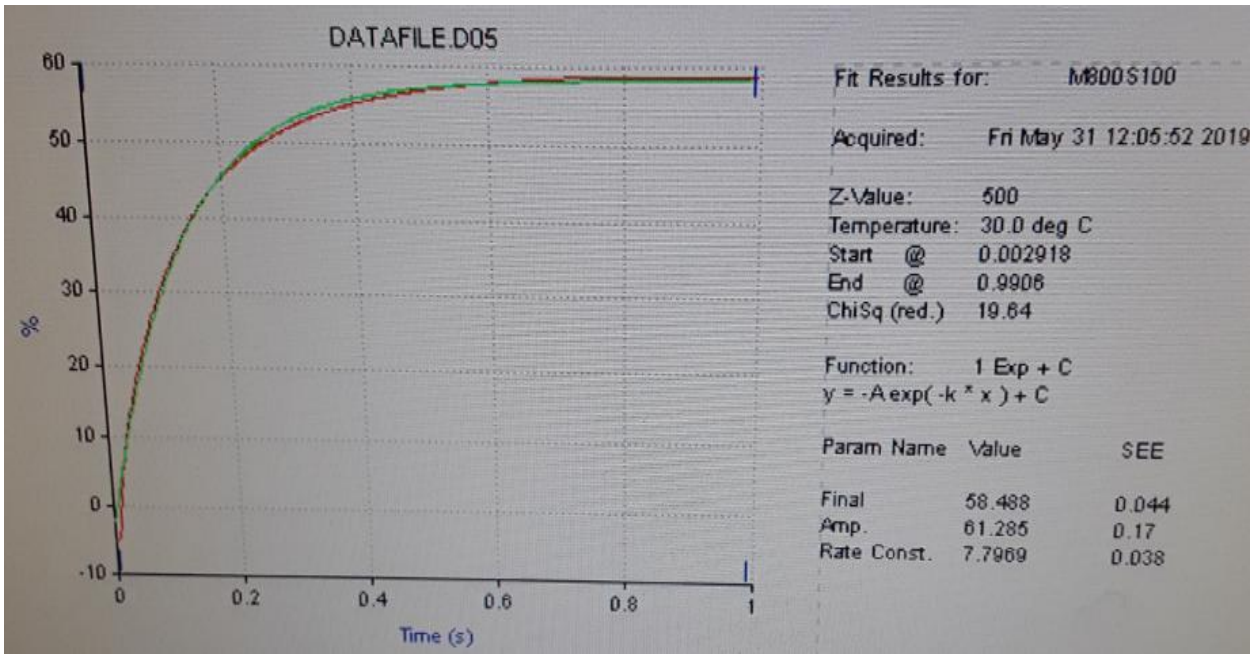

Figure IV.3. A graphical plot of the stopped-flow experiment at a set temperature

IV.2) Experimental validation:

To accurately determine the absorption kinetics of CO_2 in selected amines, the stopped-flow apparatus was first used to measure the reaction kinetics of CO_2 with an aqueous solution of MEA, to ensure the accuracy of data from the equipment. This reaction has been widely studied by numerous research scientists, with data available in reputable literature publications using the stopped flow technique. To test the validity of the stopped flow technique, several runs were carried out to measure the kinetics of MEA with CO_2 with a concentration range of (5 to 34) mol/m^3 at a temperature range of (298.15 to 313.15) K, and the results were compared with corresponding published data as shown in figure IV-4. The reproducibility was better than 3 % (absolute average deviation of 15 set of values from mean values). The values obtained in this study compare favorably with those published by Sodiq et al. (2014), with an absolute average deviation (AAD %)(Average absolute deviation) less than 5 % for all concentrations and temperatures. The results of the experiment conducted in this research work using MEA, validate that the procedure used is very accurate and can, therefore, be used as a reliable method for producing accurate reaction kinetics data for our selected solvents.

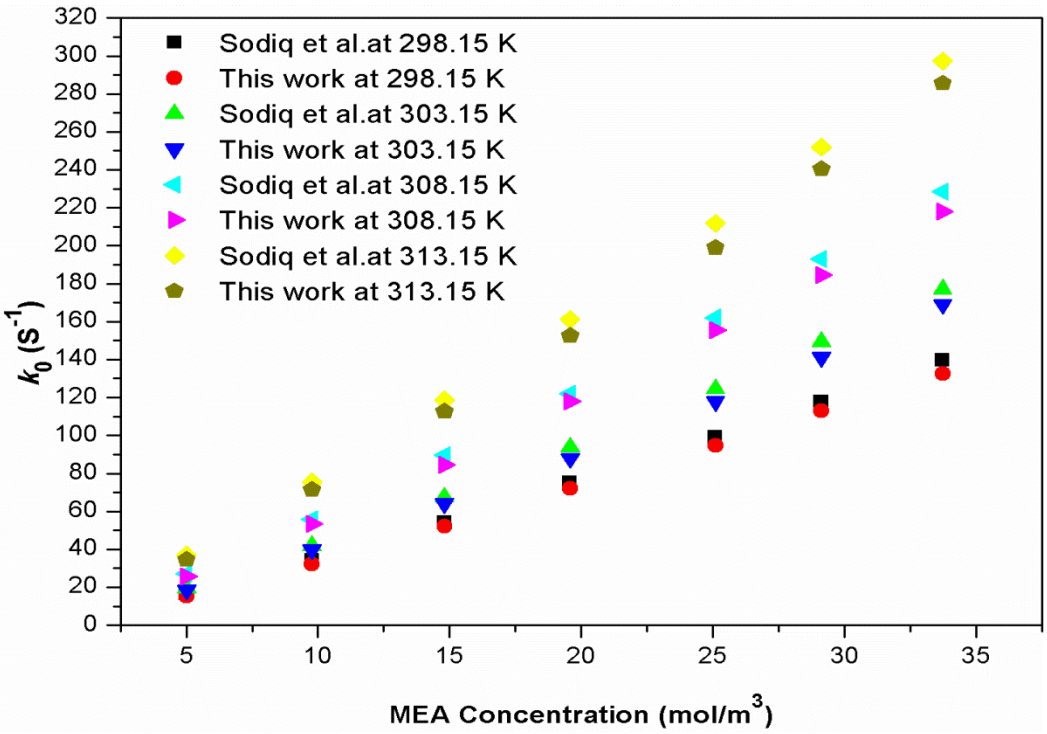

Figure IV.4: Comparison of k_0 values for CO_2 reaction with aqueous MEA with those published by Sodiq et al., (2014) at different temperatures and concentrations

IV.3) Kinetics of CO_2 absorption into aqueous amine solutions:

The kinetics of CO_2 absorption into aqueous amine solutions have been studied for a number of years with a wide variety of aqueous amine solutions such as MEA, DEA, MDEA, AMP, MDEA-MEA, MEA-AMP, MDEA-PZ, and AMP-PZ (Versteeg and Van Swaaij, 1988b; Saha and Bandyopadhyay, 1995; Mandal et al., 2001; Zhang et al., 2001; Sun et al., 2005 ; Edali et al., 2009). Saha and Bandyopadhyay (1995) conducted the experiment for measuring the rate of CO_2 absorption into aqueous AMP solutions using a wetted wall column over temperature and AMP concentration ranges of 294 K to 318 K and 0.5 M to 2 M, respectively. The Zwitterion mechanism was applied in their work. The reaction rate constant and the order of reaction with respect to concentration of CO_2 and AMP were determined using a graphical method. Ramachandran et al., (2006) performed an experiment using a laminar jet absorber for studying the kinetics of CO_2 absorption into an aqueous solution of CO_2 loaded, blended MEA-MDEA. The experimental apparent rate constants were fitted with the Zwitterion mechanism rate expression or the termolecular mechanism rate expression to obtain the rate constants. Rinker et al., (1995 and 2000) studied the kinetics of CO_2 absorption in aqueous unloaded solutions of

MDEA and blended DEA-MDEA using a wetted sphere absorber over a temperature range of 293 K to 342 K and concentration range of 10% to 30% mass MDEA. Their comprehensive reaction rate/kinetics models also take into account the coupling between chemical equilibrium, mass transfer, and chemical kinetics of all possible chemical reactions. Recently, the comprehensive reaction rate/kinetics model has been extended to other promising amines systems such as blended MEA-MDEA and blended (MDEA -PZ) (Edali et al., 2007 and 2009).

Several comprehensive investigations have been undertaken to study the kinetics of the reactions in alkanolamine processes. Compared with the instantaneous proton transfer reaction when H_2S reacts with an alkanolamine, the reaction between CO_2 and alkanolamines is more complex, and the reaction rate depend highly on the structure of the alkanolamine molecule. Primary and secondary amines have the capability to react with CO_2, forming carbamate ions. These are amines with one or two carbon containing groups attached to the nitrogen atom. Tertiary amines, like TEA and MDEA, with three carbon-containing groups attached to the nitrogen atom, cannot form carbamates, and bicarbonate formation becomes the only main reaction.

One of the mechanisms stipulates that primary and secondary alkanolamines react directly and reversibly with CO_2 through the formation of a Zwitterion intermediate which is deprotonated by the bases present in the solution to form a stable carbamate. The mechanism was originally proposed by Caplaw (1968) and reintroduced by Danckwerts (1979). In contrast, tertiary alkanolamines do not react directly with CO_2 to form carbamates. In aqueous solutions, tertiary amines catalyse CO_2 hydrolysis to form bicarbonate ions and a protonated amine as was first proposed by Donaldson and Nguyen (1980).

IV.4) Reaction mechanisms:

IV.4.1) Reaction kinetics of CO_2 in aqueous PZ:

The kinetic reaction can be described as a Zwitterion mechanism according to the steps shown below

$$PZ + CO_2 \overset{(K_2, K_{-1})}{\Longleftrightarrow} PZ^+ COO^- \qquad \text{(IV.2)}$$

$$PZ^+COO^- + B \overset{(K_b, K_{-b})}{\Longleftrightarrow} PZCOO^- + BH^+ \qquad \text{(IV.3)}$$

Where $K_{2,PZ}$ forward second order reaction rate constant for the formation of the PZ Zwitterion ($m^{3/}$mol. s), K_b Zwitterion deprotonation rate constant by B (m^3 /mol. s),and K_{-b} reverse Zwitterion deprotonation rate constant by base *B* (amine or water) (m^3/ mol. s).

According to Blauwhoff et al. (1984), any base present in solution will contribute to the deprotonation of the Zwitterion. The suffix B represents any base, which can be an amine, a hydroxyl ion, or water. In aqueous solution, the deprotonation proceeded mainly via water and the amine according to Versteeg and van Swaajj (1988 a) and others because OH^- ion contribution is in general negligible in the Zwitterion dissociation.

$$r_{CO2} = \frac{[PZ][CO_2]}{\frac{1}{K_2}+\frac{K_{-1}}{K_2 \sum K_{base}[B]}} \quad \text{(IV.4)}$$

Where r_{CO2} is the overall forward reaction rate (mol/ m^3 .s)

Equation (IV.4) can be simplified to,

$$r_{CO2}=\frac{[PZ][CO_2]}{\frac{1}{K_2}+\frac{1}{\sum K_b[B]}} \quad \text{(IV.5)}$$

$$K_b = \frac{K_{base}K_2}{K_{-1}} \quad \text{(IV.6)}$$

Under pseudo-first-order conditions, the concentration of the amine *[Am]* is always much in excess of that of CO_2, and equation (IV.5) can be written as:

$$r_{CO_2} = K_0[CO_2] \quad \text{(IV.7)}$$

Then, the observed pseudo-first-order reaction rate constant K_0 becomes,

$$K_0 = \frac{[PZ]}{\frac{1}{K_2}+\frac{1}{\sum K_b[B]}} \quad \text{(IV.8)}$$

Two limiting cases exist for equation (IV.5). If the inverse of K_2 was much bigger than the inverse of $\sum K_b$, this means that the Zwitterion was deprotonated relatively fast in comparison with the reversion rate of CO_2 and amine. Equation (IV.8) simplifies to,

$$K_0 = K_2[Amine] \quad \text{(IV.9)}$$

But if the inverse of K_2 is much smaller than $(1/\sum K_b\,[B])$, then K_0 will become:

$$K_0 = [Amine](\sum K_b\,[B]) \quad \text{(IV.10)}$$

The reaction mechanism of the (CO_2+PZ+H_2O) system can be evaluated using a single-step-termolecular mechanism proposed by Crooks and Donnella.(1989), This mechanism has been reviewed by da Silva and Svendsen.(2004). It assumes that an amine reacts simultaneously with one molecule of CO_2 and one molecule of a base. The reaction proceeds in a single step via a loosely-bound encounter complex as the intermediate (rather than a zwitterion).

$$CO_2 + Am\ldots H \Longleftrightarrow AmCOO^- \ldots BH^+ \quad \text{(IV.11)}$$

The complex breaks up to form reactant molecules, while a small fraction reacts with a second molecule of amine, or a water molecule, to give ionic products. In our system, the concentration of water is so much greater than the amine concentration that it can be assumed to be constant, and then the expression of the overall reaction rate is shown as:

$$r_{CO_2} = k_0^T[CO_2] = \sum k_b\,[B][CO_2][PZ][CO_2] \quad \text{(IV.12)}$$

$$r_{CO_2} = (k_{PZ}^T[PZ]+k_{H_2O}^T[H_2O] + k_{OH^-}^T[OH^-])[PZ][CO_2] \quad \text{(IV.13)}$$

Little et al.(1990) found that the concentration of OH^- ions in amine solution is very low due to the very fast reaction rate of CO_2 with OH^- leading to the hydroxyl ions being quickly consumed, and the effect of hydroxide ions on the overall reaction rate can be neglected, therefore all the experimental observed pseudo first-order reaction rate constants k_0 were fitted to the Termolecular mechanism represented by Equation (IV.14)

$$k_0^T = (k_{PZ}^T[PZ]+k_{H_2O}^T[H_2O])[PZ] \quad \text{(IV.14)}$$

IV.4.2) Reaction kinetics of CO_2 in aqueous MDEA:

MDEA is today the most used tertiary amine for acid gas removal. MDEA has outdone for example TEA, which was the first amine to be used for gas sweetening purposes (Bottoms, 1930). When the correct additives are used, MDEA offers several advantages over other amines also for bulk CO_2 removal (Bullin et al., (1990, 1992)). In aqueous solutions of tertiary amines, the overall reaction to take place with CO_2 is the bicarbonate formation. Carbamate formation does not occur in the case of tertiary amines like MDEA, because the MDEA molecule does not have a hydrogen atom attached to the nitrogen atom. This leads to a slower absorption rate than for primary and secondary amines, since the bicarbonate reaction occurs relatively slowly. In order to speed up the reaction, activating agents can be added to the MDEA solution. Such agents are for instance other amines with higher reaction rates. With H_2S, MDEA will react directly following the same fast reaction mechanism as for primary and secondary amines. This is the reason why MDEA as a tertiary amine is heavily used in selective absorption of H_2S when CO_2 is present. MDEA can be used in high concentrations up to 50wt%, in combination with high CO_2 loadings. Also the loss of amine using MDEA solutions will be small, due to low vapor pressure and slow degradation rates. MDEA solutions are also less corrosive than other amines such as MEA and DEA (Bullin et al., 1990).

The most accepted mechanism for the bicarbonate formation reaction involving MDEA is that the amine acts as a base catalyst for the CO_2 hydration reaction. MDEA acts as a homogenous catalyst for CO_2 hydrolysis. Versteeg and Van Swaaij (1988b) also conclude that the base catalysis of the CO_2 hydration describes the reaction between CO_2 and tertiary amines.

The kinetic reaction can be described as a base catalyzed hydration of CO_2 according to the Donaldson and Nguyen (1980):

$$MDEA + H_2O + CO_2 \overset{K_2}{\Rightarrow} MDEA^+ + HCO_3^- \quad \text{(IV.15)}$$

The following reactions also occur:

$$CO_2 + OH^- \overset{K_{OH^-}}{\Longleftrightarrow} HCO_3^- \quad \text{(IV.16)}$$

$$CO_2 + H_2O \overset{K_{H_2O}}{\Longleftrightarrow} H_2CO_3 \quad \text{(IV.17)}$$

$$r_{CO2} = K_0[CO_2] = [CO_2](K_2[MDEA] + K_{H_2O}[H_2O] + K_{OH^-}[OH^-]) \quad \text{(IV.18)}$$

In aqueous solutions, the contribution of un-catalyzed equation (IV.17) to the overall reaction is usually negligible, as the reaction rate is slow with respect to mass transfer compared to equations (IV.15) and (IV.16) according to Littel et al., (1990):

$$Am + H_2O \overset{K_p}{\Leftrightarrow} AmH^+ + OH^- \quad \text{(IV.19)}$$

Where K_p is amine protonation rate constant .

According to Littel et al., (1990), reactions (IV.15) and (IV.16) are parallel pseudo first order reactions, and they reduced the expression for the reaction rate constant from Equation (IV.18) to:

$$r_{CO_2} = K_0[CO_2] = [CO_2](K_2[MDEA] + K_{OH^-}[OH^-]) \quad \text{(IV.20)}$$

This mechanism leads to the increase of the reactivity towards the carbon dioxide and the weakness of the O-H bond in the water because of the formation of a hydrogen bond between the tertiary amine and water. By considering the contribution of OH^- ions to be negligible, this expression reduces to the following rate expression:

$$r_{CO_2} = K_0[CO_2] = [CO_2](K_2[MDEA]) \quad \text{(IV.21)}$$

The equation (IV.15) becomes:

$$K_0 = K_2[MDEA] \quad \text{(IV.22)}$$

IV.4.3) Reaction kinetics of CO2 in blended Aqueous MDEA-PZ system:

For MDEA/PZ system, a combination of Zwitterion and base-catalysis mechanisms was used as suggested by Ali et al. (2010):

$$K_0 = K_{2,MDEA}[MDEA] + \frac{[PZ]}{\frac{1}{K_{2,PZ}} + \frac{1}{K_{PZ,PZ_Z}[PZ] + K_{MDEA,PZ_Z}[MDEA] + K_{w,PZ_Z}[w]}} \quad \text{(IV.23)}$$

MDEA as a tertiary chemical alkanolamines contributes of the deprotonation of the Zwitterion.

A second model is also commonly used to correlate amine blends namely the Termolecular model. In an aqueous system, tertiary amines do not directly react with CO_2.

The main reaction is in this case the termolecular reaction between PZ and CO_2 involving the tertiary amine and PZ itself as alkaline substance. The total reaction rate of CO_2 absorption using the Termolecular mechanism can be represented as follows:

$$r_{CO_2} = k_0^T[CO_2] = (k_{PZ}^T[PZ] + k_{MDEA}^T[MDEA] + k_{H_2O}^T[H_2O] + k_{OH^-}^T[OH^-])\ [PZ][CO_2] \quad \text{(IV.24)}$$

As mentioned above, the concentration of OH- ion in amine system is very low, so the contribution of hydroxide ions can be neglected. Therefore, Equation IV.24 becomes:

$$k_0^T = (k_{PZ}^T[PZ] + k_{MDEA}^T[MDEA] + k_{H_2O}^T[H_2O])\ [PZ] \quad \text{(IV.25)}$$

IV.4.4) Reaction kinetics of CO2 in blended Aqueous MDEA-Sulfolane system: The main reaction is CO_2 with MDEA and second, the subordinate reactions are CO_2 with water and the hydroxyl ion, OH^-, besides physical absorption by Sulfolane and water. The mechanism of these reactions is well-understood and presented by Donaldson and Nguyen (1980). It is called a "base catalyzed hydration" mechanism and is generally applied to the description of the reaction between CO_2 and tertiary amines. According to Xu et al., (1991), Sulfolane as a physical solvent can only contribute to the deprotonation of the Zwitterion in aqueous solutions.

$$k_0 = k[MDEA]^n \quad \text{(IV.26)}$$

Data obtained in this study were modelled separately keeping Sulfolane concentrations constant to obtain the reaction order for MDEA. Values for reaction order (n) were very close to one for all concentrations of Sulfolane tested that were kept constant while MDEA concentration was allowed to change for each temperature studied.

IV.4.5) Reaction kinetics of CO_2 in blended Aqueous PZ-Sulfolane system:

Both Zwitterion and Termolecular models were able to fit well the experimental data for the aqueous blended (PZ + Sulfolane). PZ zwitterion is deprotonated by PZ, Sulfolane and water:

$$k_0 = \frac{[PZ]}{\frac{1}{k_{2,PZ}} + \frac{1}{k_{PZ,PZ_Z}[PZ] + k_{sul,PZ_Z}[Sul] + k_{w,PZ_Z}[H2O]}} \quad \text{(IV.27)}$$

$$k_0^T = (k_{PZ}^T[\text{PZ}] + k_{Sul}^T[\text{Sulfolane}] + k_{H_2O}^T[\text{H}_2\text{O}])[\text{PZ}] \quad \text{(IV.28)}$$

To check the accuracy of these correlations of different above systems, two different deviation functions such as the coefficient of determination (R^2) and Absolute Average Deviation (AAD) were determined. R^2 specifies how good the data points are fitted by the correlation (Shafeeyan et al.2015).

$$R^2 = 1 - \left(\frac{\sum_{i=1}^{n}\left(k_0^{exp} - k_0^{cal}\right)^2}{\sum_{i=1}^{n}\left(k_0^{exp} - k_0^{\overline{exp}}\right)^2}\right)\left(\frac{n-1}{n-N}\right) \quad \text{(IV.29)}$$

Where, n denotes the number of experimental data, N is number of parameters.

$$AAD\% = \frac{100}{n}\sum_{i=1}^{n}\left|\frac{k_{0,exp} - k_{0,cal}}{k_{0,exp}}\right| \quad \text{(IV.30)}$$

The deviation of the experimental and correlated results is basically considered to evaluate the reliability of the model.

IV.5) Results and discussion:

IV.5.1) Absorption kinetics of CO_2 in aqueous MDEA:

Aqueous MDEA concentrations ranging from (200 to 800 mol/m^3) were studied at (298.15, 303.15, 308.15, and 313.15) K, with a temperature interval of 5 K. The observed pseudo-first-order rate constants *(K_0)* for MDEA in aqueous solution are shown in Figure IV.5 as a function of the MEDA concentration. The amine concentration was kept at least 10 times the CO_2 concentration in order to maintain the pseudo first-order reaction conditions. The pseudo first order reaction constants K_0(s^{-1}) increase with the increase in aqueous MDEA concentration, as well as in temperature (Table IV.1).

Table IV.1. Experimental kinetic data for (CO_2-MDEA-Water) at different temperatures

[MDEA)] (mol/m^3)	**T (K)**			
	298.15	**303.15**	**308.15**	**313.15**
	k_0 **(s^{-1})**			
200	1.79±0.03	2.79±0.08	3.62±0.09	4.81±0.13
300	2.87±0.07	4.18±0.10	5.39±0.16	7.19±0.19
400	3.51±0.09	5.62±0.14	7.22 ±0.20	9.62±0.28
500	4.51±0.11	7.09±0.18	9.08±0.24	12.11±0.33
600	5.45±0.14	8.38±0.20	10.78±0.29	14.39±0.41
700	6.31±0.15	9.81±0.25	12.61±0.35	16.79±0.50
800	7.32±0.18	11.22±0.29	14.38±0.39	19.21±0.55

Table IV.1 shows all the values of pseudo-first order reaction rate constants (K_0) obtained from the experimental procedure for MDEA within a temperature range of (298.15-313.15) K. The experimental values of the pseudo-first order reaction rate constant, K_0 was plotted against the concentration of *N*-Methyldiethanolamine, [MDEA] and shown in figure IV.5

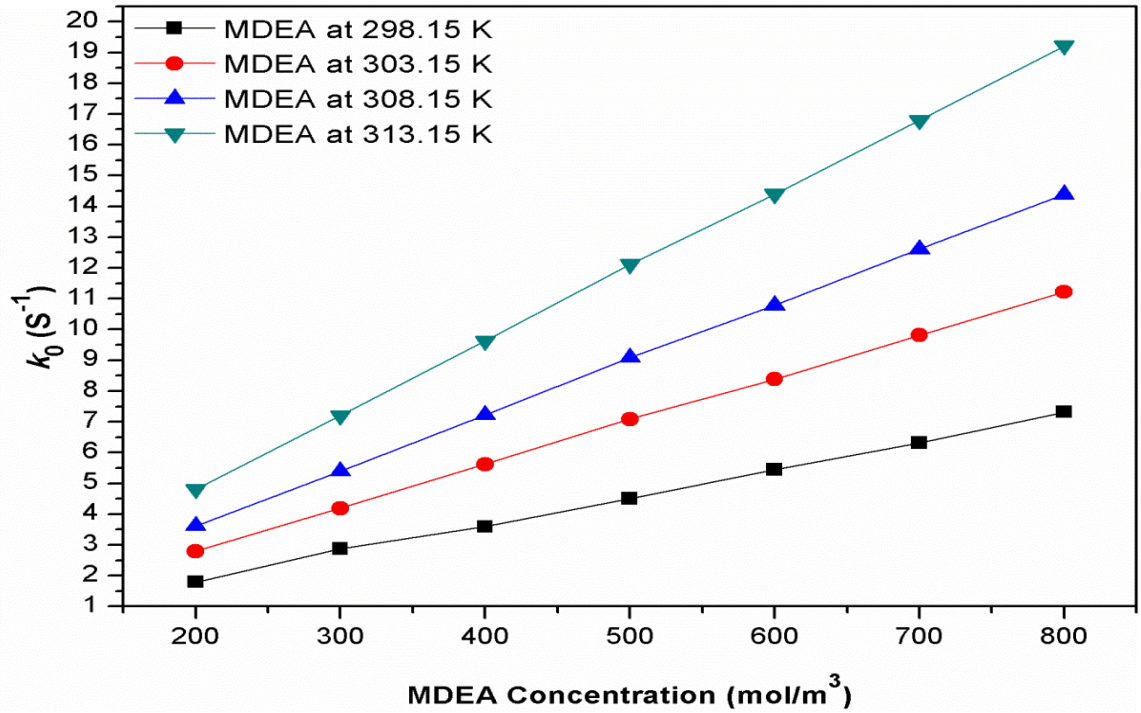

Figure IV.5. Plot of pseudo-first-order reaction rate constants K_0 versus MDEA concentrations at different temperatures

According to the graphical plot shown in figure IV.5, all values on the y-axis and x-axis represent the pseudo-first order reaction rate constant (K_0) and amine concentration respectively. When looking at the plot in Figure IV.5, it can be observed that the values of the slope increase progressively as the temperature of the experiment increases, which is evident because of the rate constant increases steadily with increasing temperature. At all temperatures the values of the pseudo-first order reaction rate constant (K_o) increase steadily with increasing concentration of amine. The accelerated rate of kinetics is due to the basicity of the solvent.

The pseudo first-order reaction rate constants of aqueous MDEA over a temperature range of (298.15 to 313.15) K were correlated with power-law kinetics as a function of concentrations

$$K_0 = K_{Am}[Am]^n \qquad \text{(IV.31)}$$

Where, K_{Am} is the power law constant (m^{3n}/mol^n. s), *[Am]* is the concentration of the amines and n is the order of reaction.

By fitting the empirical power-law kinetics to the data of experimentally observed pseudo-first order constants for CO_2 in Figure 3, the reaction orders were determined to be 0.992, 1.002, 0.997, and 0.999, with respect to [MDEA] for 298.15, 303.15, 308.15, and 313.15 K,

respectively. This empirical curve fitting approach gives a reaction order of approximately 1 with respect to [MDEA].

The Arrhenius plot for this reaction is obtained by plotting the Ln values of the second-order rate constant of ($Ln\ K_2$) for MDEA at different temperatures against the inverse of the experimental temperature (1/T) in Kelvin as shown in Fig IV.7.

$$K_2 = Aexp\left(-E_a/_{RT}\right) \qquad \text{(IV.32}$$

Where A,is Arrhenius constant (m^3/mol. s), E_a, The activation energy (kJ/mol), and R, the universal gas constant (0.008315 kJ/ mol K), respectively.

Figure IV.6 displays the corresponding Arrhenius plot from which the activation energy (E_a) for the the reaction of aqueous CO_2 with aqueous MDEA was determined to be 49.65 kJ/mol.

Arrhenius equation for CO_2-MDEA system was derived as:

K_2 (m^3/mol. s) = 4.71710^6 Exp (-5972/T) , [R^2 = 0.9865] (IV.33)

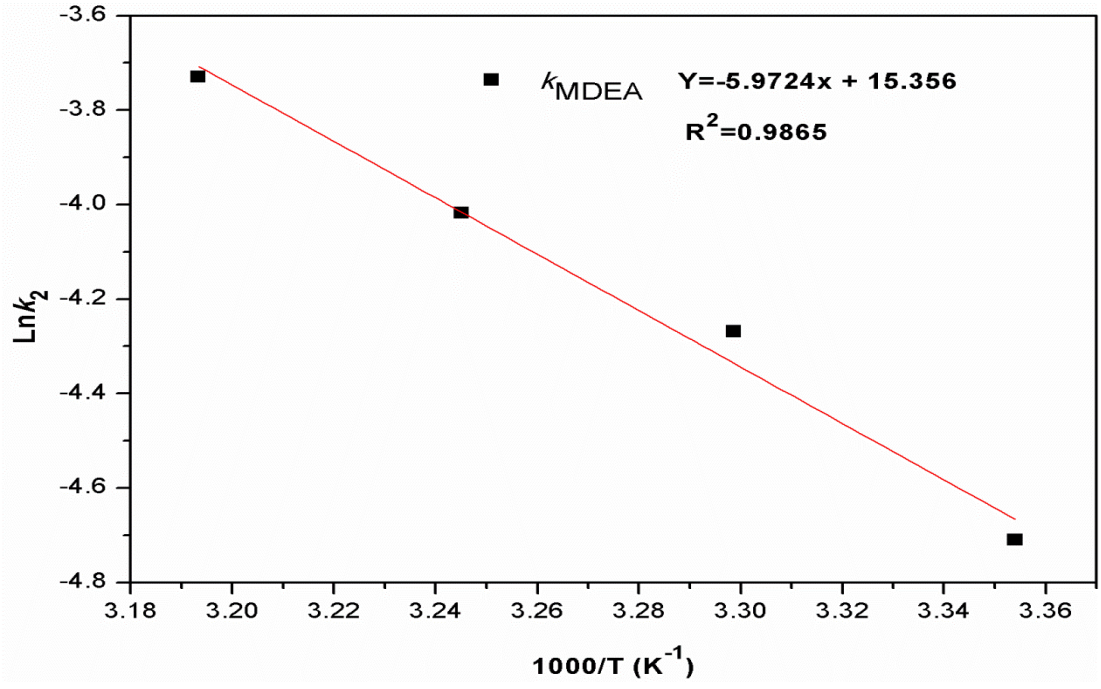

Figure IV.6. Arrhenius plots of aqueous (CO_2-MDEA) rate constants using base catalysis mechanism

Table IV.2 displays the estimates of K_2 obtained in this work and those selected literature values determined by the use of different research methods. The second-order rate constants K_2 (m^3/mol. s), as shown in Table IV.2, displayed an increasing trend with respect to increase in concentration and temperature and these values were compared with those in the literature.

Table IV.2. Second-order rate constants *(K_2)* of MDEA with CO_2 at different temperatures

T (K)	K_2 (m^3/mol. s)				
	MDEA[a]	MDEA[b]	MDEA[c]	MDEA[d]	MDEA[e]
298.15	0.012	0.009	0.007	0.00603	0.005
303.15	0.016	0.014	0.01	0.00832	0.007
308.15	0.022	0.018	0.015	0.01183	0.01
313.15	0.028	0.024	0.021	0.01518	0.013

[a]Versteeg and Swaaij(1996), [b]This work, [c]Kiezkowska-Pawlak et al,(2011), [d] Benamor et al (2016), [e]Ko and Li (2000).

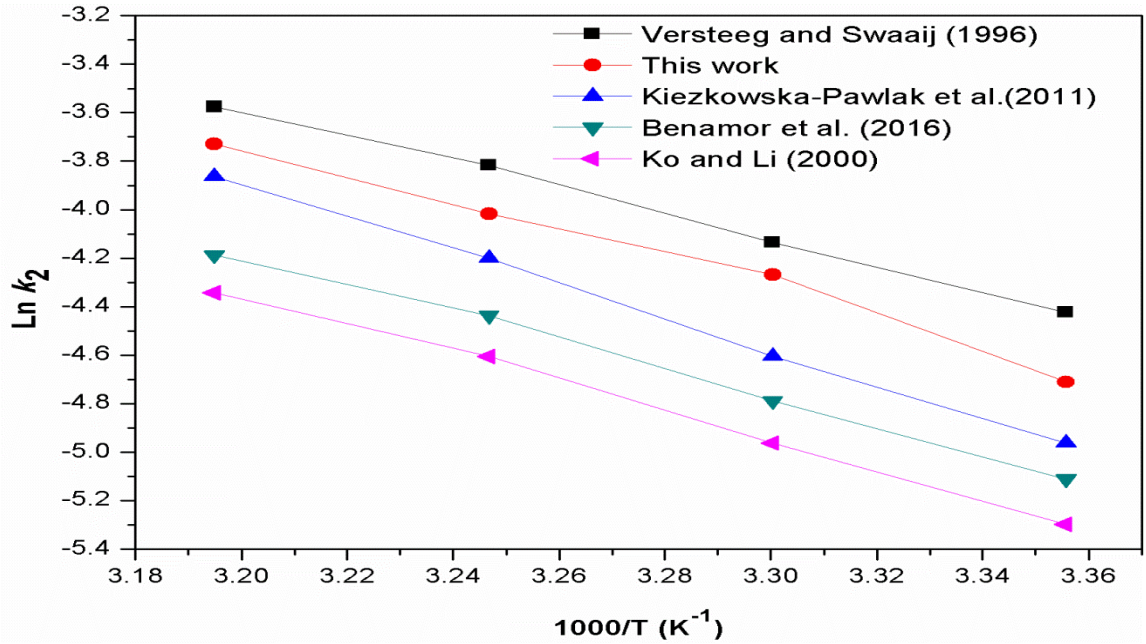

Figure IV.7. Comparison of Arrhenius plots of aqueous (CO_2-MDEA) rate constants of this work and the literature

The estimates of K_2 are plotted in Figure IV.7 for comparison with selected literature values determined by the use of different research methods. The values of K_2 obtained in this work are in good agreement with those derived by Versteeg and Swaaij,(1996), over the whole temperature range. As shown in Figure IV.7, the K_2 of Kieskowska-Pawlak et al., (2011), Benamor et al. (2016), and K_0 and Li (2000) are slightly smaller than the present ones. These discrepancies may mainly result from a different, heterogeneous experimental technique, the assumptions involved in the processing and subsequent interpretation of the kinetic rate data, and the uncertainty about the physical properties such as solubility and diffusivity of CO_2 in MDEA aqueous solutions which have an influence on the estimation of the reaction rate constant of the reaction between CO_2 and MDEA.

The use of MDEA, a tertiary amine, results in several processing advantages over the use of MEA, a primary amine, or DEA, a secondary amine. First MDEA can selectivity removes H_2S from gas streams. The reaction with H_2S through a proton transfer mechanism is very fast. The reaction rate of CO_2 with MDEA is finite and slow. Since MDEA does not react directly with CO_2 during absorptive process, the stripping can easily be achieved by simple pressure reduction. Accordingly, the stripping energy can be very small compared to conventional amines. Because of its low vapor pressure, MDEA can be used in high concentrations. MDEA is highly resistant to thermal and chemical degradations and is essentially noncorrosive. It has a low specific heat and heats of reaction with H_2S and CO_2 and is sparingly miscible with hydrocarbons. (Henni, 2002)

IV.5.2) Absorption kinetics of CO_2 in aqueous PZ:

To examine the CO_2 absorption kinetics of aqueous PZ, the absorption experiment was done using the stopped-flow apparatus over a PZ concentration range of 10–60 mol/m^3, and a temperature range of 298.15–313.15 K with temperature interval of 5 K. By applying pseudo-first-order reaction respected to the concentration of CO_2, the overall absorption rate of CO_2 can, then be expressed as presented in Equation IV.5. The pseudo-first-order reaction rate constant (K_0) extracted from the stopped-flow apparatus are presented in Table IV.3 and plotted in Figure IV.8. The amine concentration was kept at least 10 times the CO_2 concentration in order to maintain the pseudo first-order reaction conditions. The values were found to be closer to each

other with the mean relative deviation (MRD) that is less than 03% in all the four temperatures that were tested.

$$MRD = \frac{1}{n}\sum_n Abs\left(\frac{Experimental\ K_0 - Correlated\ K_0}{Experimental\ K_0}\right) * 100 \qquad \text{(IV. 34)}$$

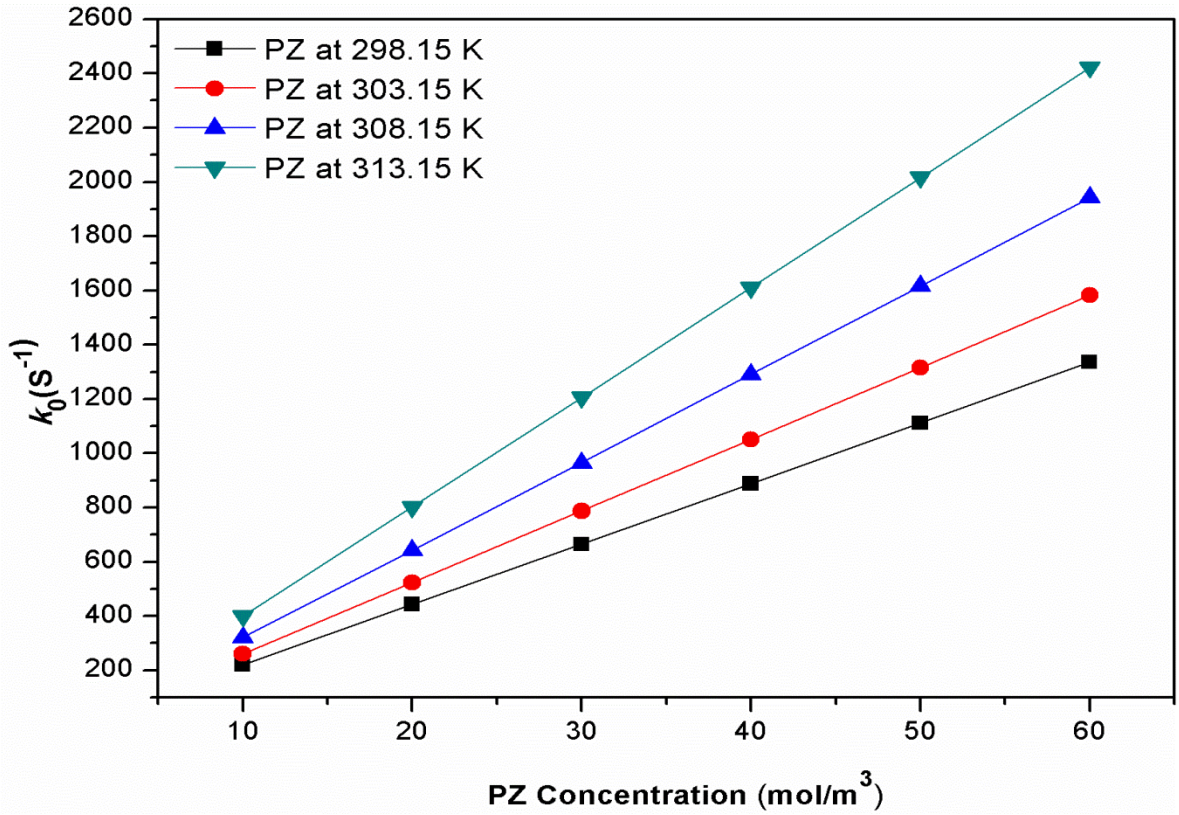

Figure IV.8. Plot of pseudo-first-order reaction rate constants K_0 versus PZ concentrations at different temperatures .

As expected, it can be seen from Figure IV.8 and Table IV.3 that the absorption kinetics of PZ increased as the concentration of PZ and/or the temperature increased over ranges of concentration and temperature of 10–60 mol/m^3 and 298.15–313.15 K, respectively.

Table IV.3. Experimental kinetic data for (CO_2-PZ-Water) at different temperatures

		T (K)			
Concentration (mol/m^3)		**298.15**	**303.15**	**308.15**	**313.15**
[PZ]	**[Water]**	k_0 **(s^{-1})**			
10	55446	220±5	261±6	320±7	400±9
20	55398	442±10	523±12	642±15	802±19
30	55350	664±17	787±18	965±24	1205±28
40	55321	886±23	1050±27	1290±32	1610±40
50	55255	1111±28	1315±32	1615±37	2015±48
60	55207	1335±33	1582±39	1942±48	2422±58

It was observed that the reaction kinetics of CO_2 in *PZ* with respect to the pseudo first order reaction rate constant (K_o), appreciated in values for every increase in amine concentration within a given temperature.

The pseudo first-order rate constants K_0 obtained experimentally from the stopped flow apparatus were interrelated using the empirical power law relationship to determine the reaction order for the CO_2-PZ reaction. By fitting the empirical power-law kinetics (Equation IV.31) to the data of experimentally observed Pseudo-first order constants for CO_2, the reaction orders were determined to be 1.004, 1.004, 1.004, and 1.004, with respect to [PZ] for 298.15, 303.15, 308.15, and 313.15 K, respectively. This empirical curve fitting approach gives a reaction order of approximately 1.00 with respect to [PZ].

The Arrhenius plots (ln K_2 against 1/T) for the aqueous-PZ system is shown in Figure IV.9. The activation energies for the Zwitterion formation step (E_{act}) for this system are calculated from the slope of their respective lines.

Figure IV.9 displays the corresponding Arrhenius plot from which the activation energy (E_a) for the the reaction of aqueous CO_2 with aqueous MDEA was determined to be 31.05 kJ/mol.

Arrhenius equation for CO_2-MDEA system was derived as:

$K_2(m^3/mol.\ s) = 5.89x\ 10^6\ Exp\ (-3731.4/T)$, $[R^2 = 0.9942]$ (IV.35)

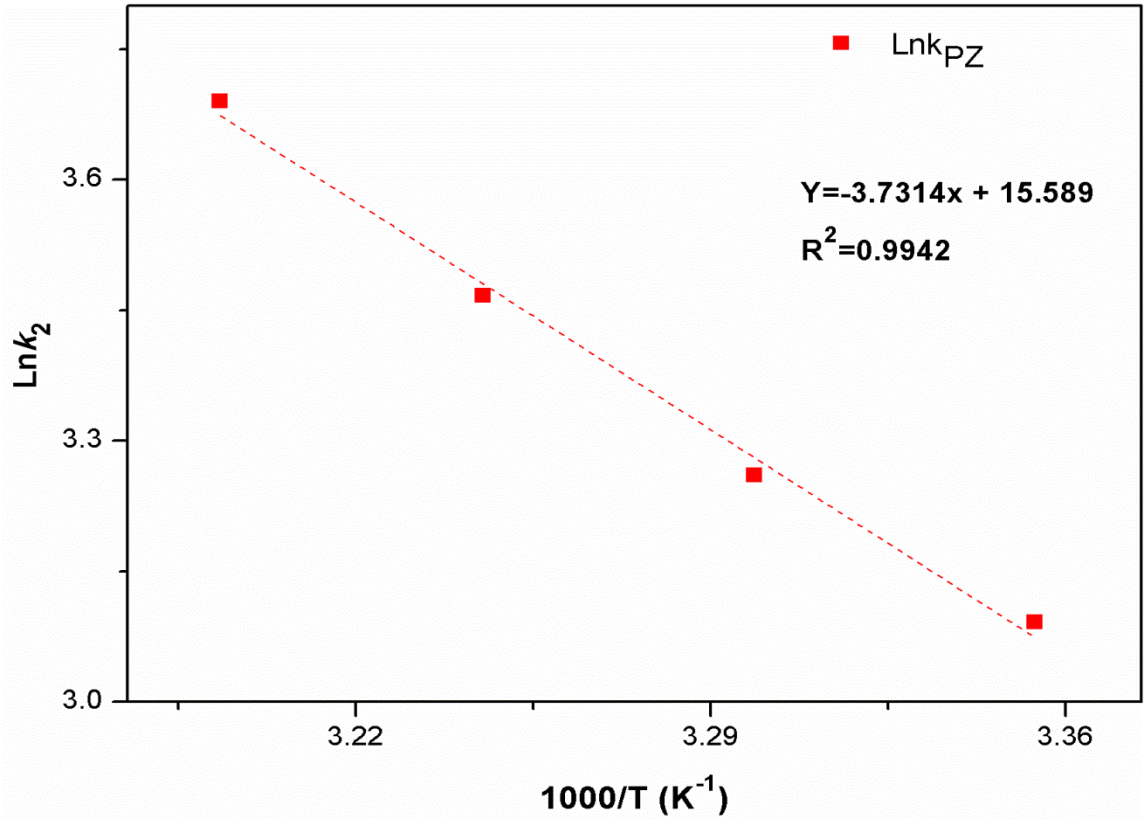

Figure IV.9. Arrhenius plots of aqueous (CO_2-PZ) rate constants using Zwitterion mechanism.

In this work, the termolecular mechanism was also used to correlate the experimentally observed pseudo first-order reaction. From the data obtained, it can be seen that k_0 strongly depends on the PZ concentration, as shown in Figure IV.10.The values of k_0 divided by the concentration of PZ result in a linear equation expressed in Equation IV.14. Plots of this equation in Figure IV.10 gave good fit of the experimental. k_{PZ}^T and that of water, k_{H2O}^T, were calculated from the plots, and the results reported in Table IV.4. From this figure, it can be seen that reaction order with respect to PZ is 1.

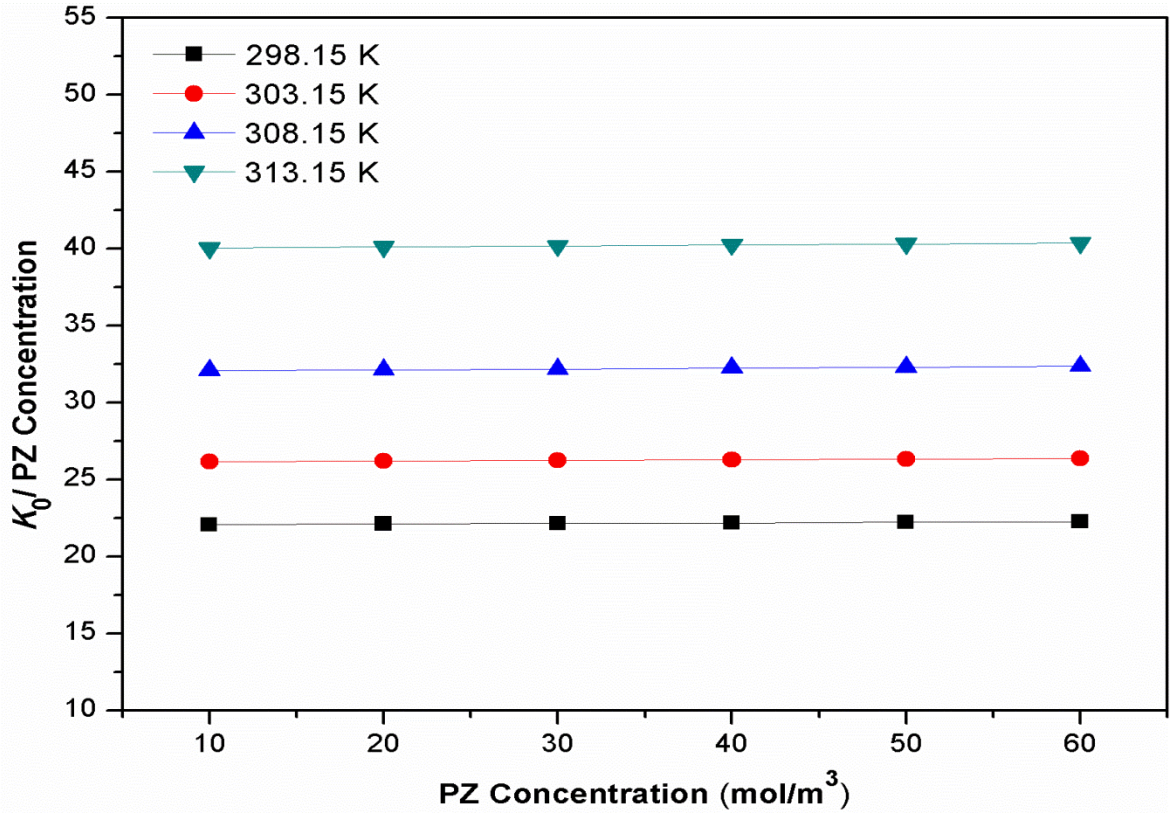

Figure IV.10. Variation of {k_o/PZ concentration} with PZ concentration over a range of temperatures from 298.15 to 313.15K.

In Figure IV.11, the fitting Arrhenius plot is shown. All experimentally observed pseudo first order reaction rate constants k_0 were fitted to the termolecular mechanism, represented by Equation IV.14.

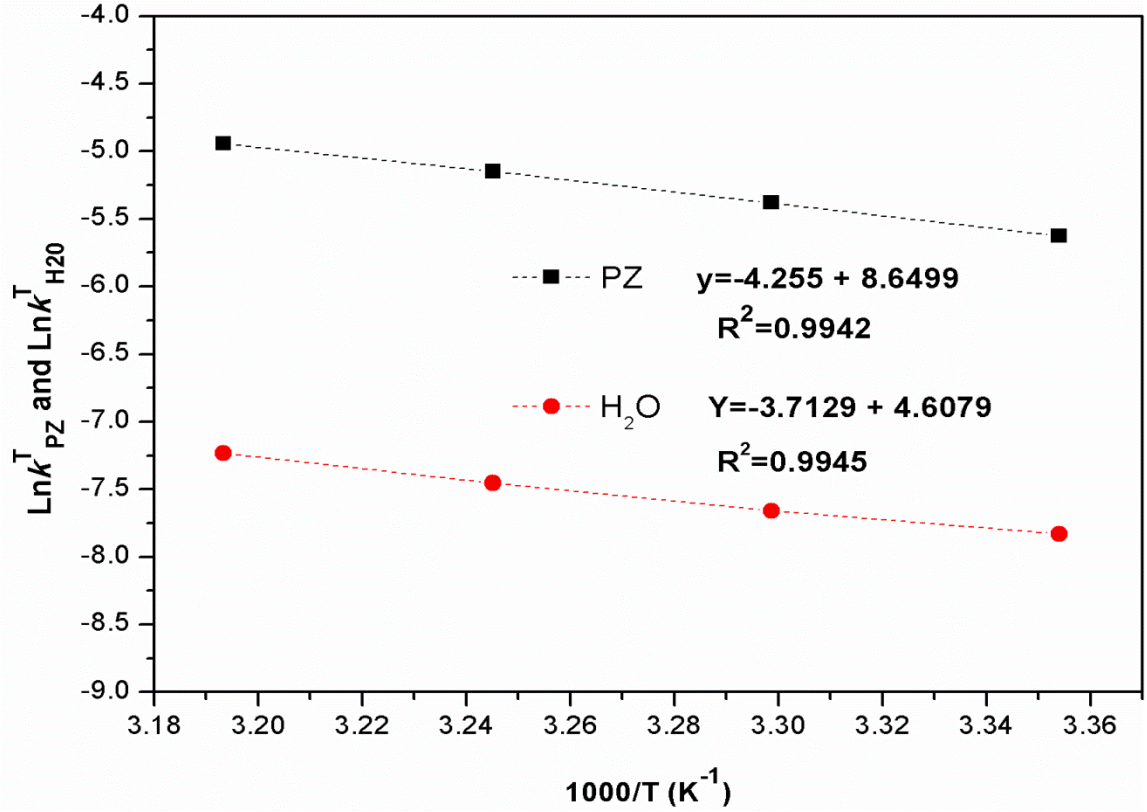

Figure IV.11. Arrhenius plot of rate constants for (CO_2+PZ+Water) system using the Termolecular mechanism.

A multiple linear regression procedure was applied to find the fitting parameters (k_{PZ}^{T} and k_{H2O}^{T}) at each temperature. These fitting parameters and the standard deviation between the experimental and the fitted model are presented in Table IV.4. The dependence of the kinetics parameters k_{PZ}^{T} and k_{H2O}^{T} on temperature is given by:

k_{PZ}^{T}($m^6/mol^2 \cdot s$) = 5.681 x 10^3 Exp (-4255.0/T) , [R^2 = 0.9994] (IV.36)

k_{H2O}^{T}($m^6/mol^2 \cdot s$) = 1 x 10^2 Exp (-3712.9/T) , [R^2 = 0.9945] (IV.37)

The calculated second order reaction constants for piperazine (PZ) are listed in Table IV.4 with their statistical analysis. It can be observed that Equation IV.8 corresponding to the Zwitterion mechanism and Equation IV.14 corresponding to the termolecular mechanism fit the data well.

The Termolecular doing a better job at that. This confirms that Zwitterion deprotonation is the rate-determining step and the deprotonation of Zwitterion is slower compared to the reverse reaction.

The following Figures IV.12 and IV.13 are plots of the experimentally obtained k_0 values against the correlated values using the generated reaction constants in Equations IV.8, and IV.14. These figures clearly indicate that a good overall parity exists between these two sets of values.

Table IV.4. Rate constants based on Zwitterion mechanism for CO_2 reaction with aqueous PZ

Equation	Parameters	T(K)			
		298.15	303.15	308.15	313.15
IV.8	k_2(m^3 /mol·s)	22.02	26.06	32.04	40.04
	k_a(m^6 /mol^2·s)	2.136 E-02	2.574 E-02	2.852 E-02	3.245 E-02
	k_{H2O}(m^6 /mol^2·s)	1.56 E-04	1.84 E-09	1.88 E-04	1.96 E-04
	R^2	1.00	1.00	1.00	1.00
	AAD%	0.63	0.75	0.56	0.43
IV.9	k_2(m^3 /mol·s)	21.90	25.80	31.90	39.78
	R^2	1.00	1.00	1.00	1.00
	AAD%	1.18	1.74	1.00	1.06
IV.14	k^T_a(m^6 /mol^2·s)	3.60E-03	4.60E-03	5.80E-03	7.12E-03
	K^T_{H2O}(m^6 /mol^2·s)	3.98E-04	4.72E-04	5.79E-04	7.22E-04
	R^2	1.00	1.00	1.00	1.00
	AAD%	0.12	0.11	0.14	0.12

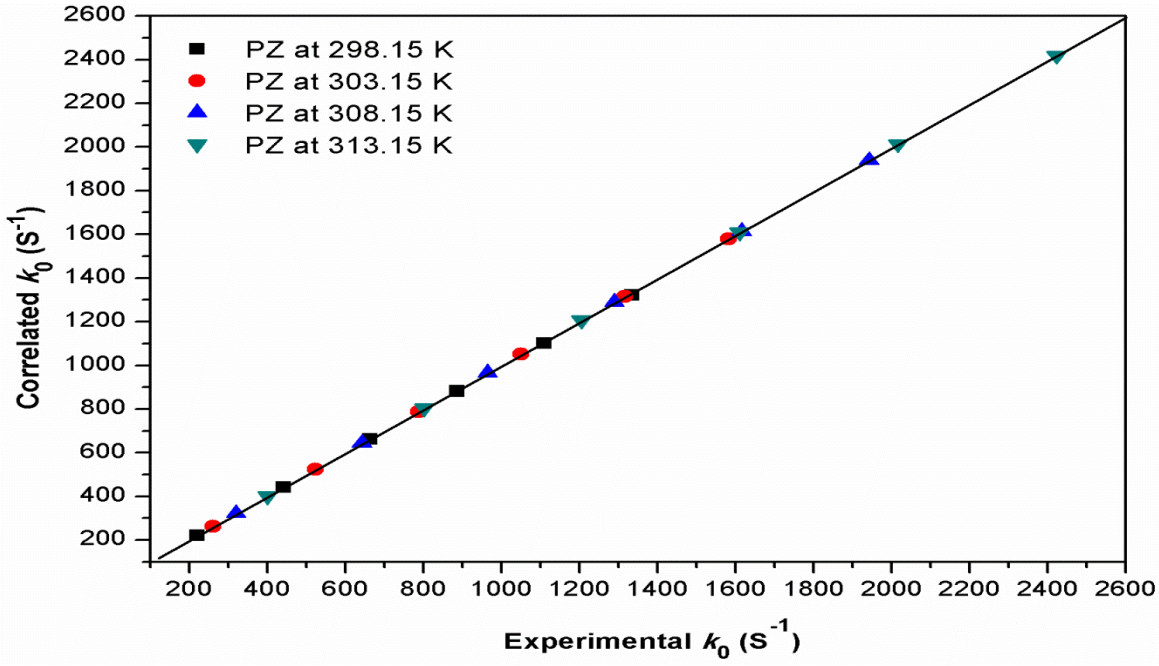

Figure IV.12. Correlation between the measured and predicted pseudo first-order rate constant based on Zwitterion mechanism.

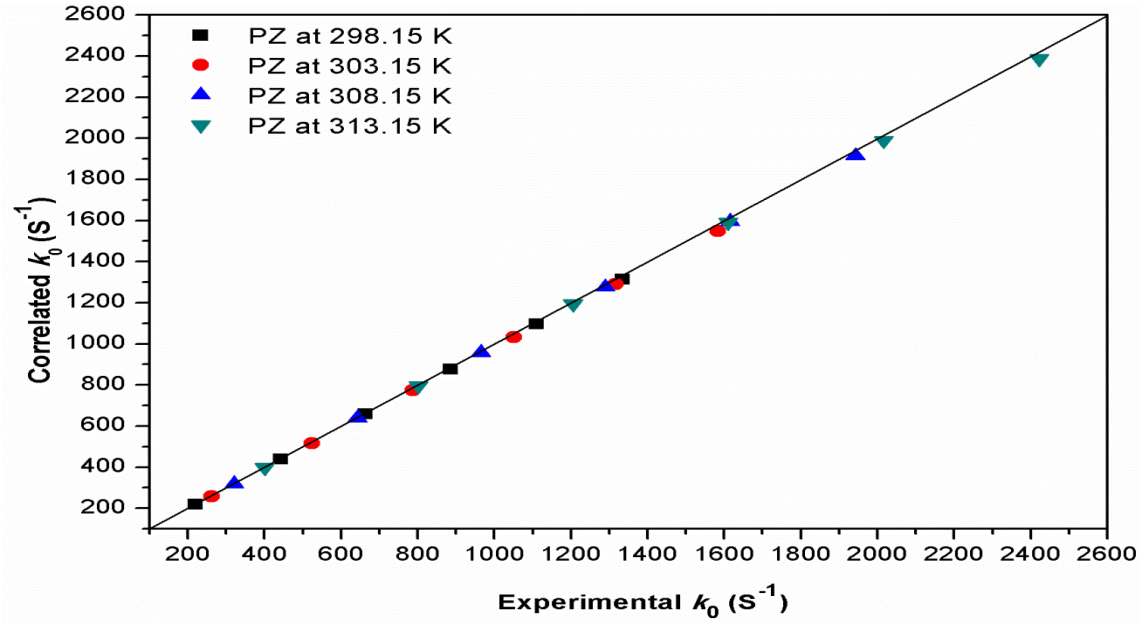

Figure IV.13. Correlation between the measured and predicted pseudo first-order rate constant based on Termolecular mechanism.

Figure IV.12 and IV.13 are plots of the experimentally obtained K_0 values against the correlated values using the generated reaction constants in Equations IV.8 and IV.14 . These figures clearly indicate that a good overall parity exists between these two sets of values.

IV.5.3) Absorption kinetics of CO2 in aqueous blended (MDEA + PZ) system: Reaction kinetics of the reaction of aqueous CO_2 with aqueous MDEA/PZ was carried out using a stopped flow technique, over concentration range of (200 to 800) mol/m^3 for MDEA and (10 to 40) mol/m^3 for PZ at a temperature range of (298.15 to 313.15) K, with an interval of 5 K. The reaction rate of the PZ reactions is much higher than the MDEA catalyzed hydration reaction. Therefore the main reaction occurring in a blended (MDEA + PZ) solution is the carbamate formations.

A model based on hybrid reaction rate, with a Zwitterion mechanism for PZ and a simplified first-order reaction for MDEA is used to correlate the overall reaction rate constant,K_0. The kinetics data are well represented by Eq. (IV.23). The observed pseudo first-order rate constants K_0 (s^{-1}) of the reaction between aqueous MDEA+PZ and aqueous CO_2 obtained from this work are shown in Figures, IV.14, 15, 16, and IV.17. The figures also show the expected trend of increasing the reaction rate, relative to increases in both concentration and temperature, as evidenced by the K_0 values.

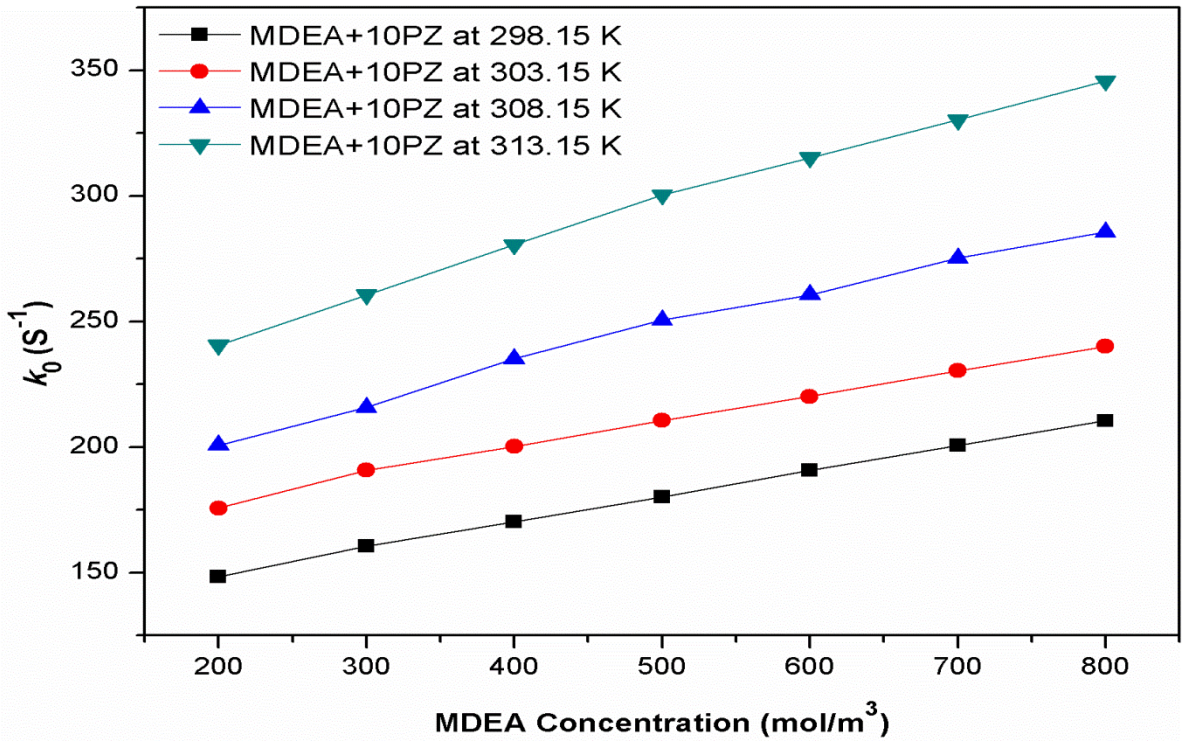

Figure IV.14. K_0 values of the reaction between aqueous CO_2 and aqueous [MDEA+PZ at 10 mol/m^3)] solutions at different concentrations and temperatures.

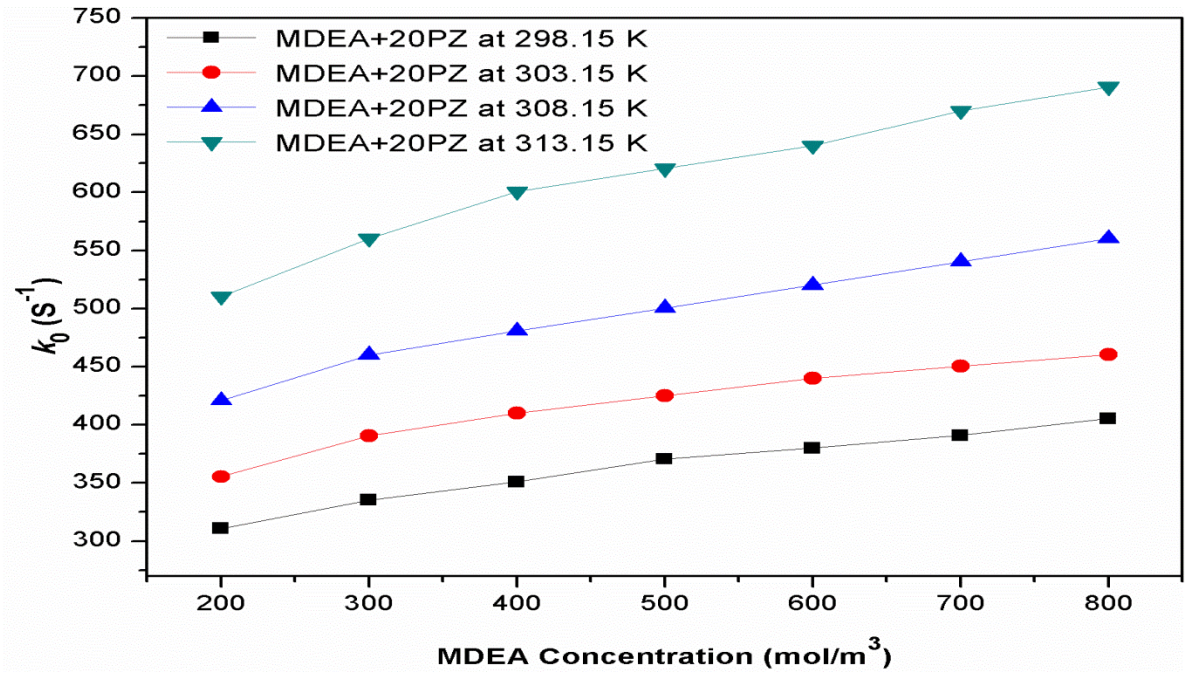

Figure IV. 15. K_0 values of the reaction between aqueous CO_2 and aqueous [MDEA+PZ at 20 mol/m^3)] solutions at different concentrations and temperatures.

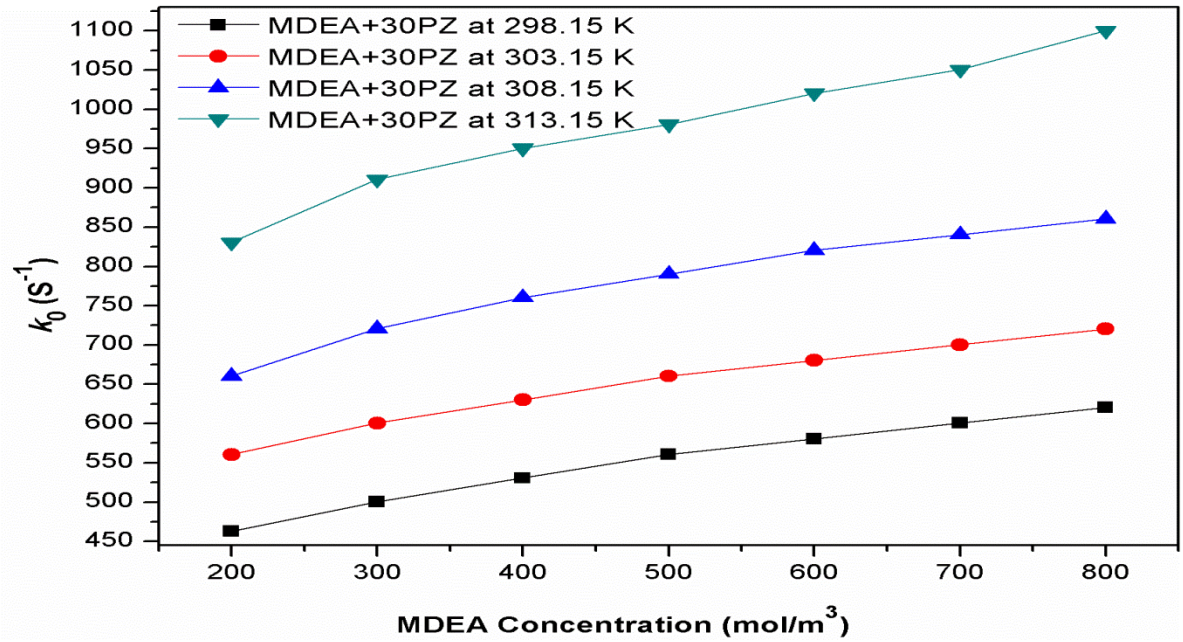

Figure IV.16. K_0 values of the reaction between aqueous CO_2 and aqueous [MDEA+PZ at 30mol/m^3)] solutions at different concentrations and temperatures.

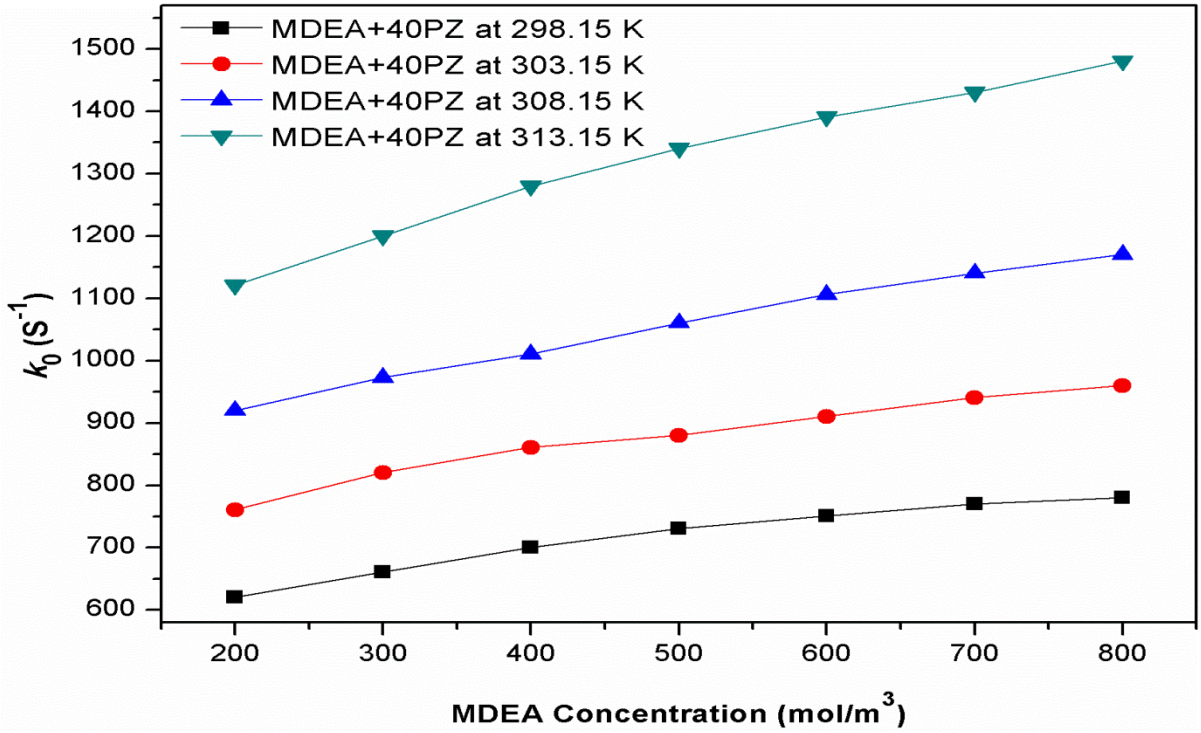

Figure IV. 17. K_0 values of the reaction between aqueous CO_2 and aqueous [MDEA/ PZ (40mol/m^3)] at different concentrations and temperatures.

Based on k_0 values, the concentration of PZ has strongly impacted the CO_2 absorption rate blended (MDEA + PZ) solutions. Higher concentrations of PZ in (MDEA + PZ) solution gave much higher k_0 values at all temperatures.

After replacing the values of the known rate constants $k_{2,PZ}$, $k_{PZ/PZZ}$, $k_{W/PZZ}$, and $k_{2,MDEA}$ reported in Tables IV.2 and IV.4, the only unknown remaining is $k_{\text{MDEA}/PZZ}$. This value is obtained by regressing the kinetic data with Equation IV.23 using Excel's Solver program and the results are reported in Table IV.5.

Table IV.5 displays the variation of k_2 (m^3/mol· s) valued for both MDEA and PZ as temperature increases. The constants are found to increase in the sequence of $k_{MDEA,PZZ} > k_{PZ,PZ} > k_{W/PZZ}$ at all temperatures. The table also shows that the MDEA molecule has more strength in deprotonating the PZ zwitterion than water. The extent of the reaction enhancement taking place depended on the specific amine, and the concentration of each amine constituent.

Table IV.5. Rate constants regressed using Equation IV.23 for aqueous (MDEA+PZ) systems

T (K)	$k_{2,PZ}$ [a]	$k_{2,MDEA}$ [b]	$k_{PZ,PZZ}$ [b]	$k_{MDEA,PZZ}$	$k_{W,PZZ}$ [b]	R^2	AAD%
298.15	22.00	0.009	0.02136	0.1951	1.56 E-04	0.9911	1.77
303.15	26.06	0.014	0.02574	0.2355	1.84 E-04	0.9943	1.27
308.15	32.04	0.018	0.02852	0.2700	1.88 E-04	0.9997	2.16
313.15	40.04	0.024	0.03245	0.3135	1.96 E-04	0.9966	2.16

[a] Table 2; [b] Table 4

Figure IV.18 is a parity plot for the predicted values of the pseudo first-order reaction rate constants against the experimental values for blended (MDEA +PZ) systems. It clearly indicates that a good overall parity exists between these two sets of values.

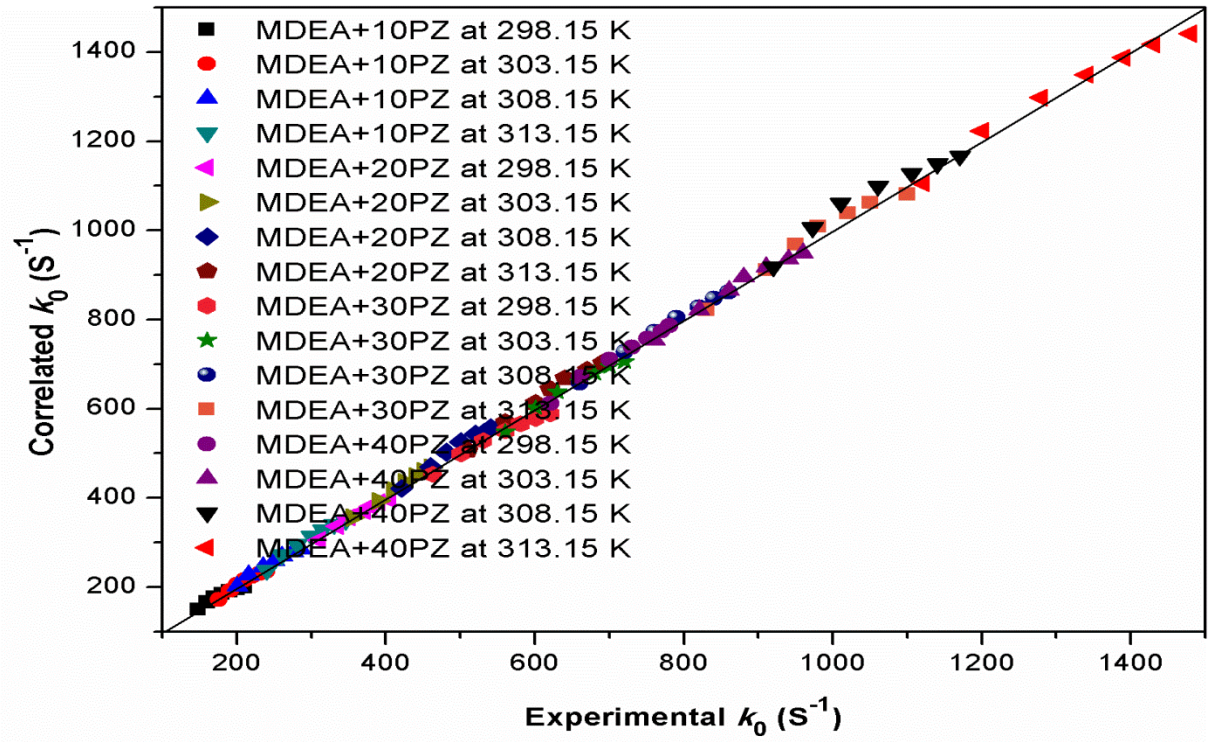

Figure IV.18. Parity plot for the experimental and predicted pseudo first-order rate constants for aqueous solutions of (MDEA+PZ) at different temperatures using Zwitterion mechanism.

The Termolecular model was also used to correlate the data. According to the proposed model Equation IV.25 in the present work, the experimental data of blended DEEA/MEA solutions were correlated to obtain the second-order reaction rate constants listed in Table IV.6.

The blended MDEA / PZ solutions were found to have a much higher CO_2 reaction rates than the individual aqueous MDEA solutions, primarily due to the higher absorption rate of PZ. The addition of PZ enhances the reaction rate of MDEA.

Table IV. 6 shows that the values of k^T_{MDEA},and k^T_{PZ}increased with temperature and are independent of PZ and MDEA concentrations. Note that k^T_{PZ} was an order of magnitude higher than k^T_{MDEA}.

Table IV.6. Rate constants regressed using Equation IV.25 for aqueous (MDEA+PZ) systems

Equation	Parameters	T(K)			
		298.15	303.15	308.15	313.15
IV.25	k^T_{MDEA}(m^6 /mol^2.s)	9.00E-03	1.10E-02	1.30E-02	1.45E-02
	K^T_{PZ}(m^6 /mol^2.s)	8.10E-02	9.58E-02	1.14E-01	1.46E-01
	K^T_{H2O}(m^6 /mol^2.s)	2.17E-04	2.61E-04	3.05E-04	3.71E-04
	R^2	0.9900	0.9834	0.9923	0.9943
	AAD%	1.81	1.60	3.18	4.12

The Arrhenius equation was used to correlate the reaction rate constants (k^T_{MDEA}, and k^T_{PZ}) with the variation of temperature. The resulting constants are plotted in Figure IV.19 and a parity plot is shown in Figure IV.20. By fitting the experimental data, the activation energies for k^T_{MDEA}, and k^T_{PZ} were found to be 24.78, and 30.32 kJ/mol, respectively. The expressions can therefore be written as:

$k^T_{MDEA} = 2.01 \times 10^2 \exp(-2980.6/T)$, $R^2 = 0.9858$ (IV.38)

$k^T_{PZ} = 1.60 \times 10^4 \exp(-3647.2/T)$, $R^2 = 0.9883$ (IV.39)

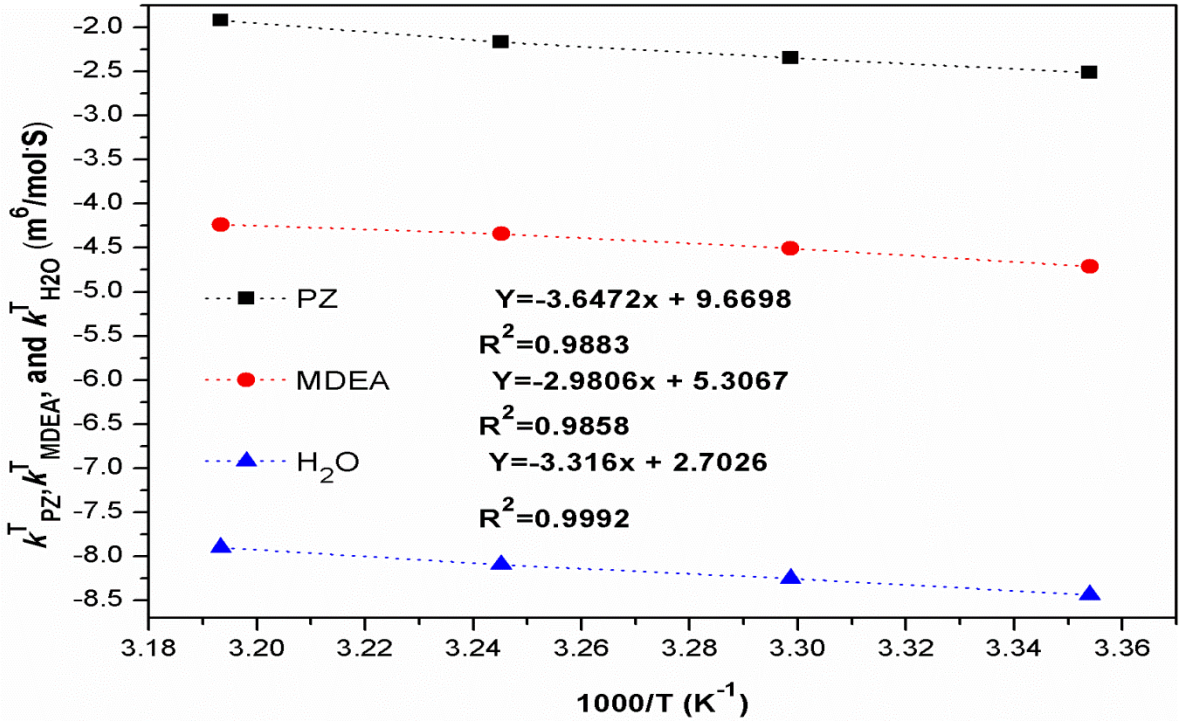

Figure IV.19. Arrhenius plot of (CO_2+MDEA+PZ+ Water) rate constants using the Termolecular mechanism.

Figure IV.20 shows a parity plot scheme for the predicted values of the pseudo first-order reaction rate constant against the experimental values for the blended (MDEA +PZ) system. It clearly indicates that a good overall parity exists between these two sets of values, with an acceptable AAD% of 2.68

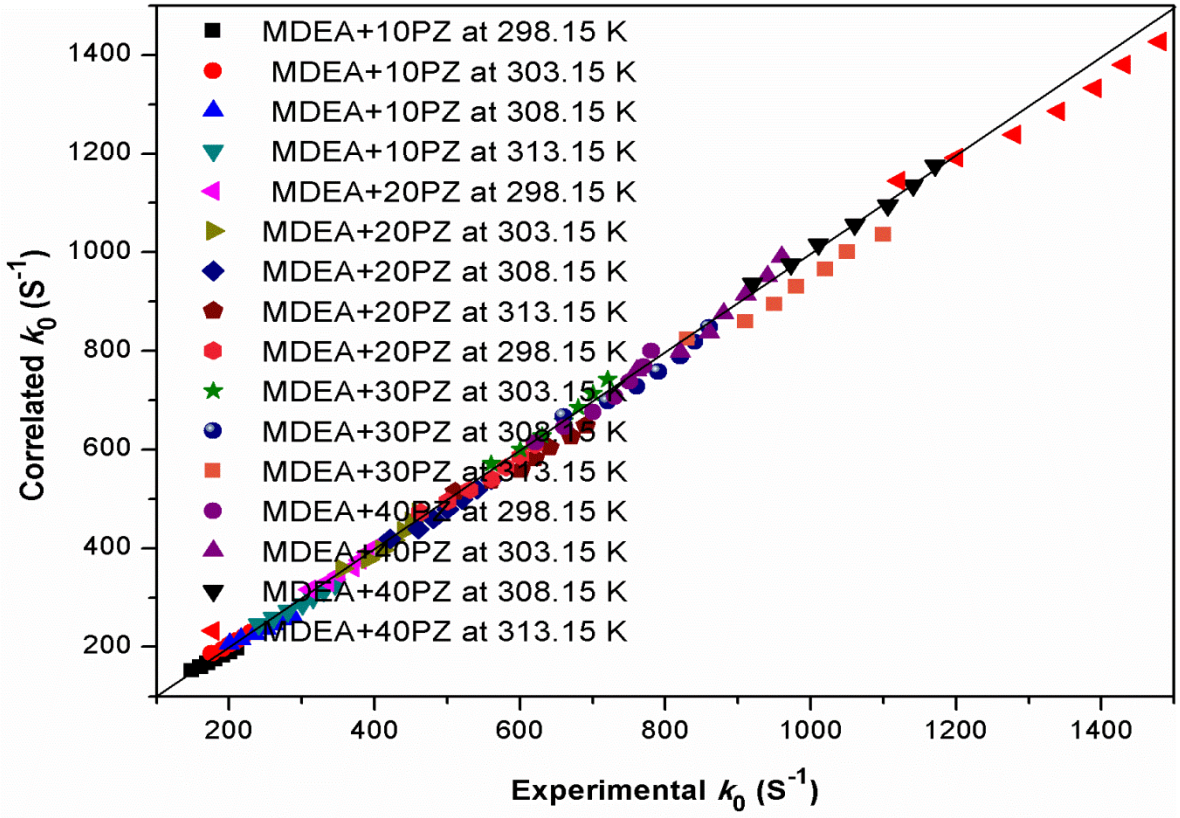

Figure IV.20. Parity plot for the experimental and predicted pseudo first-order rate constants for aqueous solutions of (MDEA+PZ) at different temperatures based on termolecular mechanism.

IV.5.4) Reaction of aqueous CO_2 with aqueous MDEA + Sulfolane:

To fully understand the reaction kinetics of CO2 and (MDEA-Sul) as a promising solvent for chemical absorption, an experiment was performed using the stopped-flow apparatus. Different samples of (MDEA-Sul) , were prepared with a concentration range of (200–1000) and (10-200) mol/m3,respectively, and the experimental temperature set within a range of 298.15 to 313.15K.

Graphical plots of the pseudo first order of selected values against the concentration of (MDEA-Sul) (mol/m^3) is provided in Figures IV.21, 22, 23,24 and IV. 25.

By comparing the absorption kinetics of (MDEA-Sul) with that of MDEA, it will provide valuable information about utilizing (MDEA-Sul) as a promising alternative absorbent for Carbon dioxide capture.

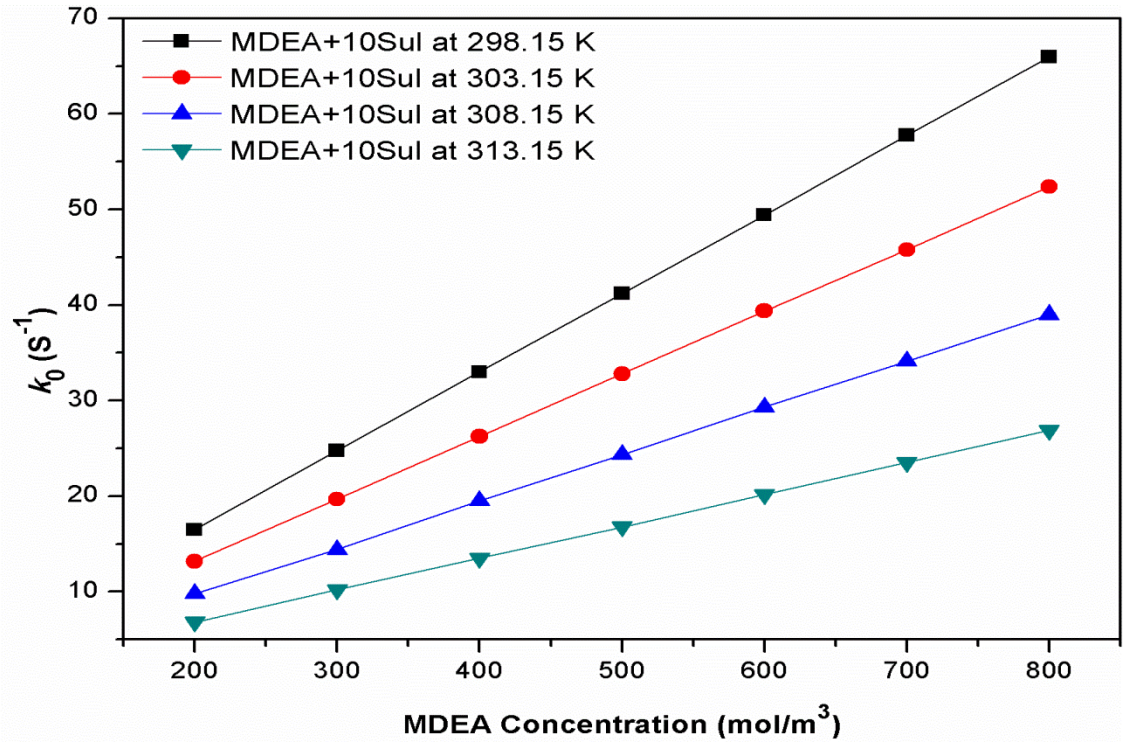

Figure IV.21. Comparison of K_0 values of the reaction between aqueous CO_2 and aqueous MDEA, and aqueous blended [MDEA+ Sulfolane at 10 mol/m^3] solutions at different concentrations and temperatures.

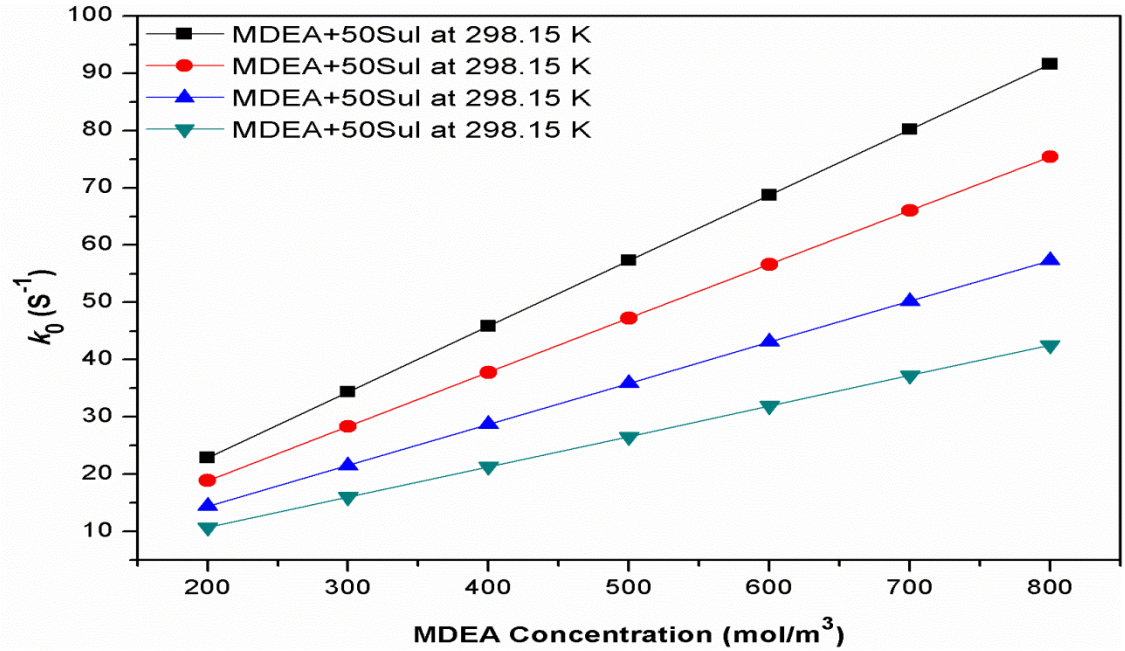

Figure IV.22. Comparison of K_0 values of the reaction between aqueous CO_2 and aqueous MDEA, and aqueous blended [MDEA+ Sulfolane at 50 mol/m^3] solutions at different concentrations and temperatures.

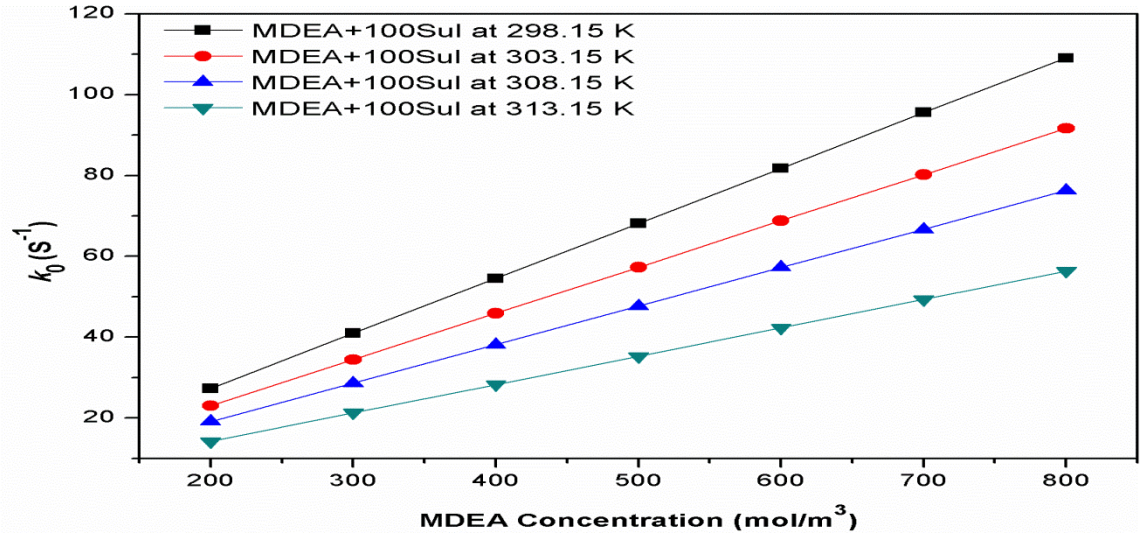

Figure IV.23. Comparison of K_0 values of the reaction between aqueous CO_2 and aqueous MDEA, and aqueous blended [MDEA+ Sulfolane at 100 mol/m^3] solutions at different concentrations and temperatures.

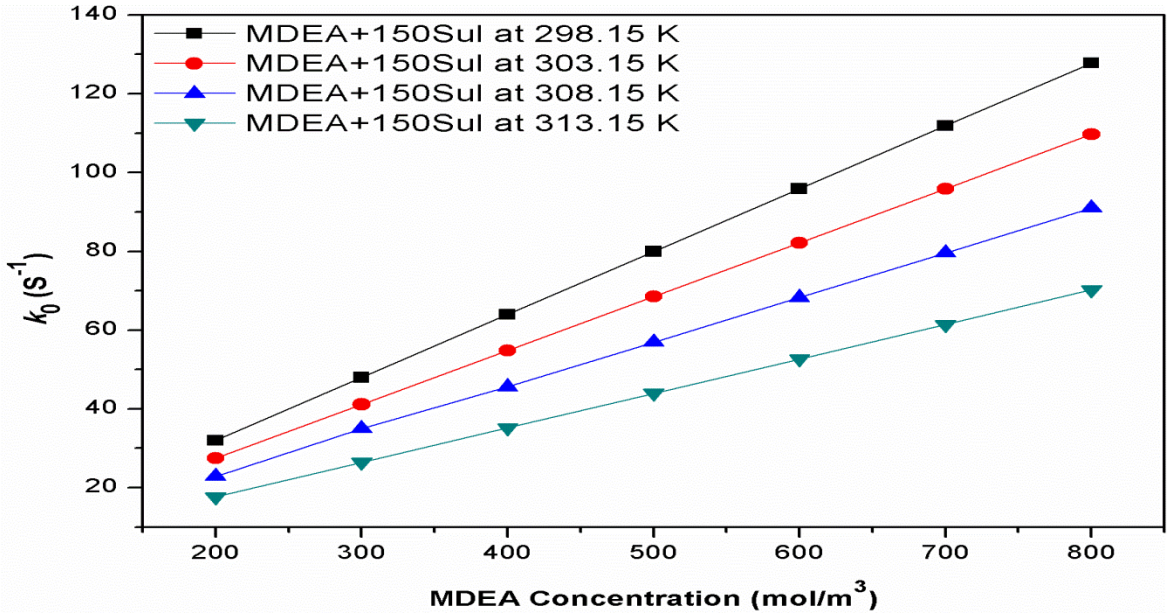

Figure IV.24. Comparison of K_0 values of the reaction between aqueous CO_2 and aqueous MDEA, and aqueous blended [MDEA+ Sulfolane at 150 mol/m^3] solutions at different concentrations and temperatures.

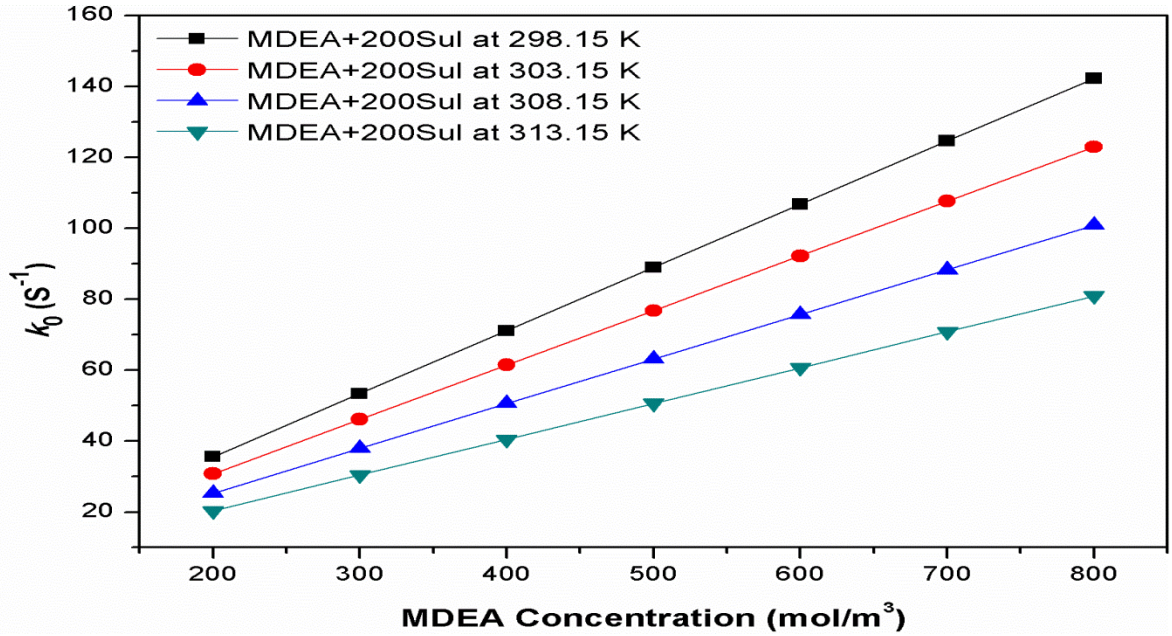

Figure IV.25. Comparison of K_0 values of the reaction between aqueous CO_2 and aqueous MDEA, and aqueous blended [MDEA+ Sulfolane at 200 mol/m^3] solutions at different concentrations and temperatures.

The absorption rates of carbon dioxide in the aqueous mixed solvent solution of (MDEA,

Sulfolane) were higher and faster than those of stand –alone MDEA of the same concentrations

at all temperatures (298.15-313.15 K). This is a direct proof that the absorption of CO_2 in aqueous MDEA is enhanced by the presence of Sulfolane, a polar solvent , justifying in part the commercial use of the Sulfinol-M process technology. According to the work that has been done by Xu et al. (1991) for investigating the effect of Sulfolane on the absorption of CO_2 in the mixed solvent, the apparent kinetic rate of Sulfolane with CO_2 is so small that it can be neglected. Only the contribution of the Sulfolane to the deprotonation need be taken into account. The addition of Sulfolane to MDEA resulted in a significant enhancement of CO_2 absorption rates mechanism was used to correlate the kinetic rates. Reaction orders were found to be practically equal to 1 at all temperatures and Sulfolane concentrations. We have modelled the obtained data when Sulfolane concentrations were kept constant and varied MDEA concentrations.

Table IV.7. Reaction orders of aqueous (MDEA + Sulfolane) systems at different temperatures and Sulfolane concentrations

[MDEA] (mol/m^3)	[Sul] (mol/m^3)	Order [n]			
		298.15K	303.15K	308.15 K	313.15 K
200-800	10	1.0001	0.9960	1.0016	0.9902
200-800	50	0.9997	0.9985	0.9974	0.9944
200-800	100	0.9997	0.9965	0.9987	0.9932
200-800	150	0.9991	0.9986	0.9904	0.9954
200-800	200	0.9995	0.9987	0.9971	0.9974

In Table IV.8, a comparison is presented between different values of k_2 (m^3/mol·s) for the reaction between CO_2 in both aqueous MDEA and aqueous (MDEA + Sulfolane) mixtures using the base catalyst mechanism. The addition of Sulfolane to water with MDEA resulted in a significant enhancement of CO_2 absorption rates. The absorption kinetic rate constants for CO_2 in

in the aqueous mixed solvent solution of (MDEA + Sulfolane) were much higher (59 % to 92 %) than those in standalone aqueous MDEA at all temperatures as shown in Table IV.7 and Figure IV.26. Note that in both cases the order with respect to MDEA was practically 1. Note also that contrary to aqueous MDEA, the rate constants were higher at lowest temperature and decreased with higher temperature. Note the very low values of k_2 in aqueous MDEA solutions, the addition of Sulfolane greatly enhances the reaction.

Table IV.8. Values of k_2 (m^3/mol·s) for the reaction between CO_2 and aqueous MDEA and (MDEA+ Sulfolane) solutions based on base catalyst mechanism

T(K)	k_2 (aq. MDEA+ Sulfolane) (m^3/mol·s)	k_2 (aq. MDEA) (m^3/mol·s)	Increase (%)
298.15	0.121	0.009	92.6
303.15	0.101	0.014	86.2
308.15	0.080	0.018	77.6
313.15	0.059	0.024	59.0

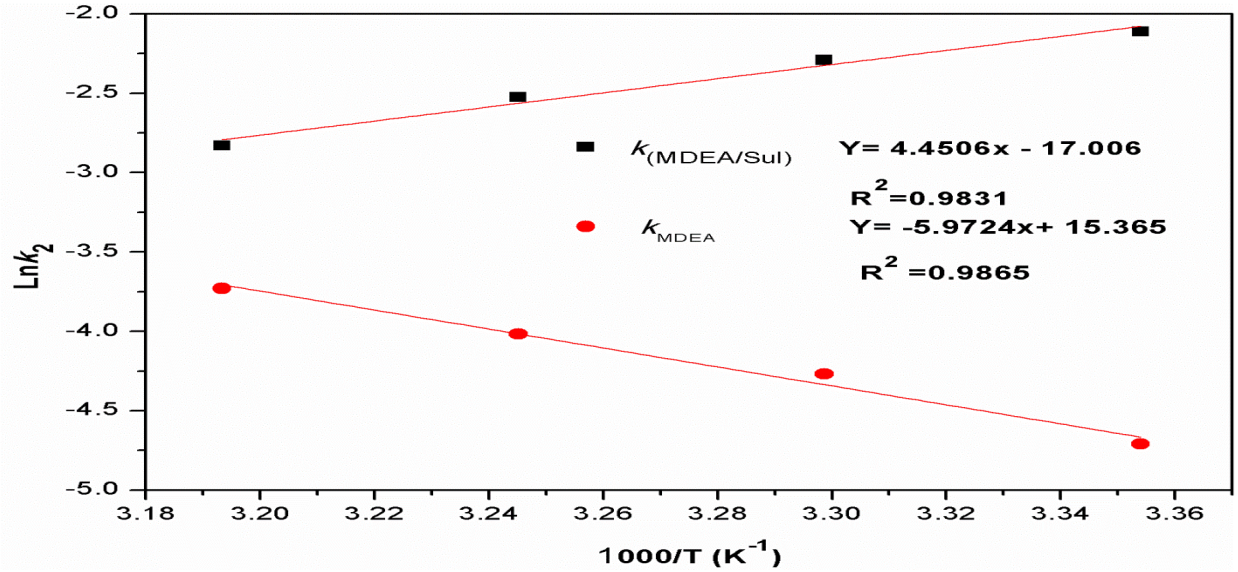

Figure IV.26. Variation of k_2 as function of temperature for aqueous (CO_2+MDEA) and aqueous (CO_2+MDEA+Sulfolane) systems.

The regression of the k_2 values results in the following Arrhenius equation:

$k_{MDEA/Sul}$ (m^3/mol·s) = 4.11 x 10^{-8} Exp (-4450.6/T), R^2 =0.9831 (IV.40)

The AAD between the experimental pseudo first-order reaction rate constant (k_0) and those calculated based on the kinetics model was 0.52 % and the parity plot is shown in Figure IV.27, indicating that the base catalyzed reaction mechanism was successfully applied in the aqueous (MDEA + Sulfolane) system.

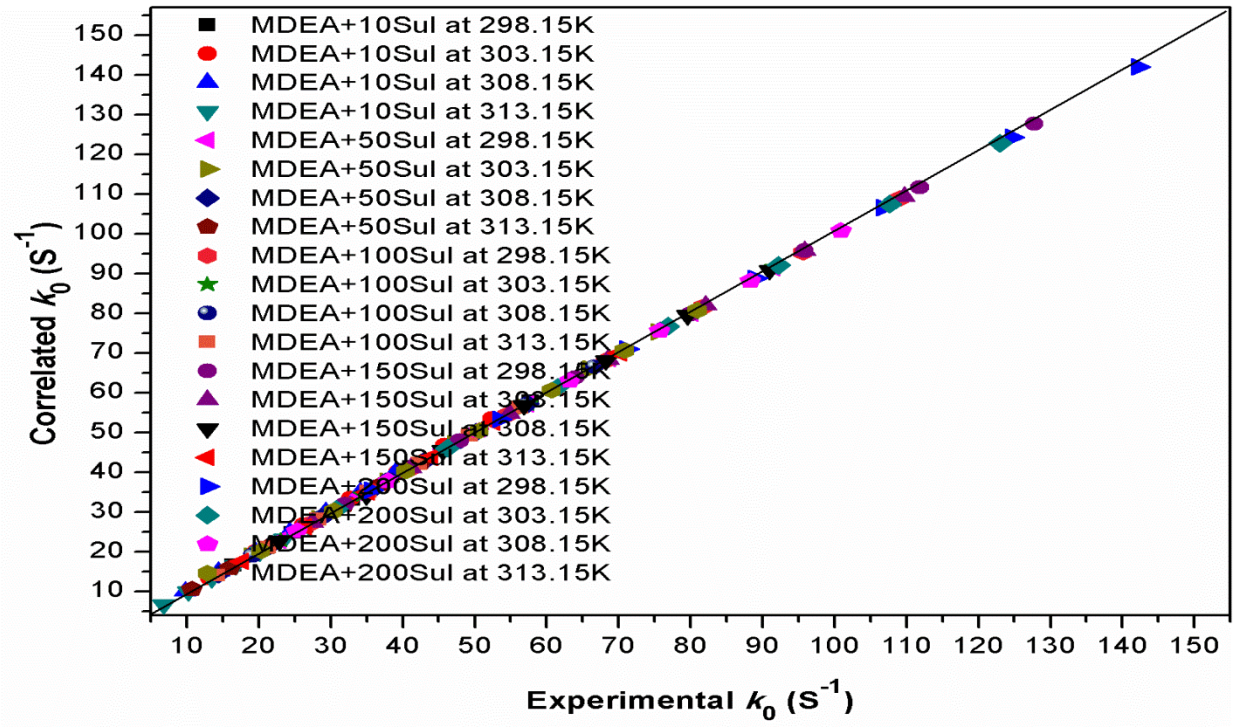

Figure 27. The correlation between the measured and predicted pseudo first-order rate constant based on base catalyzed mechanism.

IV.5.5) Absorption kinetics of CO_2 in (PZ + Sulfolane) system

The kinetics rates of CO_2 reactions in aqueous solutions of (PZ+ Sulfolane) were measured and reported in the form of pseudo-first-order rate constants *(k_0).* The observed rate constants are shown in Figures IV.28, 29, 30,31, and IV.32 as a function of PZ concentration. This concentration was kept at least ten times higher than CO_2 concentration. The addition of the different quantities of Sulfolane (10 to 200 mol/m^3) to the aqueous PZ solutions led to a noticeable increase in the reaction rates at high Sulfolane concentrations as shown in the next five figures when compared to aqueous PZ values presented earlier. The obtained k_0 values of CO_2 absorption in these mixed solutions of (PZ+ Sulfolane) are strongly influenced by Sulfolane concentration, and increased with the increase in Sulfolane concentrations. The results

demonstrate that the absorption of CO_2 in aqueous PZ solution is enhanced by the addition of Sulfolane.

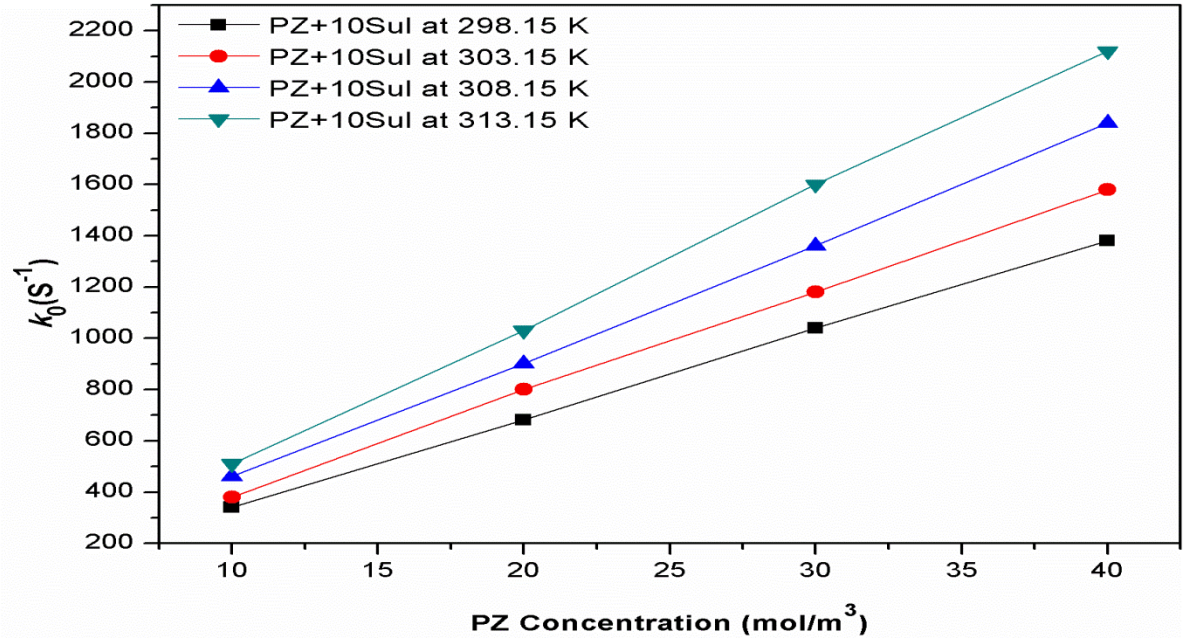

Figure IV.28. Comparison of K_0 values of the reaction between aqueous CO_2 and aqueous PZ, and aqueous [PZ+ Sulfolane at 10 mol/m^3] solutions at different concentrations and temperatures.

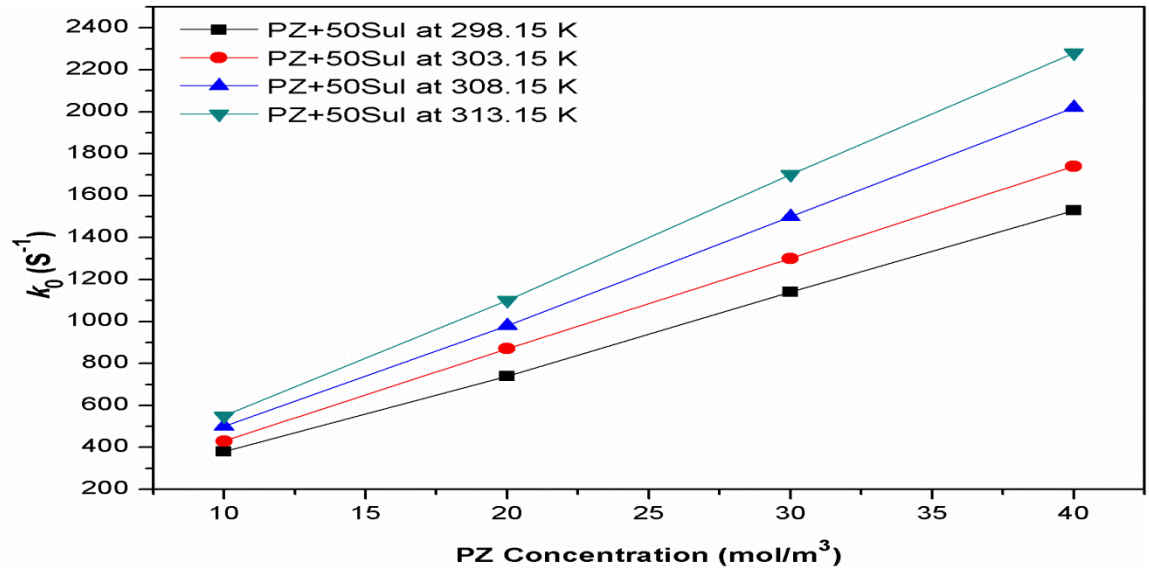

Figure IV.29. Comparison of K_0 values of the reaction between aqueous CO_2 and aqueous PZ, and aqueous [PZ+ Sulfolane at 50 mol/m^3] solutions at different concentrations and temperatures.

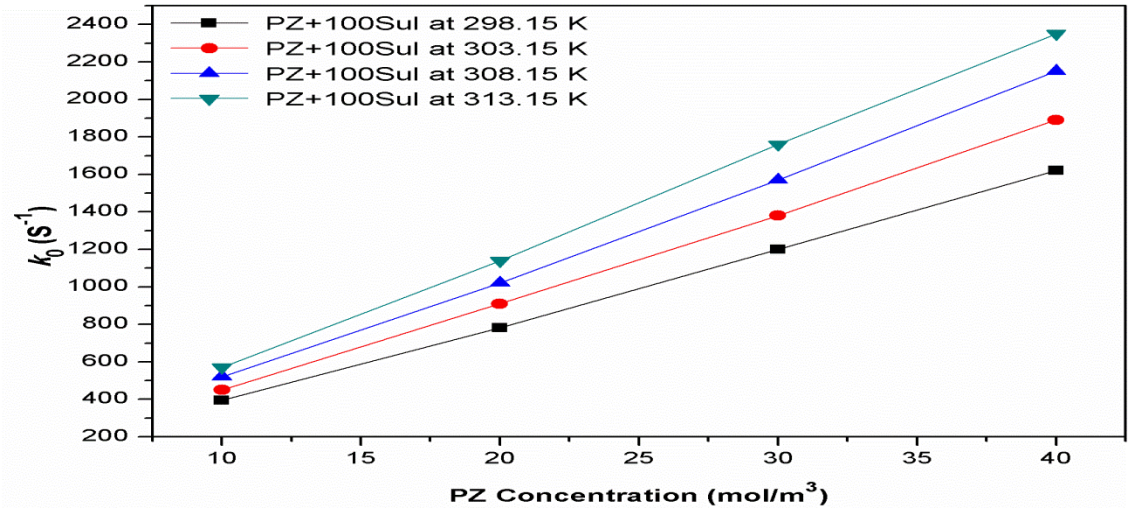

Figure IV.30. Comparison of K_0 values of the reaction between aqueous CO_2 and aqueous PZ, and aqueous [PZ+ Sulfolane at 100 mol/m^3] solutions at different concentrations and temperatures.

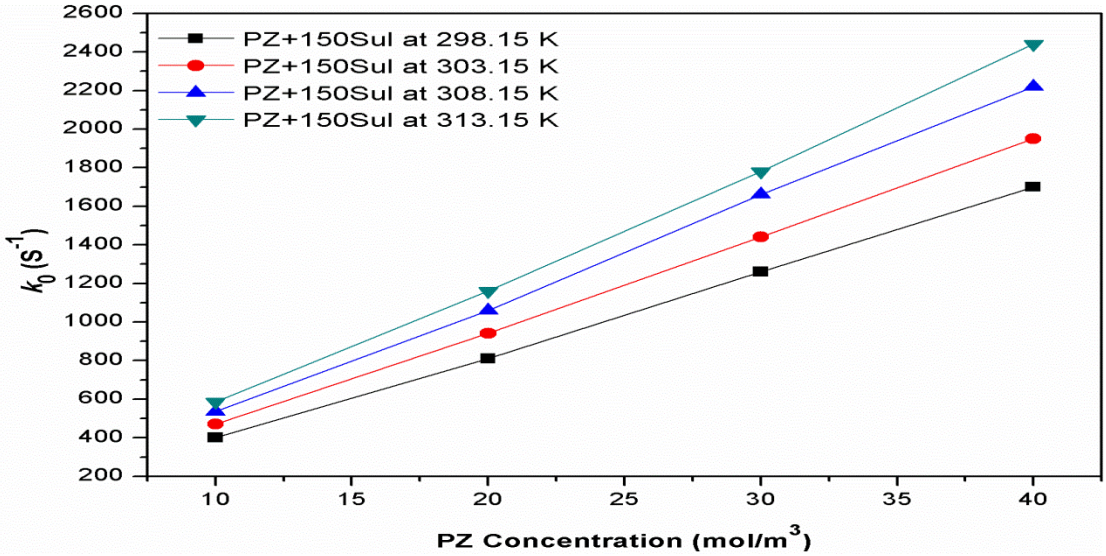

Figure IV.31. Comparison of K_0 values of the reaction between aqueous CO_2 and aqueous PZ, and aqueous [PZ+ Sulfolane at 150 mol/m^3] solutions at different concentrations and temperatures.

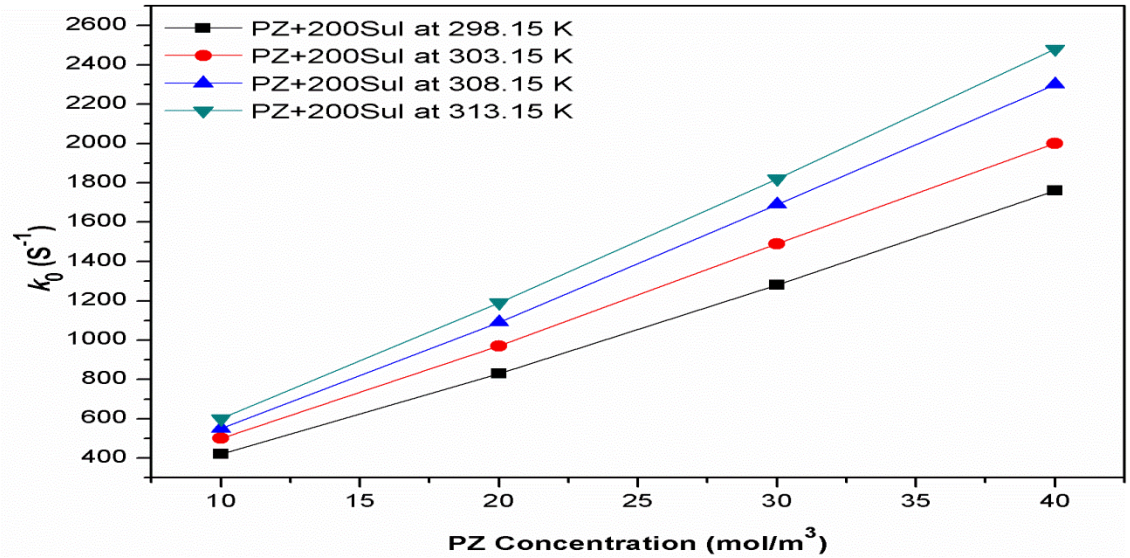

Figure IV.32. Comparison of K_0 values of the reaction between aqueous CO_2 and aqueous PZ, and aqueous [PZ+ Sulfolane at 200 mol/m^3] solutions at different concentrations and temperatures.

The plots clearly show the positive effect Sulfolane has on k_0 as it increases with Sulfolane concentrations A multiple linear regression procedure was used to determine the fitting

parameters (k_{PZ}^{T} , k_{Sul}^{T} and k_{H2O}^{T}) at each temperature. These fitting parameters and the average deviation between the experimental data and the fitted model are shown in Table IV.9.

Dependences of kinetics parameters k_{PZ}^{T} , k_{Sul}^{T} and k_{H2O}^{T} on temperature are given by:

$k_{PZ}^{T} = 2.10 \times 10^{3}$ Exp (-2807.4/T), R^2 =0.9943 (IV.40)

k_{H2O}^{T} =1.84 Exp (-2368.9/T), R^2 =0.9935 (IV.41)

k_{Sul}^{T} =2.57 Exp (-1982/T), R^2 =0.9802 (IV.42)

Table IV.9. Rate constants determined according to the termolecular mechanism for the aqueous (PZ + Sulfolane) systems

Equation	Parameters	T(K)			
		298.15	303.15	308.15	313.15
IV.28	K^{T}_{PZ}(m^6 /mol^2·s)	1.64E-01	1.85E-01	2.26E-01	2.61E-01
	K^{T}_{Sul}(m^6 /mol^2·s)	3.41E-03	3.69E-03	4.06E-03	4.68E-03
	K^{T}_{H2O}(m^6 /mol^2·s)	6.41E-04	7.52E-04	8.54E-04	9.43E-04
	R^2	0.9988	0.9989	0.9990	0.9992
	AAD%	4.16	4.16	3.74	3.54

Figure IV.33 is a representation of an Arrhenius plot between the rate constants and temperature, for k_{pz}^{T} and k_{H2O}^{T}extracted by fitting data to the Termolecular mechanism and confirming this relationship Equation IV.28 over a temperature range varying from (298.15 to 313.15) K.

The order was practically one at all temperatures and for all Sulfolane concentrations.

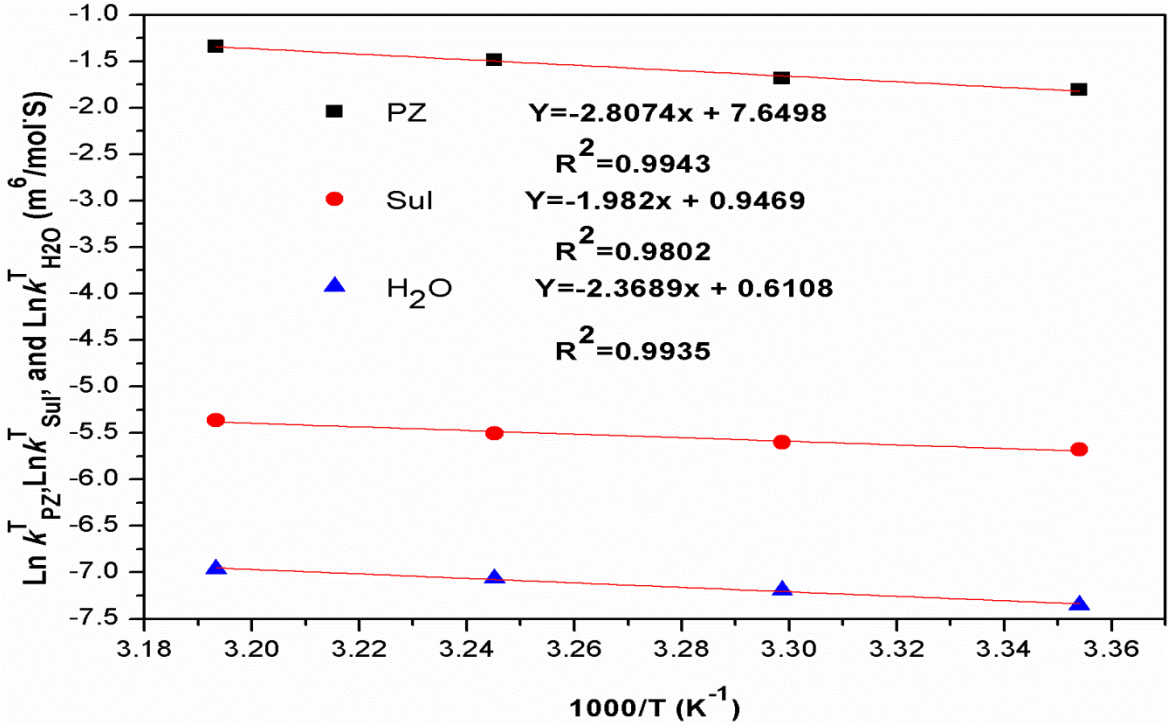

Figure IV. 33. Arrhenius plot of aqueous (CO_2+PZ+Sulfolane) rate constants using the Termolecular mechanism.

k_{cal} values were plotted in Figure IV.34, and were found to compare favorably with the corresponding experimentally observed k_o values. The average deviation between these two sets of values was found to be 3.54%.

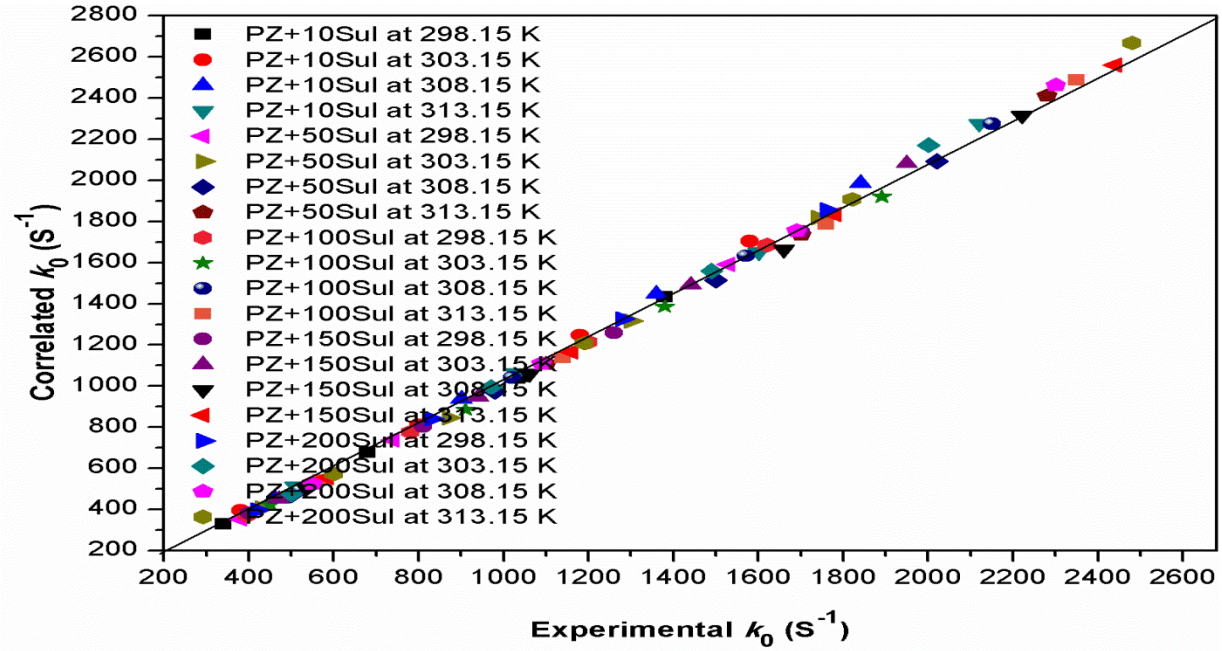

Figure IV.34. Parity plot for the experimental and predicted pseudo first-order rate constants for aqueous solutions of (PZ + Sulfolane) at different temperatures based on Termolecular.

From the obtained k_0 values of CO_2 absorption in these mixed solutions of (PZ+ Sulfolane) are strongly influenced by Sulfolane concentration. Values of the rate constants $k_{2,PZ}$, k_{PZ,PZ_Z}, k_{sul,PZ_Z}, k_{W,PZ_Z}, were obtained by regressing the kinetic data with Equation IV.27 using Excel's Solver program are shown in Table IV.10. The determined rate constants were found to increase at all temperatures in the sequence $k_{PZ,PZZ} > k_{sul,PZ} > k_{W/PZZ}$.

Table IV.10. Rate constants determined according to Equation IV.27 for the aqueous (PZ + Sulfolane) systems

T (K)	[a]Aq. $k_{2,PZ}$	$k_{2,PZ}$ *(% increase)*	$k_{PZ,PZZ}$	$k_{sul\ ,PZZ}$	$k_{W,PZZ}$	R^2	AAD%
298.15	22.02	38.24 (74 %)	0.2436	2.12 E-05	4.25 E-07	0.9990	3.50
303.15	26.06	44.83 (72 %)	0.3630	2.83 E-05	6.15 E-07	0.9993	3.17
308.15	32.04	50.80 (58 %)	0.4620	3.92 E-05	7.84 E-07	0.9995	3.48
313.15	40.04	56.24 (40 %)	0.4850	4.46 E-05	8.92 E-07	0.9995	3.33

[a] Table IV.4 for aqueous PZ systems

The regression of k_2 values from the table above results in the following Arrhenius equation:

$k_2(m^3/\ mol{\cdot}s) = 1.19 \times 10^5\ Exp\ (-2394.5/T)$, $[R^2 = 0.9928]$. (IV.43)

Correlated k_o values and the experimentally obtained were found to compare favorably with the corresponding experimentally observed *k*o values Figure IV.35. The percentage average deviation between these two values was found to be 3.36 %.

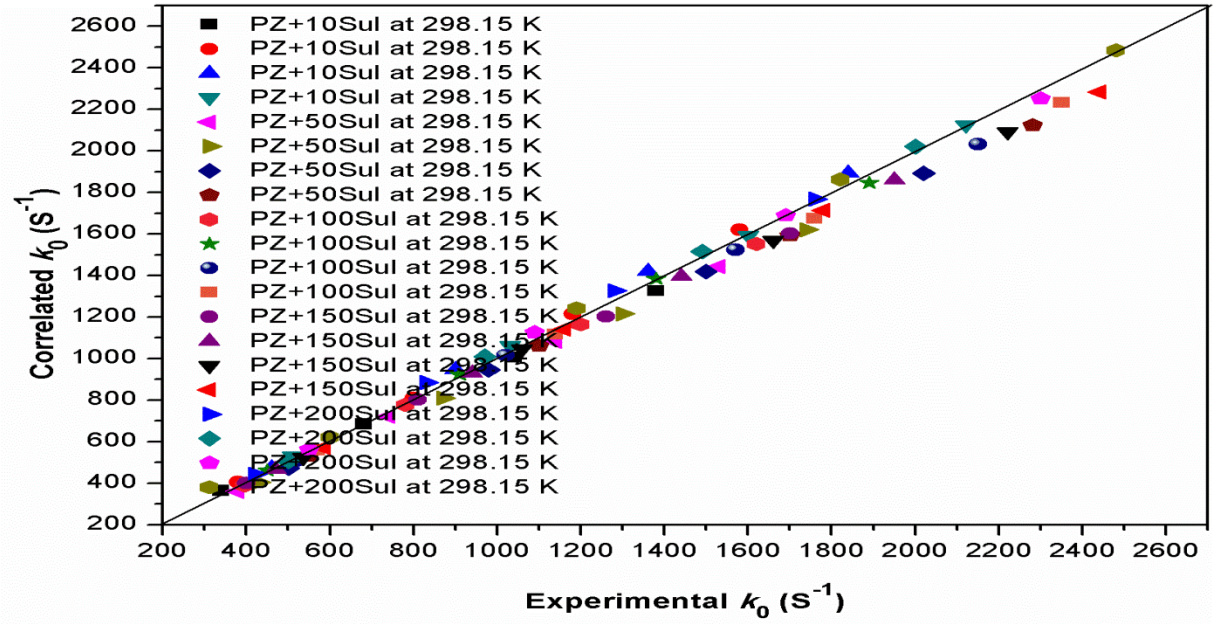

Figure IV.35. Parity plot for the experimental and predicted pseudo first-order rate constants for aqueous solutions of (PZ+ Sulfolane) at different temperature based on Zwitterion.

Conclusion:

Pseudo first order constants (k_0) for the reactions of CO_2 in aqueous PZ, MDEA, (MDEA + PZ), (MDEA + Sulfolane), and (PZ + Sulfolane) solutions were measured at (298.15, 303.15, 308.15 and 313.15) K using the stopped flow technique. MDEA reacts relatively slowly with CO_2 due to its tertiary amine characteristics. The base catalyst mechanism correlated the standalone MDEA data very well. The reaction kinetics of CO_2 in aqueous standalone MDEA and PZ increased with increasing temperature and concentration. The addition of small quantities of PZ to MDEA resulted in an important enhancement of CO_2 absorption rates.

New data for the reaction kinetics of carbon dioxide in aqueous amine solutions with Sulfolane (MDEA+ Sulfolane), and (PZ+ Sulfolane) were also reported. The absorption rates of carbon dioxide in aqueous mixed solvent solutions of (MDEA+ Sulfolane) were higher than those for standalone MDEA at the same concentrations at all temperatures from (298.15 to 313.15) K. The optimum temperature for the kinetic rates was 208.15 K and values decreased with temperature. Enhancement by Sulfolane over aqueous solution varied from 59 % to 92 % if the kinetic data were regressed with the same base catalyst model used for tertiary amines.

The absorption rates of carbon dioxide in aqueous mixed solvent solutions of (PZ+ Sulfolane) were higher than those for standalone PZ at the same concentrations at all temperatures (298.15 K to 313.15 K). Enhancement in the rate constants varied from 40 % to 74 %. In this case, the kinetic rates increased with increasing temperatures. The Termolecular reaction mechanism was used to successfully regress the kinetic data for aqueous (PZ+Sulfolane) solutions.

A hybrid model (base catalyst and Zwitterion) was capable of correlating very well all data for aqueous amine blends of (PZ+MDEA). Results show that addition of PZ enhanced the kinetic rates compared to standalone MDEA.

The kinetic study confirms the advantage of commercially available Sulfinol technology over standalone amine-based processes.

Chapter V

Solubility of CO_2 in Aqueous Solutions of blended (MDEA- Sulfolane), and (MDEA-PZ)

Chapter V: Solubility of CO_2 in Aqueous Solutions of blended (MDEA- Sulfolane), and (MDEA-PZ)

Introduction

The removal of acid gas impurities such as CO_2, H_2S, COS and CS_2 from natural and industrial gases is a frequently encountered operation in process industry. Natural gas contains varying amounts of these acid gas components. Physical and chemical absorption processes have proved successful for the purification of gaseous streams. Physical absorption is preferable when the acid gas to be removed has a high partial pressure since loading increases almost proportionally to the partial pressure; chemical absorption, characterized by a saturation phenomenon above a certain partial pressure, should be used when the partial pressure of the acid gas is low. Since the economics of absorption processes mainly depends on the chosen solvent, it is very important to carry out studies to select better solvents. Therefore the investigation of equilibrium solubilities of gaseous solutes in liquids is of fundamental importance for this purpose. Industry would prefer to use less corrosive and more advanced solvent systems which could be formulated along with the plant design and operation, according to the feed and exit streams specifications of plants.

The solubility of gases in liquids is a fundamental property for the design of gas absorption and stripping columns and gas-liquid and gas-liquid-solid reactors in the chemical industry. In addition, solubility results over a wide range of temperature are useful for studying the solution properties in the chemical, biochemical, environmental protection, and energy industries. The alkanolamine solutions can be generally classified as chemical or physical solvents. Chemical solvents are characterized by liquid phase reactions between the acid gas, such as CO_2, and a soluble base such as alkanolamine. Although the chemical reactions allow for a high solubility even at low partial pressures, the solubility, however, is limited by the stoichiometry of the reactions and the solution cannot be easily loaded once the reactant has been depleted (Roberts, and Mather, 1988)**.** Physical solvents, on the other hand, absorb by physical dissolution without chemical reaction and the solubility is approximately linear with the CO_2 partial pressure. Thus, physical solvent have a much lower capacity for CO_2 absorption than chemical solvents at low pressures, but since they lack stoichiometry limits they may be loaded to higher levels at high partial pressures (Roberts, and Mather, 1988). Solubility data of acid gases in the aqueous

alkanolamines solutions at various temperatures, pressure, and concentrations are required to design and simulate acid gas removal units. So far, several investigators have carried out the measurement of the solubility of CO_2 in the various aqueous alkanolamines.

Aqueous solutions of MDEA along with a rate activator piperazine (PZ) have been successfully used for years in the natural gas industry for removal of CO_2 and/or hydrogen sulfide (H_2S) (Bishnoi and Rochelle, 2002) reported the absorption rate of CO_2 into PZ/MDEA aqueous solution in the specified range of pressure and temperature. Their results showed that the solubility of CO_2 in the aqueous PZ/MDEA solutions is higher than the blends of the MEA/MDEA, DEA/MDEA and MDEA. (Tan and Chen, 2006) investigated the removal efficiency of CO_2 in a blend of AMP+MEA mixed with PZ (piperazine). They showed that the CO_2 removal efficiency enhanced 2 to 4 times in the presence of piperazine. (Haghtalabet al., 2014), (Haghtalab and Ghahremani, 2015) measured the solubility of CO_2 in the aqueous blends of DIPA + AMP+PZ, MDEA+AMP+PZ, DIPA+AMP, DIPA+PZ and DIPA solutions at(313.15, 328.15 and 343.15 K) and pressure range of (100 - 4000 kPa). They found that the presence of PZ as a chemical activator in the DIPA and MDEA aqueous solutions led to enhancing the absorption of CO_2 in these blended alkanolamine solutions. Due to certain advantages of (MDEA + PZ) solvent, it is the focus of many recent research activities on gas treating **(**Zoghi et al., 2012). As a tertiary amine, MDEA does not form a carbamate and it does not easily undergo amine polymerization like the primary and secondary amines Closmann et al.(2009). Both MDEA and PZ are more resistant to thermal and oxidative degradation Freeman et al.(2010). Besides, MDEA is much less corrosive **(**Jenab et al., 2005). The heat of absorption of this mixed solvent (MDEA + PZ) at high CO_2 loading is low **(**Svensson et al.,2013), hence solvent regeneration energy is reasonable for the CO_2 capture operation. . A number of such processes make use of mixed solvents composed of a non-aqueous physical solvent and an aqueous amine to take advantage of both physical and chemical absorptions. The best known example of such mixed solvents is the mixture of sulfolane (TMS) and aqueous solution of amine, either di-isopropanolamine (DIPA) or methyldiethanolamine (MDEA**)** (Korens et al.,2002; Klinkenbijl et al.,1999) as used in the sulfinol process (Flynn,1981). One of the advantages of the aqueous sulfolane–amine process for acid gas removal is the ability to simultaneously remove mercaptans and COS (Carbonyl sulfide), which are not removed by pure chemical solvents **.**Klinkenbijl et al.(1999).

Solvents such as triethylene glycol dimethyl ether (TEGDME), 1-methyl-2-pyrolidinone (NMP), and tetramethylene sulfone or sulfolane (TMS), are non-reactive organic polar compounds, which physically dissolve CO_2 and H_2S acid gases in high-pressure gas streams in industrial gas treatment processes. Physical solvents are less corrosive than chemical solvents because no chemical reaction occurs between the acid gases and these solvents and they are usually used when the concentration of acid gas impurities in the total gas streams is high (Kohl, and Nielsen, 1997). Sulfolane, known as tetramethylene sulfone (TMS), is frequently used as a physical solvent that is added to MDEA as a chemical activator.

Sulfolane has high physical absorption capacity for CO_2 and H_2S, hence used in physical and hybrid solvent processes (e.g., sulfinol-M process) (Angaji et al.,2013**).** The physical characteristics of the aqueous sulfolane–amine solution make it possible to tune the hybrid solvent by varying the relative amounts of water and sulfolane in order to reduce the solvent regeneration energy. Macgregor and Mather evaluated the solubility of H_2S, CO_2, and their mixtures at 40C and 100C in the mixed solvent consisting of MDEA (20.9 wt%) + sulfolane (30.5 wt.%) (Macgregor, and Mather, 1991). In that work, their results were compared with the same composition system, which contains AMP instead of MDEA. In 2016, Dash and Bandyopadhyay investigated the solubility of carbon dioxide in the aqueous mixture of N-methyldiethanolamine with piperazine and sulfolane (Dash, and Bandyopadhyay, 2016). They showed that the CO_2 solubility in the hybrid sulfolane based solvent reduces at the gas partial pressure of the lower range (i.e.10–100 kPa) while it enhanced at the higher partial pressure range of (100–1000) kPa at 323 K. In 2015, the solubility of CO_2 and H_2S in sulfolane and the density and viscosity of the saturated liquid binary mixture of (sulfolane + H_2S) and (sulfolane + CO_2) was reported by Jalili et al., 2015. However, the limited works have been performed to evaluate the solubility of Sulphur components such as mercaptans in solvent mixtures.

In fact, using hybrid solvents allows one to take the advantage of both physical and chemical absorption of CO_2. use of a physical solvent, e.g., sulfolane in varying concentration, has been developed to take advantage of the VLE of each class of solvents (Wang et al., 2010).

In view of this, Sulfolane has been chosen as one of the solvents of the hybrid solvent system in this study. The mixing of the chemical solvent, MDEA, and the physical

solvent sulfolane, is expected to increase the CO_2 loading capacity, while PZ will act as a rate activator. The physical character of the aqueous sulfolane–amine solution makes it possible to vary the relative amounts of water and sulfolane and to lessen the energy needed for regeneration.

The objectives of our study are: First, investigating the effect of temperature and pressure on the solubility of CO_2. The second is to investigate the effect of increasing sulfolane, and amine concentration as a physical and chemical solvent, respectively, on the solubility of CO_2 in the mixed solvent.

V.1) Experimental setup and procedure:

The experimental apparatus consists of an Autoclave glass reactor cell ($1108.366172 \times 10^{-6}$ m^3) (Erie, PA, USA). The cell is connected to a water bath (programmable temperature controller, polyscience) maintained at ± 0.04 °C by a temperature controller (Erie, PA, USA). The temperature in the cell was measured by an Omega thermocouple. The fluid pressure in the cell was measured with a calibrated digital transducer (PX 800-010GV and an indicator DP 40 from Omega) with an estimated accuracy ± 0.1%. There are valves for the inlet of gas and liquid and a connection to a vacuum pump (Figure V.1).

Figure V.1. Solubility experimental equipment for measuring equilibrium solubility of CO_2 (Autoclave reactor).

Prior to the introduction of the fluid, the apparatus was brought to the desired temperature and purged with nitrogen to remove traces of oxygen. Initially, a vacuum was applied to the reactor effectively to generate absolute pressures below 13.3 pa. Then, the reactor was charged with 250 mL of liquid. The temperature was then adjusted to the desired value through the external heating jackets.

To ensure that equilibrium was reached, the mixer was started and kept in operation for six to eight hours. To calculate the CO_2 loading, the method of Park and Sandall (Park and Sandall, 2001), also used by Zoghi et al.(Zoghi et al., 2012),was implemented.

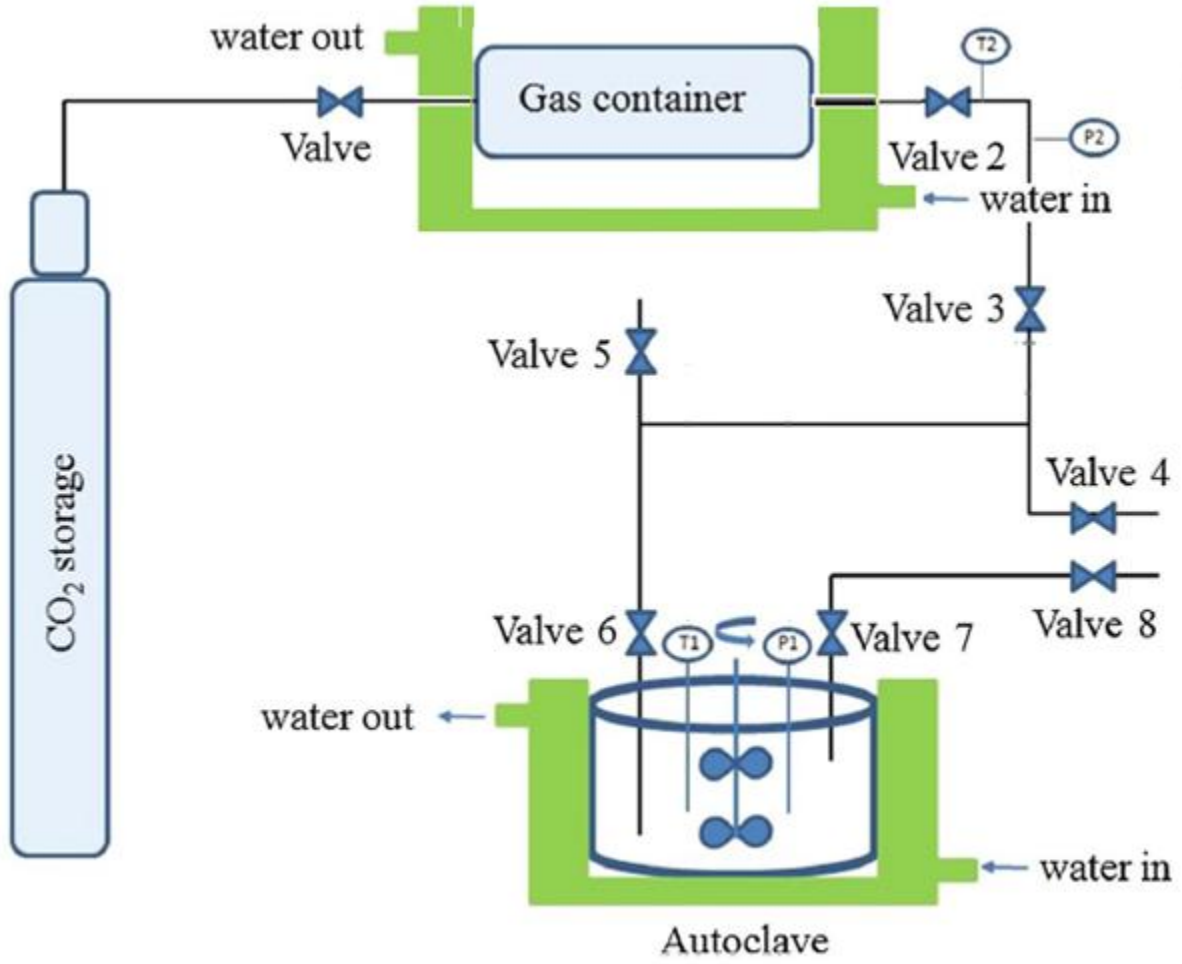

Figure V.2. Schematic of the experimental apparatus: autoclave; P1: pressure sensor no. 1; P2: pressure sensor no. 2; T1: temperature sensor no.1; T2: temperature sensor no. 2

The reactor temperature (T) was then set to the desired value by the water recirculation bath. The initial pressure of the gas container before CO_2 injection (P_1) was measured. Then,CO_2 was injected to the reactor containing the solution. Then the final pressure of the gas container (P_2) was measured after injection. The initial number of moles of CO2 existing in the gas container (n_1) and the final CO_2 moles(n_2) can be calculated by Equation.

$$n_{CO2} = \frac{V_T}{RT_a}\left(\frac{P_1}{Z_1} - \frac{P_2}{Z_2}\right) \qquad \text{(V.1)}$$

Where V_T denotes the volume of the CO_2 gas container, Z_1 and Z_2 are the compressibility factors corresponding to the initial pressure P_1 and the final pressure P_2 in the gas container before and after transferring the CO2, R is the gas constant and T_a is the temperature of transferred CO_2. Compressibility factors were calculated using equation of state Peng-Robinson (PR), within the HYSYS process simulator for the range of pressure and temperature conditions tested. Following reaching the solution to a given temperature, the vapor pressure of the aqueous solution in the equilibrium cell was measured using a pressure transducer. The equilibrium state was achieved when no change in the pressure of the equilibrium cell (P_{tot}) was observed following about 01 hour. Thus, the equilibrium partial pressure of CO_2 (P_{CO2}) can be calculated as

$$P_{CO_2} = P_{tot} - P_v \qquad \text{(V.2)}$$

Where P_v presents the vapor pressure of the aqueous alkanolamine solution at the given temperature.

The moles of remaining CO_2 in the gas phase n_{CO2}^gwere determined from:

$$n_{CO2}^g = \frac{V_g P_{CO2}}{Z_{CO_2} RT} \qquad \text{(V.3)}$$

Therefore a known quantity of CO_2, n_{CO2}, was introduced (Transferred) into the reactor from the gas container of known volume:

$$n_{CO2} = \frac{V_T}{RT_a}\left(\frac{P_1}{Z_1} - \frac{P_2}{Z_2}\right) \qquad \text{(V.4)}$$

Where V_T denotes the volume of the gas container, Z_1 and Z_2 are the compressibility factors corresponding to the initial pressure P_1 and the final pressure P_2 in the gas container before and after transferring the CO2, and T_a is the temperature of transferred CO_2. Compressibility factors were calculated using equation of state Peng-Robinson (PR), within the HYSYS process simulator for the range of pressure and temperature conditions tested. The moles of remaining CO_2 in the gas phase n_{CO2}^g was determined from:

$$n_{CO2}^g = \frac{V_g P_{CO2}}{Z_{CO_2} RT} \qquad \text{(V.5)}$$

Where V_g is the gas-phase volume in the autoclave corrected with the consideration of liquid volume change due to the solubility of CO_2.

$$V_g = V_{Autoclave\ reactor} - V_{solution} \quad \text{(V.6)}$$

Finally, the number of moles of CO_2 absorbed by the solution (n'_{CO2}) and the CO_2 loading in the liquid phase (α) are calculated:

$$n'_{CO2} = n_{CO2} - n^g_{CO2} \quad \text{(V.7)}$$

$$\alpha = \frac{n'_{CO2}}{n_{amine}} \quad \text{(V.8)}$$

Where n_{amine} is the number of moles of amine and loading is defined as the ratio of the moles of CO_2 absorbed to the moles of amine (mol/mol).

The different chemicals used in our study are shown in table 1.

Table V.1. Specifications and sources of chemicals used in this work.

Name	Abbreviation	Molecular formula	Supplier	Purity
N-methyl diethanolamine	MDEA	$CH_3N(C_2H_4OH)_2$	Sigma-Aldrich	99 wt%
Piperazine	PZ	$C_4H_{10}N_2$	Sigma-Aldrich	99 wt%
Tetramethylene sulfone	Sulfolane	$C_4H_8O_2S$	Sigma-Aldrich	99 wt%
Carbon dioxide	CO_2	CO_2	Praixair	99.99V%

V.2) Results and discussion:

V.2.1) Validation test:

Because of the low vapor pressure of pure MDEA, PZ, and Sulfolane in the temperature range considered here, the partial pressure contributions of MDEA, PZ, and Sulfolane in the vapor phase were neglected. (Xu et al., 1991).

In order to verify the accuracy of the experimental apparatus, and the reliability of the present measured data, the solubility of CO_2 in the aqueous solution of MDEA (50 wt.%) was determined at 313.15 and 333.15 K, and compared with those results given by (Dasha and.

Bandyopadhyayb, 2016)**,** as displayed in Figure. V.3. Experimental data of CO_2 partial pressure and their loading is reported in Table V.2. As seen, there is a good agreement between the present results and those data given in the literature.

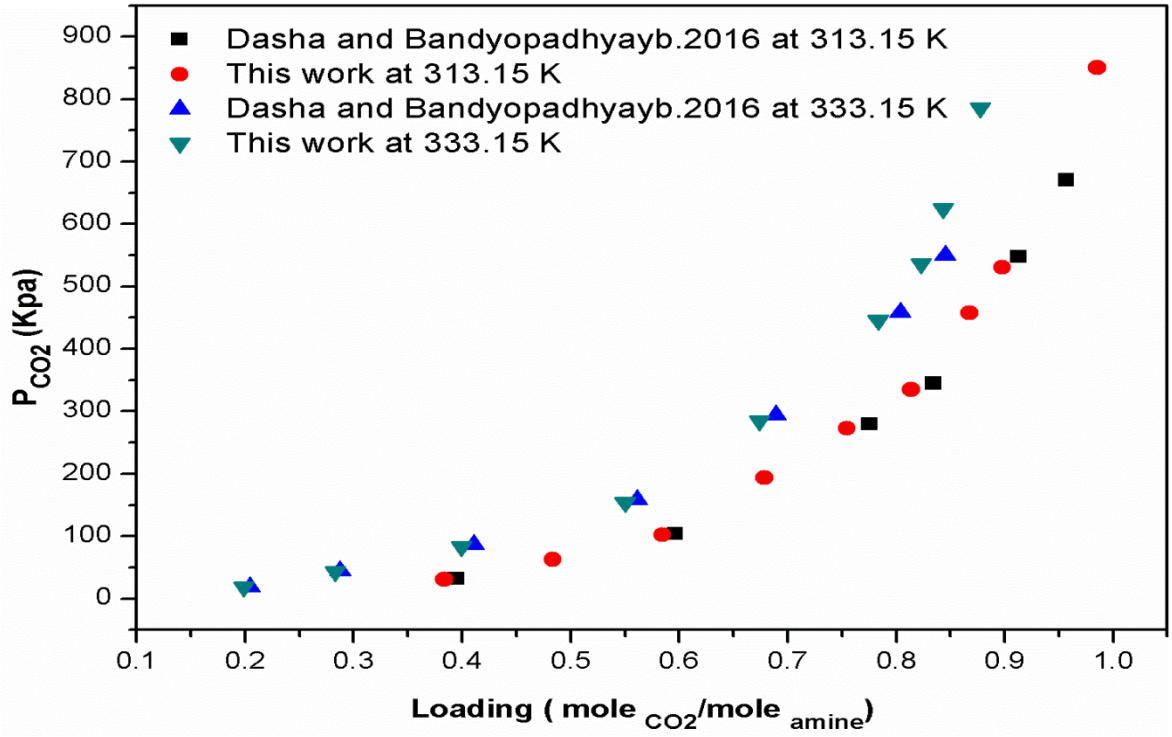

Figure V.3. Measurements of the partial pressure of CO_2 versus its gas loading for the solubility of CO_2 in the aqueous mixture of MDEA (50 wt.%) at 313.15 and 333.15K,for (Dasha and. Bandyopadhyayb,2016), and this work.

Table V.2. Experimental measurements of the partial pressure of CO_2 versus its gas loading for the solubility of CO_2 in the aqueous mixture of MDEA (50 wt %) at 313.15 K for (Dasha and. Bandyopadhyayb, 2016), and this work.

Dasha and. Bandyopadhyayb		This work	
α_{CO2}	P_{CO2} (Kpa)	α_{CO2}	P_{CO2} (Kpa)
313.15K		**313.15 k**	
0.39461	32.0512	0.38356	31.218
0.59658	103.81	0.48340	62.763
0.77578	279.71	0.58465	102.149
0.83460	344.78	0.67873	193.765
0.91323	547.30	0.75479	272.717
0.95708	670.26	0.81373	334.781
		0.86753	457.875
		0.89770	530.881
		0.98543	850.678
Dasha and. Bandyopadhyayb		This work	
α_{CO2}	P_{CO2} (Kpa)	α_{CO2}	P_{CO2} (Kpa)
333.15K		**333.15 k**	
0.20439	18.62006	0.19867	18.100
0.28753	44.61320	0.28300	43.453
0.41068	86.18844	0.39920	82.741
0.56135	157.89367	0.55012	154.420
0.68922	293.58202	0.67406	284.187
0.80372	457.88351	0.78362	445.520
0.84509	550.34189	0.82312	536.583
		0.84360	624.674
		0.87764	785.659

V.2.2) Density measurements:

The densities of the aqueous alkanolamine solutions were measured by the DSA 5000 M density and sound velocity meter (Anton Paar: DSA5000 M), which combines the world's most accurate density measurement, highly accurate sound velocity measurement and a state-of-the-art user interface. It determines the density and sound velocity of your sample in one cycle and at the same sample conditions. This unique measuring combination even reduces the error margin for concentration measurement of binary mixtures and is frequently used in industrial chemical laboratories and in research. Other applications include quality control in production processes, preparing process solutions and determining the concentration of ternary solutions.

Figure V.4. Density and sound velocity Meter (Anton Paar: DSA5000 M)

The sample is introduced into a U-shaped tube made from borosilicate glass that is excited to oscillate at its characteristic frequency which is directly related to the density of the sample. After reaching a stable oscillation, the excitation is switched off and the oscillation fades out freely. This excitation and fade-out pattern is repeated continuously. By evaluating this pattern, highly precise density results are obtained, the sample´s viscosity is even measured and air bubbles or particles are detected.

Table V.3. Comparison of the present experimental values for density of the pure MDEA at different temperatures with the literature values.

T(K)	293.15	303.15	313.15	323.15	333.15	343.15	Ref
Density	1.04136	1.03323	1.025825	1.01806	1.01041	1.00244	this work
(g/Cm^3)	1.04160	1.03410	1.02652	1.01888	1.01143	1.00332	a
	-	1.03200	1.02445	1.01666	1.00900	1.00124	b

a : Bernal-García et al., (2003), b : Maham et al., (1995)

Table V.3 presented the data comparison for the density of the pure MDEA at different temperatures between the data from this work and from the values reported in literatures .It presents the very satisfactory agreement between the measurements and the literature data.

Table V.4. Experimental values of the density (ρ) measurements of 50 wt% MDEA at various temperatures.

T(K)	303.15	313.15	323.15	333.15
Density (g/Cm^3)	1.03907	1.032584	1.025629	1.018260

V.2.3) Density of the alkanolamine mixture

The densities of the aqueous alkanolamine solutions were measured at 313.15, 318.15, 323.15, 328.15, 333.15, 338.15 and 343.15 K and their results are shown in Table V.5 and Figure V.5.We have correlated the densities of the four aqueous alkanolamine solutions against temperature and mass fraction of amines as follows (Shirazizadeh and Haghtalab, 2019) .

$$\rho = F(T) + B(X_{MDEA}) + C(X_{Sulfolane}) \quad (V.9)$$

Where F(T) is a function of temperature that is written as: $F(T) = A_1 + \frac{A_2}{T}$ (V.10)

Where, ρ is the density (g/Cm^3), T is absolute temperature in Kelvin, (X_{MDEA}, and $X_{Sulfolane}$) the mass fractions of MDEA, and Sulfolane, respectively. The parametersA_1 , A_2, B, C and were determined by optimization of the experimental data through the following objective function:

$$AAD\% = \frac{100}{n}\sum_{i=1}^{n}\left|\frac{\rho_{i,exp}-\rho_{i,cal}}{\rho_{i,exp}}\right| \quad (V.11)$$

Where $\rho_{i,exp}$ and $\rho_{i,cal}$ stand for the experimental and calculated values of density, respectively, and n is the number of data point.

Table V.5. Experimental values of the density (ρ) measurements at various temperature and composition for the different alkanolamine mixtures

MDEA	Sulfolane	Water	T(K)				
wt .%			313.15	323.15	328.15	333.15	343.15
40	20	40	1.06672	1.06207	1.05979	1.05751	1.05089
40	10	50	1.04266	1.03702	1.03455	1.03158	1.02445
30	20	50	1.05751	1.05286	1.05058	1.04781	1.04207

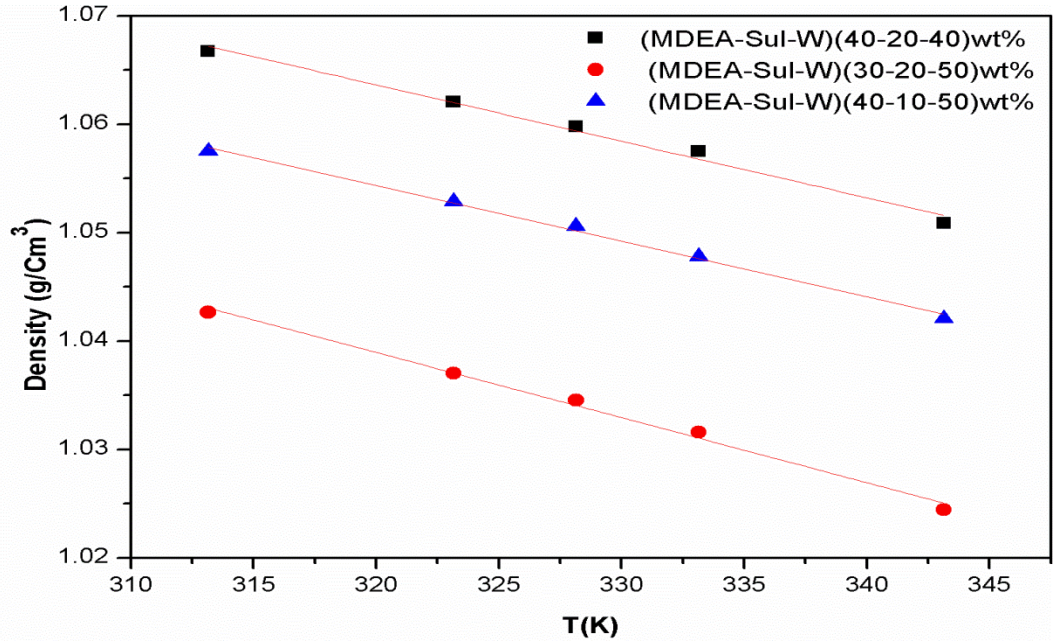

Figure V.5. Density versus temperature for the aqueous blend (MDEA-sulfolane) system with different compositions

The parameters of Equation V.9, are shown in Table V.6. This equation denotes the goodness of fit by means of the percent of absolute average deviation (AAD %) that for all data points is (0.36 %).

Table V.6. Parameters of Equation V.7 and absolute average deviation (AAD %).

Parameter	A_1	A_2	B	C	AAD %
Value	1.2100	-95.1025	0.131495	0.479272	0.36

V.2.4) Correlation of the CO_2 solubility in terms of its loading:

For regression of the partial pressure of CO_2 as function of its loading, we used a correlation given by Shamiri et al. (2016) as:

$$\ln P_{CO_2} = A(ln\alpha)^2 + B(ln\alpha) + C \qquad (V.12)$$

Where A, B, and C are the adjustable parameters, and α is the gas loading. The results of this correlation are shown in Table V.7. As one can see, the values of these three parameters are presented at a given temperature for the aqueous blended systems. To check the accuracy of this correlation, the two different deviation functions as the coefficient of determination (R^2) and the

normalized standard deviation (Δq) were applied. R^2 specifies how good the data points are fit by this correlation as (Shafeeyan et al., 2015)

$$R^2 = 1 - \left(\frac{\sum_{i=1}^{n}\left(P_i^{exp} - P_i^{cal}\right)^2}{\sum_{i=1}^{n}\left(P_i^{exp} - P_i^{\overline{exp}}\right)^2}\right)\left(\frac{n-1}{n-N}\right) \quad \text{(V.13)}$$

Where n denotes the number of experimental data, N is number of parameters, and P_i^{exp} , P_i^{cal} are the experimental and calculated values of partial pressure of CO_2, respectively, and $P_i^{\overline{exp}}$ stands for the average values of the experimental partial pressure data at a given point.
The normalized standard deviation (Δq) shows the deviation between the experimental results and the calculated data and is written as (Shafeeyan et al., 2015)

$$\Delta q = 100 * \left[\frac{1}{n-1}\sum_{i=1}^{n}\left(\frac{P^{exp} - P^{cal}}{P^{exp}}\right)^2\right]^{1/2} \quad \text{(V.14)}$$

Table V.7 shows the values of R^2 and Δq, for the present aqueous alkanolamine systems used in this work. As one can observe, these values demonstrate that Equation.V.12, is a good correlation for calculation of the partial pressure against the gas loading for the present mixed solutions at the given range of the pressure and temperature.

Table V.7 . Calculated parameters of Equation.(9), associated coefficient of determination (R^2) and normalized standard deviation (Δq) for all the studied alkanolamine blends.

Aqueous solvent	T(K)	A	B	C	R^2	Δq(%)	P(Kpa)
(MDEA-Sul)(30-20)wt%	313.15	2.72684	5.66526	6.29642	0.9995	0.103	(30-1110)
	323.15	2.56840	5.32260	6.77640	0.9994	0.050	(50-980)
	333.15	2.26839	4.90102	7.29864	0.9897	0.300	(80-1000)
(MDEA-Sul)(40-10)wt%	313.15	1.01357	5.58250	6.44034	0.9991	0.112	(25-850)
	323.15	1.06360	5.38251	6.84034	0.9997	0.074	(20-940)
	333.15	1.13358	5.21249	7.20341	0.9998	0.073	(20-1000)
(MDEA-Sul)(40-20)wt%	313.15	1.00509	5.97759	6.70542	0.9999	0.027	(10-950)
	323.15	1.28051	5.02760	7.29054	0.9998	0.083	(15-1000)
	333.15	1.30150	4.92376	7.69056	0.9991	0.395	(25-1000)
(MDEA-PZ)(40-10)wt%	313.15	1.18049	5.87375	6.65005	0.9999	0.053	(05-1020)
	323.15	1.22710	5.46378	6.81060	0.9999	0.085	(05-900)
	333.15	1.29098	5.06374	7.23101	0.9996	0.110	(15-900)
(MDEA-PZ)(40-05)wt%	313.15	1.41096	5.96377	6.87100	0.9999	0.032	(15-970)
	323.15	1.54098	5.63760	7.10054	0.9996	0.039	(30-860)
	333.15	1.64096	5.13762	7.35056	0.9999	0.0003	(40-880)

V.2.5) Effects of temperature and pressure on the solubility of CO_2:

In this work solubility of CO_2 was measured in the various compositions of the prepared aqueous solutions. The solubility of the present gas CO_2 was measured into the aqueous mixed (MDEA + sulfolane),(MDEA+ PZ) systems with three various compositions as ,(30. 20.0), (40.0–10.0), (40.0–20.0), (40.0–05.0), and (40.0–10.0)wt%, respectively.

These compositions were selected with wo scenarios so that at the first one, the sulfolane concentration was kept constant at 20.0 wt% and the concentration of MDEA increased from (30 to 40) wt%, and at the second scenario, the concentration of MDEA was maintained at 40% by weight with change in sulfolane concentrations from (10 to 20), and Piperazine from (05 to 10) wt%. All measurements were carried out at (313.15, 323.15 and 333.15) K in a pressure range of (05 to 1150) kPa. The experimental results are presented to achieve two goals. First, the effect of temperature and pressure on the solubility of CO_2. The second goal is to investigate the effect of increasing sulfolane, and amine concentration as a physical and chemical solvent, respectively, on the solubility of CO_2 in the mixed solvent.

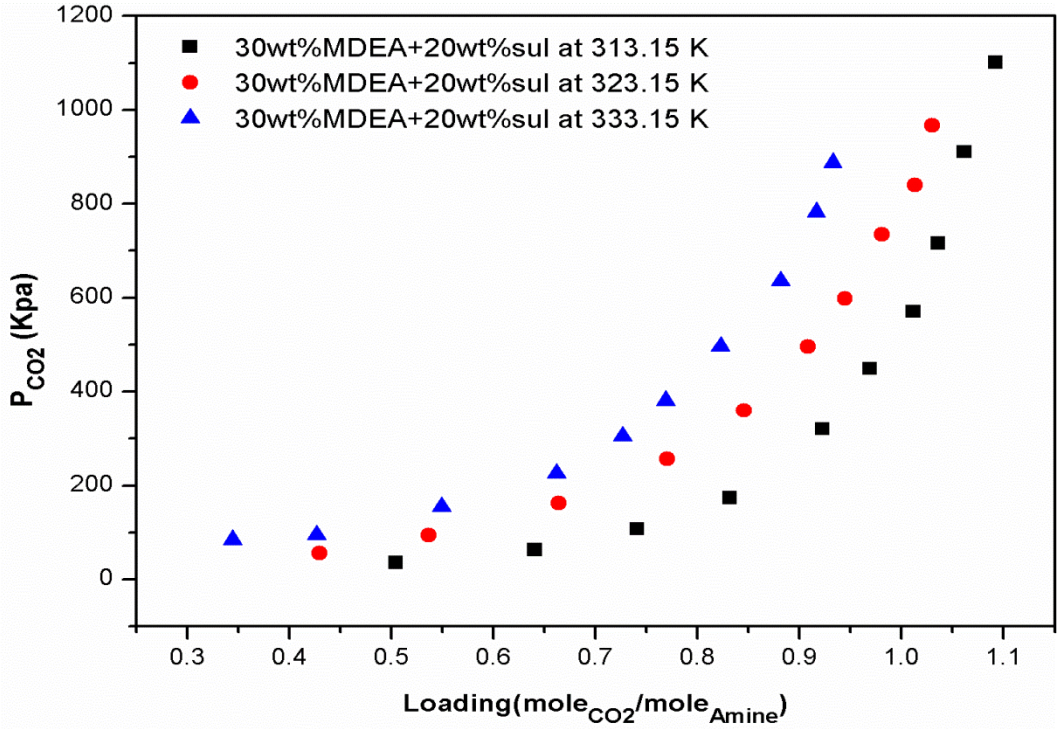

Figure V.6. Partial pressure of CO_2 versus the loading of acid gas for the aqueous mixed (30 wt % MDEA + 20% wt Sulfolane) at different temperatures.

Table V.8. Experimental measurements of the partial pressure of CO_2 versus its gas loading for the solubility of CO_2 in the aqueous mixture of (MDEA-Sulfolane) (30-20) wt %. at different temperatures.

α_{CO2}	P_{CO2} (Kpa)	α_{CO2}	P_{CO2} (Kpa)	α_{CO2}	P_{CO2} (Kpa)
313.15K		**323.15 K**		**333.15 k**	
0.50468	35.503	0.42946	55.761	0.34414	84.135
0.64069	62.639	0.53653	94.530	0.42703	94.530
0.74083	106.856	0.66380	162.800	0.54910	154.923
0.83156	173.304	0.77047	257.330	0.66164	225.820
0.92282	320.325	0.84562	359.737	0.72660	304.595
0.96895	449.015	0.90810	496.280	0.76892	380.744
1.01154	570.197	0.94450	598.687	0.82273	496.280
1.03580	715.625	0.98082	735.230	0.88162	635.448
1.06152	910.254	1.01311	840.262	0.91646	782.494
1.09201	1100.653	1.03012	967.418	0.93265	887.527

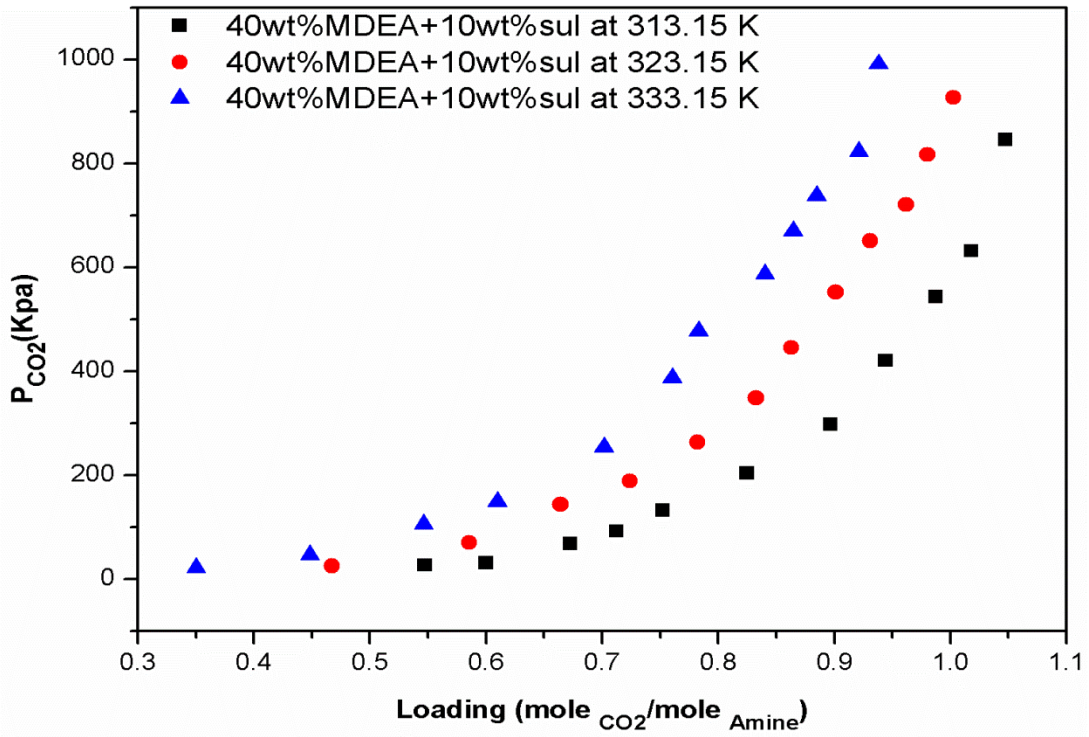

Figure V.7. Partial pressure of CO_2 versus the loading of acid gas for the aqueous mixed (40 wt % MDEA + 10% wt Sulfolane) at different temperatures.

Table V.9 . Experimental measurements of the partial pressure of CO_2 versus its gas loading for the solubility of CO_2 in the aqueous mixture of (MDEA-Sulfolane) (40-10) wt %. at different temperatures.

α_{CO2}	P_{CO2} (Kpa)	α_{CO2}	P_{CO2} (Kpa)	α_{CO2}	P_{CO2} (Kpa)
313.15K		323.15 K		333.15 k	
0.54757	27.102	0.46743	25.571	0.35043	22.636
0.60011	31.501	0.58550	71.082	0.44836	46.935
0.67262	68.514	0.66416	144.106	0.54640	106.011
0.71251	92.354	0.72403	189.241	0.60982	149.738
0.75245	132.265	0.78217	263.852	0.70155	253.611
0.82507	204.100	0.83267	349.201	0.76042	386.918
0.89689	297.436	0.86283	445.361	0.78298	477.685
0.94432	420.333	0.90117	552.247	0.84026	587.286
0.98747	543.278	0.93080	651.183	0.86466	670.175
1.01830	631.512	0.96182	720.679	0.88477	737.004
1.04750	845.621	0.98029	816.972	0.92132	822.608
		1.00260	926.621	0.93803	991.112

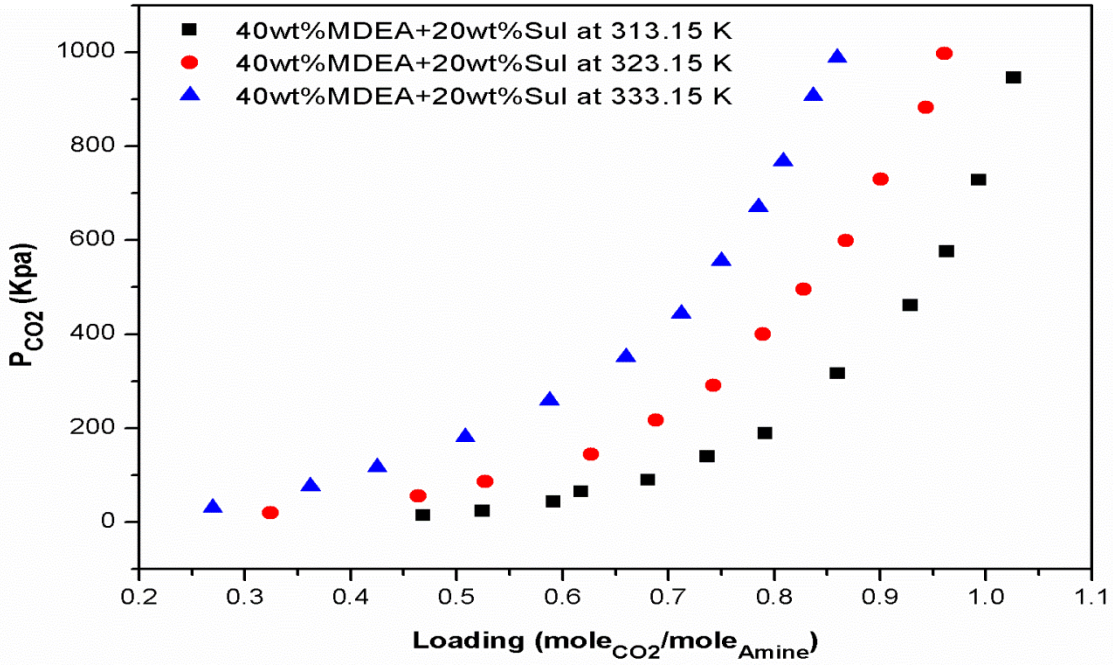

Figure V.8. Partial pressure of CO_2 versus the loading of acid gas for the aqueous mixed (40 wt % MDEA + 20% wt Sulfolane) at different temperatures

Table V.10 . Experimental measurements of the partial pressure of CO_2 versus its gas loading for the solubility of CO_2 in the aqueous mixture of (MDEA-Sulfolane) (40-20) wt %. at different temperatures.

α_{CO2}	P_{CO2} (Kpa)	α_{CO2}	P_{CO2} (Kpa)	α_{CO2}	P_{CO2} (Kpa)
313.15K		323.15 K		333.15 k	
0.46866	14.540	0.32420	19.957	0.26985	30.522
0.52467	23.678	0.46366	55.692	0.36193	75.804
0.59151	43.029	0.52685	86.795	0.42511	116.628
0.61775	65.052	0.62712	144.347	0.50816	181.426
0.68089	89.820	0.68835	217.300	0.58757	257.977
0.73703	139.078	0.74246	291.015	0.65972	350.821
0.79177	188.245	0.78916	400.161	0.71199	443.575
0.86025	316.447	0.82785	495.579	0.74977	555.311
0.92883	460.885	0.86735	599.111	0.78490	669.711
0.96299	575.326	0.90083	729.829	0.80824	767.776
0.99350	727.845	0.94313	882.356	0.83695	906.682
1.02654	945.321	0.96084	996.747	0.85948	988.371

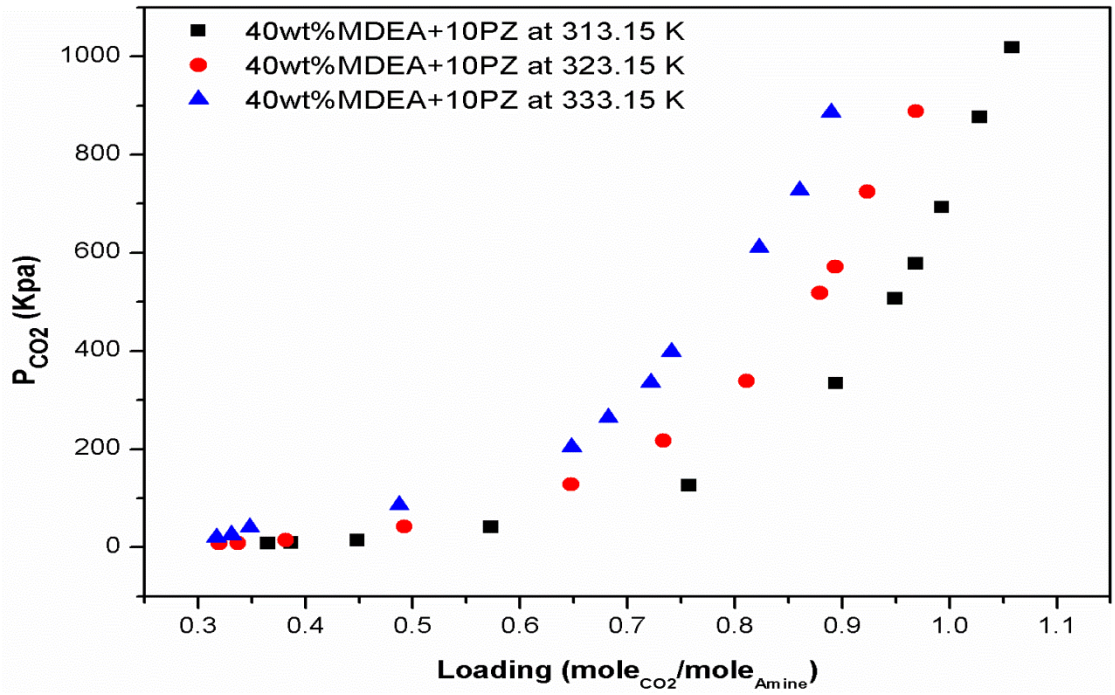

Figure V.9. Partial pressure of CO_2 versus the loading of acid gas for the aqueous mixed (40 wt % MDEA + 10% wt PZ) at different temperatures.

Table V.11 . Experimental measurements of the partial pressure of CO_2 versus its gas loading for the solubility of CO_2 in the aqueous mixture of (MDEA-PZ) (40-10) wt %. at different temperatures.

α_{CO2}	P_{CO2} (Kpa)	α_{CO2}	P_{CO2} (Kpa)	α_{CO2}	P_{CO2} (Kpa)
313.15K		**323.15 K**		**333.15 k**	
0.36510	07.690	0.31963	07.780	0.31720	19.688
0.38700	08.782	0.33702	08.870	0.33131	25.267
0.44865	14.235	0.38190	14.487	0.34817	40.600
0.57310	41.475	0.49228	42.437	0.48736	86.494
0.75733	125.540	0.64724	128.577	0.64806	204.326
0.89420	334.032	0.73360	216.866	0.68230	264.121
0.94925	506.430	0.81080	338.811	0.72150	334.950
0.96855	577.350	0.87920	517.885	0.74100	397.934
0.99300	692.250	0.89344	571.303	0.82272	610.571
1.02856	876.325	0.92340	724.348	0.86044	726.710
1.05820	1017.652	0.96868	888.521	0.88973	885.690

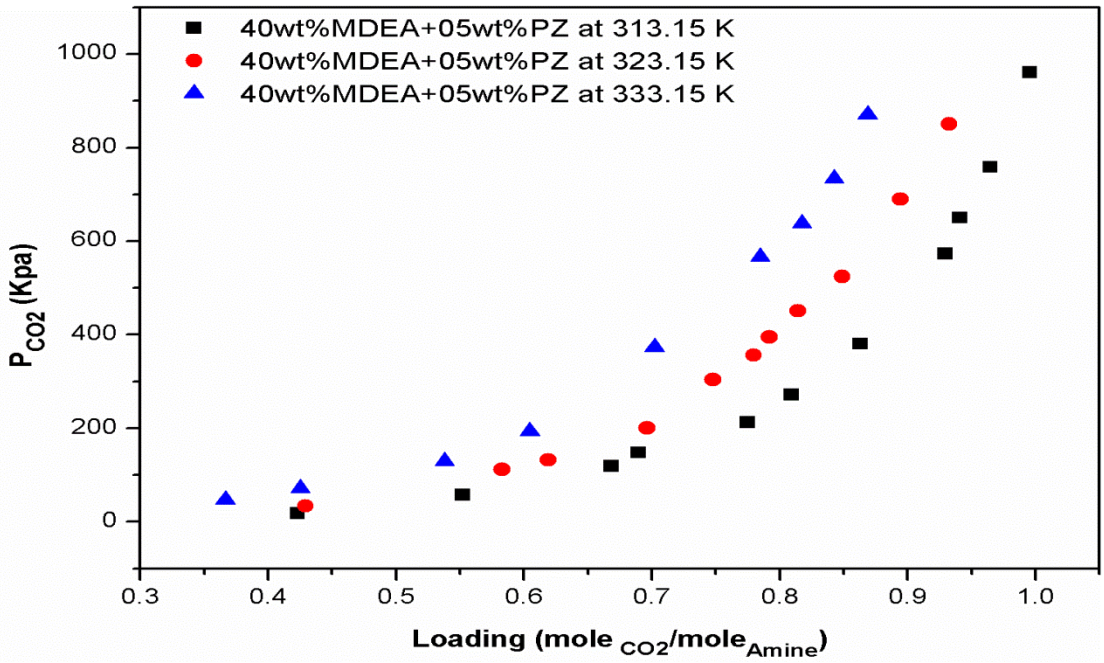

Figure V.10. Partial pressure of CO_2 versus the loading of acid gas for the aqueous mixed (40 wt % MDEA + 05% wt PZ) at different temperatures.

Table V.12. Experimental measurements of the partial pressure of CO_2 versus its gas loading for the solubility of CO_2 in the aqueous mixture of (MDEA-PZ) (40-05) wt %. at different temperatures.

α_{CO2}	P_{CO2} (Kpa)	α_{CO2}	P_{CO2} (Kpa)	α_{CO2}	P_{CO2} (Kpa)
313.15K		**323.15 K**		**333.15 k**	
0.42300	17.612	0.42910	34.163	0.36667	46.533
0.55236	56.988	0.58292	112.154	0.42526	72.281
0.66850	119.120	0.61900	132.552	0.53760	129.272
0.68960	147.711	0.69627	200.431	0.60460	193.793
0.77470	212.072	0.74780	304.083	0.70210	372.683
0.80940	270.937	0.77956	356.370	0.78463	565.650
0.86300	380.534	0.79163	395.050	0.81738	638.170
0.92964	572.872	0.81433	451.132	0.84255	733.510
0.94109	649.805	0.84880	524.421	0.86860	869.880
0.96466	758.200	0.89422	689.885		
0.99564	960.654	0.93242	850.326		

The solubility of carbon dioxide in all aqueous mixed solvents increases with increasing CO_2 partial pressure and decreases with increasing temperature. At lower CO_2 partial pressure, CO_2 solubility increases rapidly with increasing pressure, and the difference in gas solubility between

313.15 K and 333.15 K is not obvious because of the experimental uncertainty in the range of low pressure. At higher CO_2 partial pressure, CO_2 solubility increases slowly with increasing pressure, and the difference in gas solubility between 313.15 and 333.15 K becomes obvious as shown in figures and tables above.`

The CO_2 loading increases with enhancing partial pressure of CO_2 in all temperatures and composition of amines. By increasing partial pressure of CO_2, the physical as well as chemical absorption intensify through increasing the mass transfer rate so that at the high gas loading the physical absorption dominates.

Figures and tables clearly show that the CO_2 solubility in the aqueous mixtures increases with rising of the gas partial pressure, but it decreases with increasing temperature. Solubility of acidic gases in physical solvents in almost linear. Thus, in low partial pressures, they don't have much absorption power but in low partial pressures, solubility of acidic gases in the chemical solvents in due to the high reaction. However, in high partial pressures, chemical solvents have Stoichiometric limitation.

As conclusion, the results showed that the CO_2 solubility is inversely proportional to temperature increasing. In low partial pressures, the capacity of physical solvents to adsorb the acidic gases is lower than chemical solvents. But in higher pressure, due to absence of stoichiometric limitation of reaction, the capacity of physical solvent is higher than chemical solvents.

The solubility of CO_2 in aqueous solutions of blended (MDEA-Sulfolane), and (MDEA-PZ) decreases as temperature increases because the solubility of CO_2 declines with increasing temperature; thus, the system tends toward CO_2 desorption rather than CO_2 absorption. The partial pressure and the temperatures are parameters that influence the amount of CO2 absorption. Utilizing the mixture of physical and chemical solvents (Sulfinol-M), is possible to benefit from the capabilities of this solvent in a wide range of partial pressures.

V.2.6) Influence of sulfolane, PZ and MDEA concentrations on the solubility:

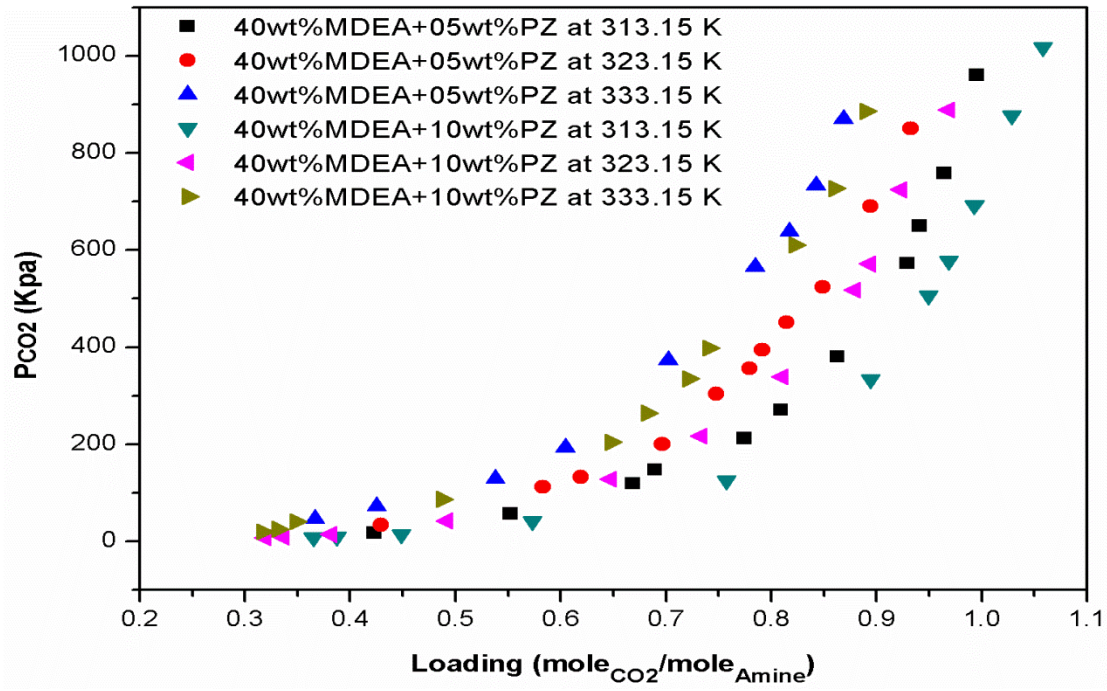

Figure V.11. Partial pressure of CO_2 versus the loading of acid gas for the aqueous mixed (MDEA + PZ) at different temperatures and concentrations

The effect of piperazine concentration on the CO_2 loading was found to be dependent on both the CO_2 partial pressure and solution temperature. Figure above depicts the effect of piperazine concentration on CO_2 loading at low and high partial pressure. As observed, the CO_2 solubility increases upon the enhancement of PZ concentration from (05 to 10) wt.% so that this trend is taking place at all temperatures. It is clear in this figure that a significant increase in loading is observed with the increase in Piperazine concentration. The addition of small amounts of Piperazine into aqueous MDEA, results in the increase of equilibrium solubility of CO_2 in the blended solution. PZ can be used as a chemical activator by introducing to the MDEA system so that the selectivity to CO_2 was intensified. The CO_2 loading increases with partial pressure and also with PZ concentration. It is evident that activated MDEA shows improved VLE. The solubility of CO_2 increases with PZ concentration and this proves that PZ is an effective component in absorbing CO_2 into (MDEA+ PZ) system.

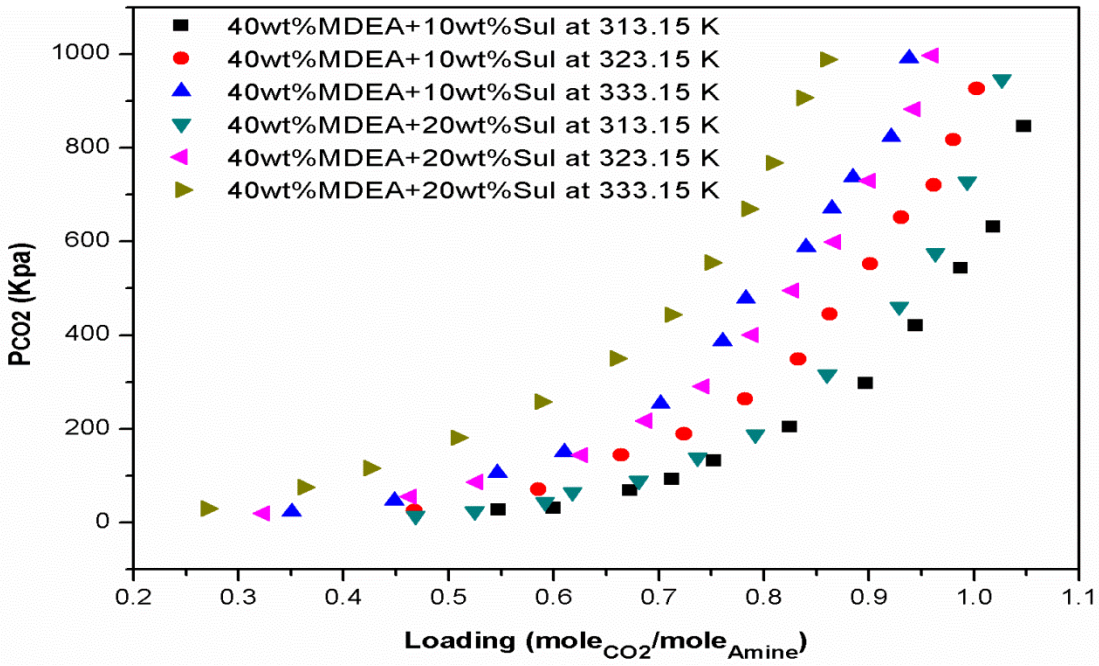

Figure V.12. Partial pressure of CO_2 versus the loading of acid gas for the aqueous mixed (MDEA + Sul) (40, 10-20) wt% at different temperatures.

Figure V.12 shows the effect of the sulfolane concentration (10.0 and 20.0 wt. %) on the solubility of CO_2 into the aqueous system of the fixed MDEA concentration (40.0 wt.%) at the different temperatures. As seen at fixed MDEA concentration, increasing sulfolane (physical solvent) and replacing with water lead to decreasing the loading of CO_2. These results are in agreement with those given by Zong and Chen (Zong and Chen, 2011). They reported that at low acid gas loading, the CO_2 absorption was mostly influenced by the chemical absorption through MDEA. In fact, the enhancement of the sulfolane concentration in the mixed-solvents would raise CO_2 partial pressures in the low gas loading. On the other hand, at higher acid gas loading, the enhancement of the acid gas absorption primarily depends on the physical absorption through sulfolane. In low partial pressures, the capacity of physical solvents to absorb the acidic gases is lower than chemical solvents. But in higher pressures, due to absence of stoichiometric limitation of reaction, the capacity of physical solvent is higher than chemical solvents. The solubility of CO_2 in (MDEA + sulfolane) solutions decreases with sulfolane concentration. It is probably due to the fact that at lower partial pressure the physical absorption of CO_2 in sulfolane is not much realized. In fact, solubility of the gases in the solvents mixture is physically. Thus, low physical solubility of acidic gases in low loading in the solvents mixture is due to sulfolane

effect. It's evident that the solubility of CO_2 decreases with Sulfolane. The fact that CO_2 cannot be ionized in Sulfolane can explain the lower capacity of blends when Sulfolane replaces water in the solutions.

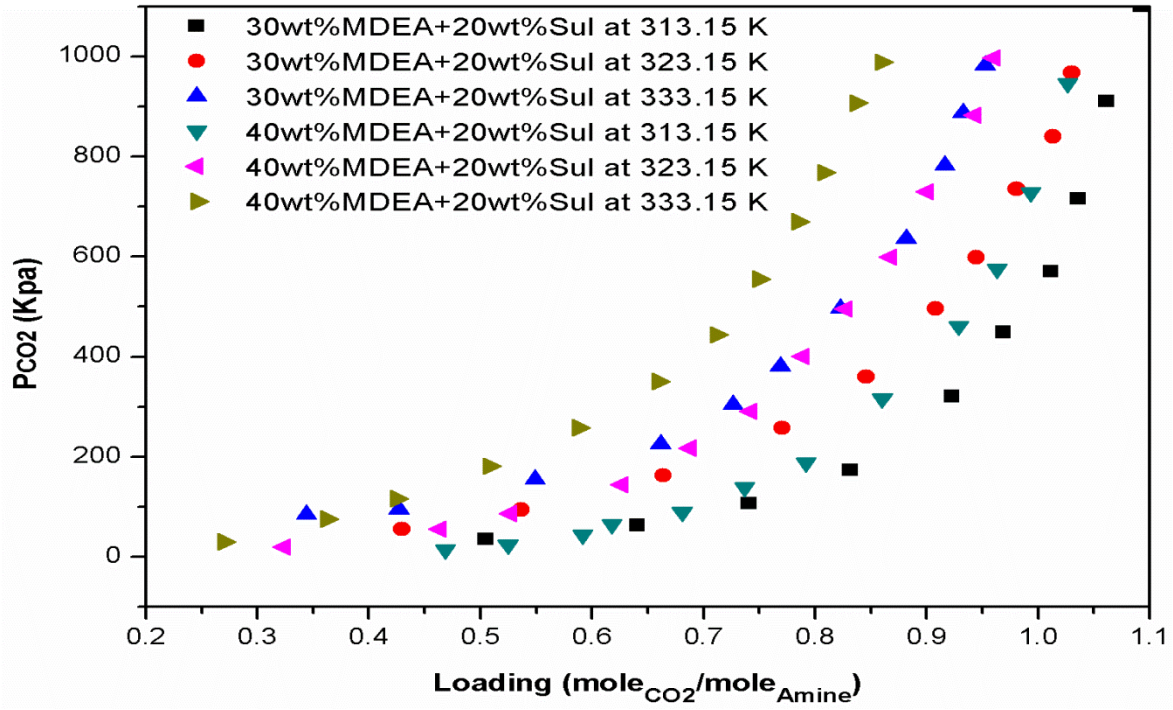

Figure V.13. Partial pressure of CO_2 versus the loading of acid gas for the aqueous mixed (MDEA+ Sul) (30-40, 20) wt% at different temperatures.

Figure V.13 demonstrates the influence of increasing MDEA concentration (30.0–40.0 wt.%) at the fixed concentration of sulfolane (20.0 wt.%) on the CO_2 loading. the solubility of the CO_2 increases by enhancing MDEA from (30.0 to 40.0) wt.% at the fixed concentration of sulfolane in all temperatures. Thus, both enhancements of sulfolane and MDEA concentration intensify the absorption of carbon dioxide (CO_2). Therefore the CO_2 was absorbed by the aqueous MDEA. Indeed, the present results may explain that the total physical and chemical absorption of CO_2 into the mixed solvent is higher than its chemical and physical absorption in the aqueous MDEA. At low acid gas loading, acid gas absorption mainly depends on the chemical absorption with MDEA. Lowering rate of water does not affect on its absorption. But reaction of CO_2 to the amine must be performed in aqueous medium. And decreased water amount will lower this

reaction. This indicates the selectivity state of Sulfinol-M solvent. (Zong and Chen, 2011; Simoni et al., 2007; Wei et al., 2010). By increasing concentration of Sulfolane, partial pressures of gases will decrease. In low partial pressures, the capacity of physical solvents to adsorb the acidic gases is lower than chemical solvents. But in higher pressured, due to presence of stoichiometric limitation of reaction, the capacity of physical solvent is higher than chemical solvents.

At low acid gas loading, the CO_2 absorption was mostly influenced by the chemical absorption through MDEA. In fact, at higher acid gas loading, the enhancement of the acid gas absorption primarily depends on the physical absorption through sulfolane. However high amount of sulfolane leads to the reduction of the CO_2 partial pressures . Since the chemical absorption of CO_2 in MDEA is very limited, its physical absorption is more significant than its chemical absorption. The CO_2 loading decreases by an increase in the MDEA concentration at the fixed sulfolane concentration. These results are in agreement with those given by Jou et al(1999).

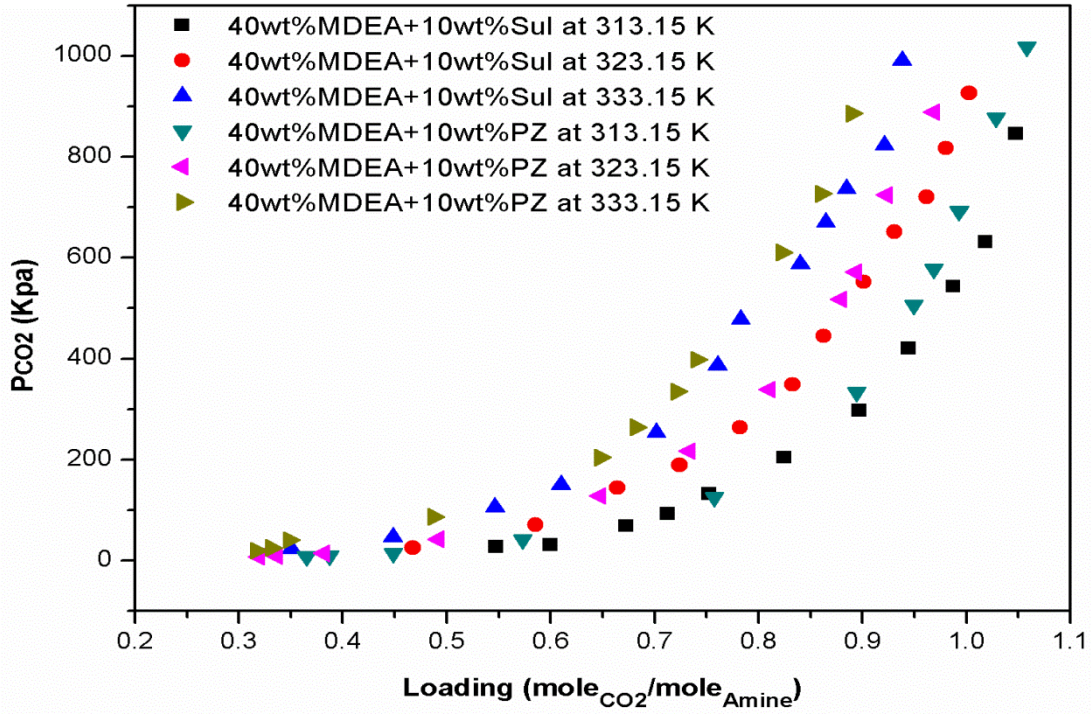

Figure V.14. Partial pressure of CO_2 versus the loading of acid gas for the aqueous mixed (40 MDEA + 10PZ) , and (40MDEA + 10Sul) wt% at different temperatures .

We have found that the effect of activators such as PZ and sulfolane on the tertiary amine MDEA has an influencing factor on the CO_2 absorption capacity of the present amine mixtures. Increasing in activators weight percent leads to more acid gas loadings. As observed in figure V.14 the influence of sulfolane is more than PZ in enhancing of the gas physical solubility. Solubility in the mixed solvent was higher as carbon dioxide was much more soluble in Sulfolane.

The physical Solubility in the mixed aqueous solvent of (MDEA-Sulfolane) is higher than that of aqueous mixed (MDEA-PZ), as if there was a kind of "enhancement" in the solubility when MDEA was used with solubility. As a conclusion, the presence of the additives such as sulfolane and PZ in MDEA solution promotes the absorption capacity. The mixed solvent (MDEA+Sulfolane) has shown a potential in the absorption of carbon dioxide at high partial pressure. As shown in figure 13, It's observed that the solvent capacity increases with the Sulfolane mass% at higher partial pressure range but decreases at lower partial pressure. This indicates that the promoter action of PZ is realized more in the lower partial pressure range, which is similar to the CO_2 partial pressure condition of the natural gas plants. It is also noticeable that Sulfolane is a better activator than PZ for increasing the solution capacity for CO_2 absorption. Due to the presence of physical solvent in solvent mixture, the physical solubility of acidic gases in the solvents mixture is higher than aqueous solution.

Conclusion:

In this work, a solubility reactor cell was used to obtain a new set of experimental values for the simultaneous solubility of carbon dioxide in the aqueous mixtures of MDEA as a chemical alkanolamine, Piperazine and sulfolane as activators. The measurements were carried out using the (MDEA + sulfolane + H_2O), (MDEA + Piperazine + H_2O) systems at the compositions of (40–20–40) wt.%, (40–10–50) wt.% , (30–20–50) wt.%, (40–05–50) wt.% , and(40–10–50) wt.% and (313.15, 323.15 and 333.15) K. In addition, the influence of temperature on the solubility of CO_2 into the mixtures was studied. In the present study our target was to investigate the effect of, temperature, partial pressure, and weight percent of sulfolane, PZ and MDEA on the solubility of CO_2. Acid gases don't react chemically in physical solvents medium. They are absorbed only physically and their solubility in the gases changes almost linearly by partial pressure.

The solubility of CO_2 in aqueous solutions of blended (MDEA-Sulfolane), and (MDEA-PZ) decreases as temperature increases because the solubility of CO_2 declines with increasing temperature; thus, the system tends toward CO_2 desorption rather than CO_2 absorption. For the effect of CO_2 partial pressure, the equilibrium solubility of CO2 increases as CO_2 partial pressure increases due to the higher driving force for CO_2 absorption at higher CO_2 partial pressure.

At low acid gas loading, the CO_2 loading was reduced by enhancing the sulfolane concentration. By increasing concentration of Sulfolane, partial pressures of gases will decrease. At low partial pressures, the capacity of physical solvents to absorb the acidic gases is lower than chemical solvents, but at higher pressure, due to absence of stoichiometric limitation of reaction, the capacity of physical solvent is higher than chemical solvents. The use of the sulfolane and PZ as activators for the MDEA solution leads to enhance the acid gas loading. On the other hand, the CO_2 equilibrium solubility in the present alkanolamine mixtures enhances effectively with increasing pressure and decreasing temperature. At fixed MDEA concentration, and increasing sulfolane (physical solvent) and replacing with water lead to decreasing the loading of CO_2. The fact that CO_2 cannot be ionized in Sulfolane can explain the lower capacity of blends when Sulfolane replaces water in the solutions.

Solubility in the mixed solvent was higher as carbon dioxide was much more soluble in Sulfolane.

The partial pressure, the temperatures, and the concentration are parameters that influence the amount of CO2 absorbed.

The presented research work may be considered as a screening survey for examination of the performance of adding piperazine and sulfolane as activators besides a tertiary amine for CO_2 absorption.

The physical Solubility in the mixed aqueous solvent of (MDEA-Sulfolane) is higher than that of aqueous mixed (MDEA-PZ), as if there was a kind of "enhancement" in the solubility when MDEA was used with solubility .

Utilizing the mixture of physical and chemical solvents (Sulfinol-M), is possible to benefit from the capabilities of this solvent in a wide range of partial pressures.

General conclusion and Recommendations

General Conclusion and Recommendations

Chemical solvents are characterized by liquid phase reactions between the acid gas, such as CO_2, and a soluble base such as alkanolamine. Although the chemical reactions allows for a high solubility even at low partial pressures, the solubility, however, is limited by the stoichiometry of the reactions and the solution cannot be easily loaded once the reactant has been depleted**.**

Physical solvents, on the other hand, absorb by physical dissolution without chemical reaction and the solubility is approximately linear with the CO_2 partial pressure. Thus, physical solvent have a much lower capacity for CO_2 absorption than chemical solvents at low pressures, but since they lack stoichiometry limits they may be loaded to higher levels at high partial pressures.

Removal of acid gases is usually achieved by absorption in solvents consisting of aqueous amine solutions.

In mixtures of a physical and a chemical solvent the solubility phenomenon is a combined one; that is, at a low partial pressure of the solute (low loading in the mixture), the kinetics of the reaction between the acid gas and the chemical solvent prevails over the physical absorption, whereas at high partial pressure of the solute the contrary occurs. In amine-based acid gas capture, acid gas reacts with an aqueous amine solution, forming different electrolyte species.

Pseudo first order constants K_o for the reaction of CO_2 in aqueous PZ, MDEA, aqueous (MDEA - PZ), aqueous (PZ - Sulfolane), and aqueous (MDEA - Sulfolane) solutions were measured at 298.15, 303.15, 308.15 and 313.15 K using the stopped flow technique. The overall reaction rate was found to depend on the amine concentration, solvent type and temperature. MDEA reacts relatively slowly with CO_2 due to its tertiary amine characteristics. The addition of small amounts of PZ to MDEA results in a significant enhancement of CO_2 absorption rates. A reaction model consisting of a first-order reaction mechanism for MDEA and a zwitterion mechanism for PZ was used to regress well the kinetic data.

The reaction kinetics of the aqueous standalone MDEA and PZ in reaction with aqueous CO_2 increase with increasing temperature and concentration. Base catalysis mechanism correlated the standalone MDEA data successfully. A hybrid model of zwitterion and base catalysis mechanisms correlated the experimental data of the MDEA/PZ system quite well.

The reaction kinetics of carbon dioxide in the aqueous mixed solvent solution of (MDEA-Sulfolane), and (PZ- Sulfolane) were studied for the first time using the stopped-flow technique. The absorption rates of carbon dioxide in the aqueous mixed solvent solution of (MDEA-Sulfolane) and (PZ- Sulfolane) were higher than those of standalone MDEA and PZ at the same concentrations at all temperatures from 298.15 to 313.15 K.

The study indicates a higher kinetic rate for the mixed system (MDEA- Sulfolane) at the lowest temperature (298.15). In the absorption process of CO_2 involving a chemical reaction, the absorption rate is dominated by the CO_2 transfer rate in the liquid film close to the interface. The rate is determined by the opposing effects of lower solubility at higher temperatures and higher diffusivity.

It confirms the advantage of the commercially available Sulfinol technologies over standalone amine-based processes. Other advantages for these systems are the higher solubility of CO_2 in Sulfolane compared to water and the lower energy used to regenerate the mixed system.

The solubility results over a wide range of temperature are useful for studying the solution properties in the chemical, biochemical, environmental protection, and energy industries.
The alkanolamine solutions can be generally classified as chemical or physical solvents.
In this work, a solubility reactor cell was used to obtain a new set of experimental values for the simultaneous solubility of carbon dioxide in the aqueous mixtures of MDEA as a chemical alkanolamine, Piperazine and sulfolane as activators. The measurements were carried out using the (MDEA - Sulfolane - H_2O), (MDEA - Piperazine - H_2O) systems at the compositions of (40–20–40) wt.%, (40–10–50) wt.% , (30–20–50) wt.%, (40–05–50) wt.% , and(40–10–50) wt.% and (313.15, 323.15 and 333.15) K. In addition, the influence of temperature on the solubility of CO_2 into the mixtures was studied.
The solubility of CO_2 in aqueous solutions of blended (MDEA-Sulfolane), and (MDEA-PZ) decreases as temperature increases because the solubility of CO_2 declines with increasing temperature; thus, the system tends toward CO_2 desorption rather than CO_2 absorption. For the effect of CO_2 partial pressure, the equilibrium solubility of CO_2 increases as CO_2 partial pressure increases due to the higher driving force for CO_2 absorption at higher CO_2 partial pressure.

At low acid gas loading, the CO_2 loading was reduced by enhancing the sulfolane concentration. By increasing concentration of Sulfolane, partial pressures of gases will decrease.

At low partial pressures, the capacity of physical solvents to absorb the acidic gases is lower than chemical solvents, but at higher pressure, due to absence of stoichiometric limitation of reaction, the capacity of physical solvent is higher than chemical solvents.

The use of the sulfolane and PZ as activators for the MDEA solution leads to enhance the acid gas loading. On the other hand, the CO_2 equilibrium solubility in the present alkanolamine mixtures enhances effectively with increasing pressure and decreasing temperature.

At fixed MDEA concentration, and increasing sulfolane (physical solvent) and replacing with water lead to decreasing the loading of CO_2. The fact that CO_2 cannot be ionized in Sulfolane can explain the lower capacity of blends when Sulfolane replaces water in the solutions. Solubility in the mixed solvent was higher as carbon dioxide was much more soluble in Sulfolane.

The partial pressure, the temperatures, and the concentration are parameters that influence the amount of CO_2 absorbed.

The presented research work may be considered as a screening survey for examination of the performance of adding piperazine and sulfolane as activators besides a tertiary amine for CO_2 absorption.

The physical Solubility in the mixed aqueous solvent of (MDEA-Sulfolane) is higher than that of aqueous mixed (MDEA-PZ), as if there was a kind of "enhancement" in the solubility when MDEA was used with Sulfolane.

Utilizing the mixture of physical and chemical solvents (Sulfinol-M), is possible to benefit from the capabilities of this solvent in a wide range of partial pressures.

It is predicted that replacement of Sulfinol-M solvent has better performance and suitable economics compared to present solvent and other amine solvents, reduce energy consumption and reduce investment costs.

Based on the results obtained from this research in terms of reaction kinetics and absorption capacity, it can be concluded that the aqueous solution of blended (MDEA-Sulfolane) have good potential to be used as the alternative solvent for capturing acid gas in Khrechba gas processing plant (In Salah).

Recommendations

It has been demonstrated through this research that the aqueous blended (MDEA+Sulfolane) have a good potential to be used as the promising alternative solvent for capturing acid gases from natural gas in terms of their absorption capacity, absorption rate, and regeneration energy. However, It is suggested to further study the transport and physico–chemical properties, degradation and corrosion tendencies and most importantly the energy needed for its regeneration for a complete evaluation of blended (MDEA-Sulfolane) used in acid gas removal applications.

References

References

Aboudheir, A., Tontiwachwuthikul, P., Chakma, A., Idem, R., 2004.Novel design for the nozzle of laminar jet absorber. Ind. Eng. Chem. Res.43, 2568-2574.

Aboudheir, A., Tontiwachwuthikul, P., Chakma, A., Idem, R., 2003.Kinetics of the reactive absorption of carbon dioxide in high CO_2-loaded, concentrated aqueous monoethanolamine solutions. Chem. Eng. Sci. 58, 5195–5210.

Abrams, D.S., Prausnitz, J.M.1975.Statistical thermodynamics of liquid mixtures: a new expression for the excess Gibbs free energy of partly or completely miscible systems, AIChE J. 21,116-128.

Ali, S. H., Al-Rasheed, O., Merchant, S. Q., 2010.Opportunities for faster carbon dioxide removal: A kinetic study on the blending of methyl Monoethanolamine and morpholine with 2-amino-2-methyl-1-propanol. Sep. Purif. Technol.74,64-72.

Ali, S. H., Merchant, S.Q., Fahim, M.A., 2000. Kinetic study of reactive absorption of some primary amines with carbon dioxide in ethanol solution, Separation and Purification Technology .18,163-175.

Angaji, M.T., Ghanbarabadi, H., Gohari, F.K.Z., 2013.Optimizations of sulfolane concentration in proposed sulfinol-M solvent instead of MDEA solvent in the refineries of sarakhs. J. Nat. Gas Sci. Eng. 15, 22-26.

Anufrikov, Y.A., Kuranov, G.L., Smirnova, N.A., 2007.Solubility of CO_2 and H_2S in alkanolamine containing aqueous solutions. Russian Journal of Applied Chemistry. 80, 515-527.

Alper E., 1990.Reaction mechanism and kinetics of aqueous solutions of 2-amino-2-methyl-1-propanol and carbon dioxide. Ind. Eng. Chem. Res.29, 1725 -1728.

Alvarez-Fuster, C., Midoux, N., Laurent, A., Charoentier, J.C., 1980. Chemical kinetics of carbon dioxide with amine in pseudo m–n^{th} order conditions in aqueous and organic solutions. Chem. Eng. Sci.35, 1717-1723.

Aly, F. A., Lee, L.L., 1981. Self -consistent equations for calculating the ideal gas heat capacity, enthalpy and entropy," Fluid Phase Equilibria. 6, 169-179.

Appl, M., Wagner, U., Henrici, H.J., Kuessnet K., Volkamer, F., Ernst-Neust N., 1982.Removal of CO_2 and/or H_2S and/ or COS from gases containing these constituents. US Patent 4336233.

Astarita, G., Savage, D.W., Bisio, A., 1983.Gas Treating with Chemical Solvents. John Wiley, NY,USA .

Aspen Technology, Inc., 2016.Physical Property Methods & Models. Version 9.

Austgen, D., Rochelle, G.T., Chen, C. C., 1991.A model of vapor- liquid equilibria for aqueous acid gas-alkanolamine systems. I. Representation of H2S and CO2 solubility in aqueous MDEA with MEA or DEA, Ind. Eng. Chem. Res. 30, 543-555.

Austgen, D.M. , Rochelle, G.T. , Peng, X. , Chen, C. C.,1989.Model of vapor- liquid equilibria for aqueous acid gas-alkanolamine systems using the electrolyte-NRTL equation, Ind. Eng. Chem. Res.28, 1060-1073.

Baker, R. W., 2004.Membrane Technology and Applications (2^{nd}edition), John Wiley & Sons. ISBN 0-470-85445-6,West Sussex.

Barvek, O., Alper, E., 1999.Reaction Mechanism and Kinetics of Aqueous Solutions of Primary and Secondary Alkanolamines and Carbon Dioxide,'' Turk. J. Chem. 23, 293-300.

Belveze, L.S. , Brennecke, J.F. , Stadtherr, M.A.,2004.Modeling of activity coefficients of aqueous solutions of quaternary ammonium salts with the electrolyte NRTL equation, Ind. Eng. Chem. Res. 43, 815-825.

Benamor, A., Al-Marri, M. J., Khraisheh, M., Nassera, M. S., Tontiwachwuthikul, P., 2016.Reaction kinetics of carbon dioxide in aqueous blends of N-methyldiethanolamine and glycine using the stopped flow technique, Journal of Natural Gas Science and Engineering.33, 186-195.

Bernardo, P., Drioli, E., Golemme, G., 2009.Membrane gas separation: a review/state of the art. Industrial & Engineering Chemistry Research.48, 4638-4663.

Bernal-García, J.M., Ramos-Estrada, M., Iglesias-Silva, G.A., Hall, K.R.,2003. Densities and Excess Molar Volumes of Aqueous Solutions of n-Methyldiethanolamine (MDEA) at Temperatures from (283.15 to 363.15) K,J. Chem. Eng. Data.48,1442-1445.

Bhide, B.D., Voskericyan, A., Stern, S.A., 1998. Hybrid processes for the removal of acid gases from natural gas. Journal of Membrane Science .140, 27-49.

Bishnoi, S., Rochelle, G.T., 2002. Thermodynamics of Piperazine-Methyldiethanolamine-Water-Carbon dioxide, Ind. Eng.Chem.Res.41 , 604-612.

Bishnoi, S., Rochelle, G.T., 2002.Absorption of carbon dioxide in aqueous piperazine-methyldiethanolamine. AIChE. J. 48, 2788-2799.

Blauwhoff, P. M. M., Versteeg ,G.F., van Swaaij, W.P.M., 1983.A study on the reaction between CO_2 and alkanolamines in aqueous solution. Chem. Eng. Sci.38, 1411-1429.

Blizzard, G., Parro, D., Hornback, K., 2005.Mallet gas processing facility uses membranes to efficiently separate CO_2. Oil and Gas Journal.103, 48-53.

Blauwhoff, P. M. M., Versteeg, G. F., van Swaaij, W. P. M. A., 1984.Study on the reaction between CO_2 and alkanolamines in aqueous - solutions. Cheat. Eng. Sci.39, 207-225.

Bord, N., Cretier, G., Rocca, J.L., Bailly, C., Souchez, J.P., 2004.Determination of diethanolamine or N-methyldiethanolamine in high ammonium concentration matrices by capillary electrophoresis with indirect UV detection: application to the analysis of refinery process waters. Anal Bioanal Chem .380, 325-332.

Bosch, H., Versteeg, G.F., van Swaaij, W.P.M., 1990. Kinetics of the reaction of CO_2 with the sterically hindered amine 2-amino-2-methylpropanol at 298 K. Chem. Eng. Sci.45,1167-1173 .

Bottoms, R.R., 1930.Process for separating acidic gases, U.S. Patent1783901.

Bp., 2014.Energy Outlook 2035.

BP., 2013.Statistical Review of World Energy.

Brelvi, S.W., O'Connell, J .P.,1972.Corresponding States Correlations for Liquid Compressibility and Partial Molar Volumes of Gases at Infinite Dilution in Liquids. AIChE J .18, 1239-1243.

Bruder, P., Grimstvedt, A., Mejdell, T., Svendsen, H.F., 2011. CO_2 capture into aqueous solutions of piperazine activated 2-amino-2-methyl-1-propanol. Chem. Eng. Sci.66, 6193-6198 .

Bullin, J.A., Polasek, J.C., Iglesias-Silva, G.A., 1992. Presented at the 71st GPA Annual Convention, Anaheim, CA .

Bullin, J.A., Polasek, J.C., Donnelly, S.T., 1990.Proceedings of the 69th GPA Annual Convention, Phoenix, AZ.135-139.

Burggraaf, A. J., 1996.Important characteristics of inorganic membranes.Membrane Science and Technology. 4, 21-34.

Caplow, M., 1968.Kinetics of carbamate formation and breakdown, J. Am. Chem. Soc.24, 6795-6803.

Caro, J., Noack, M., Kölsch, P., Schäfer, R., 2000. Zeolite membranes-state of their development and perspective. Microporous and mesoporous materials.38,3-24.

Cavenati, S., Grande, C.A., Rodrigues, A.E., 2006. Removal of carbon dioxide from natural gas by vacuum pressure swing adsorption. Energy & Fuels.20,2648-2659.

Chakraborty, A.K., Astarita, G., Bischoff, K.B., 1986.CO_2 absorption in aqueous solutions of hindered amines. Chem. Eng. Sci.41,997-1003.

Chakravarty, T., Phukan, U. K., Weiland, R. H., 1985.Reaction of acid gases with mixtures of amines," Chem. Eng. Prog.81, 32-36.

Chen, C. C., 2006.Toward development of activity coefficient models for process and product design of complex chemical systems, Fluid Phase Equilib. 241 , 103-112.

Chen, C. C., Song, Y., 2004.Generalized electrolyte NRTL model for mixed solvent electrolyte systems, AIChE J.50, 1928-1941.

Chen, C. C., Mathias, P. M., 2002.Applied Thermodynamics for Process Modeling". AIChE J. 48,194-200.

Chen, C.C., Bokis, C.P., Mathias, P.M., 2001. A segment-based excess Gibbs energy model for aqueous organic electrolyte systems, AIChE J.47, 2593-2602.

Chen, C. C., Zhu, Y., Evans, L.B., 1985.Phase partitioning of biomolecules: solubilities of amino acids, Biotechnol. Prog.5, 111-118.

Chen, C. C., Gibson, J., Phipps, D., Collier, P., 1988. A physical property model for caustic evaporator, in: Paper Presented at ASPENWORD 88, Amsterdam, The Netherlands.13–16.

Chen, C. C., Goldfarb, S.M., 1988. A representation of thermodynamic properties of aqueous sulfuric acid, in: Paper Presented at the 10^{th} Symposium on Thermophysical Properties, National Bureau of Standards, Gaithersburg , MD.

Chen, C.C., Evans, L.B., 1986. A local composition model for the excess Gibbs energy of aqueous electrolyte systems, AIChE J.32 , 444-454.

Chen, C. C., Boston, J.F., Britt, H.I., Evans, L.B.,1982. A local composition model for the excess Gibbs energy of electrolyte systems. Part I. Single solvent, single completely dissociated electrolyte systems, AIChE J.28, 588-596.

Chen, C.C., Boston, J.F., Britt, H.I., Evans, L.B.1979. Extension and application of the Pitzer equation for vapor–liquid equilibrium of aqueous electrolyte systems with molecular solutes, AIChE J.25 , 820–831.

Closmann, F., Nguyen, T., Rochelle, G.T., 2009. MDEA/ Piperazine as a solvent for CO_2 capture. Energy Procedia.1, 1351–1357.

Correljé, A.F., 2013.Markets for Natural Gas, in: Reference Module in Earth Systems and Environmental Sciences, Elsevier.

Crooks, J.E., Donnellan, J.P., 1989.Kinetics and mechanism of the reaction between carbon dioxide and amines in aqueous solutions. J. Chem. Soc. Perkin Trans. 2, 331-333 .

Cullinane, J.T. , Rochelle, G.T.,2005. Thermodynamics of aqueous potassium carbonate, piperazine, and carbon dioxide. Fluid Phase Equilibria. 227, 197–213.

Cullinane, J.T., Rochelle, G.T., 2004.Carbon dioxide absorption with aqueous potassium carbonate promoted by piperazine. Chem. Eng. Sci.59, 3619–3630.

Danckwerts, P.V., 1979.The reaction of CO_2 with ethanolamine. Chem. Eng. Sci.34, 443-446.

Dang, H.Y., Rochelle, G.T., 2003. CO_2 absorption rate and solubility in monoethanolamine / piperazine / water. Sep. Sci. Tech.38, 337-357.

Dasha, S. K., Bandyopadhyayb, S. S., 2016.Studies on the effect of addition of piperazine and sulfolane into aqueous solution of N-methyldiethanolamine for CO_2 capture and VLE modelling using e-NRTL equation, International Journal of Greenhouse Gas Control. 44 227-237.

Da Silva, E.F., Svenden, H.F., 2004. Ab initio study of the reaction of carbamate formation from CO2 and alkanolamines. Ind. Eng. Chem. Res.43, 3413-3418.

Davison, J.; , Freund, P., Smith, A.,2001. Putting carbon back into the ground (1st edition), IEA Greenhouse Gas R&D Programme. ISBN 1 898373 28, Cheltenham.

De Lange, R. S. A., Keizer, K., Burggraaf, A.J., 1995.Analysis and theory of gas transport in microporous sol-gel derived ceramic membranes. Journal of Membrane Science. 104, 81-100.

Derks, P.W.J., Kleingeld, C., van Aken, C., Hogendoorn, J.A., Versteeg, G.F., 2006.Kinetics of absorption of carbon dioxide in aqueous piperazine solution. Chem. Eng. Sci. 61, 6837-6854.

Donaldson, T. L., Nguyen, Y. N., 1980. Carbon dioxide reaction kinetics and transport in aqueous amine membrane," Ind. Eng. Chem. Fundam.19, 260-266.

Dortmundt, D., Doshi, K., 1999. Recent Developments in CO_2 Removal Membrane Technology, In design consideration.16.08.11.

Dunn, C. L., Freitas, E. R., Goodenbour, J. W., Henderson, T., Papadopoulos, N., 1964. Sulfinol Process.Oil. Gas J.62, 95-98.

Ebenezer, S. A., Gudmunsson, J. S.,2005.Removal of Carbon Dioxide from Natural Gas for LPG Production. Semester project work, academia.edu.

Economides, M. J., Wood, D. A.,2009. The state of natural gas, J. Nat. Gas Sci. Eng.1,1-13.

Edali, M., Idem, R., Aboudheir, A., 2010.1D and 2D absorption-rate/kinetic modeling and simulation of carbon dioxide into aqueous solutions of MDEA and PZ in a laminar jet apparatus. Int. J. Greenh. Gas Control.4, 143-151.

Edali, M., Aboudheir, A., Idem, R., 2009.Kinetics of carbon dioxide into mixed aqueous solutions of MDEA and MEA using laminar jet apparatus and a numerically solved 2D absorption rate/kinetics model. International Journal of Greenhouse Gas Control.3, 550-560.

Edali, M., Aboudheir, A., Idem, R., 2007.Kinetics of carbon dioxide absorption into mixed aqueous solutions of MDEA and MEA using laminar jet apparatus and numerically solved absorption-rate/kinetic model. The COMSOL Conference, Boston.

Energy information, A. , Administration, U. S. E. I., 2011. International Energy Outlook 2011, In: Natural gas. 22.08.11, Available from: http://205.254.135.7/forecasts/ieo/pdf/0484(2011).pdf.

Falk-Pedersen, O., Dannstrom, H., 1997.Separation of carbon dioxide from offshore gas turbine exhaust. Energy Conversion and Management.38, 81-86.

Figueroa, J. D., Fout, T., Plasynski, S., McIlvried, H., Srivastava, R. D., 2008. Advances in CO_2 capture technology; The U.S. Department of Energy's carbon sequestration program. Int. J. Greenhouse Gas Control.2, 9-20.

Flynn, A.J., Wallace, C.B., Christensen, R.G., Knowles, W.T.,1981.Annual Convention of the Gas Processors Association.60, 149–151.

- Freeman, S.A., Dugas, R., Wagener, D.H.V. , Nguyen, T., Rochelle, G.T.,2010. Carbon dioxide capture with concentrated, aqueous piperazine. Int. J. Greenh. Gas Control.4, 119-124.

Gilliland, E. R., Baddour, R. F., Perkinson, G.P., Sladek, K.J.,1974.Diffusion on surfaces. I. Effect of concentration on the diffusivity of physically adsorbed gases. Industrial & Engineering Chemistry Fundamentals.13, 95-100.

Glasscock, D. A., 1990.Modeling and experimental study of carbon dioxide absorption into aqueous alkanolamines, PhD thesis. University of Texas at Austin, Texas.1-292

Goldstein, A. M., Edelman, A. M., Beisner, W. D., Ruziska, P. A.,1984. Hindered Amines Yield Improved Gas Treating. Oil Gas J.82, 70−76.

Gorensek, G.M., Hang, T., Koffman, L.D.,2003. Development of an electrolyte NRTL property set for dynamic models of the high level waste evaporators at the savannah river site, in: Paper Presented at the Aspen Tech User Group Meeting, New Orleans, LA.

Haghtalab, A., Afsharpour, A., 2015. Solubility of CO_2/H_2S gas mixture into different aqueous N-methyldiethanolamine solutions blended with 1-butyl-3-methylimidazolium acetate ionic liquid. Fluid Phase Equilib.406, 10-20.

Haghtalab, A., Izadi, A.,2014.Simultaneous measurement solubility of carbon dioxide + hydrogen sulfide into aqueous blends of alkanolamines at high pressure. Fluid Phase Equilibria.2014, 375, 181-190.

Hagewiesche, D.P., Ashour, S.S., Al-Ghawas, H.A., Sandall, O.C., 1995. Absorption of carbon dioxide into aqueous blends of Monethanolamine and N-methyldiethanolamine. Chem. Eng. Sci.50, 1071–1079.

Hashemifard, S. A., Ismail, A. F., Matsuura, T., 2010.Prediction of gas permeability in mixed matrix membranes using theoretical models. Journal of Membrane Science.347, 53-61.

Henni, A., 2002. Solubility of Gases in Physical Solvents and Absorption of CO_2 in a Mixed Solvent (Doctoral dissertation, PhD. Dissertation, University of Regina, Saskatchewan, Canada).

Hermann, W., Bosshar, P., Hung, E., Hunt, R., Simon, A.J., 2005.An Assessment of Carbon Capture Technology and Research Opportunities, In: Physical Adsorption.25.08.11

Hessen, E.T., Haug-Warberg, T., Svendsen, H.F., 2010. The refined e-NRTL model applied to CO_2-H_2O-alkanolamine systems.Chemical Engineering Science.65, 3638-3648.

- Hilliard, M. D., 2008. A Predictive Thermodynamic Model for an Aqueous Blend of Potassium Carbonate, Piperazine, and Monoethanolamine for Carbon Dioxide Capture from Flue Gas," PhD, The University of Texas at Austin, Austin Texas**.**

Huang, Y. M., Soriano, A.N., Caparanga, A.R., Li, M. H., 2011.Kinetics of absorption of carbon dioxide in 2-amino-2-methyl-l-propanol + *N*-methyldiethanolamine + water, J. Chem. Eng.42, 76-85.

International Energy Agency (IEA).,2014.CO_2 emissions from fuel combustion highlights. Website;⟨http://www.iea.org/publications/free publications/publication/⟩.

Jalili, A.H., Shokouhi, M., Samani, F., Hosseini-Jenab, M., 2015.Measuring the solubility of CO_2 and H_2S in sulfolane and the density and viscosity of saturated liquid binary mixtures of (sulfolane + CO_2) and (sulfolane + H_2S). J. Chem. Thermodyn.85,13-25.

Javaid, A., 2005.Membranes for solubility-based gas separation applications. Chemical Engineering Journal.112, 219-226.

Jenab, M.H., Abdi, M.A., Najibi, S.H., Vahidi, M., Matin, N.S.,2005. Solubility of carbon dioxide in aqueous mixtures of N-methyldiethanolamine + piperazine + sulfone. J. Chem. Eng. Data.50, 583-586.

Jou, F.Y., Mather, A.E., Schmidt, K.A., Ng, H. J.,1999.Vapor- Liquid Equilibria in the System Ethane thiol + Methyldiethanolamine + Water in the Presence of Acid Gases, J. Chem. Eng. Data .44 , 833–835.

Jou, F. Y., Deshmukh, R.D., Otto , F.D., Mather, A.E.,1990. Solubility of H_2S, CO_2, CH_4 and C_2H_6, in Sulfolane at elevated pressures, Fluid Phase Equilibria.56, 313-324.

- Ismail, A. F., David, L. I. B.,2001.A review on the latest development of carbon membranes for gas separation. Journal of Membrane Science.193, 1-18.

Karadas, F., Atilhan, M., Aparicio, S. A., 2010. Review on the Use of Ionic Liquids(ILs)as Alternative Fluids for CO_2 Capture, and Natural Gas Sweetening, Energy Fuels.24, 5817-582.

Khoze, B., Mathias, P.M., 2004.Thermodynamic model for Bayer alumina process, in: Paper Presented at Aspen World, Orlando, FL. 10-15.

Ko, J.J., Li, M.H., 2000.Kinetics of the absorption of carbon dioxide into solutions of N-methyldiethanilamine + water. Chem. Eng. Sci.55,4139-4147.

Kohl, A. L., Riesenfeld, F. C., 1997. Gas Purification, Gulf Publishing Co, Houston, 5th edition.

Kohl, A.L. , Nielsen, R.B.1979.Gas purification. Houston: Gulf Publishing Co, 5th edition.

Kerry, F. G., 2007.Industrial Gas Handbook: Gas Separation and Purification, CRC.ISBN 978-0-8493-9005-0,New York.

Kierzkowska-Pawlak, H., Siemieniec, M., Chacuk, A.,2011.Reaction kinetics of CO_2 in aqueous Methyldiethanolamine solutions using the stopped-flow technique. Chem. Process Eng. 33, 7-18.

Kim, Y. S., Jang, J. H., Lim, B. D., Kang, J. W., Lee, C. S.,2007.Solubility of mixed gases containing carbon dioxide in ILs: Measurements and predictions. Fluid Phase Equilib.256,70-74.

Klinkenbijl, J.M., Dillon, M.L., Heyman, E.C.,1999.Gas pre-treatment and their impact on liquefaction processes, in GPA Nashville TE meeting.

Korens, N., Simbeck, D.R., Wilhelm, D.J., 2002.Process Screening Analysis of Alternative Gas Treating and Sulfur Removal for Gasification, SFA Pacific, Inc., Mountain View, CA.

Kovvali, A. S., Sirkar, K. K., 2002.Carbon dioxide separation with novel solvents as liquid membranes. Industrial & Engineering Chemistry Research.41, 2287-2295.

Kumelan, J., Kamps, A. P. S.,Tuma, D.,Maurer, G.,2006. Solubility of CO_2 in the ILs [bmim][CH_3SO_4] and [bmim][PF_6].J. Chem. Eng. Data.51, 1802-1807.

Laddha, S.S.; Danckwerts, P.V., 1981.Reaction of CO_2 with ethanolamine; kinetics from gas absorption. Chem. Eng. Sci.36, 229-230.

Langston, L., Lee, S.L., 2010. A bright natural gas future, Mech. Eng. (New York, N.Y.1919). 132, 49.

Li, B., Duan, Y., Luebke, D., Morraele, B., 2013. Advances in CO_2 capture technology: a patent review, Appl. Energy.102, 1439–1447.

Li, J., Henni, A., Tontiwachwuthikul, P.,2007.Reaction kinetics of CO_2 in aqueous ethylenediamine, ethyl ethanolamine, and diethyl monoethanolamine solutions in the temperature range of 298-313 K using stopped-flow technique. Ind. Eng. Chem. Res.46,4426-4434.

Liss, W., 1990. Demand outlook: a golden age of natural gas, Chem. Eng. Prog.108, 35-40.

Littel, R.J., Van Swaaij, W.P.M., Versteeg, G.F., 1990. Kinetics of carbon dioxide with tertiary amines in aqueous solution, AIChE J.11,1633–1640.

Liu, H. B., Zhang, C. F. ;, Xu, G. W.,1999.A study on equilibrium solubility for carbon dioxide in methyldiethanolamine - piperazine - water solution. Ind. Eng. Chem. Res.38, 4032-4036.

Lorant, J.L., Davoine, P.,1991.Modeling of Solvay bicarbonate column, in: Paper Presented at the Conference on Thermodynamic Challenges for Chemical Processes, Karlsruhe, Germany.

Macgregor, R.J., Mather, A.E.,1991.Equilibrium solubility of H_2S and CO_2 and their mixtures in a mixed solvent , Can. J. Chem. Eng.69,1357–1366.

Maham, Y., Teng, T.T., Mather, A.E., Hepler, L.G.,1995.Volumetric properties of (water + diethanolamine) systems , J. Chem.73 , 1514-1519.

Ma'mun, S., Dindore, V.Y., Svendsen, H.F., 2007.Kinetics of the reaction of carbon dioxide with aqueous solutions of 2-2-aminoethyl-amino- ethanol. Ind. Eng. Chem. Res.46, 385-394.

Mandal, B.P., Guha, M., Biswa, A.K., Bandopadhyay, S.S., 2001.Removal of carbon dioxide by absorption in mixed amines modeling of absorption in aqueous /MEA and AMP/MEA solutions. Chem. Eng. Sci.51, 6217-6244.

Mangers, R.J., Ponter, A.B., 1980.Effect of Viscosity on liquid film resistance to mass transfer in a packed column. Ind. Eng. Chem. Proc. Des. Dev.19, 530-537.

Mathias, P.M., O'Connell, J.P., 2012.The Gibbs-Helmholtz equation and the thermodynamic consistency of chemical absorption data. Ind. Eng. Chem. Res.51, 5090-5097.

Mathias, P.M., Brown, L.C., Ramrus, D., Chen, C. C., 2001.Thermodynamic model for the HI–I2–H_2O system, in: Paper Presented at the AIChE Annual Meeting, Reno, NV.4-9.

Mersmann, A., Kind, M., Stichlmair, J., 2011.Thermal Separation Technology Principles, Methods, Process Design, Springer. ISBN 978-3-642-12524-9, New York.

Messnaoui, B.,; Bounahmidi, T.,2005.Modeling of excess properties and vapor–liquid equilibrium of the system H_3PO_4–H_2O, Fluid Phase Equilibria.237, 77-85.

Meyers, R. A., 2001.Chemical Engineering. Encyclopedia of Physical Science and Technology 3rd edition), Ramtech, Inc. California.

Mirzaei, S., Shamiri, A., Aroua, M.K., 2015.A review of different solvents, mass transfer, and hydrodynamics for post-combustion CO_2 capture. Chem. Eng.31, 521-561.

Mock, B., Chen, C. C., Evans, L.B., 1986.Thermodynamic representation of phase equilibria in mixed-solvent electrolyte systems. AIChE .J.32, 1655–1664.

Muraoka, T., 2005. Application of aspen ratesep for nitric acid absorber, in: Paper Presented at the Aspen User Group Meeting, Amsterdam, The Netherlands.7–8.

Natural Gas. org., 2010.Overview of Natural Gas, In: Background. 22.06.11, Available from: http://www.naturalgas.org/overview/background.asp.

Pal, R., 2007.New models for thermal conductivity of particulate composites. Journal of Reinforced Plastics and Composites.26,643.

Park, M.K., Sandall, O.C., 2001.Solubility of carbon dioxide and nitrous oxide in 50 mass methyldiethanolamine. J. Chem. Eng. Data.46, 166-168.

Pilate, A., Kelchtermans, H., Vansina, H., 1988. Simulation of pyrometallurgical and hydrometallurgical processes at metallurgies Hoboken-over pelt, in: Paper Presented at Aspen World 88, Amsterdam, The Netherlands.13–16.

Pandey, P., Chauhan, R. S., 2001. Membranes for gas separation.Progress in Polymer Science. 26, 853-893.

Pani, F., Gaunand, A., Cadours, R., Bouallou, C., Richon, D., 1997.Kinetics of absorption of CO_2 in concentrated methyldiethanolamine solutions in the range 296 K to 343 K. J. Chem. Eng. Data .42, 353–359.

Pinsky, M.L., Gruber, G.,1994. Phase Equilibria in aqueous systems containing Na^+,K^+,Mg^{+2},Cl^- , and SO_4^{-2} ions using the NRTL model, AIChE Symp. Ser.298 , 112-126.

Pitzer, K. S., Simonson, J. M., 1986.Thermodynamics of Multicomponent, Miscible, Ionic Systems: Theory and Equations," American Chemical Society.90, 3005-3009.

Pitzer, K.S., 1980.Electrolytes: from dilute solutions to fused salts, J. Am. Chem. Soc.102 , 2902-2906.

Polasek, J., Bullin, J., 1984.Selecting amines for sweetening units. Energy Progress.4, 146-149.

Poling, B. E., Prausnitz, J. M., O'Connell, J. P.,2001. The Properties of Gases and Liquids, 5th ed. Mc GRAW-HILL.

Porter, M. C., 1990.Handbook of Industrial Membrane Technology, Noyes Publications.ISBN 08155-1205-8, New Jersey.

Ramachandran, N., Aboudheir, A., Idem, R., Tontiwachwuthikul, P., 2006. Kinetics of the absorption of CO_2 into mixed aqueous loaded solutions of monoethanolamine and methyldiethanolamine. Ind. Eng. Chem. Res.45,2608–2616.

Rashin, A.A. , Honig, B.,1985.Re-evaluation of the Born Model of Ion Hydration, " J. Phys. Chem. 89, 5588-5593 .

Renon, H., Prausnitz, J.M., 1968. Local compositions in thermodynamic excess functions for liquid mixtures, AIChE J.14 ,135-144.

Rinker, E.B., Ashour, S.S., Sandall, O.C., 2000.Absorption of carbon dioxide into aqueous blends of diethanolamine and methyldiethanolamine. Ind. Eng. Chem. Res.39,4346-4356.

Rinker, E.B., Ashour S.S., Sandall, O.C.,1996.Kinetics and modeling of carbon dioxide absorption into aqueous solutions of diethanolamine. Ind. Eng. Chem. Res.35, 1107-1114.

Rinker, E.B., Ashour, S.S., Sandall, O.C.,1995.Kinetics and modeling of carbon dioxide absorption into aqueous solutions of N-methyldiethanolamine. Chem. Eng. Sci.50, 755-768.

Ritter, J. A., Ebner, A. D., 2007.Carbon Dioxide Separation Technology: R&D Needs For the Chemical and Petrochemical Industries, In: Recommendation for future R&D. 22.06.11.

Roberts, B. E., Mather, A. E.,1988.Solubility of CO_2 and H_2S in A Mixed Solvent. Chem. Eng. Commun.72, 201-211.

Robinson, R. A., Stokes, R. H.,1970.Electrolyte Solutions, 2nd ed. Butterworth, Oxford, U.K.

Rodriguez, H., Mello, L., Salvagnini, W., de Paiva, J.L.,2011.Absorption of Carbon Dioxide into Aqueous Solutions of alkanolamines in a Wetted Wall Column with Film Promoter. Chemical Engineering Transactions.25, 51-56.

Saha, A.K., Bandyopadhyay, S.S., Biswas, A.K., 1995.Kinetics of absorption of CO_2 into aqueous solutions of 2-amino-2-methyl-1-propanol.Chem. Eng. Sci. 50, 3587–3598.

Sartori, G., Savage, D. W., 1983.Sterically Hindered Amines for CO_2 Removal from Gases. Ind. Eng. Chem. Fundam. 22, 239−249.

Say, G.R., Heinzelmann, F.J., Iyengar, J.N., Savage, D.W., Bisio, A., Sartori, G.,1984. A New hindered amine Concept for Simultaneous Removal of CO_2 and H_2S from Gases. Chem. Eng. Prog. 80, 72−77.

Seo, D.J., Hong, W.H., 2000. Effect of piperazine on the kinetics of carbon dioxide with aqueous solutions of 2-amino-2-methyl-1-propanol. Ind. Eng. Chem. Res. 39, 2062–2067.

Shafeeyan, M.S., Daud, W.M.A.W., Shamiri, A., Aghamohammadi, N., 2015.Modeling of carbon dioxide adsorption onto ammonia-modified activated carbon: kinetic analysis and breakthrough behavior. Energy & Fuels. 29, 6565-6577.

Shamiri, A., Shafeeyan, M., Tee, H., Leo, C., Aroua, M., Aghamohammadi, N., 2016. Absorption of CO_2 into aqueous mixtures of glycerol and monoethanolamine. J. Nat. Gas Sci. Eng. 35, 605-613.

Shekhawat, D., Luebke, D. R., Pennline, H. W., 2003. A review of carbon dioxide selective membranes: A topical report (No. DOE/ NETL-2003/1200).

Shirazizadeh, H. A., 2019.Haghtalab, A. Simultaneous solubility measurement of (ethyl mercaptan + carbon dioxide) into the aqueous solutions of (N-methyl diethanolamine + sulfolane + water), J. Chem. Thermodynamics .133,111–122.

Shimekit, B., Mukhtar, H. , Murugesan, T.,2011. Prediction of the relative permeability of gases in mixed matrix membranes. Journal of Membrane Science.373, 152-159.

Simoni, D., Lin, Y., Brennecke, J., Stadtherr, M.,2007. Modeling Liquid-liquid Equilibrium of Ionic Liquid Systems With NRTL, Electrolyte-NRTL, and UNIQUAC. Department of Chemical and Bio-molecular Engineering University of Notre Dame, Notre Dame, IN 46556,USA.

Sodiq, A., Rayer, A., Abu-Zahra, M.R.M., 2014. The Kinetic Effect of Adding Piperazine Activator to Aqueous Tertiary and Sterically-Hindered Amines Using Stopped-Flow Technique, Energy Procedia .63,1256 –1267.

Sridhar, S., Smitha, B., Aminabhavi, T.M., 2007.Separation of carbon dioxide from natural gas mixtures through polymeric membranes-a review. Separation & Purification Reviews.36, 113-174.

Stern, A., 1994. Polymers for gas separations: the next decade. Journal of Membrane Science . 94, 1-65.

Sun, W. C., Yong, C. B., Li, M. H., 2005. Kinetics of the absorption of carbon dioxide into mixed aqueous solutions of 2-amino-2-methyl-1-propanol and piperazine. Chem. Eng. Sci.60, 503–516.

Svensson, H., Hulteberg, C., Karlsson, H.T., 2013. Heat of absorption of CO_2 in aqueous solutions of N-methyldiethanolamine and piperazine. Int. J. Greenh. Gas Control .17, 89–98.

Tan, C.S., Chen, J. E., 2006. Absorption of carbon dioxide with piperazine and its mixtures in a rotating packed bed. Sep. Purif. Technol.49, 174-180.

Tennyson, R. N., Schaaf, R. P., 1977.Guideline can help choose Proper Process for Gas Treating Plants, Oil and Gas Journal. 10, 78-85.

Tobin, J., Shambaugh, P., 2006. The crucial link between natural gas production and its transportation to market in: stages in the production of pipeline-quality natural gas and NGLs. 13.07. 11.

Vaidya, P.D., Kenig, E.Y., 2007. Gas–liquid reaction kinetics: a review of determination methods. Chem. Eng. Comm. 194, 1543 –1565.

Van Ness, H. C., Abbott, M. M.,1979. Vapor-Liquid Equilibrium: Part VI. Standard state Fugacities for Supercritical Components. AIChE. J. 25, 645–653.

Versteeg, G.F., VanDijck, VanSwaaij, W.P.M.,1996. On the kinetics between CO_2 and alkanolamines both in aqueous and non-aqueous solutions. An overview, Chem. Eng. Commun. 144, 113-158.

Versteeg, G. F., Van Swaaij,W. P. M.,1988a.On the kinetics between CO_2 and alkanolamines both in aqueous and non-aqueous solutions-I. Primary and secondary amines. Chem. Eng Sci.43, 573-587.

Versteeg, G.F., van Swaaij, W.P.M., 1988b.On the kinetics between CO_2 and alkanolamines both in aqueous and non-aqueous solutions-II. Tertiary amines. Chem. Eng. Sci.43, 587-591.

Vu, D. Q.,2001.Formation and Characterization of Asymmetric Carbon Molecular Sieve and Mixed Matrix Membranes for Natural Gas Purification, PhD thesis. University of Texas at Austin, Texas. 1-362.

Wang, C. W., Soriano, A.N. , Yang, Z.Y., Li, M.H.,2010. Solubility of carbon dioxide in the solvent system (2-amino-2-methyl-1-propanol + sulfolane + water).Fluid Phase Equilib. 291, 195–200.

Wappel, D., Gronald, G., Kalb, R.; Draxler, J., 2010. ILs for post-combustion CO_2 absorption. Int. J. Greenhouse Gas Control.4, 486–494.

Wilson, G.M., 1964. Vapor- liquid equilibrium. XI. A new expression for the excess free energy of mixing, J. Am. Chem. Soc.86 , 127–130.

Wei, C., Soriano, A., Yang, Z. Hui, Li., 2010. Solubility of carbon dioxide in the solvent system.(2-amino-2-methyl-1-propanolþsulfolaneþwater). Fluid Phase Equi. 291 , 195-200.

Xiao, J., Li, C.W., Li, M.H., 2000. Kinetics of absorption of carbon dioxide in aqueous solutions of 2-amino-2-methyl-1- propanol + mono-ethanolamine. Chem. Eng. Sci.55, 161–175.

Xu, G. W., Zhang, C. F., Qin, A. J., Gao, W. H., Liu, H. B.,1998.Gas-liquid equilibrium in a CO_2 -MDEA- H_2O system and the effect of piperazine on it. Ind. Eng. Chem. Res. 37, 1473–1477.

Xu, S., Wang, Y., Otto, F.D., Mather, A.E.,1993.The physicochemical properties of the mixed solvent of 2-piperidineethanol, sulfolane and water, J. Chem. Technol. Biotechnol.56 , 309–316.

Xu, G. W., Zhang, C. F., Qin, A. J., Wang, Y.W., 1992. Kinetics study on absorption of carbon dioxide into solutions of activated methyldiethanolamine. Ind. Eng. Chem. Res.31, 921–927.

Xu, S., Qing, S., Zhen, Z., Zhang, C., Carroll, J. J.,1991. Vapor Pressure Measurements of Aqueous N-Methyldiethanolamine Solutions. Fluid Phase Equilibria. 67,197-201.

Xu, S., Wang, Y., Otto, F. D., Mather, A. E.,1991.Rate of Absorption of CO_2 in a Mixed Solvent, Ind. Eng. Chem. Res. 30, 1213-1217.

Yang, R. T. , Wiley, J.,2003. Adsorbents: fundamentals and applications, John Wiley & Sons. 2003. ISBN 9780471297413, New Jersey.

Yang, R.,1997.Gas Separation by Adsorption Processes, Imperial College Press. ISBN 9781860940477, Singapore.

Yeh, J.T., Pennline, H.W., Resnik, K.P.,2001. Study of CO_2 Absorption and Desorption in a Packed Column, Energy Fuels. 15, 274–278.

Yih, S.M., Shen, K.P., 1988. Kinetics of carbon dioxide reaction with sterically hindered 2-amino-2-methyl-1-propanol aqueous solutions. Ind. Eng. Chem. Res.27, 2237–2241.

Yu, W.C., Astarita, G., Savage, D.W.,1985.Kinetics of carbon dioxide absorption in aqueous solutions of methyldiethanolamine. Chem. Eng. Sci. 40, 1585–1590.

Zhang, X., Wang, J., Zhang, C. F., Yang, Y. H., Xu, J. J.,2003. Absorption rate into a MDEA aqueous solution blended with piperazine under a high CO_2 partial pressure. Ind. Eng. Chem. Res.42,118–122.

Zhang, X., Zhang, C.F., Qin, S.J., Zheng, Z.S., 2001.A kinetics study on the absorption of carbon dioxide into a mixed aqueous solution of methyldiethanolamine and piperazine. Ind. Eng. Chem. Res. 40, 3785-3791.

Zhang Y., Chen, C. C., 2011. Thermodynamic Modeling for CO2Absorption in Aqueous MDEA Solution with Electrolyte NRTL Model, Ind. Eng. Chem. Res. 50 , 163–175.

Zhu, Y., Chen, C. C., Evans, L.B., 1990.Representation of phase equilibrium behavior of antibiotics, Biotechnol. Prog. 6, 266–272.

Zoghi, A.T., Feyzi, F., Zarrinpashneh, S.2012. Equilibrium solubility of carbon dioxide in a 30 wt% aqueous solution of 2-((2-aminoethyl) amino) ethanol at pressures between atmospheric and 4400 KPa: An experimental and modeling study. J. Chem. Thermodyn. 44, 66–74.

Zoghi, A.T., Feyzi, F., Zarrinpashneh, A.,2012. Experimental investigation on the effect of addition of amine activators to aqueous solutions of N-methyldiethanolamine on the rate of carbon dioxide absorption. Int. J. Greenhouse. Gas Control. 7, 12–19.

Zong, L., Chen, C.C.,2011.Thermodynamic modeling of CO_2 and H_2S solubilities in aqueous DIPA solution, aqueous sulfolane–DIPA solution, and aqueous sulfolane–MDEA solution with electrolyte NRTL model, Fluid Phase Equilibria. 306, 190–203.

Publications and Conferences

Publications and Conferences

1-**Ahmed Abdelmouiz , Ahmed Hadjadj, Abdenacer Guibadj , Amr Henni.**
Measurement of the Absorption Rates of Carbon Dioxide in Aqueous Solutions of Piperazine and Sulfolane Using the Stopped-flow Technique. 15th International Conference on Greenhouse Gas Control Technologies, GHGT-15 Abu Dhabi, UAE. 15th -18th March 2021**.**

2- Ahmed Abdelmouiz, Amr Henni, Abdenacer Guibadj, Ahmed Hadjadj. Enhancement of Kinetic Rates of CO_2 in Aqueous Solutions of Piperazine and Methyldiethanolamine with Addition of Sulfolane .Canadian Journal of Chemical Engineering, June 2021, **DOI: 10.1002/cjce.24222**